Enhancing Breast Cancer Detection in Digital Mammograms through Hybrid HHO-CS, Multi-Feature and Triplet Learning Frameworks

A thesis submitted to the University of Calicut
in partial fulfilment of the requirements for the award of the degree of

DOCTOR OF PHILOSOPHY IN **COMPUTER SCIENCE**
Under the Faculty of Science

By

Haris U.

Under the Guidance of

Dr. Kabeer V.

PG AND RESEARCH DEPARTMENT OF COMPUTER SCIENCE
FAROOK COLLEGE (AUTONOMOUS)
Affiliated to University of Calicut
Farook College P.O., Kozhikode
Kerala, India, PIN - 673 632

December 2024

FAROOK COLLEGE (AUTONOMOUS)
AFFILIATED TO UNIVERSITY OF CALICUT

Farook College P.O., Kozhikode

Kerala, India, PIN - 673 632.

CERTIFICATE

This is to certify that the thesis entitled "**Enhancing Breast Cancer Detection in Digital Mammograms through Hybrid HHO-CS, Multi-Feature and Triplet Learning Frameworks**" is a report of original work carried out by **Mr. Haris U.** under my supervision and guidance in the Department of Computer Science, Farook College (Autonomous), Affiliated to University of Calicut and that no part there of has been presented for the award of any other degree.

Dr. Kabeer V.
Head & Research Supervisor
Department of Computer Science
Farook College (Autonomous)
Affiliated to University of Calicut

University of Calicut

December 16, 2024

FAROOK COLLEGE (AUTONOMOUS)
AFFILIATED TO UNIVERSITY OF CALICUT

Farook College P.O., Kozhikode

Kerala, India, PIN - 673 632.

DECLARATION

I hereby declare that the work presented in the thesis entitled "**Enhancing Breast Cancer Detection in Digital Mammograms through Hybrid HHO-CS, Multi-Feature and Triplet Learning Frameworks**" is based on the original work done by me under the guidance of **Dr. Kabeer V.** in the Department of Computer Science, Farook College (Autonomous), Affiliated to University of Calicut and has not been included in any other thesis submitted previously for the award of any degree. The contents of the thesis are undergone plagiarism check using **iThenticate** software at C.H.M.K. Library, University of Calicut, and the similarity index found within the permissible limit. The thesis incorporates all corrections and suggestions recommended by the adjudicators. I also declare that the thesis is free from AI generated contents.

Haris U.
Research Scholar

Dr. Kabeer V.
Head & Research Supervisor

University of Calicut

December 16, 2024

Dedicated to my Family, Teachers, Students & Friends

Table of Contents

List of Tables

List of Figures

Abstract

Breast cancer remains a significant global health concern, with a high incidence rate among women and a leading cause of cancer-related mortality. Early detection is paramount for improving patient health well-being, and mammography plays a central role in breast cancer screening. While Computer Aided Detection and/or Diagnosis (CAD) systems have bolstered cancer detection rates by assisting radiologists in mammogram interpretation, challenges persist in conventional detection methods, particularly in cases of false negatives, especially in dense breast tissue. Subjectivity in manual image interpretation also contributes to diagnostic variability.

In recent years, the fusion of medical science with artificial intelligence, specifically deep learning, has introduced a transformative approach to breast cancer detection. Deep learning, primarily leveraging Convolutional Neural Networks (CNNs), offers a promising solution to address the limitations of traditional detection methods. The integration of deep learning has led to the development of CADet systems that significantly enhance accuracy while reducing false positives and negatives.

This thesis embarks on a comprehensive exploration of various phases aimed at elevating the precision and quality of mammographic image analysis techniques. The research work encompasses four distinct studies, each contributing to the advancement of breast cancer detection methodologies.

In Study-1, an innovative approach is introduced for pectoral muscle segmentation, incorporating watershed transformation and regularization techniques with masking. Experimental results on the MIAS database demonstrate a remarkable accuracy of 97.20%.

Study-2 focuses on breast image segmentation techniques, enabling the detection of breast tumors through machine learning methods, particularly support vector machines. A novel hybrid model, HHO-CS MKSVM, is proposed, exhibiting an

impressive accuracy of 94.08% on the DDSM dataset.

In Study-3, we investigate into mammography-based breast cancer diagnosis, leveraging deep learning methods to enhance both segmentation and classification. A multifeature learning framework is developed, encompassing preprocessing, segmentation, feature extraction, and classification phases. The model achieves accuracies of 95.43% and 95.82% on the INbreast and MIAS datasets, respectively, showcasing its effectiveness in improving breast cancer diagnosis.

Study-4 represents an innovative fusion of Explainable AI, a Triplet Deep Learning model, and an Adaptive Deep Neural Network (A-DNN) to further enhance segmentation and classification. Impressively, it achieves an accuracy of 97.98% on the DDSM dataset, bridging the gap between advanced AI and medical diagnostics.

Collectively, these studies highlight the potential of deep learning-based methodologies to revolutionize breast cancer detection and diagnosis. By addressing challenges in segmentation, classification, and interpretability, these innovative algorithms offer promising avenues for improving the accuracy and efficiency of mammographic image analysis, ultimately contributing to the early detection and improved management of breast cancer.

Keywords: mammogram, breast cancer, deep learning, support Vector machine, CAD, preprocessing, image segmentation, feature extraction, image classification, medical diagnostics.

സംഗ്രഹം

സ്തനാർബുദം എന്നത് സ്ത്രീകൾക്കിടയിൽ വളരെ ഉയർന്ന രോഗവ്യാപനനിരക്കുള്ളതും അർബുദവുമായി ബന്ധപ്പെട്ട മരണത്തിന്റെ പ്രധാന കാരണവുമാണ്. അതുകൊണ്ട് തന്നെ സ്തനാർബുദം എന്നത് ആഗോളതലത്തിൽ ഒരു പ്രധാന ആരോഗ്യപ്രശ്നമായി തുടരുന്നു. രോഗിയുടെ ചികിത്സാഫലങ്ങൾ മെച്ചപ്പെടുത്തുന്നതിന് മുൻകൂട്ടിയുള്ള രോഗനിർണ്ണയം പരമപ്രധാനമാണ്. സ്തനാർബുദങ്ങൾ നേരത്തെ കണ്ടെത്തുന്നതിനും രോഗനിർണയം നടത്തുന്നതിനും വേണ്ടി സ്തനങ്ങൾ പരിശോധിക്കാൻ ഉപയോഗിക്കുന്ന കുറഞ്ഞ ഡോസ് ഉപയോഗിച്ചുള്ള എക്സ്-റേ ഇമേജിംഗ് രീതിയാണ് മാമോഗ്രാഫി. പരമ്പരാഗത ഡിറ്റക്ഷൻ രീതികൾ ഉപയോഗിച്ചുള്ള മാനുവൽ ഇമേജ് വ്യാഖ്യാനത്തിൽ ഒരുപാട് വെല്ലുവിളികൾ നിലനിൽക്കുന്നതിനാൽ അതെല്ലാം തന്നെ രോഗനിർണയത്തിലെ വ്യത്യാസത്തിന് കാരണമാകുന്നു, പ്രത്യേകിച്ച് ഫാൾസ് നെഗറ്റീവ് കേസുകളിലും, ഇടതൂർന്ന സ്തനകോശങ്ങളുടെ കാര്യത്തിലും. കംപ്യൂട്ടർ എയ്ഡഡ് ഡിറ്റക്ഷൻ / ഡയഗ്നോസിസ് (CAD) സംവിധാനങ്ങൾ റേഡിയോളജിസ്റ്റുകളെ മാമോഗ്രാം വ്യാഖ്യാനത്തിൽ സഹായിക്കുന്നതിനാൽ കാൻസർ നിർണയ നിരക്ക് വളരെയധികം വർധിപ്പിക്കാൻ സാധിച്ചിട്ടുണ്ട്.

സമീപ വർഷങ്ങളിൽ നിർമിത ബുദ്ധി, ഡീപ് ലേണിംഗ് രീതികൾ എന്നിവയുമായി വൈദ്യശാസ്ത്രത്തിന്റെ സംയോജനം സ്തനാർബുദം കണ്ടെത്തുന്നതിനുള്ള ഒരു ട്രാൻസ്ഫോർമേറ്റീവ് സമീപനം അവതരിപ്പിച്ചു. പ്രാഥമികമായി കൺവലൂഷണൽ ന്യൂറൽ നെറ്റ്വർക്കുകൾ (CNN) പ്രയോജനപ്പെടുത്തിക്കൊണ്ടുള്ള ഡീപ് ലേണിംഗ് രീതികൾ പരമ്പരാഗത കണ്ടെത്തൽ രീതികളുടെ പരിമിതികൾ പരിഹരിക്കുന്നതിന് ഒരു നല്ല പരിഹാരമാണ്. ഡീപ് ലേണിംഗുമായുള്ള സംയോജനം ഫാൾസ് പോസിറ്റീവുകളും നെഗറ്റീവുകളും കുറയ്ക്കുന്നതിനാൽ അത് കൃത്യത വർദ്ധിപ്പിക്കുന്ന CAD സംവിധാനങ്ങളുടെ വികാസത്തിലേക്ക് നയിക്കുന്നു. മാമോഗ്രാഫിക് ഇമേജ് അനാലിസിസ് ടെക്നിക്കുകളുടെ കൃത്യതയും ഗുണനിലവാരവും ഉയർത്തുവാനുള്ള നാല് വ്യത്യസ്ത പഠനങ്ങളാണ് ഈ തീസിസിൽ ഉൾക്കൊള്ളിച്ചിരിക്കുന്നത്.

പഠനം-1 ൽ, പെക്റ്റൊറൽ മസിൽ സെഗ്മെന്റേഷനു വേണ്ടി വാട്ടർഷെഡ് ട്രാൻഫോർമേഷൻ, റെഗുലറൈസേഷൻ, മാസ്കിംഗ് തുടങ്ങിയ സാങ്കേതികതകൾ

ഉൾപ്പെടുത്തിക്കൊണ്ടുള്ള ഒരു നൂതനമായ സമീപനമാണ് അവതരിപ്പിക്കുന്നത്. ഇതുപയോഗിച്ചുകൊണ്ടുള്ള MIAS ഡാറ്റാബേസിലെ പരീക്ഷണഫലങ്ങൾ 97.20% കൃത്യതയുള്ളതാണ്.

പഠനം-2 ൽ, സപ്പോർട്ട് വെക്റ്റർ മെഷീനുകൾ (SVM) ഉപയോഗിച്ചുകൊണ്ടുള്ള മെഷീൻ ലേണിംഗ് രീതികളിലൂടെ ബ്രെസ്റ്റ് ഇമേജ് സെഗ്മെന്റേഷൻ ടെക്നിക്കുകളിൽ ശ്രദ്ധ കേന്ദ്രീകരിച്ചുകൊണ്ട് സ്തനാർബുദം കണ്ടെത്തുന്നതിനുള്ള ഒരു പുതിയ ഹൈബ്രിഡ് മോഡൽ നിർദ്ദേശിക്കപ്പെട്ടിരിക്കുന്നു. ഹാരിസ് ഹോക്സ് ഓപ്റ്റിമൈസേഷൻ (HHO), കുക്കൂ സെർച്ച് (CS) എന്നിവയെ SVM മായി സംയോജിപ്പിച്ചുകൊണ്ടുള്ള ഈ മോഡൽ (HHO-CS: MKSVM) DDSM ഡാറ്റാസെറ്റിൽ 94.08% കൃത്യത കൈവരിച്ചിട്ടുണ്ട്.

പഠനം-3 ൽ, മാമോഗ്രാഫി അടിസ്ഥാനമാക്കിയുള്ള സ്തനാർബുദ രോഗനിർണയം മെച്ചപ്പെടുത്തുന്നതിന് വേണ്ടി ഡീപ് ലേണിംഗ് രീതികൾ പ്രയോജനപ്പെടുത്തിക്കൊണ്ട് പ്രീപ്രോസസിംഗ്, സെഗ്മെന്റേഷൻ, ഫീച്ചർ എക്സ്ട്രാക്ഷൻ, ക്ലാസ്സിഫിക്കേഷൻ എന്നിവ ഉൾക്കൊള്ളുന്ന ഒരു മൾട്ടിഫീച്ചർ ലേണിംഗ് ഫ്രെയിംവർക്ക് വികസിപ്പിച്ചെടുത്തിട്ടുണ്ട്. സ്തനാർബുദ രോഗനിർണയം മെച്ചപ്പെടുത്തുന്നതിൽ വളരെയധികം ഫലപ്രാപ്തി കാണിക്കുന്ന ഈ മോഡൽ, ഇൻബ്രെസ്റ്റ് (INbreast), MIAS എന്നീ ഡാറ്റാസെറ്റുകളിൽ യഥാക്രമം 95.43%, 95.82% കൃത്യത പ്രകടമാക്കുന്നു.

സെഗ്മെന്റേഷൻ, ക്ലാസ്സിഫിക്കേഷൻ എന്നിവ കൂടുതൽ മെച്ചപ്പെടുത്തുന്നതിനായി എക്സ്പ്ലൈനബിൾ AI, ട്രിപ്പ്ലെറ്റ് ഡീപ് ലേണിംഗ് മോഡൽ, അഡാപ്റ്റീവ് ഡയലേറ്റഡ് ഡീപ് ന്യൂറൽ നെറ്റ്വർക്ക് (AD-DNN) എന്നിവ ഉപയോഗിച്ചുകൊണ്ടുള്ള നൂതനമായ ഒരു ഫ്യൂഷൻ ഫ്രെയിംവർക്കാണ് പഠനം-4 ൽ പ്രതിനിധീകരിക്കുന്നത്. DDSM ഡാറ്റാസെറ്റിൽ ഈ ഫ്രെയിംവർക്ക് 97.98% കൃത്യത കൈവരിക്കുന്നു.

മൊത്തത്തിൽ, ഈ പഠനങ്ങൾ എല്ലാം തന്നെ സ്തനാർബുദം കണ്ടെത്തുന്നതിലും രോഗനിർണയത്തിലും വിപ്ലവം സൃഷ്ടിക്കുന്നതരത്തിലുള്ള ഡീപ് ലേണിംഗ് അധിഷ്ഠിത രീതികളുടെ സാധ്യതകൾ ഉയർത്തിക്കാട്ടുന്നു. സെഗ്മെന്റേഷൻ, ക്ലാസ്സിഫിക്കേഷൻ എന്നിവയിലെ വെല്ലുവിളികൾ അഭിമുഖീകരിക്കുന്നതിലൂടെ, മാമോഗ്രാഫിക് ഇമേജ് വിശകലനത്തിന്റെ കൃത്യതയും കാര്യക്ഷമതയും മെച്ചപ്പെടുത്തുന്നതിന് ഈ നൂതന അൽഗോരിതങ്ങൾ മികച്ച വഴികൾ വാഗ്ദാനം ചെയ്യുന്നു. ഇത് ആത്യന്തികമായി സ്തനാർബുദം നേരത്തേ കണ്ടെത്തുന്നതിനും കൈകാര്യം ചെയ്യുന്നതിനും സഹായിക്കുന്നു.

കീവേഡുകൾ: മാമോഗ്രാം, സ്തനാർബുദം, ഡീപ് ലേണിംഗ്, സപ്പോർട്ട് വെക്റ്റർ മെഷീൻ, CAD, ഇമേജ് പ്രീപ്രോസസിംഗ്, ഇമേജ് സെഗ്മെന്റേഷൻ, ഫീച്ചർ എക്സ്ട്രാക്ഷൻ, ഇമേജ് ക്ലാസ്സിഫിക്കേഷൻ.

Acknowledgements

I, Haris U., a Research Scholar under the able guidance of Dr. Kabeer V., Head of the Research Department of Computer Science at Farook College (Autonomous), affiliated to the University of Calicut, extend my heartfelt gratitude to all those who have contributed to the realization of this thesis. As an Assistant Professor in the Department of Computer Science at KAHM Unity Women's College, Manjeri, I am grateful to the supportive academic and personal community that has been instrumental in this journey.

I extend my deepest appreciation and gratitude to Dr. Kabeer V., my esteemed supervisor, for his unwavering guidance, insightful feedback, and invaluable support, which have been the cornerstone of this research endeavor. His mentorship, distinguished by academic rigor and profound expertise, has been instrumental in navigating the complexities of this work. Dr. Kabeer's encouragement and belief in my potential have been a constant source of motivation, inspiring me to strive for excellence and persevere through challenges. His role in my academic journey has been immeasurable, and for that I am eternally grateful.

My gratitude extends to Dr. K.A. Aysha Swapna, Principal of Farook College (Autonomous), for fostering an environment of academic excellence and research innovation. I also wish to acknowledge the contributions of the former principal, Dr. K.M. Naseer, whose efforts have significantly shaped the institution's legacy of educational leadership.

The management and principal at KAHM Unity Women's College, Manjeri, deserve special thanks for their encouragement and the resources they have provided,

which have been crucial in facilitating my research endeavors.

I also wish to acknowledge my co-researchers, Afsal K and Sainul Abideen Nannat, for their collaborative spirit, shared insights, and the synergistic efforts that have enriched this research work. My colleagues at both Farook College (Autonomous) and KAHM Unity Women's College have provided a supportive academic atmosphere, and I am thankful for the engaging discussions and camaraderie we have shared.

A special acknowledgment to my parents, whose boundless love, care, and sacrifices have been the foundation of my strength and resilience. Their unwavering support and encouragement have been my guiding light through this journey.

A special note of appreciation to my wife, Dr. Aysha Muhsina K, whose support and patience have been fundamental to my ability to pursue this research with dedication and resilience.

I extend a heartfelt thanks to my sisters, in-laws, father-in-law, and mother-in-law for their unwavering love and encouragement. Their support has been a cornerstone of my journey, providing me with the strength and motivation to pursue my academic endeavors. Additionally, my gratitude goes out to my friends for their understanding and support. Despite the time spent away from them due to my commitments, their patience and encouragement have been invaluable, making this journey not only possible but also more rewarding.

To my students, past and present, their enthusiasm for learning and their questions have continually inspired me to explore further into the field of study.

This journey would not have been possible without the collective contributions of everyone who directly or indirectly supported me. Your unwavering support has not only facilitated the successful completion of this thesis but has also been a catalyst for personal growth and learning.

Above all, I am profoundly thankful to the Almighty for the grace and strength provided throughout this journey.

University of Calicut **Haris U.**

December 16, 2024 Reg. No. FKAQRSE003

Glossary

ACR	American College of Radiology
AD-DNN	Adaptive Dilated Deep Neural Networks
AFF	Adaptive Fuzzy based median filtering
ANFIS	Adaptive Neuro-Fuzzy Inference System
AI	Artificial Intelligence
ANN	Artificial Neural Network
AUC	Area Under the Curve
AGF	Adaptive Gaussian Filter
AWF	Adaptive Wavelet Filter
BCDR	Breast Cancer Digital Repository
BI-RADS	Breast Imaging Reporting and Data System
BOA	Butterfly Optimization Algorithm
CAD	Computer Aided Detection and/or Diagnosis
CBIS-DDSM	Curated Breast Imaging Subset of DDSM
CC	Cranio-Caudal View
cGAN	conditional Generative Adversarial Network
CLAHE	Contrast-Limited Adaptive Histogram Equalization
CMMD	Chinese Mammography Database
CNN	Convolutional Neural Network
COA	Coati Optimization Algorithm
CS	Cuckoo Search

Continued on the next page

CSO	Cuckoo Search Optimization
CSA	Crow Search Algorithm
CSDCNN	Class Structure-based Deep Convolutional Neural Network
CS-ELM	crow Search Optimized Extreme Learning Machine
DALY	Disability-Adjusted Life Year
D-CNN	Deep Convolutional Neural Networks
DDSM	Digital Database for Screening Mammography
DFS	Depth-First Search
DLH	Dimension Learning-Based Hunting
DNN	Deep Neural Networks
DRLBP	Discriminative Robust Local Binary Pattern
DRLTP	Discriminative Robust Local Ternary Pattern
ELBP	Elliptical LBP
ELM	Extreme Learning Machine
EMO	Electromagnetism Optimization
FC-NN	Fully Connected Neural Network
FDim	Fractal Dimension
FN	False Negative
FNR	False Negative Rate
FP	False Positive
FPR	False Positive Rate
FrCN	Full-Resolution Convolutional Network
GC	Grayscale Conversion
GLCM	Gray Level Co-Occurrence Matric
GLDS	Gray-Level Difference Statistics
Grad-CAM	Gradient-weighted Class Activation Mapping
GRU	Gate Recurrent Unit
GT	Geometric Transformations
HE	Histogram Equalization
HED	Holistically-Nested Edge Detection
HHO	Harris Hawks Optimization

Continued on the next page

HSV	Hue, Saturation, Value
IA	Image Augmentation
KFLI	Knowledge-driven Feature Learning and Integration
LBP	Local Binary Pattern
LDA	Linear Discriminant Analysis
LDP	Local Directional Pattern
LF	Levy Flight
LM	Lateromedial View
LOH	Local Orientation Histograms
LSTM	Long Short-Term Memory
MACNN	Multiscale All Convolutional Neural Network
MACSO	McCulloch's Algorithm inspired Cuckoo Search Optimization
MC	Microcalcifications
MCC	Matthews Correlation Coefficient
MCET	Cross Entropy Thresholding
ME	Masi Entropy
MFO	Moth Flame Optimizer
MIAS	Mammographic Image Analysis Society Database
MKSVM	Multi-Kernel Support Vector Machine
MLO	Medio-Lateral Oblique View
MME	Multi-level Masi Entropy
MOEA	Multi-Objective Evolutionary Algorithm
MQSA	Mammography Quality Standards Act
NMD	National Mammography Database
NPV	Negative Predictive Value
NRDR	National Radiology Data Registry
OMI-DB	OPTIMAM Mammography Image Database
OMLTS-DLCN	Optimal Multi-Level Thresholding-based Segmentation with a Deep Learning enabled Capsule Network
PACS	Picture Archiving and Communication System
PEIPA	Pilot European Image Processing Archive

Continued on the next page

PGM	Portable Gray Map
PSO	Particle Swarm Optimizer
RGB	Red, Green, and Blue
RLL	Regularized Logistic Loss
RMSE	Root Mean Square Error
RNN	Recurrent Neural Networks
ROI	Region of Interest
RPN	Region Proposal Network
RSO	Rat Swarm Optimization
SAE	Sparse Autoencoders
SAWSO	Self-Adaptive War Strategy Optimization
SE	Sum Entropy
SL	Straight Lateral view
SLO	Sea Lion Optimization
SSAE	Stacked Sparse Autoencoders
STDO	Self-Adaptive Tasmanian Devil Optimization
SURF	Speeded-Up Robust Features
SV	Sum Variance
SVM	Support vector machine
TDO	Tasmanian Devil Optimization
TFR-CNN	Triplet Fast Region Based Convolutional Neural Networks
TSO	Tuna Swarm Optimization
TTCNN	Transferable Texture Convolutional Neural Network
VQA	Visual Question Answering
WHO	World Health Organization
WNN	Wavelet Neural Network
WSO	War Search Optimization
WSOA	War Strategy Optimization Algorithm
XCC	Extended CC view

Chapter 1

Introduction

This thesis investigates cancer detection using image processing techniques in mammogram images, focusing on early breast cancer detection, crucial for effective treatment and better patient health well-being and outcomes. It aims to improve mammography's accuracy and efficiency, a key tool in breast cancer screening. This chapter outlines the thesis's background, motivation, problem statement, objectives, and scope, providing a comprehensive overview of the methodologies, technologies, and impact of image processing in early breast cancer detection, highlighting its importance in the medical field.

The beginning of the 21st century has witnessed remarkable strides in medical technology, particularly in the realms of cancer detection and treatment. As one of the leading causes of mortality worldwide, cancer poses a significant public health challenge, necessitating continual advancements in diagnostic and therapeutic methods. According to the World Health Organization (WHO), cancer accounted for nearly 10 million deaths in 2020, underscoring its devastating impact on global cancer statistics [Ferlay et al., 2020, World Health Organization, 2020].

Among various cancer types, breast cancer remains the most diagnosed cancer globally. In 2020 alone, there were an estimated 2.3 million women diagnosed with breast cancer, with the disease also being the leading cause of cancer-related deaths among women [Sung et al., 2021]. Figure 1.1 illustrates the most common types of cancer deaths and their share.

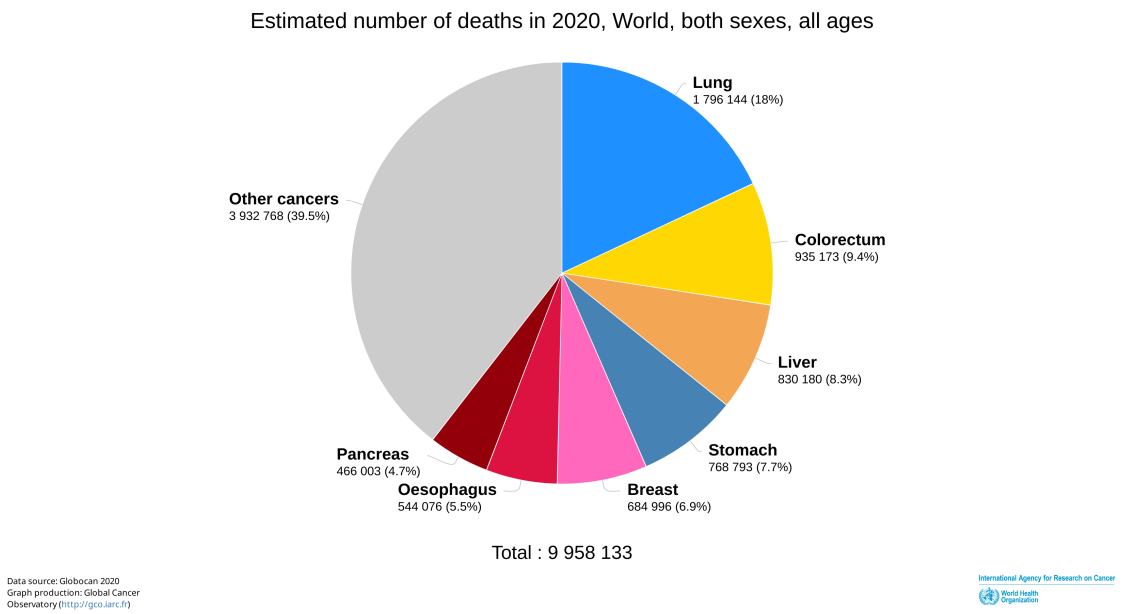

Figure 1.1: The most common types of cancer deaths in 2020 [Ferlay et al., 2020]

1.1 Background

The breast, situated on the chest wall, is a complex organ comprising components that function collectively to produce and secrete milk, nourish infants, and offer support and protection to underlying tissues. Various tissues exist in a woman's breast, including glandular, connective, adipose, nervous, and blood vessels/lymphatics. Glandular tissue produces milk, while connective tissue offers structural support. Adipose tissue cushions and supports the mammary gland, varying based on age, weight, and hormonal fluctuations. Nervous tissue supplies sensation, while blood vessels and lymphatics maintain blood supply and facilitate waste removal [National Cancer Institute, 2012, Ruud et al., 2020].

Breast density refers to the proportion of tissue types (glandular, fibrous, adipose) in a woman's breast. Dense tissue, comprising more glandular and fibrous tissue, poses challenges in tumor detection on mammograms, as both dense tissue and cancerous growths appear white on imaging. Women with dense breast tissue face an increased risk of breast cancer, yet breast density alone isn't a reliable predictor,

other factors like age, family history, and lifestyle play roles [Haji Maghsoudi et al., 2021].

1.1.1 Breast Cancer

Breast cancer manifests as uncontrolled growth of abnormal breast cells forming tumors that, if unchecked, can spread throughout the body, potentially becoming fatal. While predominantly affecting females, approximately 0.5–1% of breast cancers occur in men. Breast cancer originates in the lining cells of the breast ducts or lobules. Initially confined ("in situ") with minimal potential for spread, it may progress to invasive breast cancer, infiltrating surrounding tissues and possibly metastasizing to lymph nodes or other organs, becoming fatal if widespread [Anderson, 1985]. Treatment modalities encompass surgery, radiation therapy, and medication [de Martel et al., 2020]. Breast cancer contributes significantly to disability-adjusted life years (DALYs) among women globally. Survival improvements since the 1980s in countries with early detection programs and diverse treatment modes underscore the significance of early diagnosis and treatment strategies [Arnold et al., 2022]. Several factors, including age, obesity, alcohol use, family history, reproductive history, tobacco use, and postmenopausal hormone therapy, increase breast cancer risk [Ibrahim et al., 2022b].

1.1.2 Type of Breast Cancer Abnormalities

Major abnormalities include breast masses, calcifications, architectural distortions, and bilateral asymmetry, each with distinctive characteristics and implications for patient management and treatment. Understanding these abnormalities is essential for healthcare providers, as they guide the decision-making process regarding further diagnostic testing and treatment options [Helvie and Patterson, 2014, Venkataraman et al., 2021].

Breast Masses: Breast masses are areas of abnormal breast tissue that appear distinct from the surrounding tissue on a mammogram. They can vary in size, shape, and density. Not all masses indicate cancer; they can also be cysts or

non-cancerous solid tumors. The likelihood of malignancy increases with irregular shapes and indistinct or spiculated margins [Bozek et al., 2008, Cheng et al., 2006].

Calcifications and Microcalcifications: Calcifications in the breast tissue are small calcium deposits visible as white spots on a mammogram. There are two types: macrocalcifications, which are larger and typically benign, and microcalcifications, which are smaller and can be more concerning. Tight clusters or lines of microcalcifications are particularly suspicious and may indicate breast cancer. It's important to note that not all calcifications are linked to cancer; they can also result from aging, injuries, inflammation, or past breast surgery [Bankman et al., 1997].

Architectural Distortion: Architectural distortion refers to a change in the normal appearance of breast tissue, often without a visible mass. It can be a subtle finding and is commonly missed in traditional 2D mammograms. The causes of architectural distortion are diverse, ranging from benign conditions like fibrosis and radial scars to malignant entities. 3D tomosynthesis has improved the detection of architectural distortions, but this also comes with a higher rate of false positives. The presence of architectural distortions alongside other findings, like a distinct mass or calcifications, is typically considered higher risk [Rangayyan et al., 2010].

Bilateral Asymmetry: Bilateral asymmetry occurs when there is a significant difference in the appearance of breast tissue between the two breasts. Some asymmetry is normal, but new or increasing asymmetry may require further evaluation. This type of asymmetry can be a sign of an underlying pathology, but it can also be due to differences in positioning or compression during imaging [Rangayyan et al., 2007b].

1.1.3 Breast Cancer Screening

Breast cancer screening is a critical component in the early detection of breast cancer. Screening tests are designed to find breast cancer before it causes symptoms, like a lump that can be felt. Early detection of breast cancer often leads to a wider range of treatment options, less extensive surgery, and better outcomes. Recent studies have reinforced the value of regular screening. For instance, the

American Cancer Society reports that the 5-year relative survival rate for localized breast cancer (cancer that has not spread outside the breast) is 99%. This high survival rate is largely attributed to early detection through screening [American Cancer Society, 2022]. However, screening can have downsides, such as false-positive results that require further testing and cause anxiety. Moreover, there's the risk of overdiagnosis, where screening identifies a cancer that would not have caused harm in the person's lifetime. The balance of these factors is an essential consideration in the decision-making process for screening [Welch and Black, 2010]. The American College of Radiology recommends annual screening mammography starting at age 40 for women at average risk of breast cancer [American College of Radiology, 2021, Centers for Disease Control and Prevention, 2023].

1.1.4 Mammography - The Common Screening Test for Breast Cancer

Mammography is the most common breast cancer screening tool and is widely recommended for women of certain age groups or risk factors. It involves taking an X-ray picture of the breast to detect early signs of cancer that are not yet palpable [Centers for Disease Control and Prevention, 2023]. Figure 1.2 shows mammographic images.

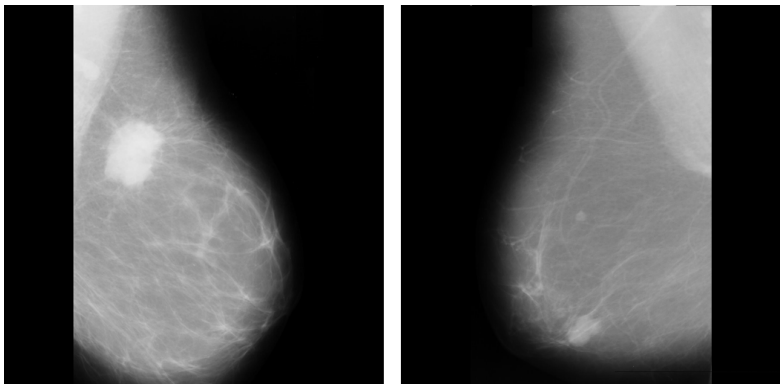

Figure 1.2: Sample Mammographic Images taken from MIAS Database [Suckling et al., 1994].

1.1.5 Computer Aided Detection and/or Diagnosis

Computer Aided Detection and/or Diagnosis (CAD) of cancer is a groundbreaking approach that harnesses the power of artificial intelligence and machine learning to assist healthcare professionals in the accurate and efficient detection of various types of cancer [Doi, 2007]. CAD systems are designed to analyze medical images, such as X-rays, CT scans, MRIs, and mammograms, with a level of precision and consistency that complements human expertise. These systems use sophisticated algorithms to identify patterns, abnormalities, and potential signs of cancer in the images, providing radiologists and clinicians with valuable insights and a second opinion [Rangayyan et al., 2007a]. By doing so, CAD not only enhances the accuracy of cancer detection but also helps in early diagnosis, which is critical for improving treatment outcomes and patient survival rates. Moreover, CAD systems are continually evolving, becoming more adept at detecting subtle or complex lesions, thereby playing a vital role in the fight against cancer and contributing to advancements in medical imaging and healthcare overall.

CAD of breast cancer is a significant approach that is revolutionizing breast cancer. Texture analysis, a sophisticated image processing technique, allows CAD systems to scrutinize the intricate patterns and structures within mammographic images of breast tissue [Masood and Ali Al-Jumaily, 2013]. By analyzing the subtle variations in texture, CAD can spot anomalies that might go unnoticed by the human eye, including microcalcifications, masses, or distortions, which could indicate the presence of breast cancer [Tourassi, 1999]. This technology serves as a crucial ally for radiologists, providing them with an additional layer of analysis and assisting in the early detection of breast cancer. Through texture analysis and CAD, healthcare professionals can enhance the accuracy of their diagnoses, enabling more timely interventions and better outcomes for individuals facing breast cancer [Petrosian et al., 1994, Duda et al., 2013]. This innovative blend of medical imaging and computational analysis offers great promise in the ongoing battle against breast cancer, offering hope for improved detection, treatment, and ultimately, more lives

saved.

The phases of a Digital Mammogram CAD system are crucial steps in the processing and analysis of mammography images for the detection of breast cancer. Each phase plays a specific role in enhancing the accuracy and efficiency of the diagnostic process:

Preprocessing: This phase is focused on enhancing the quality of the mammogram images. Techniques such as noise reduction and contrast enhancement are applied to improve clarity and visibility of the breast tissues. This step ensures that the subsequent phases have the highest quality data for analysis.

Region of Interest (ROI) Selection: In this phase, specific areas within the mammogram that may contain abnormalities are identified. This selection can be performed manually by a radiologist or automatically through algorithms designed to detect irregularities in breast tissue. The accuracy of ROI selection is critical for the effectiveness of the subsequent phases.

Segmentation: During segmentation, the system isolates and outlines specific structures or potential abnormalities within the selected ROI. This involves differentiating the suspected lesion from the surrounding normal breast tissue. Accurate segmentation is vital for ensuring that the feature extraction phase focuses on the correct areas.

Feature Extraction: Here, quantitative features from the segmented regions are extracted. These features may include the shape, size, texture, and intensity of the suspected lesions. The nature and quality of these extracted features play a pivotal role in the accuracy of the final classification phase.

Automatic Classification: In the final phase, the system uses the extracted features to classify the findings. Advanced algorithms, often incorporating machine learning techniques, analyze the features to determine whether the lesions are likely benign or malignant. This classification aids radiologists in making a more informed diagnosis.

Figure 1.3 visually represents these sequential phases, depicting the progression from image acquisition to the final classification and diagnosis. Each phase

builds upon the previous one, culminating in a sophisticated analysis that assists radiologists in the early detection and treatment of breast cancer.

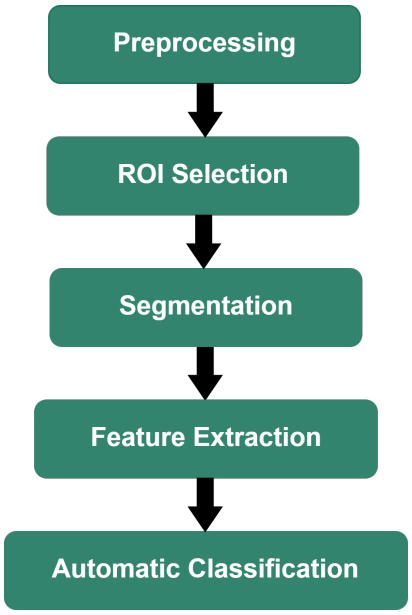

Figure 1.3: Mammogram CAD Flow

1.1.6 Artificial Intelligence in Medical Image Analysis

Machine learning and deep learning, subsets of AI, address challenges in medical imaging applications like CAD, lesion segmentation, and image analysis. Convolutional neural networks (CNNs), especially, have proven effective in medical imaging tasks, offering high accuracy rates. Deep learning algorithms show promise in automating feature learning from mammogram images, potentially enhancing breast cancer screening and diagnosis. Challenges such as data availability, bias, and interpretability require attention for ensuring clinical effectiveness and safety of these algorithms [Doi, 2007, Rangayyan et al., 2007a, Masood and Ali Al-Jumaily, 2013].

1.2 Motivation and Objectives

The pervasiveness of breast cancer globally is not just a health concern but a clarion call for enhanced detection and management strategies. The statistics are stark, highlighting not only the widespread nature of this affliction but also the urgent

need for more effective diagnostic methodologies. The critical role of medical image analysis, particularly through advanced imaging technologies like mammography, MRI, and ultrasound, has become a central pillar in the early detection of breast cancer. Such early detection is vital, significantly improving prognosis and survival rates. In fact, studies indicate that early-stage detection can lead to survival rate exceeding 90% [American Cancer Society, 2022]. However, the journey towards efficient and accurate breast cancer diagnosis is fraught with challenges. Despite technological advancements, variability in diagnostic accuracy persists, influenced by factors like healthcare access and imaging technology quality. Additionally, the interpretation of medical images often varies among radiologists, further complicating the diagnostic process [Smith et al., 2021]. This thesis is anchored in the backdrop of these challenges and the transformative potential of artificial intelligence in medical imaging. It aims to explore and harness advanced image processing techniques and AI algorithms for the detection of breast cancer, focusing on mammogram analysis. The integration of AI in interpreting medical images has shown promising results in enhancing diagnostic accuracy and reducing human error [Lei et al., 2020, Dileep and Gianchandani, 2022]. The goal is to contribute to enhancing diagnostic accuracy and developing more efficient, reliable, and universally accessible breast cancer detection methods and frameworks. This research is fuelled by a blend of a critical evaluation of existing screening modalities and the potential of technological innovations that could significantly improve diagnostic precision, accuracy and efficiency.

1.2.1 Problem Statement

The primary focus of this research is to refine and implement advanced CAD systems for more effective breast cancer detection and diagnosis in digital mammography. Digital mammograms, while essential in breast cancer screening, pose unique challenges due to the diverse textures, patterns, and densities of breast tissue, and the presence of noise and artifacts [Doi, 2007]. These complexities often lead to diagnostic inaccuracies, including missed diagnoses or false positives, affecting patient care [Geras et al., 2019].

To address these issues, the proposed CAD system integrates Support Vector Machine and deep learning methods. These techniques systematically evaluate mammograms, identifying subtle abnormalities and providing accurate assessments to medical professionals [Vu et al., 2020]. Such methods are increasingly vital, as they can discern intricate details and anomalies in breast tissue that might escape human analysis [Elkorany and Elsharkawy, 2023]. Utilizing deep learning models, the system is designed to handle the nuances of mammography datasets [Mridha et al., 2021, Zakareya and et al., 2023].

The development of this CAD system aims to augment the diagnostic process, increasing sensitivity and specificity, reducing interpretational errors, and facilitating early cancer detection. It's imperative to tailor the system to accommodate the complexities of breast tissue imaging and to integrate smoothly into existing healthcare workflows.

The overarching goal of this research is to enhance detection accuracy in breast cancer, particularly for early-stage malignancies, through a CAD system that efficiently differentiates between benign and malignant lesions. This involves addressing image quality issues and the optimization of machine learning algorithms for improved sensitivity and specificity [Elkorany and Elsharkawy, 2023]. The successful implementation of this system promises to bolster healthcare providers' capabilities, leading to better diagnostic outcomes and patient care in addressing breast cancer.

1.2.2 Research Objectives and Scope

The objectives of this research are designed to address identified gaps in the field of breast cancer detection using digital mammography. These include:

Development of a Robust CAD System Frameworks: Creating CAD system frameworks capable of accurately detecting suspicious lesions in digital mammograms.

Enhancement of Diagnostic Accuracy: Improving the sensitivity and specificity of breast cancer detection in digital mammograms to minimize false positives and negatives.

Comparative Evaluation with Radiologists: Assessing the diagnostic performance of the CAD system by comparing its results with those of experienced radiologists using a varied dataset of digital mammograms.

The scope of this research encompasses multiple key areas, ensuring a thorough examination and comprehensive understanding of the subject matter:

Development of Deep Learning Frameworks: Developing deep learning frameworks tailored to the unique characteristics of digital mammograms for improved detection of breast abnormalities.

Diverse Dataset Utilization: Gathering a wide-ranging and representative dataset of digital mammograms, encompassing various breast cancer types, stages, and patient profiles, to confirm the CAD system's applicability across different clinical environments.

Evaluation of Diagnostic Parameters: Assessing the sensitivity, specificity, positive predictive value, and overall diagnostic accuracy of the CAD system.

Impact on Patient Health Well-being and Outcomes: Analyzing the potential influence of the CAD system on patient health well-being and outcomes, including earlier cancer detection, reduction of false positives, improved treatment planning, and overall clinical significance.

Contribute to Continuous Improvement and Validation: Continuously refining the CAD system's algorithms and parameters and validating its performance using independent datasets to ensure reliable and consistent results.

1.3 Outline of the Thesis

This thesis is structured to provide a comprehensive examination of breast cancer detection using advanced medical imaging techniques. The organization of the thesis is as follows:

Chapter 1: This chapter outlines significant advances in medical technology for cancer detection and treatment, focusing on the prevalence and challenges of diagnosing breast cancer. It discusses the complexities of breast tissue and the role

of mammography in early detection, highlighting the importance of CAD systems. The chapter emphasizes the need for enhanced CAD systems to improve accuracy and efficiency in diagnosing breast cancer, addressing the challenges in interpreting medical images and the critical role of advanced imaging techniques.

Chapter 2: It presents a thorough analysis of current knowledge and methodologies, segmented into three primary areas: preprocessing, segmentation, and classification of medical images. Each section provides a paragraph-wise discussion of existing literature, offering a critical evaluation of past work and identifying gaps that this thesis aims to address.

Chapter 3: This chapter explores mammogram databases, views, classification standards, and preprocessing techniques crucial for breast cancer detection and diagnosis. It begins with an overview of the importance of mammogram databases and their role in research and medical practice. The chapter then examines various databases like DDSM, CBIS-DDSM, MIAS, INbreast, OPTIMAM, BCDR, NMD, CMMD, and BreaKHis, detailing their features and contributions. Next, it discusses mammogram views, classification standards (BI-RADS), and preprocessing techniques, emphasizing their significance in improving image quality and aiding early cancer detection. This chapter concludes by highlighting the critical role of these resources and techniques in advancing breast cancer detection.

Chapter 4: This chapter introduces an innovative approach for automated pectoral muscle segmentation in digital mammograms, vital for enhancing breast cancer detection accuracy. It begins by outlining the significance of pectoral muscle segmentation in mammogram interpretation and the challenges associated with it. The chapter then presents the proposed methodology, comprising orientation normalization, noise removal, and pectoral muscle detection phases. Each phase is explained in detail, highlighting the techniques employed and their contributions to accurate segmentation. Furthermore, the chapter discusses the results and discussions, showcasing the effectiveness of the proposed method through accuracy assessments and comparative evaluations. This chapter concludes by emphasizing its potential in improving breast cancer detection accuracy and reducing radiologist workload.

Chapter 5: Chapter 5 presents an advanced Hybrid SVM Framework tailored for breast cancer detection, comprising Support Vector Machines (SVM), Harris Hawks Optimization (HHO), and Cuckoo Search (CS) algorithms. It begins with an overview of SVM and the challenges in medical image analysis, followed by an explanation of HHO and its integration with CS. The chapter introduces Multi-Kernel Based Support Vector Machine (MKSVM) and its optimization using HHO-CS. Results and discussions include implementation details, dataset evaluation, and comparative analysis with existing methods. The chapter concludes by summarizing findings, discussing implications, and transitioning to Chapter 6.

Chapter 6: This chapter examines advanced techniques for breast cancer detection using multi-feature deep learning and image processing methods. It highlights the importance of geometric transformations and image augmentation in aligning and diversifying medical image datasets. Additionally, it discusses grayscale conversion, enhanced segmentation with modified Faster R-CNN, multi-layered feature extraction, and advanced classification strategies involving Autoencoders and LSTM models. Evaluation metrics and results from datasets like INbreast and MIAS demonstrate the efficacy of the proposed framework in improving breast cancer detection accuracy.

Chapter 7: Chapter 7 explores into cutting-edge methodologies to enhance detection accuracy by leveraging triplet deep learning and explainable AI. It introduces Adaptive Dilated Deep Neural Networks (AD-DNN) and Self-Adaptive Tasmanian Devil Optimization (STDO), showcasing their pivotal roles in refining classification capabilities. By incorporating these advanced techniques into the proposed Triplet Deep Learning Framework, the chapter underscores the collaborative benefits of Deep Learning and Explainable AI in improving medical imaging analysis. Performance analysis on the CBIS-DDSM dataset demonstrates the framework's exceptional accuracy and precision, highlighting its potential to significantly enhance early breast cancer detection rates while providing interpretable insights into the decision-making process.

Chapter 8: This final chapter provides a summary of the research, encapsulating the overall results and conclusions drawn from each component of the

study, outlines key contributions, and offers recommendations for future research. It reaffirms the significance of the research findings in the context of breast cancer detection and medical imaging.

The thesis concludes with a comprehensive bibliography containing full citations for all referenced works, encompassing various research papers, articles, and relevant literature consulted throughout the study. Additionally, a list of the author's publications related to the research topic is included, highlighting their contributions to the field.

Chapter 2

Review of Literature

2.1 Introduction

This chapter presents an in-depth literature review of preprocessing, segmentation, feature extraction, classification methods and multiple obstacles related to mammographic image analysis. The emphasis is given on including several features into the process of learning that would enhance the preciseness and dependability of breast cancer classification frameworks.

Mammograms, which are X-ray images of the human breast, serve a critical purpose in the detection and diagnosis of alterations in breast tissues. Regular screening mammography is recommended for asymptomatic women, particularly after reaching a specific age. These mammograms provide crucial insights that aid breast radiologists in identifying suspicious lesions, aiming to detect these abnormalities before they progress to late-stage cancer, a phase that poses significant challenges for effective treatment and recovery. The critical review emphasizes the significant strides made in mammography screening and systemic treatment, marking notable advancements in both areas.

Since its inception in 1956, mammography screening was initially introduced for the "detection of early cancer of the breast" [Gold et al., 1990]. During the 1970s, multiple randomized controlled trials provided substantial evidence confirming the positive impact of mammography screening on reducing breast cancer mortality [Elmore et al., 2005]. This benefit primarily applies to women between the ages of 50

to 74 years and is most pronounced, estimated at around 30%, within the age bracket of 60 to 69 years [Hubbard et al., 2011][Schousboe et al., 2011]. The overarching goal of mammography screening process is to decrease breast cancer-specific mortality. This is achieved by minimizing the risk of diagnosing breast cancer at an advanced stage and by optimizing the efficacy and safety of anticancer treatments, thereby positively influencing prognosis. The introduction of mammography involved x-ray units exclusively designed for the purpose, utilizing x-ray film alongside paired fluorescent screens to capture images, known as screen-film mammography. However, starting in the early 2000s, a gradual transition commenced towards digital mammography units, supplanting the conventional screen-film approach [Song et al., 2019][Souza et al., 2013][Nelson et al., 2009][Mandelblatt et al., 2016][Pisano et al., 2005][Nelson et al., 2016].

Mammography's diagnostic accuracy relies on several factors including breast structure, density, and the expertise of the radiologist. Studies indicate that in screening mammography, approximately 70% of missed breast cancers result from misinterpretation, while 30% are due to overlooked lesions. To enhance mammographic examination sensitivity, CAD systems have been developed. By aiding radiologists in mammogram interpretation, CAD systems play a significant role in elevating cancer detection rates. These systems are crucial in the screening process, enabling more accurate analysis and diagnosis. These systems identify suspicious regions such as microcalcifications and masses [Muralidhar et al., 2008][Warren Burhenne et al., 2000][Freer and Ulissey, 2001]. The U.S. Food and Drug Administration approved the first CAD system for mammogram in 1998 [U.S. Food and Drug Administration, 1998][U.S. Food and Drug Administration, 2004].

The essential phases of a typical Computer-Aided Diagnosis (CAD) system, including preprocessing, segmentation, feature extraction, and classification, are developed using a blend of digital image processing and machine learning techniques. The development and improvement of these techniques are of paramount importance in medical imaging, particularly in enhancing the early detection of breast cancer. This can significantly increase the chances of successful treatment, thereby reducing

mortality rates. This literature review will delve into various methodologies, advancements, and challenges in this field, contributing to the broader understanding and ongoing research in the classification breast cancer.

Subsequent sections will present a theoretical analysis and a review of pertinent literature, focusing on the latest and most sophisticated techniques and algorithms which are employed in this research study and applied by researchers in the evolution of each stage of CAD systems.

2.2 Review of Preprocessing Techniques

Preprocessing stands as a pivotal technique in the initial phases of image processing, crucial for augmenting image quality and removing unwanted noise [Bandyopadhyay, 2010]. It involves tasks such as orientation correction, noise reduction, and contrast enhancement to ensure optimal inputs for segmentation methods. The need for effective preprocessing methods is evident from the literature, as they contribute significantly to the success of subsequent segmentation techniques. Eliminating noise is paramount as it aids in intensifying variations across image segments, thus assisting CAD systems in subsequent detection processes and enhancing the accuracy of detection models [Haralick and Shapiro, 1985][Besl and Jain, 1988][Sahoo et al., 1988].

2.2.1 Noise Removal Process

The noise artifacts such as film strips, scratches, image marks, patient identification details, seals, logos, hospital or clinic information, dates, times, as well as various unwanted scanning and tapping artifacts, objects or substances (cloth, button, jewellery, etc.), grid lines, equipment parts, water marks can arise from different stages including image acquisition, transmission, and processing. These artifacts can be caused by a variety of factors, including patient-specific issues, errors made by technologists, problems with the mammography equipment, and issues in the processing phase [Chaloeykitti et al., 2006][Van Ongeval et al., 2008]. As a result,

it becomes challenging for radiologists to distinguish between normal and abnormal tissues, leading to missed cancer diagnoses in some cases.

Majid et al. and colleagues found that 10% to 30% of breast cancers are missed in mammograms, often due to dense breast tissue and other technical challenges. Their study, highlighting the importance of enhanced imaging techniques and detailed analysis, aims to improve cancer detection [Majid et al., 2003]. To address this, image denoising techniques are essential in preprocessing to enhance image quality and assist in accurate diagnosis. These techniques aim to remove unwanted noise and recover images that are as close to the original as possible, which is crucial for effective medical analysis and decision-making. Image Enhancement, noise reduction, edge detection, image segmentation, region of ROI extraction, image registration, morphological operations, standardization and normalization are the crucial preprocessing operations in the mammogram images for enhancing the quality and clarity of the images, which aids in more accurate diagnosis and analysis [Zebari et al., 2019][A and Lakshmanan, 2017][Fu and Mui, 1981][Besl and Jain, 1988][Haralick and Shapiro, 1985][Suradi et al., 2021].

2.2.2 Histogram Equalization

Histogram Equalization (HE) is an image preprocessing technique used to enhance the contrast of images. It functions by uniformly redistributing the gray scale values across the histogram of the image. This approach modifies the pixel intensity values in an image to achieve a more uniform and widespread distribution, leading to improved global contrast. Specifically, in an 8-bit image, which contains 256 different gray levels, HE makes the frequently occurring intensity values more evenly spread out on the histogram. This is particularly advantageous for images where the foreground and background have similar brightness, as it can significantly enhance the visibility of details that might otherwise be obscured due to poor contrast. HE is an essential tool in medical imaging where image clarity and detail are crucial [Ittannavar and Havaldar, 2022]. This approach, although time-consuming, was effective in handling mammographic images with irregular shapes and appearances of

cancerous cells. Langarizadeh et al. demonstrated a positive effect on image quality, highlighting the importance of HE in mammogram image enhancement and illustrates the practical applications and effectiveness of HE in medical imaging [Langarizadeh et al., 2011]. The study by Zhang et al. underscores the role of histogram equalization, particularly contrast-limited adaptive histogram equalization (CLAHE), in enhancing digital mammography. It highlights CLAHE's ability to significantly improve local contrast and edge definition in mammograms, aiding in the effective detection of breast abnormalities [Zhang et al., 2016]. Their finding is pivotal in demonstrating the practical benefits of histogram equalization in medical imaging, especially for early and accurate breast cancer detection. These studies highlight the diverse applications and effectiveness of Histogram Equalization and related techniques in enhancing mammogram analysis.

2.2.3 Otsu's thresholding

Otsu's thresholding operates on the gray level histogram of an image and is particularly effective for bimodal histograms. It seeks the optimal threshold that best separates two distinct classes in the image, aiming to minimize the within-class variance while maximizing the between-class variance. This thresholding technique is especially useful for automatically binarizing grayscale images into foreground and background, leveraging the variances and probabilities of the classes defined by the threshold. Otsu's method is valued for its effectiveness in global automatic thresholding in various image processing applications.

Al-Bayati and El-Zaart reveals that among the tested techniques, Otsu's method and its variants show significant effectiveness in detecting abnormalities in mammogram images, thus underscoring its utility in early breast cancer detection. This research is a crucial reference for understanding the application and impact of Otsu's thresholding in medical imaging [Al-Bayati and El-Zaart, 2013]. Liu et al. presents an algorithm combining iterative Otsu thresholding with mathematical morphological processing to segment pectoral muscles from mammograms. This method aims to reduce false positives in CAD of breast cancer by accurately identifying

and segmenting the pectoral muscle. They demonstrate the algorithm's effectiveness through extensive testing on the MIAS database, highlighting Otsu's thresholding as a critical tool in enhancing the accuracy of breast cancer detection methods [Liu et al., 2012]. We have employed Otsu's thresholding to refine the threshold value to enhance the algorithm's performance in preprocessing phase.

2.2.4 Preprocessing for Deep Learning Based Systems

Preprocessing in mammography is a crucial multifaceted process that plays a pivotal role in enhancing the quality and interpretability of mammographic images. This process involves a series of essential steps designed to refine raw mammographic data, preparing it for subsequent analysis by deep learning models. These preprocessing steps are critical as they directly impact the accuracy, efficiency, and reliability of classification systems in identifying and categorizing breast cancer indicators.

This section explores various preprocessing techniques employed in the proposed deep learning frameworks, emphasizing their vital role in addressing challenges posed by mammographic images. These challenges include low contrast, high noise levels, and varied breast densities. Specifically, we review literature on the impact of preprocessing on different deep learning architectures used in mammography, such as convolutional neural networks (CNNs), and examine how these methodologies have evolved.

A notable contribution to this field is from Ahmed et al., who developed a deep learning-based method for identifying, categorizing, and segmenting malignant regions in mammography. They proposed techniques for noise, artifact, and muscle region reduction, which are known to generate a significant number of false positives. Their preprocessing approach included transforming images into 512x512 patches, enhancing system performance and mitigating resource consumption. They utilized two publicly accessible breast cancer datasets, MIAS and CBIS-DDSM, and applied advanced deep learning-based case segmentation methods like DeepLab and Mask RCNN. This approach notably improved the width within the target's functioning curve, leveraging transfer learning techniques [Ahmed et al., 2020].

Another significant study by Maqsood et al. demonstrates a system based on deep learning that detects using an "end-to-end" learning approach. This method involves an altered contrast enhancement technique to improve the granularity of borders in the original mammography images. It then employs a transferable texture convolutional neural network (TTCNN) to enhance accuracy, including an entropy layer for texture data extraction from the convolutional layer. The TTCNN approach features three separate levels of convolution and a single energy layer. The study examined TTCNN performance using extensive characteristics of CNN models, selecting optimal layers to improve classification precision. The final phase involved combining trait vectors using a convolutional sparse image breakdown strategy and selecting the most effective characteristics through an entropy-controlled firefly technique [Maqsood et al., 2022].

In summary, these preprocessing techniques are instrumental in preparing mammographic data for deep learning algorithms, ensuring that the input images are in an optimal state for effective feature extraction and analysis. The discussed literature underscores the integral role of preprocessing in enhancing the effectiveness of deep learning-based classification systems in mammography, ultimately contributing to more accurate and early detection of breast cancer.

2.2.5 Adaptive Wavelet Filter

Adaptive wavelet filtering is an essential technique for noise reduction and feature extraction in medical imaging, particularly in mammograms. This method leverages wavelet filters to adaptively remove noise while preserving vital features within an image, crucial for accurate medical diagnosis. Recent advancements in wavelet techniques have seen a shift towards adaptive parametrized methods, tailored specifically for certain tasks like mammogram analysis. These approaches, as highlighted in the works of Vrankic and Sersic and Lin, focus on parametric models with minimal parameters to enhance efficiency [Vrankic and Sersic, 2004][Lin, 2020].

Pioneering research in the application of wavelet transform for mammogram processing has been conducted by Strickland and Hahn and Mata et al.. Their

studies explore undecimated transforms and multi-resolution analysis for detecting microcalcifications (MCs) in mammograms [Strickland and Hahn, 1994][Mata et al., 2000]. Further, Wang and Karayiannis provide a comprehensive overview of wavelet theory, particularly emphasizing its application in enhancing MC visibility in mammograms through subband suppression and nonlinear thresholding methods [Wang and Karayiannis, 1998]. The adaptive wavelet filtering approach in the context of MC detection represents a significant evolution in image processing techniques. By leveraging wavelet theory, these methods offer more effective and precise analysis for mammogram image processing.

In addition to these studies, Kavitha et al. introduced a novel tumor detection system using OMLTS-DLCN for analyzing electronic mammograms. This system employs an "Adaptive Fuzzy based median filtering (AFF)" technique to remove distortions from mammography images. Furthermore, they utilized the OKMT-SGO method in the classification of breast cancer. The system also incorporates a "CapsNet-based feature extractor and a BPNN classifier" to identify the presence of breast tumors. The diagnostic efficacy of the proposed OMLTS-DLCN approach was evaluated using the benchmark MIAS and DDSM datasets [Kavitha et al., 2021].

Overall, the adaptive wavelet filter stands out as a sophisticated tool in mammographic image processing. Its ability to adaptively filter noise while preserving essential image features positions it as an invaluable technique in the analysis of mammograms. These studies collectively demonstrate the potential of adaptive wavelet filters in enhancing the accuracy and reliability of breast cancer detection through advanced image processing methods.

2.2.6 Self-Adaptive War Strategy Optimization

The Self-Adaptive War Strategy Optimization (SAWSO) represents a novel and effective approach in the field of mammogram analysis. Inspired by military tactics, SAWSO is designed to adapt and optimize image processing techniques and deep learning model parameters, especially in the context of breast cancer detection. This algorithm is particularly adept at handling the variability and

imbalance commonly found in mammograms, ensuring a more accurate and robust diagnostic process. Its dynamic ability to balance exploring new solutions and exploiting known strategies makes it an invaluable asset in enhancing the overall accuracy of mammography diagnostics.

A significant application of this approach is evident in the work of Madhukar et al.. Their proposed method integrates a ResNet backbone with multi-scale convolution and multi-channel attention mechanisms, marking a substantial advancement in breast cancer detection within Computer-Aided Diagnosis (CAD) systems. A key aspect of this approach is the incorporation of the War Search Optimization (WSO) algorithm. WSO significantly enhances the accuracy of image segmentation, a crucial step in differentiating cancerous tissues across varied datasets. The effectiveness of their method, bolstered by WSO, is validated through metrics such as precision, accuracy, and recall, highlighting WSO's essential role in improving the reliability and precision of breast cancer diagnostics in deep learning-based CAD systems [Madhukar et al., 2023].

Further exploring the potential of WSO, Ayyarao et al. introduces a novel metaheuristic optimization algorithm inspired by ancient war strategies. The efficacy of WSO was rigorously tested on 50 benchmark functions and four engineering problems, demonstrating its superiority in comparison to ten well-established metaheuristic algorithms. The results highlight a commendable balance between the exploration and exploitation stages, a critical aspect of any optimization algorithm. The detailed mathematical modeling and extensive testing of WSO underscore its potential in solving complex engineering problems. While promising, the study suggests the need for further refinement, particularly in adapting the algorithm to specific real-world applications. The future scope of WSO could involve fine-tuning its parameters and strategies for more specialized scenarios, enhancing its applicability and effectiveness in various engineering challenges [Ayyarao et al., 2022].

In summary, the Self-Adaptive War Strategy Optimization and its variants like WSO offer innovative and effective solutions in mammogram analysis. These techniques stand out for their strategic balance in handling data and their adaptability

in optimizing image processing and deep learning models, contributing significantly to the advancements in breast cancer detection and diagnosis.

2.2.7 Geometric Transformations

Geometric transformations play a critical role in the field of deep learning for mammogram image analysis. These transformations are key to addressing the inherent variability in mammogram images, which arises due to differences in breast positioning and size. By applying transformations such as scaling, rotation, and flipping, images are standardized, enabling deep learning models to more effectively recognize patterns and anomalies. This standardization is vital for ensuring accurate diagnoses. Furthermore, geometric transformations are instrumental in augmenting limited medical image datasets. By creating diverse training samples, these transformations contribute to improved model generalization and robustness, making them an indispensable tool in preparing mammogram images for deep learning analysis.

In the realm of data augmentation using geometric transformations, Paschali et al. introduces a novel technique, ManiFool Augmentation. This method optimizes affine geometric transformations to enhance the robustness of deep learning models in medical imaging tasks, including mammogram tumor classification. The ManiFool Augmentation approach significantly improves performance on test data and surpasses traditional augmentation methods in efficacy. This study underscores the potential of geometric transformations in augmenting medical datasets, ensuring better model training and accuracy, especially in critical areas like mammogram analysis [Paschali et al., 2019].

Additionally, the study by Oza et al. investigates into the application of geometric transformations in mammogram analysis, particularly within the context of deep learning-based breast cancer diagnosis. The authors review various geometric methods, such as flipping, rotation, translation, and scaling. They acknowledge the effectiveness of these techniques in enhancing training dataset size and model generalization. However, they also note that these methods have shown limited improvement in model training. The study suggests that further refinement of these

techniques is necessary to better address the unique challenges in mammogram analysis and to improve diagnostic accuracy. This research contributes to the ongoing advancement of image augmentation in the field of medical imaging [Oza et al., 2022].

In conclusion, geometric transformations are essential in the preprocessing of mammographic images for deep learning. They not only help standardize the images for more effective pattern recognition but also augment the datasets to enhance model training and generalization. The insights from Paschali et al. and Oza et al. illuminate the evolving role of these transformations in improving the accuracy and reliability of breast cancer diagnosis through deep learning models [Paschali et al., 2019][Oza et al., 2022].

2.2.8 Image Augmentation

Image augmentation is a pivotal technique in deep learning that significantly enhances dataset size and diversity, particularly in medical imaging. This process involves applying various transformations such as rotation, scaling, and brightness adjustment to existing images. The primary goal of image augmentation is to improve model training by increasing dataset variety, which is especially crucial in fields like medical imaging where datasets can be limited. This technique ensures better model performance and reliability, specifically in disease detection scenarios.

The study by Oza et al. researches into image augmentation techniques for mammogram analysis, with a specific focus on applications in breast cancer diagnosis using deep learning. Their research examines both basic and advanced augmentation methods, highlighting their role in enhancing data diversity and bolstering model robustness against overfitting. The study stresses the significance of augmentation in overcoming dataset limitations and improving the generalization capabilities of models, thus underscoring the critical role of image augmentation in medical imaging, particularly in challenging tasks such as breast cancer detection [Oza et al., 2022].

In addition, Oyelade and Ezugwu explores the effectiveness of traditional data augmentation methods like flipping and rotating images for identifying architectural distortions in mammograms. Their approach significantly improves the performance

of convolutional neural network models, achieving an accuracy of 93.75%. This work exemplifies the value of data augmentation in enhancing deep learning models for medical imaging. It emphasizes how augmentation can help reduce false positives and increase detection accuracy in breast cancer diagnostics [Oyelade and Ezugwu, 2021].

Furthermore, Alkhaleefah et al. investigates the impact of image augmentation on breast lesion classification using transfer learning with a pre-trained VGG-19 model. The study demonstrates that specific augmentation techniques, including rotation, flipping, zooming, and adjustments in brightness and contrast, considerably improve classification accuracy, sensitivity, specificity, and AUC, achieving a final accuracy of 90.4%. This research highlights how carefully chosen augmentation methods can address limitations in breast x-ray image datasets, reducing overfitting and enhancing the overall performance of the model [Alkhaleefah et al., 2020].

In conclusion, image augmentation plays an indispensable role in the realm of deep learning for mammogram analysis. Its ability to expand and diversify datasets is crucial for training effective models, especially in the field of breast cancer detection where data availability and variety are often limited. The contributions from these studies highlight the transformative impact of image augmentation techniques, showcasing their potential in advancing deep learning models for more accurate and reliable medical imaging diagnostics.

2.2.9 Grayscale Conversion

Grayscale conversion is a fundamental preprocessing step in medical image processing and computer vision, particularly relevant in the analysis of medical images such as mammograms. This process involves converting colour images, typically composed of multiple channels like RGB (Red, Green, and Blue), into a single-channel representation in shades of gray. The primary purpose of this conversion is to significantly reduce computational complexity while retaining the essential information necessary for analysis. In medical imaging, where colour often does not provide additional diagnostic value, converting images to grayscale allows for a more efficient and effective focus on structural and textural features of the images.

In the field of deep learning applications for cancer categorization, including breast cancer, Ibrahim et al. provides a comprehensive overview, which contributes to a deeper understanding of the capabilities of deep learning in medical imaging. While this research paves the way for future explorations in specialized image processing techniques, it emphasizes the potential role of grayscale conversion in enhancing the analysis process [Ibrahim et al., 2022a].

Moreover, Oladele et al. introduces a two-stage classification model for breast cancer detection using mammograms. In this study, grayscale conversion is highlighted as a crucial part of the image preprocessing stage. By converting images to grayscale, the research indicates a significant reduction in image dimensions from a 3D array to a 2D array, which simplifies subsequent analysis. This study underscores the importance of grayscale conversion in enhancing the performance of machine learning techniques, leading to more accurate and efficient breast cancer detection [Oladele et al., 2022].

Additionally, Raghavendra et al. offers an insightful review of computer-aided diagnostic systems using thermogram images for breast cancer detection. The paper discusses various methods including segmentation and feature extraction but does not specifically delve into grayscale conversion. It focuses on evaluating machine learning approaches for breast cancer screening using thermography. Although it provides significant insights into the application of advanced technologies in medical diagnostics, the specific impact of grayscale conversion on performance accuracy is not detailed [Raghavendra et al., 2019].

In summary, grayscale conversion is an essential preprocessing technique in the analysis of medical images for breast cancer detection. Its role in reducing computational complexity while preserving necessary diagnostic information makes it a valuable tool in the preprocessing pipeline, especially for machine learning and deep learning applications. The studies reviewed highlight the varied applications and potential benefits of grayscale conversion in enhancing the effectiveness of breast cancer detection methodologies.

2.2.10 Image Normalization

Image normalization is an essential preprocessing step in image processing and deep learning, particularly in the context of mammogram analysis. This technique standardizes the intensity of images by scaling pixel values to a specific range, commonly between 0 and 1 or -1 and 1. The primary purpose of normalization is to ensure consistent data input for machine learning models and to reduce variations caused by differing imaging conditions. It is particularly crucial in medical imaging, where it aids in harmonizing images captured under various conditions, thereby improving the convergence speed of learning algorithms and enhancing the overall performance and accuracy of predictive models.

In the field of breast density evaluation using deep learning, Pérez-Benito et al. demonstrated a fully automated technique, including histogram normalization as a critical phase. The study conducted a multi-centre analysis involving mammograms of 1785 women, categorized by qualified radiologists. The histogram normalization phase played a key role in flattening the distribution difference and was integrated into an estimation framework that obtained separation variables as inherent image characteristics, evaluated against a DICE rating-based error function [Pérez-Benito et al., 2020].

Deng et al. presented an advanced CNN architecture incorporating an SE-Attention strategy for biased feature acquisition. The method was divided into three stages: data enhancement and normalization of breast images, SE-Attention training for feature re-calibration, and constructing auxiliary loss. The study utilized a technique for drawing attention, where the SE-Attention method was employed to acquire focused characteristics, enhancing autonomous breast density diagnosis in mammography [Deng et al., 2020].

Kaur et al. explored breast cancer detection enhancements using mammogram images and a multi-class SVM with deep learning classification. Their methodology included a preprocessing stage for image quality enhancement, crucial for reliable feature extraction and segmentation. The study highlighted the importance of

noise reduction and median filtering in mammography, enhancing the detection of concerning features [Kaur et al., 2019].

Mahmood et al. investigated the use of deep transfer learning for breast cancer detection from mammogram images. The research underscored the critical role of image normalization in preprocessing, demonstrating its impact on the model's ability to accurately classify breast abnormalities. The normalization process ensured data consistency and improved model performance, showing the effectiveness of this approach for future medical imaging diagnostics [Mahmood et al., 2021b].

Lastly, Li et al. focused on the classification of mammogram images for breast cancer detection using deep learning. The study emphasized the significance of zero-mean normalization in the data preprocessing stage. This technique, crucial for reducing the interference of medical images due to uneven light, was shown to enhance the model's training speed and accuracy, further suggesting its potential in medical imaging diagnostics [Li et al., 2019b].

In conclusion, image normalization emerges as a fundamental aspect of the preprocessing pipeline in mammogram analysis for deep learning models. By standardizing image intensities, it plays a pivotal role in enhancing the accuracy and efficiency of breast cancer detection, making it an indispensable technique in the field of medical imaging.

2.3 Review of Segmentation Techniques

Segmentation of mammogram images are critical steps in the CAD systems of breast cancer. Segmentation refers to the process of partitioning a digital image into multiple segments to simplify and/or change the representation of an image into something more meaningful and easier to analyze [Michael et al., 2021]. In mammography, segmentation is crucial for accurately identifying and isolating regions of interest, such as potential tumors, from the surrounding breast tissue. Classical Segmentation includes region-based, threshold-based, and edge-based techniques, which are essential for identifying distinct regions in mammograms for initial tumor

detection. Machine Learning Segmentation utilizes traditional algorithms, offering the advantage of adapting to the nuances in medical imaging data, with less reliance on predefined rules. Lastly, Deep Learning Segmentation, which encompasses both supervised and unsupervised learning approaches, is particularly effective at handling complex patterns in large datasets, making it highly suitable for detailed analysis in mammography. Effective segmentation is challenging due to the varied appearance of breast tissues and anomalies, the low contrast of mammograms, and the presence of noise and artifacts [Abdelhafiz et al., 2020]. Subsequent subsections will discuss various segmentation techniques used in this research to enhance accuracy and performance.

2.3.1 Watershed segmentation

Watershed segmentation has emerged as a pivotal technique in the realm of image processing, particularly in the field of mammogram analysis for breast cancer detection. This method, grounded in the topological characteristics of an image, merges edge detection with region-growing methods through a unique flooding simulation process on grayscale images. It aims to delineate watershed lines defining catchment basins, each correlating with a unique minimum in the image, and identifies key point types crucial for comprehensive image analysis.

The study of Gulsrud et al. provides a comprehensive examination of watershed segmentation in mammogram analysis. It underscores the method's efficacy in segmenting the pectoral muscle in mammograms, combining it with Otsu thresholding and regression analysis. This approach is particularly effective in enhancing the accuracy of computer-aided detection systems for breast cancer, reducing false positives as demonstrated through tests on the MIAS database. Such integration highlights the significant role of watershed segmentation in medical image processing [Gulsrud et al., 2005].

Further extending the application of watershed segmentation, Hefnawy discusses its use in mammography for breast cancer detection. The study proposes a hybrid algorithm that combines watershed transform with level set techniques, aimed at improving tumor segmentation. Despite its sensitivity to small image variations,

watershed segmentation is shown to be effective in accurately locating tumors under various conditions, emphasizing its potential in enhancing the accuracy and reliability of breast cancer detection in medical imaging [Hefnawy, 2013].

Similarly, Raj et al. demonstrates the importance of watershed segmentation in mammogram analysis. The study fuses Otsu's multi-thresholding with watershed segmentation to identify suspicious sections in digital mammograms. This methodology, involving multi-level thresholding for preprocessing and marker-controlled watershed segmentation for extracting affected areas, is evaluated using the Haralick texture feature. The results confirm the technique's proficiency in extracting breast malignancies, offering valuable insights into the utility of watershed segmentation in mammogram analysis for breast cancer [Raj et al., 2018].

The research of Sharma et al. focuses on augmenting mammogram segmentation using watershed segmentation combined with K-means clustering. It details a method involving preprocessing and enhancement of the initial region of interest through adaptive histogram equalization, followed by watershed transform and K-means clustering for refined segmentation. This approach effectively addresses the challenge of over-segmentation common in watershed techniques, thereby improving the accuracy of mammogram image analysis [Sharma et al., 2015].

Lastly, Shahin et al. emphasizes the enhancement of breast cancer detection in mammograms through an advanced watershed segmentation technique. Incorporating the Sobel operator for gradient calculation and key point detection, this method utilizes watershed segmentation to identify and segment tumor regions effectively, aiming to improve tumor detection reliability [Shahin et al., 2020].

From these studies, it is evident that watershed segmentation has become indispensable in mammogram analysis, enhancing breast cancer detection. Its integration with various algorithms such as Otsu thresholding, K-means clustering, and gradient calculation methods demonstrates significant improvements in tumor identification and segmentation. These methodologies not only reduce over-segmentation but also improve diagnostic accuracy, highlighting the adaptability of watershed segmentation in various preprocessing and postprocessing stages. The collective find-

ings underscore the indispensability of watershed segmentation in medical imaging, particularly in refining mammogram analysis for early and reliable breast cancer detection.

2.3.2 Pectoral Muscle Removal

The accurate segmentation and removal of the pectoral muscle in mammographic images is a critical step in enhancing the effectiveness of breast cancer diagnosis. Common noises such as the chest wall and pectoral muscle, due to their fixed positions in mammograms, often necessitate removal for consistent analysis. Several methods have been proposed to address this challenge, aiming to improve both accuracy and quality of mammogram analysis.

A novel approach to this issue is the Depth-First Search (DFS) algorithm proposed by Pawar et al. for the removal of the pectoral muscle and artifacts in digital mammograms. This method is crucial for accurate breast density classification, given the similarity between the pectoral muscle and fibro-glandular tissue that can affect density measurements. The DFS algorithm has shown robust performance across different breast density classes, achieving an overall segmentation accuracy of 86.18%, along with impressive Jaccard and Dice similarity coefficients [Pawar et al., 2021].

Similarly, Avuti et al. introduces a novel EMO algorithm for pectoral muscle segmentation from scanned mammograms, employing electromagnetism optimization (EMO). This algorithm has demonstrated its effectiveness through testing on the MIAS database, achieving a segmentation accuracy of 96.58%. The study suggests that future improvements could focus on adapting to new datasets and imaging technologies [Avuti et al., 2019].

Another significant advancement is presented by Rampun et al., which introduces a Convolutional Neural Network (CNN) inspired by the Holistically-nested Edge Detection (HED) network for pectoral muscle segmentation. This method addresses the complex shape variations of the pectoral muscle boundary and shows high segmentation accuracy in over 1000 breast pectoral muscle boundaries in MLO mammograms [Rampun et al., 2019].

Further, Qayyum and Basit proposes a methodology for detecting breast cancer in digital mammograms using SVM. This process includes segmentation, removal of the pectoral muscle, and classification of tissues into normal and abnormal categories. The methodology, validated on the MIAS database, demonstrates a high classification accuracy of 96.55% [Qayyum and Basit, 2016].

Yoon et al. introduces an innovative method for pectoral muscle detection in mammograms, employing morphological methods and the RANSAC algorithm. This research, using the MIAS database, achieves an accuracy of 92.2%, contributing significantly to the field [Yoon et al., 2016].

The study by Shi et al. showcases an automated mammogram image processing pipeline with high accuracy in breast boundary segmentation and calcification detection on the MIAS database. The authors suggest future improvements could focus on refining pixel clustering and line fitting algorithms within the pipeline [Shi et al., 2018].

Wei et al. introduces a novel method for pectoral muscle segmentation in mammograms using a curve detection method. The method achieves high accuracy and reliability, indicating significant advancements in mammographic analysis and CAD systems [Wei et al., 2016].

The segmentation method using contrast enhancement and k-means algorithm, introduced by Slavković-Ilić et al., achieved promising results on the MIAS database. However, the study points to a lower success rate in pectoral muscle segmentation due to variations in intensity and texture [Slavković-Ilić et al., 2016].

Mustra et al. presents a method focusing on scanned mammograms, addressing challenges like artifact removal and breast tissue segmentation. The study shows potential for enhancing the accuracy of CAD systems, although further refinement is needed for different types of mammograms [Mustra et al., 2013].

Shen et al. introduces a method that integrates a genetic algorithm with morphological selection. The study demonstrates an effective approach to mammogram analysis, with potential areas for further refinement [Shen et al., 2018].

A geometric rule-based algorithm is introduced by Taghanaki et al. for

pectoral muscle segmentation in mammograms. The method shows promising results, especially for challenging cases like extremely dense breasts [Taghanaki et al., 2017a].

Hazarika and Mahanta introduce a region-growing based approach for the segmentation of the pectoral muscle in mammograms. This work demonstrates the effectiveness of region-growing techniques for pectoral muscle segmentation [Hazarika and Mahanta, 2018].

Kwok et al. presents an algorithm for segmenting the pectoral muscle in mammograms, facing challenges with very clear or indistinct pectoral muscles. The study underlines the need for further refinement in handling diverse mammographic images [Kwok et al., 2001].

Shinde and Rao introduces a machine learning-based approach for segmenting the pectoral muscle in mammograms. This method achieved a significant acceptance accuracy on the mini-MIAS database [Shinde and Rao, 2019].

The article by Li et al. focuses on a novel method for segmenting the pectoral muscle in mammograms, combining homogeneous texture analysis and intensity deviation. This method achieved an acceptable rate on MIAS and DDSM databases [Li et al., 2013].

The watershed transformation-based method for pectoral muscle segmentation in mammograms, presented by Camilus et al., indicates effective segmentation but suggests further improvements in segmentation accuracy [Camilus et al., 2011].

Lastly, Moghbel et al. provides a comprehensive overview of various image segmentation techniques in mammographic image processing. The review emphasizes the need for advancements and importance of accurate segmentation in CAD systems [Moghbel et al., 2019].

In conclusion, the extensive literature on pectoral muscle segmentation in mammograms encompasses a wide range of techniques, indicating the need for ongoing improvements in accuracy rates. This justifies further investigations into the application of these methods to enhance pectoral muscle segmentation, which is crucial in the accurate diagnosis of breast cancer.

2.3.3 Segmentation for Deep Learning Based Systems

Segmentation plays a pivotal role in mammography by isolating areas of interest, particularly those that may indicate the presence of breast cancer. This section of the literature review investigates into the various deep learning approaches that have substantially enhanced the accuracy of segmentation in mammograms. The effectiveness of segmentation is crucial in addressing specific challenges associated with mammographic analysis, such as the variability in breast densities and the differentiation between benign and malignant features.

This part of the review will explore how advanced segmentation techniques have been instrumental in improving the performance of mammographic classification systems. Emphasis will be placed on how effective segmentation contributes to the early and accurate detection of breast cancer, highlighting its importance in medical imaging. The focus will be on evaluating the impact of state-of-the-art segmentation methods in deep learning, examining how they have overcome traditional obstacles in mammography and contributed to more reliable and precise diagnostics.

Through this exploration, the section aims to illustrate the significant advancements in mammographic segmentation and its vital role in enhancing the accuracy and reliability of breast cancer detection using deep learning technologies.

2.3.4 Enhanced R-CNN

The Enhanced R-CNN, particularly the Modified and Triplet Faster R-CNN models, have made significant strides in mammographic image analysis for breast cancer detection. These deep learning-based object detection approaches have been tailored to recognize and classify medical breast masses with increased accuracy and efficiency.

Zhang et al. utilized a deep learning-related object detection approach, incorporating transfer learning based on the Faster R-CNN network, and explored five feature extractors' impacts on the model. Employing the Digital Database for Screening Mammography (DDSM), their study assessed the algorithm's capabilities

in distinguishing between malignant and benign breasts using ROC trade-off curves [Zhang et al., 2019b].

Al-antari et al. developed a comprehensive CAD system powered by deep learning for identifying breast abnormalities. They utilized a localized deep learning technique known as YOLO for lesion detection, followed by a novel deep network splitting model, the Full-Resolution Convolutional Network (FrCN), for lesion separation. The system also employed traditional deep learning designs like regular feedforward CNN, ResNet50, and InceptionResNet-V2 for classifying observed lesions [Al-antari et al., 2020].

Al-Masni et al. introduced a combined detection system using a deep learning full resolution convolutional network (FrCN) for skin lesion border detection and a CNN classifier for lesion categorization. They employed various renowned classification recurrent neural networks and assessed the model using three different datasets [Al-Masni et al., 2020].

Ragab et al. introduced a new CAD approach that combines feature mining and categorization using deep learning strategies. They conducted four distinct tests to identify the best method, involving fully calibrated and optimized DCNN systems, SVM classifiers with multiple kernel functions, deep feature integration, and PCA for feature compression [Ragab et al., 2021].

Singh et al. described a multi-stage CAD system employing a modified Faster R-CNN detector with an Inception-ResNet-v2 feature extractor and a squeeze and excitation network. This system improved tumor detection and also used a conditional generative adversarial network (cGAN) for tumor segmentation and a CNN for classifying tumor shapes [Singh et al., 2021].

Cao et al. focused on lesion detection in mammograms using a deep learning-based Faster R-CNN model. This model demonstrated high accuracy in detecting various types of lesions, showcasing the potential of Faster R-CNN in medical imaging [Cao et al., 2019].

Harrison and Park highlighted the application of Faster R-CNN in tumor detection in breast histopathological images. They investigated the effects of prepro-

cessing procedures like colour normalization and patching on the model's performance, finding notable improvements in certain scenarios [Harrison and Park, 2021].

Sunardi et al. optimized breast cancer classification using Faster R-CNN by investigating image data segmentation optimization techniques. Their study demonstrated a significant improvement in accuracy rate through the application of various software tools [Sunardi et al., 2023].

In summary, the Enhanced R-CNN models, including the Modified and Triplet Faster R-CNN, have been instrumental in advancing mammographic image analysis for breast cancer detection. These studies demonstrate the models' effectiveness in lesion detection, segmentation, and classification, underscoring the potential of these deep learning approaches in improving the accuracy and reliability of breast cancer diagnostics.

2.4 Review of Feature Selection & Extraction Techniques

Feature extraction and selection are pivotal in mammogram analysis for CAD systems. These processes enhance diagnostic accuracy by isolating key characteristics from complex image data. Feature extraction identifies crucial image aspects like shapes or textures, while feature selection reduces data complexity, improving efficiency and computational resource use. Additionally, these steps boost model performance by avoiding overfitting and aid in the interpretability of the system's decisions, crucial for clinical trust. They also help in adapting to patient variability and provide detailed disease characterization, essential for accurate detection, staging, and monitoring of breast cancer. Overall, these processes are critical for precise, efficient, and reliable medical diagnoses. Optimization is crucial in this phase to determine the most relevant and informative features from the extracted data. This involves reducing the dimensionality of the feature set to improve the efficiency and effectiveness of the classification algorithm. Subsequent subsections will discuss various optimization techniques used in this research to enhance accuracy and performance.

Subsequent subsections will discuss various feature selection and extraction techniques used in this research to enhance accuracy and performance.

2.4.1 Optimization Techniques

Optimization techniques are integral to mammogram analysis, significantly enhancing breast cancer detection. These techniques are crucial for processing mammographic images, as they improve the accuracy and efficiency of tumor identification. This encompasses a range of algorithms dedicated to image enhancement, noise reduction, and accurate segmentation and feature extraction of potential cancerous regions. The value of these optimization methods lies in their ability to provide radiologists with clearer, more accurate images, which is vital for early diagnosis and effective treatment planning. Consequently, optimization emerges as an indispensable component in mammogram analysis, contributing significantly to the advancements in breast cancer diagnostics.

One key aspect of optimization in digital mammography is the spectral shape, referring to the energy distribution in the X-ray beam used for imaging. The study Fahrig and Yaffe investigates into the optimization of spectral shape in digital mammography. This optimization is pivotal in adjusting the energy distribution to enhance image contrast and detail, while also minimizing radiation exposure to the patient. By focusing on the spectral shape, this research addresses a crucial aspect of image clarity essential for accurate breast cancer detection. The optimization of spectral parameters thus plays a significant role in enhancing the effectiveness of mammography as a diagnostic tool [Fahrig and Yaffe, 1994].

Moreover, metaheuristic optimization methods, which are advanced algorithms inspired by natural phenomena, have been gaining prominence in solving complex and challenging optimization problems. These methods, known for their versatility and robustness, are ideal for diverse applications, ranging from engineering to machine learning. Their flexibility is particularly beneficial in handling nonlinear and multi-modal problems [Yang, 2011].

Among these methods, the Harris Hawks Optimization (HHO) and Cuckoo

Search (CS) algorithms stand out. HHO, inspired by the cooperative behavior and chasing style of Harris' hawks in nature, is notable for its efficiency in handling complex, nonlinear, and multi-dimensional optimization problems. It operates through exploration and exploitation phases, effectively navigating through various problem spaces. The CS algorithm, drawing inspiration from the parasitic breeding behavior of cuckoo birds, is known for its global search efficiency, simplicity in implementation, and minimal parameter requirements. These characteristics make CS particularly effective for diverse optimization problems. Both HHO and CS algorithms are valued for their flexibility and robustness, demonstrating their efficacy in various complex optimization scenarios.

In summary, optimization techniques in mammography, including the optimization of spectral shape and the application of metaheuristic algorithms like HHO and CS, play a critical role in the field. They enhance the quality of mammographic images, thereby aiding in the more accurate and efficient detection of breast cancer. These advancements in optimization techniques are vital for improving the diagnostic capabilities of mammography, making them an essential area of study in breast cancer research.

2.4.2 Harris Hawks Optimization

The Harris Hawks Optimizer (HHO) is a nature-inspired, population-based optimization technique that has garnered significant attention in recent years, particularly in the field of mammogram analysis for breast cancer detection. Introduced by Heidari et al., HHO draws inspiration from the cooperative hunting strategy of Harris' hawks, demonstrating its ability to model dynamic patterns and behaviors in optimization tasks. The effectiveness of HHO is proven through its comparison with other techniques on various benchmark and real-world engineering problems, showcasing its utility in complex problem-solving across different fields including engineering and computer science [Heidari et al., 2019].

A notable variant of HHO is presented by Rahul Hans and Kaur, which integrates an opposition-based strategy to enhance the convergence rate and effectiveness

of the original algorithm. This variant is particularly significant for its application in improving machine learning techniques in medical diagnostics. It contributes to the early detection of breast cancer through mammography analysis, emphasizing the adaptability and potential of HHO in medical applications [Rahul Hans and Kaur, 2020].

Further advancing the capabilities of HHO, Kaur et al. introduces the DLHO algorithm, which addresses limitations such as premature convergence and poor crowd diversity found in the original HHO. By integrating dimension learning-based hunting (DLH) with HHO, DLHO improves neighborhood formation and information sharing among search agents. The performance of this enhanced algorithm in breast cancer detection using mammography underlines its robustness and efficiency, suggesting its potential for broader biomedical applications and complex datasets [Kaur et al., 2021].

Another innovative application of HHO is found in image segmentation demonstrated by Rodríguez-Esparza et al. which applies HHO to multilevel thresholding for digital mammograms, showcasing the algorithm's superiority in segmentation quality over other methods. The efficiency and robustness of HHO in this context provide a promising direction for future research in image processing, especially in medical diagnostics [Rodríguez-Esparza et al., 2020].

Similarly, Rodrí¬guez-Esparza et al. focuses on the use of HHO for enhancing breast cancer detection in mammograms. By proposing a multilevel threshold segmentation technique that combines Minimum Cross Entropy Thresholding (MCET) with HHO, the study achieves significant accuracy in identifying regions of interest in mammograms. This suggests promising avenues for further research in medical image processing and early breast cancer detection [Rodrí¬guez-Esparza et al., 2020].

Additionally, Thawkar developed a hybrid algorithm, CSAHHO, combining the Crow Search Algorithm (CSA) and Harris Hawks Optimization (HHO). This algorithm excels in feature selection from mammograms using an artificial neural network (ANN) and classifies masses as benign or malignant using ANN and SVM classifiers. Tested on 651 mammograms, CSAHHO demonstrates high accuracy and

outperforms both the original CSA and HHO algorithms. Its effectiveness is further confirmed through comparisons with other state-of-the-art methods, indicating its potential in enhancing breast cancer detection [Thawkar, 2022].

In summary, the existing literature emphasizes the significance of HHO and its variants in mammogram analysis for breast cancer detection. These studies underscore the development of innovative hybrid optimization techniques, integrating the strengths of HHO with other algorithms to enhance feature extraction and classification accuracy. The adaptability and efficiency of HHO in various aspects of mammogram analysis, from feature selection to image segmentation, highlight its potential as a powerful tool in medical diagnostics and breast cancer detection.

2.4.3 Cuckoo Search Optimization

Cuckoo Search Optimization has emerged as a significant method in advancing breast cancer detection through mammogram analysis. The study of R and Kumar utilizes Cuckoo Search (CS) optimization in conjunction with a multiphase level set approach to address challenges in segmenting mammograms, especially those with low contrast and varying intensity levels. This method demonstrates superior performance over traditional techniques, particularly in segmenting both homogeneous and inhomogeneous regions. Its effectiveness is validated through quantitative measures like Jaccard and Dice coefficients, along with sensitivity, specificity, and accuracy metrics, on the MIAS dataset. The results suggest that this method surpasses classical segmentation methods, indicating its potential for future applications in medical imaging and early breast cancer detection [R and Kumar, 2022].

Further exploring the capabilities of Cuckoo Search Optimization, the study titled "McCulloch's Algorithm Inspired Cuckoo Search Optimizer Based Mammographic Image Segmentation" by Santhos et al. introduces a novel method using McCulloch's Algorithm inspired Cuckoo Search Optimization (MACSO). MACSO, combined with Otsu's method, has been found to be robust for mammogram segmentation, outperforming other nature-inspired algorithms. This research not only enhances mammogram image segmentation but also opens pathways for future advancements

in medical image analysis, underscoring the importance of further exploration of MACSO in various contexts and datasets [Santhos et al., 2020].

S R and Rajaguru proposed a computer-aided approach employing the Cuckoo Search Algorithm (CSA) for breast cancer classification from digital mammograms. Utilizing wavelet-based feature extraction on the MIAS database, the study demonstrates that CSA outperforms the Linear Discriminant Analysis (LDA) classifier, achieving an impressive 97.5% accuracy. These results underscore CSA's potential in medical image analysis and diagnosis, suggesting promising future applications in enhancing the accuracy and efficiency of breast cancer detection methods [S R and Rajaguru, 2019].

Additionally, a hybrid approach that combines a Multi-objective Evolutionary Algorithm (MOEA) with CS for detecting masses in mammograms is presented by Bhalerao and Bonde. This innovative CS-MOEA/DE method integrates nature-inspired cuckoo search with multi-objective optimization using Differential Evolution. Evaluated on both MIAS and DDSM datasets, the method achieves an overall accuracy of 96.74% for 110 images, indicating its superiority over other methods like the Otsu method and Kapur's Entropy. This showcases its potential for enhanced mammogram analysis and breast cancer detection [Bhalerao and Bonde, 2021].

The review of the literature on hybrid segmentation methods highlights the necessity for innovative approaches in this field. This leads to the development of a new hybrid segmentation and classification model, which combines the strengths of Harris Hawks Optimization (HHO) and Cuckoo Search (CS). This model is proposed to address the existing gaps and enhance the efficiency and accuracy of the segmentation and feature extraction processes in mammogram analysis.

2.4.4 Feature Extraction for Deep Learning Based Systems

Feature extraction is a crucial process in deep learning, particularly in mammogram analysis for breast cancer detection and classification. This process involves identifying and isolating relevant features from mammographic images, which is essential for accurate diagnosis. This section of the literature review explores

various feature extraction techniques employed in deep learning and how they have enhanced the performance of classification systems, particularly in distinguishing between benign and malignant lesions.

Vo et al. presented a method for extracting useful visual information for tumor categorization using deep learning models with convolutional layers. This approach demonstrated that deep learning systems could obtain more valuable characteristics than manual feature extraction techniques. Additionally, they proposed a technique to optimize the structure by successively integrating deep learning models into an improved predictor, illustrating its applicability to breast cancer histopathology images [Vo et al., 2019].

Sha et al. developed a comprehensive strategy for locating malignant spots in mammography images. The technique involved visual noise reduction, optimal segmentation using a CNN, a grasshopper optimization algorithm, and optimized feature extraction. This approach was adapted to notable breast cancer databases, and the simulation outcomes were compared with various modern techniques to evaluate the accuracy of the suggested system [Sha et al., 2020].

Xi et al. utilized deep convolutional neural networks (D-CNN) for autonomous feature learning and classifier development. They focused on programming these models on labeled photo patches and then adapting them to function on entire mammography images for localizing anomalies. The study evaluated the classification efficacy of advanced deep convolutional neural networks [Xi et al., 2018].

Feng et al. introduced a Knowledge-driven Feature Learning and Integration (KFLI) system for distinguishing malignant from benign breast tumors using mammogram images. The system employed domain expertise to drive the feature learning process, constructing multiple deep networks to gather different sub-sequence characteristics and integrating these features through an estimation module [Feng et al., 2020].

Furthermore, the literature also explores the role of enhanced R-CNN models in feature extraction. Zhang et al. utilized the Faster R-CNN network for lesion detection in mammograms, exploring the impact of various network feature extractors

[Zhang et al., 2019b]. Al-antari et al. developed a CAD system employing deep learning for breast abnormality identification, including a localized technique known as YOLO and a full-resolution convolutional network (FrCN) for lesion separation [Al-antari et al., 2020]. Ragab et al. introduced a CAD approach using deep learning for feature mining and classification, employing multiple tests to identify the best method, including deep feature integration and SVM classifiers [Ragab et al., 2021].

Singh et al. described a CAD system using a modified Faster R-CNN detector for tumor detection, demonstrating the integration of advanced neural networks [Singh et al., 2021]. Cao et al. and Harrison and Park also highlighted the application of Faster R-CNN in mammogram and breast histopathological image analysis, focusing on the model's performance improvements through preprocessing procedures [Cao et al., 2019][Harrison and Park, 2021]. Sunardi et al. emphasized the optimization of breast cancer classification using Faster R-CNN, showcasing significant improvements in accuracy [Sunardi et al., 2023].

In summary, the feature extraction process in deep learning for mammogram analysis has evolved significantly, with various techniques enhancing the detection and classification of breast cancer. The advancements in automated feature identification, particularly through enhanced R-CNN models and other deep learning approaches, have contributed to more effective and precise breast cancer screening and diagnosis.

2.4.5 Local Binary Pattern

Local Binary Pattern (LBP) is a prominent texture descriptor in image processing and computer vision, widely applied in various domains including medical imaging. LBP operates by comparing each pixel with its neighbors and assigning a binary code that reflects the texture pattern of the original image. Renowned for its simplicity, computational efficiency, and robustness to lighting changes, LBP has been extensively utilized for feature extraction in machine learning and pattern recognition tasks, particularly in mammogram analysis.

Rabidas et al. introduces the novel Discriminative Robust Local Binary Pattern (DRLBP) and Discriminative Robust Local Ternary Pattern (DRLTP) for

classifying mammographic masses. These methods enhance traditional LBP by better discriminating objects against various backgrounds and preserving edge information. DRLBP, in particular, achieved an area under the receiver operating characteristic curve of 0.982, demonstrating its potential in mammogram analysis [Rabidas et al., 2016].

Sri and Gomathi explores the use of LBP and its completed version (CLTP) in breast cancer image classification. The study reveals that CLTP, combined with Support Vector Machine (SVM) classification, yields better accuracy than traditional LBP. This improvement indicates the potential for advanced image processing techniques to enhance breast cancer diagnosis [Sri and Gomathi, 2022].

In the work of Mewada et al., an innovative approach integrates LBP with a Convolutional Neural Network (CNN) for breast cancer classification using histopathological images. This research underscores the efficacy of combining LBP-based texture information with CNN features, resulting in significant performance improvements and an accuracy of 96.46% [Mewada et al., 2021].

George and Zwiggelaar study investigate the effectiveness of various LBP descriptors in classifying breast tissue in mammograms. They assessed different LBP variants like classic LBP, Elliptical LBP (ELBP), and Local Directional Pattern (LDP) against other texture analysis methods. The findings underscored the significance of directional filters and the effectiveness of classification from regions of interest (ROIs) within the fibroglandular disk [George and Zwiggelaar, 2019].

Lastly, Farhan and Kamil focuses on the application of LBP for texture analysis in mammogram classification. Their research demonstrates the method's enhanced sensitivity, specificity, and accuracy using logistic regression classification, highlighting LBP's robustness as a feature extraction method in breast cancer diagnosis [Farhan and Kamil, 2020].

In summary, the Local Binary Pattern and its variants have shown significant promise in mammogram analysis for breast cancer detection. These studies collectively illustrate the sophistication of LBP in extracting nuanced features from mammograms, enhancing the accuracy and reliability of breast cancer screening and diagnosis through

advanced computational techniques.

2.4.6 Fractal Dimension

Fractal Dimension (FD) is a crucial feature extraction technique. It quantifies the complexity of a fractal pattern, which characterizes the roughness and self-similarity of an object. In the context of mammography, FD helps in analyzing the texture of breast tissues, aiding in the distinction between benign and malignant masses. This is particularly relevant as malignant tumors often exhibit more complex and irregular patterns compared to benign ones. Therefore, the application of FD in mammographic image analysis holds significant potential in improving the accuracy of breast cancer diagnosis and in enhancing computer-aided detection systems.

Raguso et al. presents an insightful approach to using fractal dimension in mammography to distinguish between benign and malignant breast masses. The authors report high diagnostic accuracy, indicating the potential for further enhancements in breast cancer diagnosis through this method. This study's findings suggest a significant scope for future advancements in computer-aided diagnosis and the need for further research in feature selection and classification methods [Raguso et al., 2010].

The study by Tourassi et al. focuses on the application of fractal analysis in detecting architectural distortion (AD) in mammograms. The research uses the circular average power spectrum method to calculate fractal dimension (FD) and employs receiver operating characteristics (ROC) analysis to evaluate its effectiveness. The study shows that the average FD of normal regions is significantly higher than that of AD regions, with the best ROC performance reaching 0.89 ± 0.02. The study demonstrates the effectiveness of FD in AD detection and suggests the need for further research on feature selection, classification methods, and the effect of image acquisition and digitization on FD estimates [Tourassi et al., 2006]. Dobrescu et al. presents a study on using fractal measures for diagnosing breast cancer from mammograms. The research involves a morphological study of mammographic images, focusing on differentiating between benign and malignant tumors. The study employs fractal

dimension, computed using the box-counting algorithm, and lacunarity, to analyze the mammogram textures. The results suggest that while the fractal dimension alone is insufficient for differentiation, its combination with lacunarity proves effective. This study indicates the potential of fractal measures as significant tools in breast cancer diagnosis, highlighting the need for further research to enhance accuracy and effectiveness [Dobrescu et al., 2013].

The article "A New Approach for Mammogram Image Classification Using Fractal Properties" by Don et al. introduces a novel method for classifying mammogram images based on fractal features. The study focuses on utilizing Fractal Dimension (FD) and Fractal Signature (FS) for image classification. A neural network and K-Means algorithm were used for classification and achieved a high performance rate. The study demonstrates the potential of fractal properties in mammogram image classification, suggesting that further improvements could be made in feature selection and classification techniques for even higher accuracy[Don et al., 2012].

A study by Rangayyan and Nguyen examines the use of fractal analysis in differentiating breast masses in mammograms. The study uses four methods to calculate the fractal dimension of breast mass contours, including both 1D and 2D representations. It demonstrates that fractal dimension, particularly when combined with the shape factor fractional concavity, enhances the accuracy of classifying breast masses as benign or malignant. The highest performance achieved was an area under the ROC curve of 0.93. The study emphasizes the potential of fractal analysis in breast cancer diagnosis and suggests further research to refine these methods for improved diagnostic accuracy [Rangayyan and Nguyen, 2007].

Shanmugavadivu et al. presents a novel approach to analyze digital mammograms using fractal dimensions. The research introduces a method called Fractal Hurst based Mass Segmentation for Temporal Mammograms (FHMST) to detect and segment masses in mammograms. The study focuses on temporal analysis, examining changes over time in mammograms. The methodology employs fractal dimension and fractal Hurst measures for efficient detection and segmentation of masses. The authors emphasize the potential of this approach in enhancing the accuracy of breast

cancer diagnosis. However, they suggest further research is needed to improve the precision of fractal dimension-based analysis and to develop more comprehensive diagnostic tools [Shanmugavadivu et al., 2016].

Nam and Choi presents a study on enhancing mammogram images and analyzing them using fractal dimensions in the article "A Method of Image Enhancement and Fractal Dimension for Detection of Microcalcifications in Mammogram". The research focuses on detecting microcalcifications in mammograms, a key indicator of breast cancer. The authors employ image enhancement techniques to improve image quality and then use fractal dimensions to analyze the roughness and irregularity of images, which can indicate the presence of microcalcifications. The study concludes that calculating fractal dimensions can aid in the early detection of breast cancer, suggesting the potential for these methods in diagnostic procedures. However, the authors note the need for further development in this approach to ensure more precise and reliable results [Nam and Choi, 1998].

Nguyen and Rangayyan investigates the use of fractal analysis for classifying breast masses in mammograms. The study applies box-counting and ruler methods to compute the fractal dimension of breast mass contours. Notably, the ruler method applied to two-dimensional contours achieved a high classification accuracy, with an area under the ROC curve of 0.946. The findings suggest that fractal dimension is a promising feature for distinguishing benign and malignant masses, although further research is needed to refine these techniques for enhanced diagnostic accuracy [Nguyen and Rangayyan, 2005].

Zebari et al. presents an innovative method for classifying mammogram images using multi-fractal dimensions. Their approach combines wavelet transform and machine learning for noise reduction and feature extraction. They propose a new multi-fractal dimension (M-FD) technique for feature extraction, and utilize a genetic algorithm for feature selection. The study demonstrates promising results in breast cancer detection, showing potential for future improvements and research in image processing and machine learning applications in medical diagnostics [Zebari et al., 2021].

Caldwell et al. explores the use of fractal dimension to characterize mammographic parenchymal patterns. The study aims to provide a quantitative, observer-independent method for characterizing these patterns. It evaluates the correlation between classifications made by a fractal-based system and those by radiologists. The research indicates potential use of fractal dimension in assessing risk for breast cancer and in mammographic screening programs, though further development and validation are necessary [Caldwell et al., 1990].

The collective review on fractal dimension in mammography highlights its potential in breast cancer diagnostics, yet underscores the need for continued advancements in methodology for greater accuracy.

2.4.7 Gray-level difference statistics

Gray-level difference statistics (GLDS) is a method used in image processing to analyze the texture of an image. It focuses on the statistical distribution of gray-level differences between pairs of pixels at specific distances and orientations. This technique is particularly valuable in medical imaging, where it can help in identifying patterns or anomalies in tissues, enhancing diagnostics. GLDS is effective in capturing local variations in pixel intensity, making it a robust tool for texture analysis. Its application extends across various fields, contributing significantly to automated image analysis and interpretation.

Chandy et al. introduces a gray level statistical matrix method for extracting texture features in mammograms. This method, aimed at improving content-based mammogram retrieval, demonstrates a high mean precision rate of 85.1%. The study underscores the effectiveness of the proposed approach in mammogram retrieval but suggests that further research and development are needed to optimize texture feature extraction and improve retrieval performance in different datasets [Chandy et al., 2014].

Mohd Khuzi et al. presents a method for identifying masses in mammograms using gray level co-occurrence matrices. This study, conducted at Multimedia University in Malaysia, focuses on differentiating between mass and non-mass tissues

in mammograms. It demonstrates a promising receiver operating characteristics (ROC) curve area of 0.84 for Otsu's method, 0.82 for thresholding method, and 0.7 for K-mean clustering. The authors suggest that the simplicity of their approach reduces computational time, making it suitable for real-time breast cancer diagnosis systems, but they also acknowledge the need for further improvements to enhance accuracy and reliability [Mohd Khuzi et al., 2009].

Dhawan et al. delves into the use of gray-level image structure features for analyzing microcalcifications in mammograms. The study introduces a novel approach that includes second-order histogram statistics and wavelet decomposition-based features for this purpose. While the method showed promise in identifying microcalcifications, the authors note the necessity for ongoing research and enhancement of these techniques to ensure more accurate and reliable diagnostic processes [Dhawan et al., 1996]. The analyses of various studies on gray-level difference statistics in mammography emphasize its effective role in texture analysis and mass identification, offering a promising tool for early breast cancer detection. However, there is a unanimous agreement on the necessity for further refinement and research to enhance the accuracy and reliability of GLDS methods in medical imaging.

2.5 Review of Classification Techniques

Classification involves categorizing these segmented regions into benign or malignant categories based on their features. This is typically achieved through various machine learning algorithms that analyze characteristics such as shape, size, texture, and density of the segmented regions [Šerifovic-Trbalić et al., 2014]. Classification is a vital step in providing a preliminary diagnosis, assisting medical professionals in making informed decisions.

Classification in mammogram analysis using deep learning models is a critical step where extracted features are interpreted to differentiate between benign and malignant findings. This section of the literature review examines various methodologies and algorithms that have been instrumental in achieving accurate and efficient

classification in mammography. It highlights how these systems are trained to recognize patterns indicative of breast cancer, addressing challenges such as varying image qualities and ambiguous cases. The focus is on the advancements in deep learning that have significantly improved the precision and reliability of breast cancer diagnosis through mammography. Subsequent subsections will discuss supervised learning-based Support Vector Machine (SVM) Classifier and deep learning-based classification techniques used in this research to enhance accuracy and performance.

2.5.1 Multi-Kernel Based Support Vector Machine Classifier

The Multi-Kernel Based Support Vector Machine (MKSVM) represents a significant evolution in the field of machine learning, particularly for classification and regression tasks. Building on the foundation laid by the traditional SVM, which was a substantial innovation introduced by Boser et al., MKSVM distinguishes itself by employing multiple kernel functions instead of just one. This advancement enhances MKSVM's capability to effectively handle complex and diverse data patterns [Boser et al., 1992].

Unlike its predecessor, MKSVM amalgamates various types of kernel functions, such as linear, polynomial, and radial basis functions. Each kernel type is adept at capturing different characteristics of data, making MKSVM particularly effective in modeling complex, nonlinear relationships. This flexibility is crucial in advanced applications like image and speech recognition, bioinformatics, and natural language processing. MKSVM also employs regularization strategies to prevent overfitting, ensuring robust generalization to new data. The success of MKSVM lies in the careful selection and optimization of these kernels' weights, tailored to the specific dataset, thereby enhancing its efficacy in handling high-dimensional and intricate data structures.

In the domain of medical diagnostics, MKSVM has shown promising results, especially in breast cancer detection and classification. Brata Chanda and Kumar Sarkar reports over 80% accuracy in linear classification using MKSVM for categorizing mammogram images into malignant or benign tumors. This underscores the

efficiency of MKSVM in tumor detection and highlights the importance of advanced computational techniques in medical diagnosis [Brata Chanda and Kumar Sarkar, 2018].

Further exploring the potential of MKSVM, de Lima et al. investigates its application in detecting and classifying mammographic lesions. The study combines multi-resolution wavelets and Zernike moments for feature extraction, utilizing modified kernel SVM and Extreme Learning Machine (ELM) networks for classification. The method is noted for its potential to significantly reduce learning time compared to other state-of-the-art methods, emphasizing the need for ongoing research to enhance the accuracy and efficiency of these methods in medical diagnostics [de Lima et al., 2016].

Additionally, Jothilakshmi and Raaza presents a method for detecting and classifying mass abnormalities in digital mammogram images using a Multi-Support Vector Machine classifier. This approach includes region-based segmentation and texture analysis using Gray Level Co-Occurrence Matrices (GLCMs). The study indicates a need for further improvements in feature extraction and classification algorithms, with a future scope that includes refining the model for better accuracy and reducing misclassification [Jothilakshmi and Raaza, 2017].

In summary, the MKSVM, with its integration of multiple kernels and advanced computational techniques, offers a powerful tool for medical image analysis, particularly in breast cancer detection. The continuing evolution and application of MKSVM in medical diagnostics demonstrate its potential to significantly contribute to the accuracy and efficiency of breast cancer detection methods.

2.5.2 Deep Learning Based Frameworks for Classification Systems

The advent of deep learning has revolutionized mammography, a critical component in breast cancer screening. Traditional methods of mammogram analysis, often manual and time-consuming, are being significantly enhanced by deep learning technologies. This section explores into the impact of these advancements, particularly

highlighting the role of Convolutional Neural Networks (CNNs). CNNs, with their advanced neural network architectures, have the capability to automatically extract features from mammograms with high precision, thus significantly enhancing the detection and classification of breast cancer.

One of the key contributions of deep learning frameworks in mammography is the improved accuracy in distinguishing between benign and malignant lesions. This not only aids in early detection but also plays a crucial role in reducing false diagnoses. This literature review encompasses the latest developments in deep learning approaches for mammographic image classification, emphasizing their transformative potential. By exploring these advancements, this section aims to provide insights into how deep learning is paving the way for future innovations in breast cancer screening and diagnosis.

Al-Antari et al. developed a unified CAD system using deep learning for diagnosing breast lesions, implementing a YOLO detector for tumor identification and three deep learning classifiers for categorization. The system was tested on digital X-ray mammogram datasets, showcasing its effectiveness in classification [Al-Antari et al., 2020].

Alam et al. conducted a segmentation-based analysis of breast cancer surveillance and detection. Employing a sophisticated semantic classification algorithm and a D-CNN, the study evaluated different models on a dataset of 309 patients, enhancing classification outcomes [Alam et al., 2023].

Al-Masni et al. suggested an automated diagnostic method using structural deformation and deep learning. Their mammography classification architecture, tested on three datasets, used machine vision and CNNs to categorize architectural distortion ROIs into benign and malignant classes [Al-Masni et al., 2020].

Mahmood et al. proposed a technique using ConvNet for differentiating suspicious and normal areas in mammography. They conducted experiments using end-to-end trained DCNNs and SVMs, resulting in outstanding accuracy and demonstrating the effectiveness of deep convolutional neural networks in classification [Mahmood et al., 2021a].

Wang et al. explored a breast CAD technique combining features with deep CNN characteristics. The study presented a recognition technique using CNN deep features and unsupervised ELM clustering, creating a classifier for differentiating breast tumors [Wang et al., 2019].

Duraisamy and Emperumal introduced a deep learning-driven system for mammogram analysis. Their approach involved deep learning algorithms, level set methods for feature extraction, and a multifaceted-valued relaxation network classifier for enhanced classification precision [Duraisamy and Emperumal, 2017].

Salama and Aly developed a new paradigm for image classification and segmentation. They utilized multiple algorithms for categorizing breast cancer images and a customized U-Net for segmenting breast areas, demonstrating improved detection precision with varying mammography views [Salama and Aly, 2021].

Al-Masni et al. proposed a YOLO-based CAD system for identifying and categorizing masses within the same architecture. Their system included preprocessing, feature extraction using deep convolutional networks, mass detection, and categorization using fully connected neural networks (FC-NNs) [Al-Masni et al., 2018].

Agnes et al. created the Multiscale All Convolutional Neural Network (MA-CNN) to assist in the identification of breast tumors. The MA-CNN classified mammographic images into typical, malignant, and benign categories, showing the efficacy of multiscale filters in enhancing classification system reliability [Agnes et al., 2020].

Li et al. introduced an upgraded DenseNet neural network model for the categorization of mammography images. This approach involved preprocessing, regularization, and the use of a DenseNet-II neural network, enhancing the accuracy and precision of malignant and benign image classification [Li et al., 2019a].

Saffari et al. aimed to create a fully automated breast tissue classification and segmentation system using advanced deep learning techniques. Their approach utilized cGAN for segmenting dense regions in mammograms and a CNN for categorizing mammograms based on BI-RADS calibration, employing the INbreast dataset for validation [Saffari et al., 2020].

In conclusion, the classification phase in mammogram analysis using deep learning has seen substantial advancements. These studies collectively highlight the transformative impact of various deep learning technologies in medical imaging, significantly enhancing the accuracy and reliability of breast cancer screening and diagnosis.

2.5.3 Autoencoder

Autoencoders have become increasingly significant in mammogram analysis within the field of deep learning. They are primarily utilized for feature extraction and image reconstruction, effectively compressing mammographic images into a lower-dimensional space. This compression is essential for enhancing the detection of anomalies by highlighting critical features, particularly useful in identifying subtle patterns indicative of breast cancer. Additionally, deep learning autoencoders aid in denoising mammograms, thereby improving image clarity for more accurate diagnoses.

Ghosh et al. introduced a deep convolutional autoencoder-based approach for noise removal in mammograms, employing a total variational multi-norm loss function for mammogram restoration. This autoencoder restored structural details while reducing noise more effectively than other methods, indicating potential for further optimization in medical imaging [Ghosh et al., 2022].

Naderan and Zaychenko developed a convolutional autoencoder to simplify breast cancer detection models. By training various autoencoder models with different architectures, they achieved significant accuracy in reconstructing original images from noise-added inputs. Their approach highlighted the autoencoder's efficiency in handling large datasets and its capability as an unsupervised model, contributing to the advancement of breast cancer detection techniques [Naderan and Zaychenko, 2020].

Wang et al. focused on evaluating deep learning models for discriminating breast lesions with microcalcifications. They found that the deep learning model exhibited superior accuracy compared to traditional methods, demonstrating the clinical value of these models in the early detection and treatment of breast cancer

through mammogram analysis [Wang et al., 2016].

Selvathi and Poornila presented an automated system for breast cancer detection using deep learning techniques including CNNs, sparse autoencoders (SAE), and stacked sparse autoencoders (SSAE). Their findings indicated that SSAE outperformed other methods, underscoring the need for robust and efficient non-invasive cancer detection systems and highlighting the potential of deep learning in enhancing diagnostic accuracy [Selvathi and Poornila, 2018].

Taghanaki et al. proposed a novel multi-objective optimization of deep autoencoder networks. This approach optimized mean squared reconstruction error and mean classification error, demonstrating the potential of deep learning and multi-objective optimization in medical imaging, particularly in mammography classification [Taghanaki et al., 2017b].

In conclusion, autoencoders in deep learning have proven to be a transformative tool in mammogram analysis for breast cancer screening. Their application in feature extraction, image reconstruction, and noise reduction signifies a crucial advancement towards more sophisticated, AI-driven diagnostic tools in medical imaging. These studies collectively highlight the effectiveness and potential of autoencoders in improving the accuracy and reliability of breast cancer diagnosis.

2.5.4 Long Short-Term Memory Model

Long Short-Term Memory (LSTM) models, a subset of recurrent neural networks, are increasingly recognized for their effectiveness in mammogram analysis within deep learning frameworks. LSTMs excel in processing sequential data and learning long-range dependencies, a capability that is crucial in medical image analysis. This is particularly relevant in mammogram analysis, where understanding the context and sequence of images or features is vital for accurate diagnosis. The application of LSTM models in this field signifies a notable advancement in leveraging deep learning for precise medical imaging analysis.

Li et al. conducted a study focusing on the automatic classification of breast masses in mammograms. They proposed a two-view mammogram classification

model that integrates Convolutional Neural Networks (CNN) with Recurrent Neural Networks (RNN), specifically using the Gate Recurrent Unit (GRU) structure. The model employs a modified ResNet for feature extraction from craniocaudal and mediolateral oblique views of mammograms. This integration of CNN and RNN models led to significant improvements in classification accuracy, recall, and area under the curve (AUC), demonstrating the model's effectiveness in mammogram analysis for breast cancer detection. This study presents an innovative approach by combining the strengths of CNN and RNN to enhance medical image analysis [Li et al., 2021].

Another study by Li et al. examines the use of Long Short-Term Memory (LSTM) networks in predicting breast cancer risks from mammogram screenings over multiple time points. The study reveals that LSTM classifiers, informed by deep-learning-extracted or radiomic features, show enhanced performance compared to assessments at single time points. This approach highlights the importance of tracking changes in breasts over time, including in unaffected breasts, in identifying cancer risks. The use of LSTM models in this context underscores their potential for developing more accurate and timely breast cancer detection methodologies [Li et al., 2023].

In summary, the application of LSTM models in mammogram analysis represents a significant step forward in the field of medical imaging. These models' ability to process and learn from sequences of mammographic images or features has the potential to greatly enhance the accuracy and reliability of breast cancer detection and diagnosis. The studies discussed illustrate the innovative use of LSTM in combination with other deep learning techniques, showcasing the potential of these models in advancing breast cancer diagnostics.

2.5.5 Enhanced Deep Neural Networks

Deep Neural Networks (DNN) are emerging as critical tools in mammogram analysis, significantly improving the accuracy and efficiency of breast cancer detection and classification. This section explores various advancements and applications of

DNN in the realm of medical imaging.

Chakravarthy and Rajaguru introduced an upgraded deep feature-based technique using a crow-search optimized extreme learning machine (CS-ELM). They focused on differentiating typical and unusual mammogram data and classifying the abnormal severity as benign or malignant. Deep features extracted from ResNet-18 were combined with the proposed ICS-ELM algorithm and compared to traditional ELM, PSO optimized ELM, and crow-search optimized ELM, providing empirical insights into mammogram analysis [Chakravarthy and Rajaguru, 2022].

Frazer et al. explored the application of deep neural networks in detecting breast cancer using mammograms. Various DNN models were assessed, showing notable performance with an AUC of 0.8979 and an accuracy of 81.78%. The study highlighted the potential of DNN in breast cancer screening, suggesting future enhancements through exploring diverse models and data-processing strategies [Frazer et al., 2021].

Al-antari et al. proposed an integrated CAD system utilizing deep learning for detecting and classifying breast lesions in mammograms. Employing the YOLO detector and modified deep learning models like ResNet-50 and InceptionResNet-V2, the study achieved high detection accuracies and F1-scores, underlining the potential for future improvements in CAD systems through advanced deep learning techniques [Al-antari et al., 2020].

Escorcia-Gutierrez et al. presented an advanced CAD system using mammogram images. This system utilized ResNet 34 and Wavelet Neural Network (WNN) for feature extraction and classification, enhanced by a chimp optimization algorithm for hyperparameter tuning. The promising results in accuracy and efficiency suggested significant potential for clinical applications and future advancements in deep learning for medical diagnostics [Escorcia-Gutierrez et al., 2022].

Kavitha et al. introduced a novel deep learning model for breast cancer diagnosis using mammograms. The model integrated an Optimal Multi-Level Thresholding-based Segmentation with a deep learning-enabled Capsule Network (OMLTS-DLCN). Employing techniques like Adaptive Fuzzy based median filtering for preprocessing,

the model demonstrated high accuracy rates on Mini-MIAS and DDSM datasets, indicating its effectiveness and potential for further refinement in medical imaging [Kavitha et al., 2022].

Wang and Yang introduced a DNN model to address false positives in detecting microcalcifications in mammograms. By incorporating local image features and surrounding tissue context, the DNN model showed improved performance, pointing towards a promising future for enhancing mammogram analysis accuracy using DNNs [Wang and Yang, 2018].

In summary, DNNs in mammogram analysis represent a crucial advancement in medical imaging. These studies illustrate the effectiveness of DNN in enhancing breast cancer detection, with a focus on accuracy, precision, and the potential for integration into clinical practice. The use of advanced algorithms and optimization techniques in these models underscores their significant role in transforming breast cancer diagnostics.

2.5.6 Gradient-weighted Class Activation Mapping

Gradient-weighted Class Activation Mapping (Grad-CAM) is a crucial visualization technique in deep learning, particularly within Convolutional Neural Networks (CNNs). This technique plays a significant role in enhancing the interpretability of CNN models by providing visual explanations for their decisions. Grad-CAM works by highlighting the important regions in an input image that influence its classification, thereby offering insights into the model's reasoning process. This is especially beneficial in tasks such as image classification, object detection, and segmentation. Grad-CAM is instrumental in improving model transparency and aiding in the debugging process, allowing researchers and practitioners to identify potential biases or errors in the learning process of the model.

Prodan et al. conducted a study on the application of deep learning techniques in mammography analysis, focusing on improving the efficiency of evaluation processes. The research utilized multiple models, including ViT designs and CNN, on a publicly accessible dataset. A key aspect of their approach was a data enhancement strategy

based on simulated images to increase the efficacy of the systems. Additionally, the study employed understandable AI methods to accurately interpret the decision-making process of the framework [Prodan et al., 2023].

Selvaraju et al. introduced Grad-CAM, a technique that enhances the transparency and interpretability of CNNs. Grad-CAM provides visual explanations for CNN decisions by underscoring the influential regions in images that lead to specific classifications. This method is adaptable to various CNN architectures without the need for retraining or architectural changes. The technique has shown effectiveness in tasks such as classification, captioning, and Visual Question Answering (VQA), surpassing existing methods in weakly-supervised localization tasks. Furthermore, it offers valuable insights into model failure modes and dataset biases, highlighting the potential of Grad-CAM in making deep learning models more reliable and comprehensible for practical applications [Selvaraju et al., 2017].

In conclusion, Gradient-weighted Class Activation Mapping is a transformative tool in the field of deep learning, offering significant contributions to the interpretability and transparency of CNN models. The studies discussed herein demonstrate the effectiveness of Grad-CAM in providing visual explanations for model decisions, thereby enhancing our understanding of deep learning models and their application in tasks like mammogram analysis. The integration of Grad-CAM into deep learning models presents a vital step towards making these models more understandable and reliable for use in practical and clinical settings.

2.6 Performance Evaluation Metrics

Performance evaluation metrics are essential for assessing the effectiveness of CAD systems, particularly in the context of breast mass classification. These metrics allow for a comparative analysis of different algorithms, facilitating the selection of the most suitable one for specific tasks. The fundamental definitions relevant to these metrics include [van Stralen et al., 2009]:

True Positive (TP): This is an outcome where the CAD system correctly

identifies a positive case (e.g., presence of a breast mass).

False Positive (FP): This occurs when the CAD system incorrectly identifies a case as positive (e.g., marking a healthy tissue as a breast mass).

True Negative (TN): This is an outcome where the CAD system correctly identifies a negative case (e.g., recognizing healthy tissue as normal).

False Negative (FN): This happens when the CAD system fails to identify a positive case, incorrectly marking it as negative (e.g., missing a breast mass).
Based on these definitions, several key performance metrics are used:

Sensitivity (or Recall): This metric measures the proportion of actual positive cases (TPs) correctly identified by the CAD system. It is calculated as:

$$\text{Sensitivity} = \frac{TP}{TP + FN}$$

High sensitivity indicates the system's effectiveness in identifying disease presence.

Specificity: This represents the proportion of actual negative cases (TNs) correctly identified. It is calculated as:

$$\text{Specificity} = \frac{TN}{TN + FP}$$

High specificity shows the system's ability to correctly identify normal or negative cases, reducing false alarms.

Accuracy: This is the ratio of correctly identified cases (both TPs and TNs) to the total number of cases. Calculated as:

$$\text{Accuracy} = \frac{TP + TN}{TP + FP + TN + FN}$$

It provides an overall measure of the system's performance. High accuracy means the CAD system is generally correct in its classifications.

Apart from these, other metrics are also important:

Precision (or Positive Predictive Value): This measures the proportion of positive identifications that were actually correct. It is calculated as

$$\text{Precision} = \frac{TP}{TP + FP}$$

F-Measure (F1 Score): This is the harmonic mean of precision and sensitivity, providing a balance between the two. It is particularly useful when there is an uneven class distribution. Calculated as

$$\text{F1 Score} = 2 \times \frac{\text{Precision} \times \text{Sensitivity}}{\text{Precision} + \text{Sensitivity}}$$

Signal to Mean Square Error (SMSE): It is a ratio that compares the power of the signal to the mean square error, commonly used in signal processing.

$$\text{SMSE} = \frac{\text{Signal Power}}{\text{MSE}}$$

where $\text{MSE} = \frac{1}{N}\sum_{i=1}^{N}(x_i - \hat{x}_i)^2$, x_i is the original signal, $\hat{x}_i$ is the estimated signal, and N is the number of samples.

Root Mean Square Error (RMSE): It is a measure of the differences between values predicted by a model and the values observed.

$$\text{RMSE} = \sqrt{\frac{1}{N}\sum_{i=1}^{N}(x_i - \hat{x}_i)^2}$$

Matthews Correlation Coefficient (MCC): It is a measure of the quality of binary classifications, taking into account true and false positives and negatives.

$$\text{MCC} = \frac{TP \times TN - FP \times FN}{\sqrt{(TP + FP)(TP + FN)(TN + FP)(TN + FN)}}$$

Negative Predictive Value (NPV): It is the proportion of negative results in a statistical test that are true negative results.

$$\text{NPV} = \frac{TN}{TN + FN}$$

False Positive Rate (FPR): It is the proportion of actual negatives that are incorrectly classified as positives.

$$\text{FPR} = \frac{FP}{FP + TN}$$

False Negative Rate (FNR): It is the proportion of positives that yield negative test outcomes.

$$\text{FNR} = \frac{FN}{TP + FN}$$

2.7 Summary

This literature review chapter investigates into the complexities of mammography-based breast cancer detection, emphasizing the key role of deep learning in enhancing medical imaging. It methodically examines key processes in mammogram analysis such as preprocessing, segmentation, feature extraction, and classification. This chapter highlights how advanced computational techniques, including CNN and transfer learning, significantly improve the accuracy and efficiency of tumor detection and classification. These deep learning models adeptly tackle challenges posed by the intricate nature of breast tissues and subtle anomalies, thereby bolstering early detection and precise interpretation of breast cancer. The exploration of various state-of-the-art algorithms showcases the potential of deep learning to revolutionize breast cancer diagnostics. Overall, this chapter underscores the transformative impact of deep learning in mammography, setting a foundation for future advancements in breast cancer screening and diagnosis, ultimately aiming to enhance patient care.

Chapter 3

Mammogram Databases, Views, Classification Standards and Preprocessing Techniques

3.1 Introduction

Mammogram databases play a crucial role as repositories of invaluable data for researchers and medical professionals dedicated to advancing breast cancer detection and diagnosis. These databases are comprehensive collections of mammogram images, each serving as a unique case study that contributes to a broader understanding of breast cancer. They offer a treasure trove of data that is essential for various critical applications in the medical field.

Primarily, these databases are used to train machine learning algorithms, providing a rich source of information for developing systems that can aid in the early detection and accurate diagnosis of breast cancer. By analyzing patterns and anomalies within a vast array of mammographic images, these algorithms can learn to identify signs of cancer that might be challenging for the human eye to detect. This aspect of machine learning is particularly crucial in enhancing the efficiency and accuracy of breast cancer screenings.

Furthermore, mammogram databases serve as vital resources for conducting clinical studies. Researchers utilize this wealth of data to observe trends, compare different cases, and draw meaningful conclusions about breast cancer characteristics

and behaviours. These studies can range from analyzing the effectiveness of various screening methods to understanding the impact of certain risk factors on breast cancer development.

Another significant application of these databases is in improving diagnostic techniques. By providing a diverse range of mammogram images, including those with rare or subtle signs of cancer, these databases enable radiologists and other medical professionals to refine their diagnostic skills. This is particularly important in reducing false positives and negatives in breast cancer screenings, ultimately leading to more accurate diagnoses and better patient outcomes.

3.2 Mammogram Databases

Several mammogram databases are publicly available for research and clinical use, each with its own unique features and data. Some of the well-known mammogram databases are explained below.

3.2.1 Digital Database for Screening Mammography

The Digital Database for Screening Mammography (DDSM) is a significant and pioneering mammography database extensively used in the field of breast cancer research, especially in the development and testing of CAD systems. Released in 1996, it is a collaborative effort involving Massachusetts General Hospital, Sandia National Laboratories, and the University of South Florida's Computer Science and Engineering Department. This database was created to facilitate the study of mammographic image analysis and to support the development of diagnostic algorithms.

The DDSM database contains a substantial collection of digitized screen-film mammograms. A distinctive aspect of DDSM is its historical significance, as it was one of the first large-scale resources made available for mammography research. It includes a variety of cases that represent a wide spectrum of breast tissue types and pathology. The dataset in DDSM is meticulously curated and includes images from about 2,890 cases, amounting to over 11,560 individual mammographic images.

These images cover both cranio-caudal (CC) and mediolateral-oblique (MLO) views. Each case in the DDSM is categorized into one of four distinct groups: malignant, benign, benign without callback, and normal. This classification provides a valuable framework for research and analysis, especially in the development of CAD systems [Logan et al., 2023].

One of the key characteristics of DDSM is the format and quality of the images. The images are based on scanned film mammograms, which were scanned at a resolution of between 42 and 50 microns. The images are stored in a unique file format (LJPG), which requires specific software for decompression and viewing. The use of scanned film images and a less common file format presents certain challenges, particularly when integrating this data with modern digital mammography systems [Heath et al., 2001, 1998].

Despite its extensive use, DDSM has faced criticism and limitations, particularly regarding its image segmentation accuracy and diagnostic categories. The segmentation labeling within the DDSM database has been noted to have inaccuracies, which can limit the utility of the dataset in applications that require precise localization or highly accurate diagnostic information. Furthermore, the ground truth for the benign and normal categories in DDSM is based on radiologist interpretation and follow-up results, which can introduce a degree of ambiguity[Lee et al., 2017].

In addition to its use in developing CAD systems, DDSM has been instrumental in a wide range of studies, including those examining the effectiveness of various image processing and machine learning techniques in mammography. It has been a cornerstone in facilitating the comparison of different methodologies and algorithms due to its standardized format and wide accessibility. Despite its age and some technical limitations, DDSM remains a valuable resource in the field of mammography research. Its comprehensive collection of mammographic images and associated clinical data continue to make it a go-to database for researchers and developers working on improving breast cancer detection and diagnosis.

3.2.2 Curated Breast Imaging Subset of DDSM

The Curated Breast Imaging Subset of DDSM (CBIS-DDSM) is a specialized database designed for the advancement of mammography research, particularly in the development of CAD systems for breast cancer. This database addresses the limitations of the original DDSM, which was challenging to use due to its size, format, and lack of standardization. The CBIS-DDSM provides a more accessible and curated version of the DDSM, enhancing the value of the data for research purposes [Sawyer-Lee et al., 2016].

One of the primary issues with the original DDSM was its use of outdated image formats and tools that were not compatible with modern systems. To address this, the CBIS-DDSM converted the DDSM images from the obsolete lossless JPEG format to 16-bit gray scale TIFF files, and eventually to the DICOM standard format for medical images. This process ensured a lossless transition, preserving the quality and information of the original images. Additionally, Python tools were developed for this conversion to make the process more accessible and user-friendly [Sawyer-Lee et al., 2016].

The CBIS-DDSM also offers significant improvements in terms of metadata and annotations. It provides detailed metadata, including patient age, study dates, scanner details, and resolution. The annotations for abnormalities are more precise, categorizing them as mass or calcification and including Breast Imaging Reporting & Data System (BI-RADS) descriptors. This level of detail is critical for research accuracy and consistency.

Another key feature of the CBIS-DDSM is its handling of questionable cases. A trained mammographer reviewed the dataset to identify and remove images where a mass was not clearly visible, enhancing the dataset's reliability. The CBIS-DDSM also includes both full mammogram images and cropped images focusing on the abnormalities, aiding in specific research tasks that require detailed analysis of abnormal regions.

Furthermore, the CBIS-DDSM is structured with training and testing splits

based on BI-RADS categories, ensuring a balanced level of difficulty across the dataset. This stratification is vital for developing and testing CAD systems in a consistent and standardized manner. CBIS-DDSM represents a significant enhancement over the original DDSM, providing a more accessible, standardized, and detailed dataset for mammography research. Its curated nature makes it a valuable resource for advancing the field of breast cancer detection and diagnosis through computer-aided systems.

3.2.3 Mammographic Image Analysis Society Database

The Mammographic Image Analysis Society (MIAS) Database, managed by a consortium of UK research groups, is a pivotal resource in mammography and breast cancer research. This database, derived from the UK National Breast Screening Programme, includes 322 digitized mammographic films. The digitization process utilized a Joyce-Loebl scanning microdensitometer, ensuring a high-resolution capture of 50 microns per pixel edge, which was later standardized to a 200 micron pixel edge for uniformity, resulting in images of 1024x1024 pixels [Suckling et al., 2015].

A key feature of the MIAS database is the inclusion of radiologist's "truth"-markings, which denote the locations of abnormalities within the mammograms. These annotations are invaluable for research, particularly for developing and benchmarking algorithms in mammographic image analysis. The database, initially available on 2.3GB 8mm (ExaByte) tape, is now accessible in Portable Gray Map (PGM) format via the Pilot European Image Processing Archive (PEIPA) at the University of Essex [Suckling and et al, 1994].

The MIAS database, in particular, stands out for its impact on research and clinical applications. It has become a benchmark in the research community for the development and testing of image analysis algorithms. The detailed annotations and high-quality images also significantly contribute to the understanding and detection of breast cancer.

For comprehensive information and to access the database, the MIAS database page on the University of Cambridge's repository and the Mammographic Image Analysis Society's homepage are excellent resources. This database is a testament to

the collaborative efforts in advancing mammographic image analysis and breast cancer research, offering an invaluable resource for researchers and healthcare professionals. The details of the MIAS database are given in Table 3.1.

Table 3.1: Details of MIAS Database

Property	**Description**
Alternate Name	Mini Mammographic Image Analysis Society database of mammograms
Projections	MLO (Medio-Lateral Oblique)
Digitized Pixel Edge	50 Micron
Reduced Pixel Edge	200 Micron
Gray-level quantization	8 bits
Dimension	1024 x 1024 pixels (256 distinct intensity levels)
File type	PGM (Portable Gray Map)
Clipped/padded?	Yes
Digitizer	Joyce-Loebl microdensitometer SCANDIG-3
Number of studies	161
Number of images	322 (208 - Normal, 63 - Benign & 51 Malignant)
Image View Type	Mediolateral Oblique (MLO) View
Organizer	J Suckling
Co-Workers	S Astley, D Betal, N Cerneaz, D R Dance, S-L Kok, J Parker, I Ricketts, J Savage, E Stamatakis and P Taylor
Truth-Data	C R M Boggis and I. Hutt

3.2.4 INbreast Database

The INbreast database is a significant resource in the field of mammographic image analysis, particularly in the development of CAD systems for breast cancer. This database addresses the need for comprehensive and detailed mammographic

data for research and study purposes. Developed with images acquired at the Breast Centre of Centro Hospitalar de S. João in Porto, Portugal, the INbreast database includes a total of 115 cases, encompassing 410 images. These cases are divided into 90 cases from women with both breasts affected, resulting in four images per case, and 25 cases from mastectomy patients, with two images per case. The database covers a wide array of lesions, including masses, calcifications, asymmetries, and distortions [Moreira et al., 2012].

A distinctive feature of the INbreast database is its construction using full-field digital mammograms, as opposed to digitized mammograms. This approach ensures a higher quality and variability of cases, enhancing its utility for research purposes. Additionally, the database includes accurate contours of lesions, marked by specialists and provided in XML format. This feature is particularly beneficial for algorithms aiming at precise lesion detection and characterization. The INbreast database's comprehensive coverage of various types of lesions, coupled with its detailed annotations and high-quality digital mammograms, makes it a valuable resource for advancing breast cancer imaging research. Its availability to the research community has been instrumental in fostering developments in CAD systems and breast cancer detection methodologies. The INbreast database is accessible and detailed in various scientific publications and projects like the INCISIVE project, funded by the European Union's Horizon 2020 research and innovation program [INbreast, Accessed on: December 16, 2024]. This database represents a critical contribution to the field of medical imaging and breast cancer research, providing a solid foundation for future advancements in diagnosis and treatment methodologies.

3.2.5 OPTIMAM Database

The OPTIMAM Mammography Image Database (OMI-DB) is a significant resource in the field of breast cancer research and mammographic imaging. Developed and maintained through the efforts of the UK national breast screening programme, the database boasts a large collection of mammography images from over 170,000 women. This extensive dataset includes both processed and unprocessed images,

covering various types of mammograms such as 2D and 3D (tomosynthesis) images. These images are biopsy-proven and encompass a range of cases, including malignant, benign, and normal findings. A key feature of the OPTIMAM database is the inclusion of expert-determined ROI annotations, providing valuable data for precise analysis and research applications. Spanning over a decade, the dataset enables researchers to conduct longitudinal studies, offering insights into the trends and developments in breast cancer detection over time [Halling-Brown et al., 2021].

Originally collected as part of the OPTIMAM2 Research Project funded by Cancer Research UK, the data in the OMI-DB is used extensively for research and training in the field. The project primarily aimed to evaluate how various technical factors influence cancer detection in mammographic images. This included studies that mimic breast screening scenarios, using both real patient images and virtual clinical images. A summary of the cases per year included in the OMI-DB can be seen on the table 3.2.

Table 3.2: Data Table of OMI-DB for the Years 2015 to 2020

Category/Year	**2015**	**2016**	**2017**	**2018**	**2019**	**2020**
Normal	19180	52105	60274	19516	20726	60
Benign	418	1283	1520	459	612	0
Malignant Marked	999	981	868	908	834	198
Malignant Unmarked	26	23	16	25	12	1
Interval Cancers	626	564	386	282	76	0
Total	21249	54956	63064	21190	22260	259

This database is not only a tool for academic research but also plays a crucial role in developing and evaluating artificial intelligence tools for automating breast cancer detection. Such advancements are crucial for improving cancer detection rates, reducing unnecessary recalls, and efficiently utilizing resources like radiologists' time. The OPTIMAM database is available for licensing and seeks partnerships with commercial, academic, and non-profit organizations. Its widespread availability

and comprehensive data make it a pivotal resource for advancing mammography technology and breast cancer diagnostics.

3.2.6 Breast Cancer Digital Repository

The Breast Cancer Digital Repository (BCDR) is a substantial resource aimed at developing computer-based detection and diagnosis methods for breast cancer and training medical professionals. It was created through the IMED Project and involves institutions like INEGI, FMUP-CHSJ (University of Porto, Portugal), and CETA-CIEMAT, Spain. The BCDR contains data from 1734 patients, including mammography and ultrasound images, clinical history, lesion segmentation, and pre-computed image descriptors. It is divided into two parts: BCDR-FM (Film Mammography-based Repository) and BCDR-DM (Full Field Digital Mammography-based Repository), both providing valuable data for breast cancer research, including images, lesions outlines, and clinical data. The database is publicly available since April 2012 and continues to evolve, offering benchmarking datasets for research purposes [Miguel Angel Guevara López, 2012, Lopez et al., 2012].

3.2.7 National Mammography Database

The National Mammography Database (NMD), established by the American College of Radiology (ACR), is a pivotal quality improvement registry in the field of breast imaging. Its primary aim is to enable radiologists and facility staff members to monitor and enhance the quality of breast imaging services with ease and efficiency. The NMD aligns with the objectives of the National Radiology Data Registry (NRDR), focusing on data collection and performance feedback. The registry collects standardized data elements, already gathered under the Mammography Quality Standards Act (MQSA) and consistent with the ACR's BI-RADS. This integration with commercial mammography reporting software vendors and in-house systems facilitates one-click data submission to the registry. Facilities participating in the NMD receive real-time interactive and quarterly PDF performance feedback reports. These reports, highlighting various NMD measures such as recall rates and biopsy

results, enable facilities to compare their performance across various peer groups and the entire registry. Moreover, the NMD contributes significantly to advancing practice and research in mammography. The data submitted to the NMD aids in developing an extensive database, supporting research into national practice trends, care patterns, and identifying gaps in care. This database is instrumental in providing nationwide performance metrics and allowing comparison with published benchmarks [Lee et al., 2016, 2021].

3.2.8 Chinese Mammography Database

The Chinese Mammography Database (CMMD) is a significant database in the field of breast cancer research and mammography. Developed to address the limitations of existing mammography databases, such as small sample sizes and lack of diversity, the CMMD provides a more comprehensive and diverse set of data. The database was conducted on 1,775 patients from China with benign or malignant breast diseases, who underwent mammography examinations between July 2012 and January 2016. It consists of 3,728 mammography images from these patients, all with biopsy-confirmed types of benign or malignant tumors. A unique aspect of the CMMD is that for 749 of these patients (1,498 mammographies), it includes the patients' molecular subtypes. This addition is particularly valuable for research that looks into the relationships between image representation and molecular subtype, including luminal A, luminal B, HER2 positive, and Triple-negative. The image data in the CMMD were acquired using a GE Senographe DS mammography system [Cui et al., 2021, Cai et al., 2023].

The CMMD is recognized for its contributions to the field of artificial intelligence in computer-aided diagnosis. It supports advances in computer-aided detection for locating suspect lesions such as mass and microcalcification and computer-aided diagnosis for characterizing suspicious lesions or estimating their probability of onset. Moreover, the database facilitates the discovery of predictive image-based biomarkers by applying computational methods. Despite its extensive coverage, the CMMD is not without limitations. One notable limitation is the relatively small sample size.

Additionally, the Regions of Interest (ROI) are not marked in the dataset. Future plans include adding more information and increasing the data volume to enhance its utility. The CMMD, through its comprehensive and diverse data, plays a crucial role in advancing the understanding and diagnosis of breast cancer, especially in the context of mammography and AI-based analyses.

3.2.9 Breast Cancer Histopathological Database

The Breast Cancer Histopathological Image Classification (BreaKHis) database is a significant resource for the development and validation of machine learning models for breast cancer detection and diagnosis. It comprises a comprehensive collection of microscopic images of breast tumor tissue. The database includes 7,909 images collected from 82 patients, offering a wide range of samples captured at different magnifications (40X, 100X, 200X, and 400X). Notably, the BreaKHis database encompasses both benign and malignant samples, with images resized to 224x224 pixels for standardized analysis.

Developed in collaboration with the P&D Laboratory - Pathological Anatomy and Cytopathology in Parana, Brazil, the BreaKHis database is particularly structured for use in machine learning tasks involving binary and multiclass classification problems. The images, organized according to classification tasks and magnification levels, provide a detailed view of the tissue characteristics, crucial for the accurate classification of breast cancer types [Spanhol et al., 2016].

3.3 Mammogram Views

Mammography, a crucial tool in breast cancer screening and diagnosis, employs various image views to thoroughly examine breast tissue. The two most common views are the craniocaudal (CC) view and the mediolateral oblique (MLO) view. The CC view is taken from above the breast and is essential for visualizing the central and medial aspects of the breast tissue. The MLO view, captured at an angle, covers a larger volume of breast tissue, including the upper outer quadrant and the

armpit area, aiding in the examination of lymph nodes. Diagnostic mammography often necessitates additional views, especially when abnormalities are detected. These include the mediolateral and latero-medial (LM) views, which aid in lesion localization. Magnification views are employed to enhance the visibility of calcifications and small mass margins, achieved by increasing the distance between the breast and the receptor plate. Focal compression or spot views compress tissue around specific areas of interest, while rolled views separate overlapping tissues for better localization. The extended CC view (XCC) visualizes axillary or far lateral breast tissue, and tangential views are used for skin calcifications or abnormalities. Cleavage views assess medial breast abnormalities.

The selection of these supplementary views depends on the type of abnormality under investigation. Straight lateral (SL) and rolled views are typically used for parenchymal asymmetries, whereas magnification views are preferred for calcifications. In clinical practice, additional views are often complemented by ultrasound, especially when positive findings are identified, enhancing the diagnostic accuracy [Bassett et al., 1989].

3.4 Mammography Classification Standards

Mammography classification standards in breast imaging are crucial for diagnosing and managing breast cancer. These standards involve a systematic approach to categorizing mammographic findings based on specific criteria. They include detailed assessments of breast composition, the nature of masses, types of calcifications, and other radiographic features. This systematic classification is key for accurate diagnosis and effective communication in medical practice, ensuring consistent interpretations across various medical settings.

3.4.1 Breast Imaging Reporting and Data System

The Breast Imaging Reporting and Data System (BI-RADS) is a classification system developed by American College of Radiology used in mammography to

standardize reporting and help radiologists communicate breast imaging findings [D'Orsi, 2014]. It categorizes mammogram results into categories ranging from 0 (incomplete) to 6 (known biopsy-proven malignancy), with each category indicating a different level of suspicion for cancer. These categories are listed in table 3.3.

Table 3.3: BI-RADS Categories and Descriptions

Category	Description
BI-RADS 0	Incomplete - Additional imaging or previous images needed
BI-RADS 1	Negative - No masses, architectural distortion, or suspicious calcifications
BI-RADS 2	Benign - 0% Probability of malignancy
BI-RADS 3	Probably Benign - $<$ 2% Probability of malignancy; Short interval follow-up suggested
BI-RADS 4A	Suspicious - Low suspicion for malignancy (2-9%); Biopsy considered
BI-RADS 4B	Suspicious - Moderate suspicion for malignancy (10-49%)
BI-RADS 4C	Suspicious - High suspicion for malignancy (50-94%)
BI-RADS 5	Highly suggestive of malignancy - $>$ 95% Probability; Appropriate action needed
BI-RADS 6	Known biopsy-proven malignancy

BI-RADS assists in clinical decision-making and helps in determining the need for further testing, such as additional imaging or biopsy. This system plays a crucial role in ensuring consistent and effective breast cancer screening and diagnosis [D'Orsi, 2014, Eberl et al., 2006, Pesce et al., 2019, Orel et al., 1999].

3.5 Preprocessing Techniques in Digital Mammograms

Image processing in mammography is a critical aspect of modern medical imaging, aimed at improving the detection and diagnosis of breast cancer. The primary goal is to enhance image clarity and quality, making it easier for radiologists

to identify suspicious areas. Techniques like contrast enhancement and noise reduction are employed to highlight important features while minimizing distractions. The image processing methods are essential for accurately assessing and classifying potential abnormalities, facilitating early intervention and treatment. These techniques include:

Image Enhancement: It is a key preprocessing technique in digital mammography for breast cancer detection. Improves image clarity for better visualization of structures. This can involve contrast adjustment, brightness correction, histogram equalization, sharpening and noise reduction. By enhancing the image, radiologists can better detect and diagnose breast cancer at early stages, improving treatment outcomes. Effective image enhancement balances the need for clearer images with preserving the accuracy and diagnostic value of the mammogram.

Noise Reduction: It is a critical preprocessing technique in digital mammography. It focuses on minimizing the presence of random variations or 'noise' in mammogram images. This noise can obscure important details, making it harder to detect subtle signs of breast cancer. Effective noise reduction techniques enhance the clarity of mammograms, improving the visibility of tumors, microcalcifications, and other vital features. By reducing noise, radiologists can more accurately interpret mammograms, leading to better diagnosis and treatment planning. Filters like median filters, Gaussian filters, and wavelet-based methods are employed to reduce noise while preserving important features. The choice and application of noise reduction methods are crucial for maintaining image quality without losing essential diagnostic information.

Artifact Removal: It is a preprocessing technique in digital mammography that focuses on eliminating non-tissue elements from the images. These artifacts, which may include labels, markers, or dust spots, can obscure critical details and potentially lead to misinterpretation. Removing these artifacts ensures that the mammogram is clear and solely represents breast tissue, allowing for more accurate analysis and diagnosis. This process is vital for maintaining the integrity and diagnostic quality of mammograms.

Image Normalization: It is a preprocessing technique in digital mammography

designed to standardize the appearance of images. It adjusts the dynamic range and contrast of mammogram images, ensuring consistency across different scans. This process is important because it allows radiologists to more accurately compare images over time or between different imaging systems. By normalizing images, subtle changes or anomalies in breast tissue are easier to detect, aiding in the early diagnosis and treatment of breast cancer. This technique is crucial for maintaining a high quality and comparability of mammogram images.

Edge Detection and Enhancement: It is a preprocessing technique in digital mammography that emphasizes the edges within mammogram images. This process is crucial for delineating the contours of breast tissues and potential anomalies like tumors or calcifications. By enhancing the edges, this technique aids radiologists in more accurately identifying and analyzing suspicious areas, improving the diagnosis of breast cancer. Techniques like Sobel, Canny, and Laplacian filters to highlight and enhance the edges of lesions. Effective edge detection and enhancement make it easier to distinguish between normal and abnormal tissue structures, playing a significant role in early cancer detection.

Region of Interest Segmentation: It is a preprocessing technique in digital mammography where specific areas of a mammogram are isolated for detailed analysis. This process involves identifying and segmenting regions that are likely to contain abnormalities such as tumors or calcifications. ROI segmentation helps in focusing the diagnostic process on these critical areas, enhancing the efficiency and accuracy of breast cancer detection. By isolating these areas, radiologists can more closely examine potential abnormalities, which is crucial for early and accurate diagnosis. This technique plays a significant role in improving the effectiveness of breast cancer screening and analysis.

Standardization and Normalization: These are preprocessing techniques in digital mammography aimed at ensuring consistency across different mammogram images. Standardization refers to the process of adjusting the imaging parameters to a common standard, which helps in comparing images taken at different times or with different machines. Normalization involves adjusting the pixel values in the

images to a specific scale, enhancing the uniformity in brightness and contrast. These techniques are crucial for accurate interpretation and comparison of mammograms, facilitating the early detection and diagnosis of breast cancer.

Continual advancements in this field are revolutionizing mammography. These technologies offer improved accuracy in detecting subtle changes in breast tissue, aiding in the early diagnosis of breast cancer. The ongoing development of image processing techniques underscores their importance in enhancing breast cancer screening and diagnosis, ultimately contributing to better patient outcomes.

3.6 Conclusion

Mammogram databases are not just collections of images; they are pivotal in driving forward the research and practice in the field of breast cancer. Their role in training advanced machine learning models, facilitating comprehensive clinical studies, and enhancing diagnostic techniques underscores their invaluable contribution to the ongoing battle against breast cancer. As technology and medical understanding evolve, these databases will continue to be central resources in developing more effective strategies for breast cancer detection and treatment. Classification in mammography is crucial for ensuring standardized, accurate diagnoses and streamlining communication in breast cancer care. The importance of preprocessing techniques in digital mammograms, such as image enhancement, noise reduction, artifact removal, image normalization, edge detection, ROI segmentation, and standardization, is highlighted for improving detection and diagnosis accuracy. These advancements are vital for early breast cancer detection and enhancing patient care.

Chapter 4

Improved Automated Pectoral Muscle Segmentation in Digital Mammograms

4.1 Introduction

Mammography is a low energy X-ray which is widely used for the detection of breast cancer. Various studies have shown that breast cancer screening using mammography can reduce mortality rates by a good percentage. Similarly, mammogram interpretation using CAD systems has played a significant role in increasing cancer detection rates. A mammogram image is a two-dimensional image of a three-dimensional breast. The MLO view shows the highest breast projection and the presence of pectoral muscle cells in MLO view images is crucial [Logan et al., 2023]. The presence of pectoral muscle cells is far more useful in determining the position of mammography images.

The Pectoral Muscle is situated in the chest area, serving as a connection between the chest's front, the upper arm, and the shoulder. Separating the pectoral

Parts of the content in this chapter have been published in the following research article:

Haris U., Kabeer V., "Automated Breast Pectoral Muscle Segmentation in Digital Mammograms Using Holistic Regularization Method", Journal of Clinical Otorhinolaryngology, Head, and Neck Surgery, Vol: 27 Issue: 01, 2023, ISSN: 1001-1781.

muscle from mammogram images presents complexities due to individual variations in patient anatomy, age, and positioning during imaging. The pectoral muscle, varies in size, shape, and intensity across patients, sometimes covering a significant portion of the breast area. Its border can be concave, convex, or a combination, with variations in strength, intensity, and texture. While the upper borders of pectoral muscle cells are usually clearer, the lower borders are less distinct, often merging with fibroglandular cells. Breast density is calculated based on the opacity of fibro-glandular tissue reflected on digital mammograms concerning the whole area of the breast. The opacity of pectoral muscle and fibro-glandular tissue is similar to each other; hence, the small presence of the pectoral muscle in the breast area can hamper the accuracy of breast density classification. In CAD systems for breast mammography, the pectoral muscle region can easily cause a high false positive rate and misdiagnosis due to its similar texture and low contrast with breast parenchyma. So, segmenting the pectoral muscle region is a critical preprocessing step in mammography-based CAD systems. However, achieving accurate segmentation in mammograms with poor contrast remains a significant challenge in the field [Pawar et al., 2021, Avuti et al., 2019].

This chapter aims to present an innovative methodology for identifying and removing pectoral muscles from digital mammograms. Employing watershed transformation, regularization techniques, and masking methods, the proposed methodology addresses the complexity of this process. The following sections explain the details of employed methodology, analysis of the results and the conclusive findings.

4.2 Proposed Pectoral Muscle Segmentation

The suggested technique relies on region intensity, thresholding, and holistic regularization methods. It employs a comprehensive set of rules aimed at enhancing the outcomes. Assessments of these rule sets encompass all mammographic images from the MIAS database, demonstrating commendable performance. This method's algorithm primarily comprises three phases. The initial phase focuses on orientation

normalization. Subsequently, the second phase targets the elimination of noise artifacts while discerning the shape, size, and position of the pectoral muscle. Finally, the third phase concentrates on removing the pectoral muscle from the mammographic images to reveal the actual breast portion. The resulting image can be utilized for breast cancer recognition. The schematic representations of phase 1, phase 2 and phase 3 of this method are shown in figures 4.1, 4.2 and 4.3 respectively.

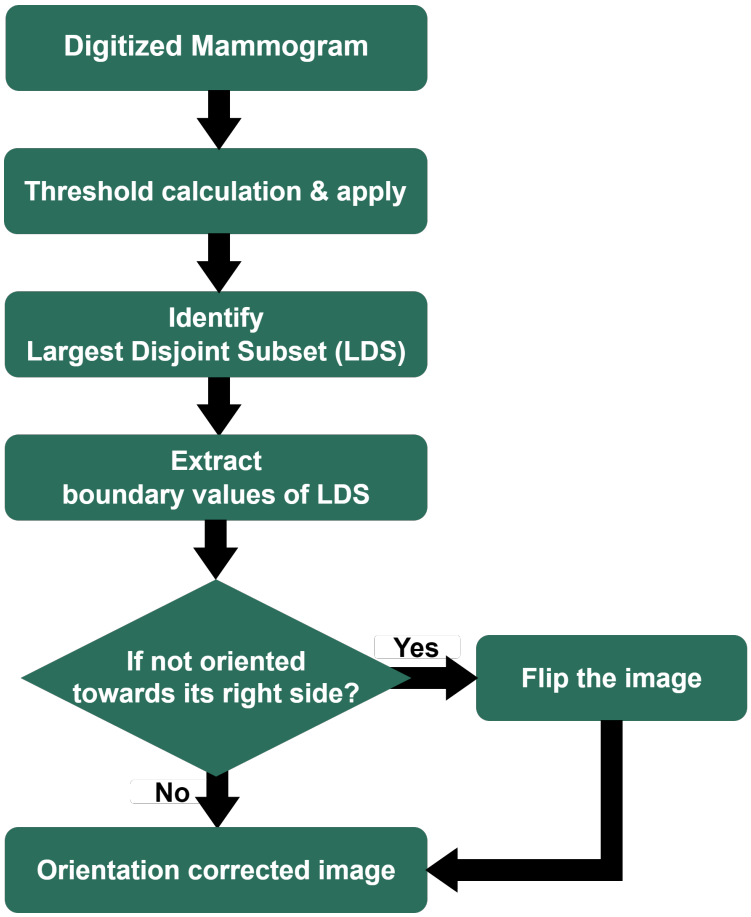

Figure 4.1: Orientation normalization of the input image

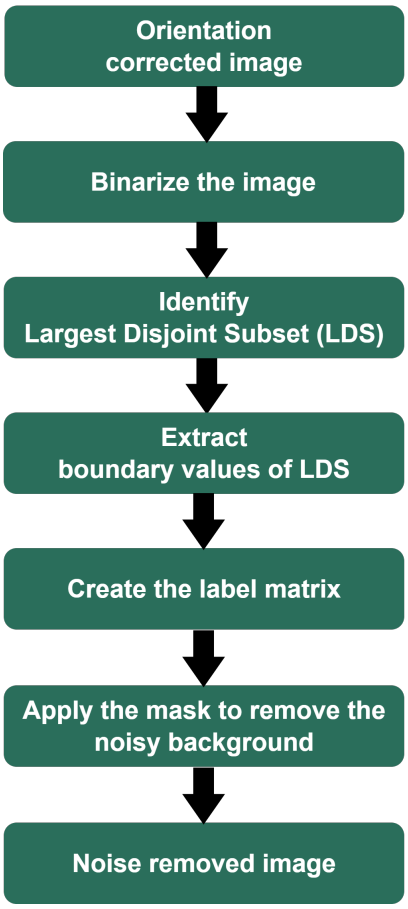

Figure 4.2: Noise Removal

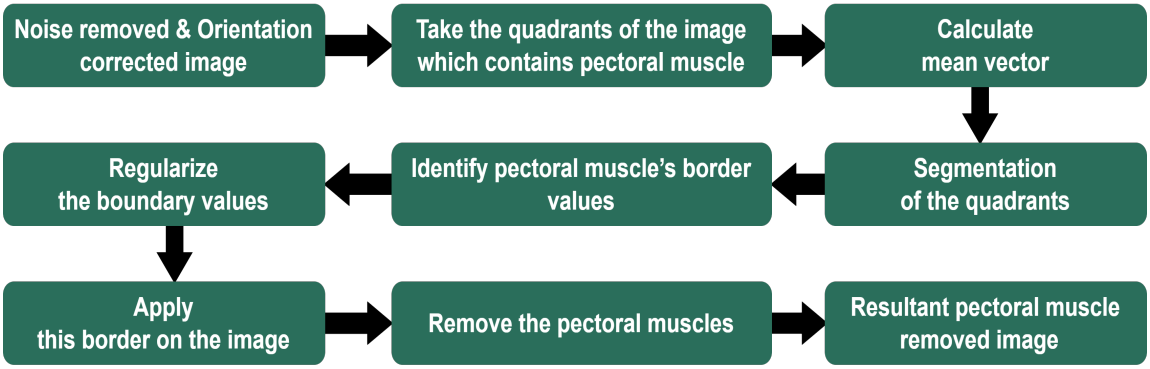

Figure 4.3: Pectoral Muscle Removal

4.2.1 Orientation Normalization

The primary objective of this phase is to establish the correct orientation for the input mammographic image, crucial for confirming the positioning of the pectoral muscle in the upper left corner. Binarization, a fundamental step in this process, becomes imperative to accurately differentiate the pectoral muscle from the surrounding elements. The algorithm employed for orientation normalization utilizes Otsu's threshold theory to compute the threshold value for image binarization.

4.2.1.1 Otsu's thresholding

Otsu's thresholding method, widely acknowledged as the best and most prevalent technique for thresholding, operates on the premise that the input image comprises two distinct pixel categories: foreground and background [Otsu, 1979, Yang et al., 2020]. By comprehensively evaluating optimal threshold values, it aims to diminish intra-class variance while enhancing inter-class variance [Qin et al., 2019, Sha et al., 2016, Sharma et al., 2013a, Sezgin and Sankur, 2004, H et al., 2014]. Its objective is to minimize internal class variance while maximizing class variation, achieved by leveraging the gray level histogram and treating the variance between classes as an objective function. This process of optimal threshold segmentation plays a vital role in accurately isolating the pectoral muscle from artifacts and other surrounding elements, enabling precise orientation normalization for mammographic images. The following part describes this method more in detail.

$$\text{Total Variance} = \text{Inside Class Variance} + \text{Among Class Variance} \tag{4.2.1}$$

Otsu's thresholding technique meticulously seeks threshold values that decrease intraclass variance, expressed as a weighted sum of variances of the two classes according to equation 4.2.2.

$$\sigma_{\omega}^2(t) = \omega_0(t)\sigma_0^2(t) + \omega_1(t)\sigma_1^2(t) \tag{4.2.2}$$

Where $\omega_0(t)$ and $\omega_1(t)$ are the probabilities of two classes divided by the threshold value t, while σ_0^2 and σ_1^2 represent the variances of these respective classes.

The initial step involves identifying the largest disjoint subset within the binarized image, which effectively delineates the area of interest - specifically, the actual breast area. Subsequently, the orientation of this largest disjoint subset, which mirrors the orientation of the breast area, is considered as the orientation of the original image. If necessary, the image is then reoriented based on this determined orientation.

To establish the orientation of the largest disjoint subset, the boundary values of this subset are computed. By examining the proximity of the curved points within these boundary values against the horizontal border line of the mammographic image, the orientation of the breast area is determined. If the image is observed to be left-oriented, it is flipped to ensure correct orientation towards its right side. This phase culminates in the successful alignment of the image towards its intended right direction. figure 4.4 shows the input image, histogram, threshold applied and orientation normalized images of this phase. The processing steps of the orientation normalization phase are given below in algorithm 1.

Algorithm 1 Orientation Normalization Algorithm

Data: Mammogram image $I = \{I_{i,j}\}$, $1 \leq i \leq m$, $1 \leq j \leq n$
Result: Orientation normalized image
$T \leftarrow$ Otsu's threshold value calculated using Otsu's theory
$HS \leftarrow m/2$
Binarize image I_b such that $I_{i,j} = 0$ when $I_{i,j} < T$ otherwise $I_{i,j} = 1$
Calculate $D_k \subseteq I_b$, $1 \leq k \leq t$, the disjoint sets of 1s in the binarized image I_b
Find $D_{\max} = \max(\{D_k\})$, the biggest disjoint set
Find (x_β, y_β), the set of boundary positions in $D_{\max}$
Compute mode $M = \text{Mod}(x_\beta)$
if $M > HS$ **then**
    $I_{i,j} \leftarrow I_{i,n-j+1}$ (i.e., re-orient the image)
else
    `// No need.`

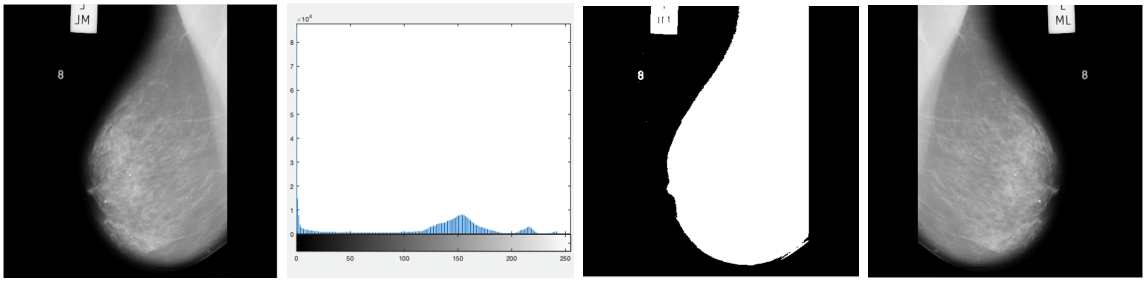

(a) (b) (c) (d)

Figure 4.4: (a) Randomly selected mammographic image from the MIAS database [mdb057.pgm] (b) Histogram of the image mdb057.pgm (c) Otsu's threshold applied on MIAS image [mdb057.pgm] (d) Orientation Normalized Image [mdb057.pgm]

4.2.2 Noise Removal Process

The primary objective of this phase is to eliminate extraneous noise artifacts situated outside the breast area in mammographic images. Such artifacts encompass film strips, scratches, image marks, patient identification details, seals, logos, hospital or clinic information, dates, times, as well as various unwanted scanning and tapping artifacts. To achieve this, a combination of the Watershed Segmentation technique along with grey level histogram and thresholding techniques are employed. These noise removal processes effectively reduce the area of the actual image intended for further processing in detection algorithms. Consequently, this reduction enhances the speed, accuracy, correctness, and overall performance of the subsequent detection process [Vala and Baxi, 2013].

Throughout this phase, we employ binarized images derived from previous results to conduct further noise reduction and generate a label matrix utilizing a parametric equation. This precise method plays a significant role in enhancing the noise elimination technique, concurrently preparing the image for subsequent stages in the analysis.

$$X(t) = X_c + a\cos t\cos\phi - b\sin t\sin\phi \tag{4.2.3}$$

$$Y(t) = Y_c + a\cos t\sin\phi - b\sin t\cos\phi \tag{4.2.4}$$

Where, (X_c, Y_c) is the object centers of the binarized image, a and b are the

major and minor axis lengths, and ϕ is the angle between the x-axis and the major axis.

The next step involves identifying the largest disjoint area denoted as B, a region consistently encompassing the scanned breast region. This area serves as a foundation for generating a mask, labeled M, specifically designed for the noise removal process applied to the background segment of the input mammographic image. Image masking, an effective technique supported by literature, is employed to eliminate artifacts like noises and scratches within the background [Bhuvaneswari et al., 2013].

Subsequently, the generated mask is applied to the original image labeled I, targeting the removal of all noise artifacts from the background section. As a result of this process, the resultant image exclusively retains the authentic breast area, effectively devoid of undesired artifacts, as illustrated in Figure 4.5. This method ensures a refined image specifically focused on the breast region, facilitating further analysis and enhancing the image's quality for the subsequent stages.

$$\text{roi} = I \cdot M \tag{4.2.5}$$

where I is the input mammographic image and M is the mask (largest disjoint subset of the threshold applied image).

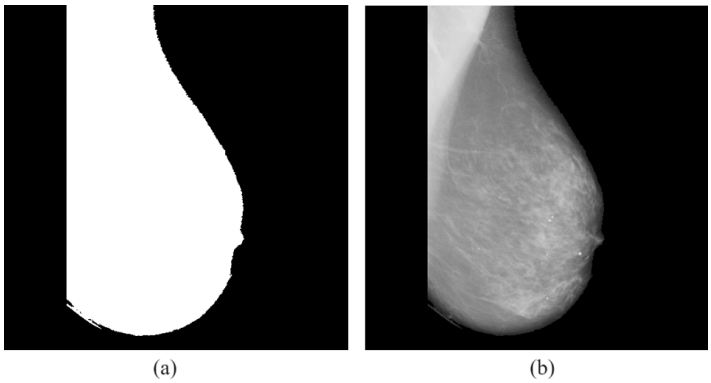

Figure 4.5: (a) The mask – largest disjoint subset of the threshold applied image [mdb057.pgm], (b) Noise removed image – Breast portion only [mdb057.pgm]

4.2.3 Pectoral Muscle Detection and Removal

The preliminary stage in CAD systems involves the crucial identification of the pectoral muscle, a task that remains challenging using existing hand-crafted methods. These methods often fall short when encountering varied shapes and indistinct boundaries of the pectoral muscle area due to its overlapping nature [Rampun et al., 2019]. To address these limitations, this phase integrates a holistic regularization method and a combination of diverse techniques aimed at accurately recognizing and eliminating the pectoral muscles from the breast area.

Ensuring the correct orientation of the image towards its right direction is imperative, as it is observed that the pectoral muscle portion consistently occupies the upper-left quadrant of the mammogram image [Moghbel et al., 2019]. However, occasional extensions of the pectoral muscles to the bottom left-hand corner, encompassing the third quadrant, pose challenges. Consequently, to compute the mean threshold value of the pectoral muscle, the second quadrant (top left-hand area) and the third quadrant are considered. This approach significantly enhances the accuracy in determining the average threshold.

The mean-vector calculation method is employed for the pectoral muscle area, followed by determining the mean of the mean vector to derive the final mean of the entire pectoral muscle area. This meticulous process contributes to more precise identification and elimination of the pectoral muscles, addressing variations in their shapes and overlapping boundaries encountered in mammographic images.

$$\bar{x} = \frac{1}{mn} \sum_{i=1}^{m} \sum_{j=1}^{n} P(i,j) \tag{4.2.6}$$

To obtain the largest disjoint subset, the area property of the binarized pectoral muscle area is identified and calculated the boundary values to get the shape of the pectoral muscle from the largest disjoint subset B. Boundary values were comprehensively adjusted, including prior knowledge, to obtain the entire area of the pectoral muscle.

The parametric equation 4.2.1 was applied to the binary image P to identify

the label matrix Rp, and the boundary values were calculated to select the pectoral muscle area. Then applied Moore-Neighbor tracing algorithm modified by Jacob's stopping criteria to identify the exterior boundaries of objects [Sharma et al., 2013b]. The state of the given pixel at time step $(t+1)$ will be determined from the states of pixels within its neighborhood at time step t.

$$P_{i,j}(t+1) = f(P_{i,j}(t) + P_{\text{neigh(i,j)}}(t)) \tag{4.2.7}$$

Where, P_i, j denotes the state of the $(i,j)^{th}$ pixel, t denotes the number of generations that have evolved, $P_{\text{neigh(i,j)}}$ denotes the set of neighbors of the $(i,j)^{th}$ pixel. Then identify the biggest from the label matrix, and this will be the final ROI.

$$(B_{p(i+1)} > B_{p_i}) \rightarrow B_p \tag{4.2.8}$$

Where, B_{p_i} is the objects in the label matrix and eventually B_p will have the biggest object which contains the pectoral muscle. Then apply this boundary line on the final noise removed image to mark the border of the pectoral muscle. Figure 4.6 shows the images from different stages of this phase and the resultant border marked pectoral muscle.

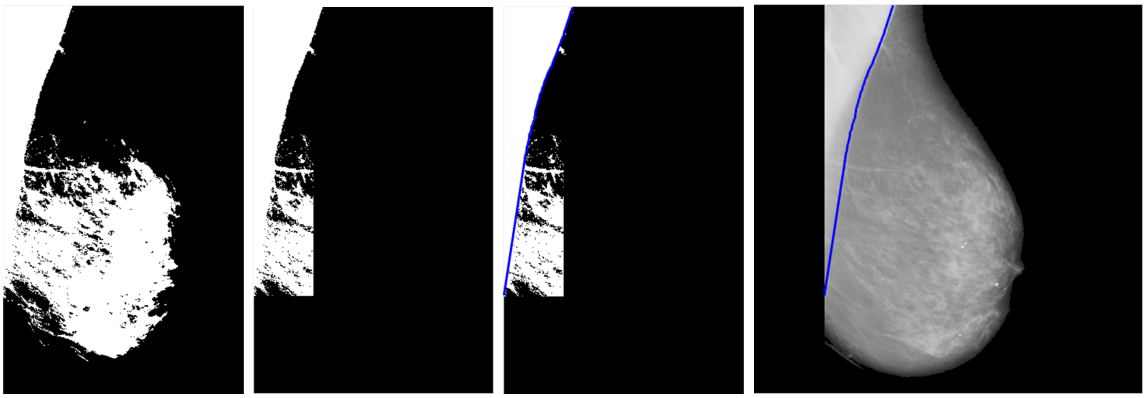

(a) (b) (c) (d)

Figure 4.6: (a) Binarized the image using mean of the pectoral muscle area [mdb057.pgm] (b) Taken only the quadrants which contains the pectoral muscle [mdb057.pgm] (c) Identified the border of the pectoral muscle and marked on it [image mdb057.pgm] (d) Applied the identified border on the actual mdb057.pgm

4.3 Results and Discussions

The proposed pectoral segmentation algorithm is applied on all the images of MIAS database which are belong to either left or right orientations and it results an accuracy of 97.20% certified by expert radiologist[1]. The results of pectoral muscle segmentation using the suggested algorithm is given in table 4.1.

Table 4.1: Experimental results of the proposed algorithm

Results Classification	Number of images falls in category out of 322 images	Result Percentage
Accurate	289	89.75%
Acceptable	24	7.45%
Inaccurate	9	2.79%

The results of this suggested method are categorized into three classes such as accurate, acceptable and inaccurate. The descriptions of these categories are explained in table 4.2.

Table 4.2: Result categories of proposed algorithm

Class	Description
Accurate	Pectoral muscles are identified as exactly same as the ground truth.
Acceptable	More than 65% of pectoral muscle area of the ground-truth was recognized.
Inaccurate	The rest of the results with accuracy less than 65%

The purpose of this evaluation is not only to ensure that all left-oriented images are reoriented towards the right direction, but also to ensure that images already in the right direction are not been affected by this algorithm. Therefore, it has been proven that we can apply this algorithm before applying any of the models,

[1]Dr. Hamna Najiya K, Department of Radio Diagnosis, Government Medical College, Calicut, Kerala, India.

regardless of the direction of the images in MLO views. This reduces the involvement of the radiologist or mammogram evaluator in manually determining the image orientation in CAD systems, which in turn reduces processing time. Table 4.3 shows a comparative evaluation of the various pectoral muscle segmentation approaches, evaluated in the MIAS database, including this specific method. Figure 4.7 displays the confusion matrix, while Figure 4.8 presents the comparison between the accuracy of the proposed work and related research. Figure 4.9 exhibits the comparison of False Positive (FP) and False Negative (FN) metrics between the proposed work and related research. Therefore, it is clear that the model proposed in this work has achieved excellent results regardless of the orientation and intensity differences of the input images.

Table 4.3: Comparative results

Method used	**Proposed by**	**Number of images used**	**Accuracy**
Proposed method	[Haris and Kabeer, 2023]	**322**	**97.20%**
Canny edge detection	[Qayyum and Basit, 2016]	322	93%
Curve fitting	[Yoon et al., 2016]	322	92.20%
Gradient-based thresholding	[Shi et al., 2018]	322	97.08%
Hough transform	[Xu et al., 2007]	52	94.50%
K-means clustering	[Slavković-Ilić et al., 2016]	322	87.57%
K-means clustering	[Yoon et al., 2016]	320	93.16%
Polynomial fitting/ Curve estimation	[Mustra et al., 2013]	322	96.60%
Polynomial fitting/ Curve estimation	[Shen et al., 2018]	322	96.81%
Region growing	[Rampun et al., 2019]	150	92%
Region growing	[Maitra et al., 2012]	322	95.65%
Region growing	[Taghanaki et al., 2017a]	322	95%

Continued on the next page

Table 4.3: Comparative results (Continued)

Method used	Proposed by	Number of images used	Accuracy
Region growing	[Hazarika and Mahanta, 2018] (2018)	150	92%
Straight line estimation and cliff detection	[Kwok et al., 2001]	322	94%
Support vector machine (SVM)	[Shinde and Rao, 2019]	306	93.70%
Texture features	[Li et al., 2013]	322	90%
Thresholding	[Maitra et al., 2012]	322	95.70%
Watershed	[Camilus et al., 2011]	84	94%

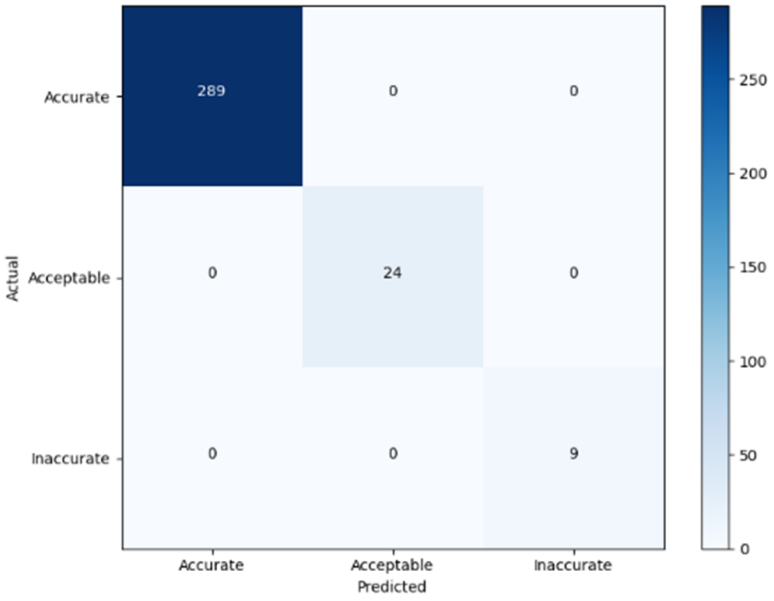

Figure 4.7: Confusion Matrix

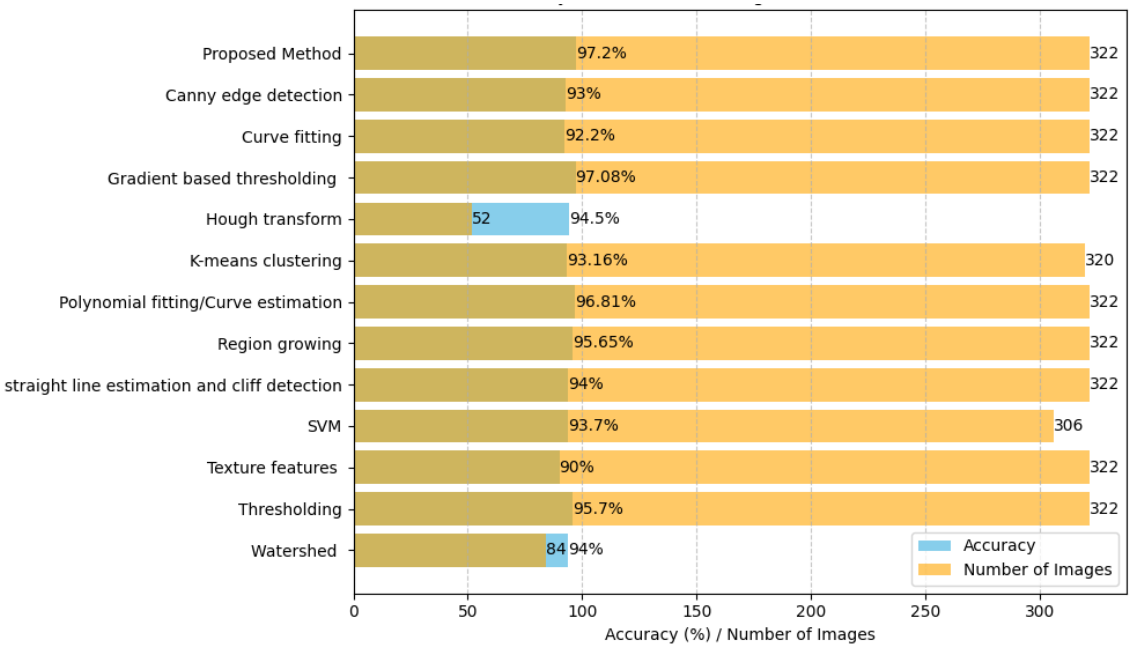

Figure 4.8: Performance of proposed work with related research in essence of accuracy.

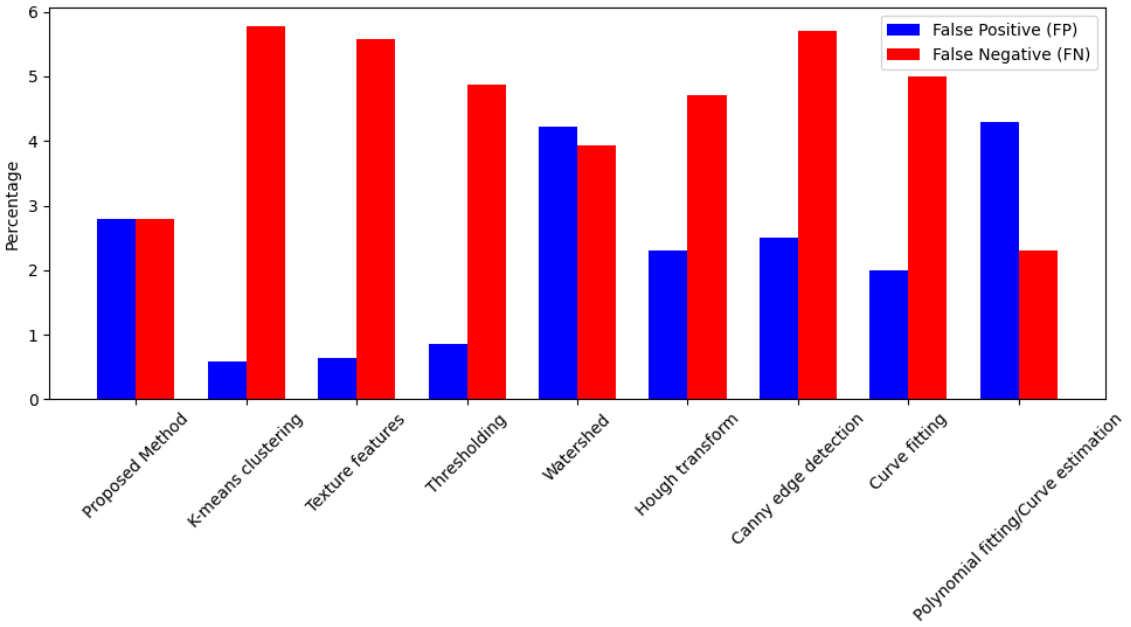

Figure 4.9: Performance of proposed work with related research in essence of FP & FN.

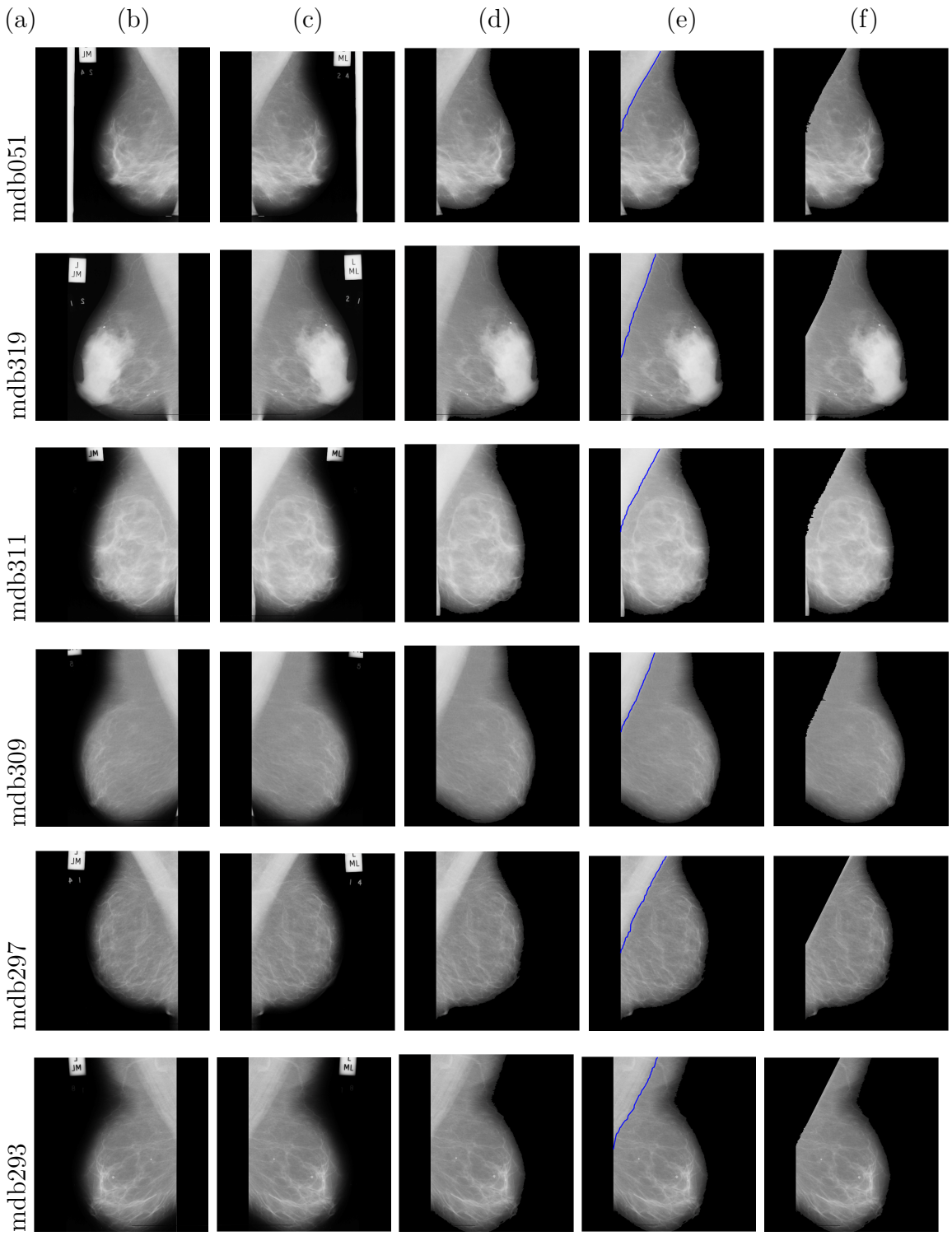

Figure 4.10: Column (a) contains the image name, column (b) shows original images from MIAS digital mammographic database, column (c) shows orientation normalized image toward right direction, column (d) shows noise removed image, column (e) shows border line between pectoral muscle and breast area, and column (f) shows only the breast area after removing noises and pectoral muscles from original image.

The images shown in figure 4.10 are the arbitrarily selected mammographic images from MIAS database. All the selected films which are left oriented are successfully reoriented towards right direction and images which are already in right direction are not been affected or changed by this proposed algorithm.

4.3.1 Stability Analysis

To validate the stability of the suggested method, a 5% Gaussian noise is added to the randomly selected images from the MIAS database. This analysis is also produced the same result as applied on the original image. It is proved that the suggested method is really a stable method and will work as expected in real data too. Figure 4.11 displays the graph representing the stability analysis, while Figure 4.12 illustrates the resultant images obtained from the stability analysis.

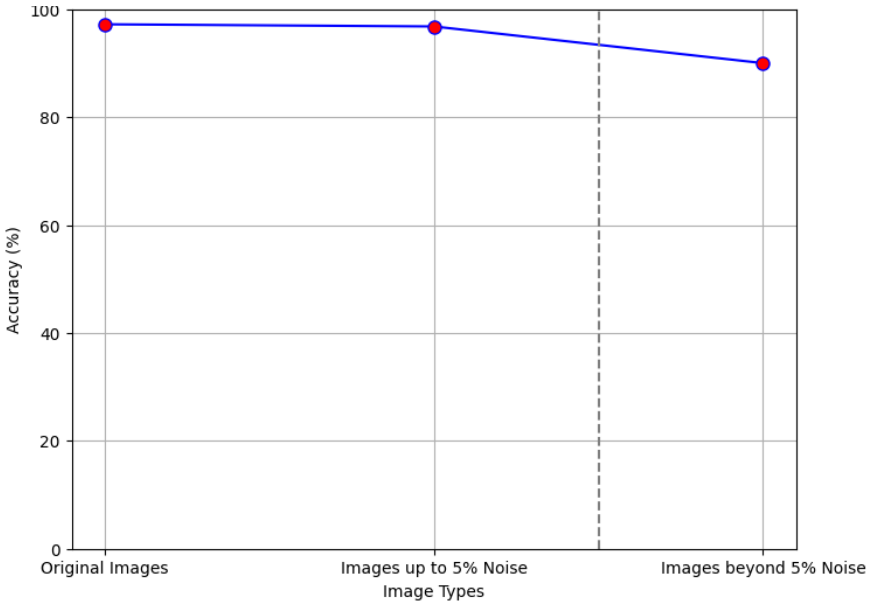

Figure 4.11: Stability analysis with 5% noise level and then showcases a potential drop in stability beyond that threshold.

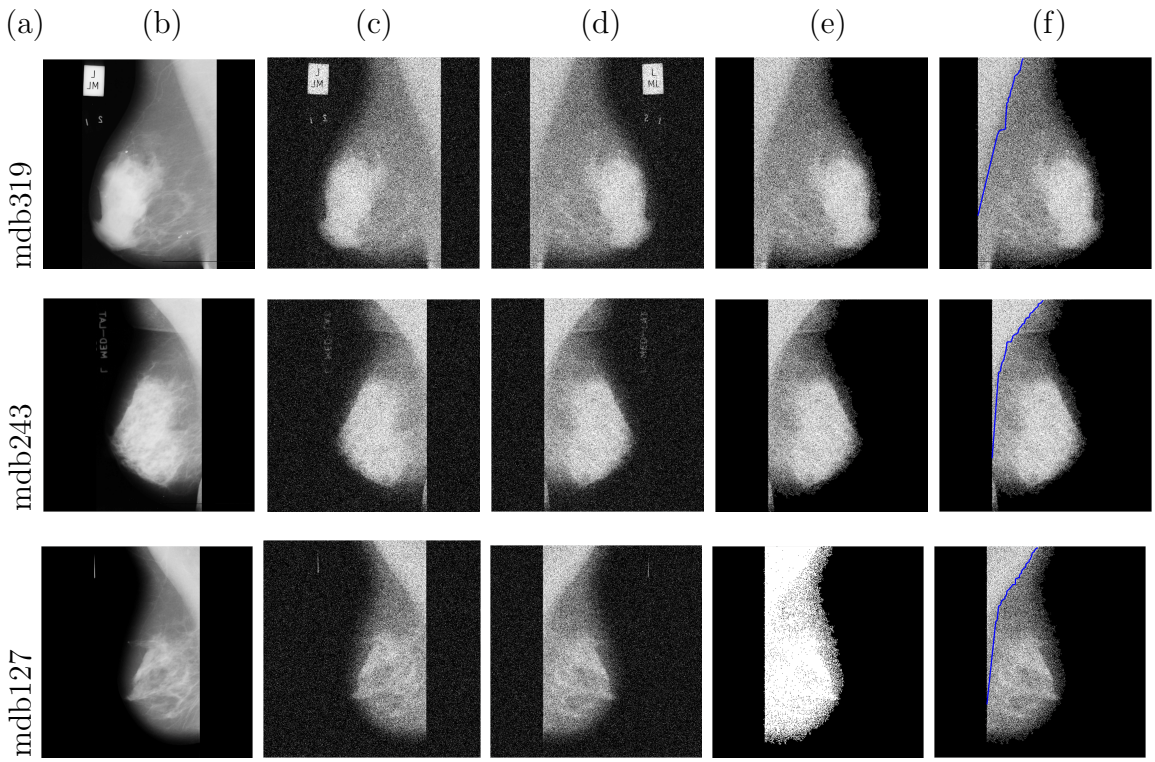

Figure 4.12: Column (a) contains the image name, column (b) shows original image from MIAS digital mammographic database, column (c) 5% noise added to the original image, column (d) shows orientation normalized image toward right direction, column (e) shows the noise removed image, and column (f) shows border line between pectoral muscle and breast area.

4.4 Conclusion

This chapter presents a pioneering method for Automated Breast Pectoral Muscle Segmentation in Digital Mammograms, addressing challenges in precise identification and removal of pectoral muscles from mammographic images. The proposed three-phase methodology—Orientation Normalization, Noise Removal, and Pectoral Muscle Detection—demonstrates exceptional accuracy, achieving an overall 97.20% accuracy rate across the MIAS database. Comparative evaluations against existing methods in the MIAS database underscore the superiority of the proposed technique in terms of accuracy and robustness. It outperforms other approaches, showcasing its reliability and consistency in pectoral muscle segmentation, even across varied image orientations and intensity differences. Furthermore, stability analysis

under a 5% Gaussian noise level confirms the method's reliability in real-world scenarios. This research introduces an automated, accurate, and reliable approach that significantly enhances Computer-Aided Diagnosis systems' effectiveness in breast cancer detection. The findings emphasize the potential practical implementation of this method in clinical settings, reducing dependency on manual interventions and accelerating the diagnostic process. This work contributes substantially to improving automated breast cancer detection systems by emphasizing the critical role of accurate pectoral muscle segmentation in enhancing diagnostic outcomes while reducing radiologists' workload.

Chapter 5

Breast Cancer Detection in Digital Mammograms using Hybrid HHO-CS MKSVM Framework

5.1 Introduction

In the quest to enhance breast cancer diagnosis using mammography, this chapter introduces a cutting-edge Hybrid SVM Framework that synergistically combines the robust classification capabilities of Support Vector Machine (SVM) with the dynamic optimization potential of Harris Hawks Optimization (HHO) and Cuckoo Search (CS) algorithms. This innovative approach aims to refine feature selection and classification processes, leveraging the precision of SVM and the adaptive search strategies of HHO and CS to navigate the complex landscape of mammographic image analysis. By tapping into the cooperative hunting strategies of Harris hawks and the unique brood parasitism behavior of cuckoo birds as metaheuristic inspirations, the framework is designed to enhance the segmentation accuracy and, consequently, the classification efficacy of mammographic images. This is particularly crucial in

Parts of the content in this chapter have been published in the following research article:

Haris U, Kabeer V, and Afsal K. "Breast Cancer Segmentation Using Hybrid HHO-CS SVM Optimization Techniques." Multimedia Tools and Applications, 2024, https://doi.org/10.1007/s11042-023-18025-7.

the context of breast cancer, where early and accurate detection can significantly impact treatment outcomes. The integration of these optimization algorithms into the SVM framework facilitates a more nuanced and effective analysis of mammographic data, promising to push the boundaries of current diagnostic methodologies. This chapter investigates into the intricacies of this Hybrid SVM Framework, exploring its components, operational mechanics, and potential impact on the field of medical imaging, particularly in the early detection and classification of breast cancer from mammographic images.

5.2 Proposed Framework

This framework presents an innovative hybrid approach to breast cancer classification by integrating Support Vector Machine (SVM) with Harris Hawks Optimization (HHO) and Cuckoo Search (CS) optimization algorithms. HHO, based on the cooperative behavior of Harris Hawks, serves as a metaheuristic optimization algorithm. It effectively explores and exploits the search space, thereby augmenting the accuracy of image segmentation in breast cancer detection. Furthermore, the CS algorithm is integrated within this approach to balance both local and global search aspects, ensuring a comprehensive optimization strategy. The optimized segmentation results derived from HHO-CS algorithm is utilized in tandem with a Multi Kernel Support Vector Machine (MKSVM) for the classification of breast cancer cases. Notably, the CS algorithm assumes an integral role in fine-tuning hyperparameters, consequently enhancing the performance of the MKSVM. This collaborative framework significantly improves the overall accuracy and efficacy of breast cancer classification, thereby contributing to advancements in the field. This proposed framework is shown in Figure 5.1.

The primary focus of this framework revolves around the development of an efficient breast cancer classification system utilizing mammographic images sourced from the Curated Breast Imaging Subset of Digital Database for Screening Mammography (CBIS-DDSM). This dataset, an enhanced iteration of the DDSM (Digital Database

for Screening Mammography), is renowned for its comprehensive compilation of mammographic examinations. It includes confirmed pathologies of benign, malignant, and normal cases, making it an invaluable resource for medical image analysis and research purposes.

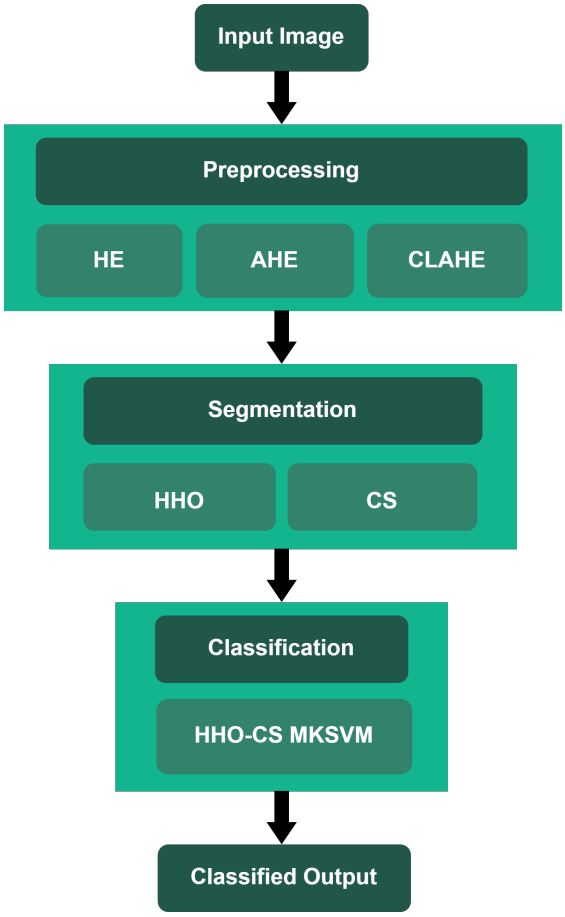

Figure 5.1: The overall Architecture of the Hybrid SVM Framework

5.3 Preprocessing

The preprocessing of mammographic images is a critical step in enhancing the diagnostic capabilities of medical imaging for breast cancer analysis. Techniques such as Histogram Equalization, Adaptive Histogram Equalization, and Contrast Limited Adaptive Histogram Equalization play pivotal roles in this phase. These methods aim to improve image contrast, enabling the clearer visibility of crucial features such as masses and microcalcifications. While HE focuses on global contrast enhancement,

AHE and CLAHE offer more localized adjustments, with CLAHE additionally controlling for noise amplification, thereby preparing images for subsequent segmentation and analysis with increased accuracy and reliability.

5.3.1 Histogram Equalization

Histogram Equalization (HE) is applied for enhancing the global contrast of the mammogram images to reveal hidden details. That is the visibility of critical features such as microcalcifications, masses, and architectural distortions can be significantly improved through HE, which redistributes the pixel intensity values to span the entire range, thereby enhancing the overall image contrast. The process of histogram equalization involves adjusting the distribution of pixel intensities by applying a transformation function to the original histogram of the image. This function is defined as:

$$T(r) = (L-1)\int_0^r p_r(w)dw \tag{5.3.1}$$

where $T(r)$ is the transformation function applied to the original pixel value r, L represents the number of possible intensity levels, and $p_r(w)$ denotes the normalized histogram of the input image.

By applying this technique, mammographic images can be standardized in terms of brightness and contrast, facilitating more consistent analysis across different images and imaging conditions. However, while HE is effective at improving global contrast, it may not address local contrast variations adequately, which are often present due to the diverse density and texture across different regions of the breast.

The need for a more localized approach to contrast enhancement in mammography leads to the application of Adaptive Histogram Equalization (AHE). AHE tailors the histogram equalization process to smaller regions within the image, allowing for customized contrast enhancement that adapts to local image characteristics. This local adaptation is crucial for highlighting subtle features in mammographic images that may indicate the presence of breast cancer, thus enhancing the diagnostic process before the images proceed to the segmentation phase.

5.3.2 Adaptive Histogram Equalization

Adaptive Histogram Equalization (AHE) advances the concept of histogram equalization by applying the contrast enhancement technique locally to small regions or tiles within a mammographic image. This localized approach allows AHE to adjust the contrast based on the specific characteristics of each region, thereby addressing the limitations of global histogram equalization in handling local contrast variations. Such local adaptations are particularly beneficial in mammography, where the breast tissue's heterogeneity can obscure critical diagnostic features. AHE enhances the visibility of local structures and anomalies by computing separate histograms for overlapping tiles across the image and applying histogram equalization to each tile independently. The transformation function for each local region can be expressed as:

$$T_i(r) = (L-1)\int_0^r p_{r_i}(w)dw \tag{5.3.2}$$

where $T_i(r)$ is the local transformation function for tile T_i, and $p_{r_i}(r)$ is the normalized histogram of the pixel intensities within the tile T_i.

While AHE significantly improves the detection of local features in mammographic images, such as masses and calcifications, it can also introduce noise and amplify artifacts, particularly in homogenous regions of the breast. This potential for noise amplification underscores the need for a more refined approach to local contrast enhancement, leading to the development of Contrast Limited Adaptive Histogram Equalization (CLAHE). CLAHE builds on the principles of AHE but incorporates a contrast limiting step to prevent the over-amplification of noise. By applying CLAHE, mammographic images are processed to enhance local contrast while maintaining the integrity of the image, thus preparing the images for subsequent segmentation with minimized noise and artifacts.

5.3.3 Contrast Limited Adaptive Histogram Equalization

Contrast Limited Adaptive Histogram Equalization (CLAHE) represents a sophisticated advancement in the preprocessing of mammographic images, specifically designed to enhance local image contrast while mitigating the drawbacks associated

with traditional AHE, such as noise amplification. CLAHE operates by dividing the image into contextual tiles and applying histogram equalization to each, with a critical contrast limiting step to prevent the over-enhancement of noise in uniform areas.

The key to CLAHE's effectiveness lies in its approach to histogram clipping, which limits the enhancement in regions where the histogram exceeds a predefined threshold. The excess is redistributed across other histogram bins before the cumulative distribution function (CDF) is computed and used for transforming pixel values. This process can be represented as follows:

- Clip the histogram at a predefined maximum height,

$$h_{clip}(r) = \min(h(r), \text{clip\_limit}) \tag{5.3.3}$$

  where $h(r)$ is the original histogram of the tile, and clip_limit is the predefined maximum height for any histogram bin.

- Redistribute the excess counts from clipped bins across other bins in the histogram.

- Compute the CDF of the modified histogram for each tile and apply it to adjust the pixel values, enhancing local contrast without significantly amplifying noise.

By ensuring that contrast enhancement is localized and controlled, CLAHE facilitates the prepares the images for more effective segmentation, allowing for detailed analysis of breast tissue components.

5.4 Segmentation

To enhance the precision and effectiveness of this segmentation phase advanced optimization algorithms like the Harris Hawks Optimization (HHO) and Cuckoo Search Optimization (CSO) are employed. These algorithms draw inspiration from natural behaviours and phenomena, exhibiting exceptional capabilities in exploring

the search space and converging towards optimal solutions efficiently. The HHO algorithm, inspired by the predatory tactics of Harris Hawks, excels in adapting its search strategy dynamically, balancing between exploration and exploitation to locate the most promising regions for segmentation. To achieve this goal, we've integrated the HHO (Harris Hawks Optimization) algorithm, which involves three key optimization stages: initialization, fitness evaluation, and update [Zhang et al., 2019a], [Heidari et al., 2019]. On the other hand, the CSO algorithm, mimicking the brood parasitism of cuckoo birds, introduces a novel approach to updating solutions, ensuring diversity and avoiding local optima. The Cuckoo Search methodology presents distinct advantages compared to other meta-heuristic methods due to its ability to balance local search and comprehensive analysis of the entire search region using only two parameters: population size and the probability of egg detection. Its unique attribute lies in the effective equilibrium it achieves between random and local search after restoration, a crucial aspect to be explored further. The CSO algorithm's simplicity, attributed to its fewer parameters, renders it more adaptable and widely applicable [Yang and Deb, 2009]. The integration of these optimization techniques into the segmentation phase not only improves the delineation of relevant features within mammograms but also contributes to the robustness and accuracy of the overall image analysis process, ultimately aiding in the early detection and effective treatment of breast cancer.

The process begins by initializing the image matrix, embedding a specific number of hawks into it. Each hawk in the population is associated with an individual fitness function, denoted as (X_i). This function is calculated by considering pixel intensity, neighbouring intensities, and image resolution. For example, the fitness function of the i^{th} hawk is formulated based on these parameters. Once fitness is estimated for all hawks, a sequential process consisting of three stages is executed to determine the best alternative. This optimization aims to enhance segmentation accuracy and effectiveness. Ultimately, this process indirectly influences the Masi Entropy (ME) metric, reducing dissimilarities between predicted and ground truth segmentation masks in mammogram images [Masi, 2005].

The ME metric serves as an evaluation tool for segmentation quality in this study. It quantifies the similarity between two segmentations, typically comparing an automated segmentation result with a ground truth or reference segmentation. ME considers overlapping regions between segmentations, assessing agreement based on the proportion of overlap and the sizes of the regions. The entropic measure named Masi Entropy, denoted as Equation (5.4.1), is used for a probability distribution that encompasses all possible outcomes $P_d = \{p_{d_1}, p_{d_2}, \ldots, p_{d_n}\}$ where p_{d_i} resides within 0 and 1, and i expands from 1 to n where $\sum_{i=1}^{n} p_{d_i} = 1$.

$$S_l = \frac{1}{1-l} \log \left[1 - (1-l) \sum_{i=1}^{n} p_{d_i} \log p_{d_i} \right] \tag{5.4.1}$$

Here $l > 0$ and $l \neq 1$ and l is known as a measure of the degree of nonextensivity in the system. According to Equation (5.4.1), if $l = 1$ then the Masi entropy diminishes to Shannon entropy $S_x = \sum_{i=1}^{n} p_{d_i} \log p_{d_i}$ [Lin, 1991]. The non-extensivity and additivity of Tsallis and Renyi entropy are combined to form Masi entropy [De Albuquerque et al., 2004], [Sahoo et al., 1997]. In Tsallis and Renyi entropy, every state of probability is in the power of q or α, whereas in Masi entropy, the entire probability function is in the power of l. As a result, when compared to other entropies, it makes the supreme objective function.

When considering the probability distribution $P_d = \{p_{d_i}\}$ and $R = \{q_i\}$ of two statistically independent systems, the Masi entropy demonstrates the additive property described by Equation (5.4.2).

$$S_l(P_d \cap R) = S_l(P_d) + S_l(R) \tag{5.4.2}$$

The application of this method extends to addressing the multi-level image segmentation challenge, exemplified by the Multi-level Masi Entropy (MME) based image segmentation approach.

Let I/P be the dimension of size $M \times N$ where the probability of the ith grey level is $a_i = \frac{n_i}{M \times N}$ subject to $a_i \geq 0$, $\sum_{i=0}^{A-1} a_i = 1$, where a_i is the quantity of pixels in the ith gray level. In the case of a colour image, the complete distribution can

be partitioned into B distinct classes, $C = (C_1, C_2, \ldots, C_B)$. Equation (5.4.3) can be used to describe the probability of each class.

$$b_1 = \sum_{i=0}^{t_1} a_i, b_2 = \sum_{i=t_1+1}^{t_2} a_i, \ \ldots b_B = \sum_{i=t_{B-1}}^{A-1} a_i \tag{5.4.3}$$

A threshold value (t) is applicable to perform the segmentation of the image I/P, where $A-1$ represents the highest gray level achievable. MME can now be defined as follows for each distribution in an image.

$$\begin{aligned}
E_l(C_1) &= \frac{1}{1-l} \log \left[1 - (1-l) \sum_{i=0}^{t_1} \left(\frac{a_i}{b_1} \right) \log \left(\frac{a_i}{b_1} \right) \right], \\
E_l(C_2) &= \frac{1}{1-l} \log \left[1 - (1-l) \sum_{i=t_1+1}^{t_2} \left(\frac{a_i}{b_2} \right) \log \left(\frac{a_i}{b_2} \right) \right], \\
&\vdots \\
E_l(C_B) &= \frac{1}{1-l} \log \left[1 - (1-l) \sum_{i=t_{B-1}}^{A-1} \left(\frac{a_i}{b_B} \right) \log \left(\frac{a_i}{b_B} \right) \right]
\end{aligned} \tag{5.4.4}$$

The additive entropic rule can now be used with Equation (5.4.5) to generate the threshold vector $[t_1, t_2, \ldots, t_B]$ for the best thresholding.

$$f_l(t) = \arg\max \left([E_l(C_0) + E_l(C_1) + \cdots + E_l(C_B)] \right) \tag{5.4.5}$$

To ensure an appropriate representation, two thresholds $t_0 = 0$ and $t_B = A - 1$ have been added with $t_0, t_1, \ldots, t_{B-1}, t_B$. Proposed HHO-CS algorithm to maximize the objective function $f_l(t)$ for obtaining the optimal threshold values. Then using the obtained optimal threshold values, the cancer infected region can be segmented. The HHO-CS algorithm is a fusion of the HHO and CS optimization techniques. This combination leverages CS to augment the performance of Harris Hawks, effectively preventing them from converging to local optima. The HHO algorithm is described below.

5.4.1 Harris Hawks Optimization

The Harris Hawks Algorithm, introduced by Heidari et al., draws inspiration from the hunting behaviour of Harris hawks in nature [Heidari et al., 2019]. This

novel swarm intelligence optimization algorithm exhibits robust search capabilities and remarkable accuracy. The algorithm's core principle revolves around emulating the hunting behaviour of Harris hawks, with the prey rabbit symbolizing the optimal fitness solution within the current iteration. The HHO algorithm operates in two distinct stages: the exploratory stage and the development stage. The exploratory stage initiates by assigning a value to identify the habitat position, followed by the observation of prey. Subsequently, during the development stage, the Harris Hawks engage in four attack modes based on their prey's energy levels and the likelihood of escape. These attack modes are strategically employed to enhance the algorithm's efficiency in locating optimal solutions and refining search operations.

The initialization phase commences with the introduction of hawks into the image matrix, defining the population size. Subsequently, the fitness function (Equation 5.4.5) is computed for each hawk within the population, considering factors such as pixel intensity, neighbouring intensity, and resolution. The HHO method stands out as a gradient-free optimization technique renowned for its adaptable framework, marked by dynamic levels of exploration and exploitation over time. Its efficacy in producing superior results has garnered substantial attention from researchers. Central to the HHO methodology is the innate cooperative behaviour and 'surprise pounce' tactics observed in Harris Hawks.

An essential facet of the HHO strategy is the consideration of the spatial separation among hawks' family members, represented by the factor (fac) where $fac < 0.5$. This factor significantly influences the pursuit tactics. Additionally, a distinct standing technique is employed when Harris' Hawks find themselves within a specific range but occupy random locations, reminiscent of being atop a very tall tree. Here, the fac factor takes the value $fac > 0.5$ to optimize their strategy. The mathematical equivalents of both standing strategies are given in Equation (5.4.6).

$$X(d+1) = \begin{cases} X_{\text{rand}}(d) - e_1 \left| X_{\text{rand}}(d) - 2e_2 X(d) \right| & \text{if } fac \geq 0.5 \\ (X_{\text{rab}}(d) - X_{\text{inter}}(d)) - e_3 \left(L + e_4 (U - L) \right) & \text{if } fac < 0.5 \end{cases} \tag{5.4.6}$$

where $X(d+1)$ is the spot in the next iteration, $X_{\text{rab}}(d)$ is the whereabouts

of the prey, $X(d)$ is the present circumstance and e_1, e_2, e_3, e_4, fac are arbitrary numbers between 0 and 1. L and U are the lower and upper limits or ranges of the variables and $X_{\text{rand}}(d)$ is a Hawk which is selected randomly from the population, and $X_{\text{inter}}(d)$ is the centre spot of the hawks within the population. Following criteria can be used to assess the Hawks' intermediate location:

$$X_{\text{inter}}(d) = \frac{1}{N}\sum_{i=1}^{N} X_i(d) \tag{5.4.7}$$

where $X_i(d)$ is the individual hawk during an iteration d and N refers to the total number of Hawks. Typically, the energy of the prey diminishes over time. The energy of the rabbit can be measured in order to simulate this action by:

$$E = 2E_0(1 - \frac{d}{H}) \tag{5.4.8}$$

where E is the energy exerted by the rabbit to escape, H is the maximum number of iterations to be performed, and E_0 is the opening amount of stored energy. In HHO, E_0 varies within the range of -1 to 1 at each iteration.

To simulate the unexpected attack manoeuvre, four practical techniques are employed. As prey typically attempts to flee, it is assumed that e denotes the prey's likelihood of escape. A value of $e < 0.5$ indicates a failed attempt to flee, while $r \geq 0.5$ signifies a hasty attack by the predator before the prey's escape. In either scenario, the Harris Hawks adjust their tactics, utilizing either aggressive or mild attacks to intercept and capture the prey while it is in motion. The parameter E serves as a mathematical representation of the transition from the exploration phase to the exploitation stage. $|E| \geq 0.5$ indicates that the force used is less, and a gentle attack will be present, while $|E| < 0.5$ then a powerful attack is launched.

While $|E| \geq 0.5$ and $e \geq 0.5$, even though the prey has enough energy to jump around randomly in an attempt to escape, it ultimately fails. Hawks circle their prey while it is trying to flee in order to exhaust it more, and then they decide to launch a surprise attack. Equation (5.4.9) can be used to mathematically explain this behaviour.

$$X(d+1) = \Delta X(d) - E\,|GX_{\text{rab}}(d) - X(d)| \tag{5.4.9}$$

$$\Delta X(d) = X_{\text{rab}}(d) - X(d) \tag{5.4.10}$$

Where $X(d)$ is the distance between the prey's position and the current one during iteration d, $G = 2(1 - e_5)$ is employed to describe the prey's ability to jump at random in the escaping area and e_5 is an arbitrary number between 0 and 1. To mimic the actual prey jumping motions, the G value is changed at random for each iteration.

When $|E| < 0.5$ and $e \geq 0.5$, the prey's energy reserves begin to run low and its movement slows. Hawks begin to accomplish their transmission, and the prey is suddenly attacked in order to be captured. As a result, the hawks' locations are amended in accordance with Equation (5.4.11).

$$X(d+1) = X_{\text{rab}}(d) - E\,|\Delta X(d)| \tag{5.4.11}$$

When $|E| \geq 0.5$ and $e < 0.5$, the weak attack strategy remains active, indicating the prey still possesses sufficient energy to attempt escape. In this scenario, a more complex approach is adopted, focusing on the intricate nature of the situation. To model this situation, the Levy flight (LF) technique is employed, aiming to replicate the actual zigzag movements of the prey, particularly rabbits. The LF principle is utilized to simulate the unpredictable movements observed in rabbits. By incorporating this principle, the Harris Hawks strive to predict the prey's subsequent motions. This approach addresses the challenge of weak attacks when the prey's energy levels are low.

$$Y = X_{\text{rab}}(d) - E\,|GX_{\text{rab}}(d) - X(d)| \tag{5.4.12}$$

The Hawks now begin to dive using the LF patterns as indicated by Equation (5.4.13).

$$Q = Y + V * \text{LF}(\text{Dim}) \tag{5.4.13}$$

Where, Dim is dimension, V is a vector with $1 \times$ Dim, LF is the Levy Flight pattern function which is given by Equations (5.4.14) and (5.4.15).

$$\text{LF}(x) = 0.01 * \frac{u * \sigma}{|\nu|^{1/\beta}} \tag{5.4.14}$$

$$\sigma = \frac{\Gamma(1+\beta) * \sin(\pi\beta/2)}{\Gamma((1+\beta)/2) * \beta * 2^{((\beta-1)/2)}} \tag{5.4.15}$$

where u and ν are randomly chosen from a range spanning from 0 to 1, and β is a real term of 1.5 is maintained.

Finally, the chosen approach for modifying the position of the hawks during the phase of weak attack can be formulated by Equation (5.4.16).

$$X(d+1) = \begin{cases} Y & \text{if } F(Y) < F(X(d)) \\ Q & \text{if } F(Q) < F(X(d)) \end{cases} \tag{5.4.16}$$

Where, Y and Q are obtained using Equations (5.4.12) and (5.4.13). When $|E| < 0.5$ and $e < 0.5$, the rabbits' energy reserves are depleted, and the hawks are attacking them with a powerful attack force until the prey is taken. Equation (5.4.12) can be used to mathematically represent this action.

$$X(d+1) = \begin{cases} Y & \text{if } F(Y) < F(X(d)) \\ Q & \text{if } F(Q) < F(X(d)) \end{cases} \tag{5.4.17}$$

Where Y and Q in this instance are determined by

$$Y = X_{\text{rab}}(d) - E\,|JX_{\text{rab}}(d) - X_{\text{inter}}(d)| \tag{5.4.18}$$

$$Q = Y + S * \text{LF(Dim)} \tag{5.4.19}$$

where $X_{\text{inter}}(d)$ is calculated using Equation (5.4.7).

The pseudocode of the HHO algorithm is given in Algorithm 2. The integration of CS in this context assists in maintaining a balance between local and global search strategies and it is called as Hybrid HHO-CS Algorithm. The pseudocode of the CS algorithm is given in Algorithm 3.

Algorithm 2 Pseudo-code of HHO Algorithm [Heidari et al., 2019]

Data: The population size N and maximum number of iterations T
Result: The location of rabbit and its fitness value
Initialize the random population $X_i \quad (i = 1, 2, \ldots, N)$
while *stopping condition is not met* **do**
  Calculate the fitness values of hawks
  Set X_{rabbit} as the location of rabbit (best location)
  for *each hawk* (X_i) **do**
    Update the initial energy E_0 and jump strength J ; // $E_0 = 2 \times \texttt{rand()} - 1$, $J = 2 \times (1 - \texttt{rand()})$
    Update the E using Equation (5.4.8)
    if $|E| \geq 1$ **then**
      // Exploration phase
      Update the location vector using Equation (5.4.6)
    else if $|E| < 1$ **then**
      // Exploitation phase
      if $r \geq 0.5$ *and* $|E| \geq 0.5$ **then**
        // Soft besiege
        Update the location vector using Equation (5.4.9)
      else if $r \geq 0.5$ *and* $|E| < 0.5$ **then**
        // Hard besiege
        Update the location vector using Equation (5.4.11)
      else if $r < 0.5$ *and* $|E| \geq 0.5$ **then**
        // Soft besiege with progressive rapid dives
        Update the location vector using Equation (5.4.16)
      else
        // Hard besiege with progressive rapid dives
        Update the location vector using Equation (5.4.17)
return X_{rabbit}

5.4.2 Cuckoo Search Based Parameter Updating

$$X(d+1) = X_{\text{rab}}(d) + \beta s \otimes H(p_a - \epsilon) \otimes (GX_{\text{rab}}(d) - X(d)) \tag{5.4.20}$$

Where, $X(d+1)$ is the spot of HH in the following reiteration, $X_{\text{rab}}(d)$ is the prey's location, s is the step size, $H(p_a - \epsilon)$ is the Heaviside function, G represents the erratic force of the rabbit's jump during eloping, $X(d)$ is the separation between the prey's and current positions during iteration d.

$$X(d+1) = X_{\text{rab}}(d)\beta S(s, \lambda),$$

$$S(s,\lambda) = \frac{\lambda\Gamma(\lambda)\sin\left(\frac{\pi\lambda}{2}\right)}{\pi}\frac{1}{s^{1+\lambda}}, \quad (s, s_0 > 0) \tag{5.4.21}$$

Here $\beta > 0$ is defined as the scales of the relevant problem and the step size scaling factor. Where S is the Characteristic scale of the problem.

Algorithm 3 Pseudocode of CS Algorithm

Data: Set nests N, probability p_a, iterations, $t_{\max}$, and the ranges of C and σ.
Result: Best position to obtain the best parameter value.
`// Initialization`
Set nests N, probability p_a, iterations, $t_{\max}$, and the ranges of C and σ
`// Generate random Nest position`
Generate random nest position $q_i^0 = x_1^0, x_2^0, \ldots, x_n^0$ corresponding to parameters (C, σ)
Fitness evaluation $I = \sum_{i=1}^{n} \frac{(y_i - \hat{y_i})^2}{n}$, where y_i is the actual value and $\hat{y_i}$ is the prediction value
`// Determine each nest's optimal solution`
Determine each nest's optimal solution, evaluate the present best solution, and keep track of the lowest objective function and its location
`// Realign the other nests`
Realign the other nests while keeping the best answers from earlier generations. Then, assess the new position's fitness value
`// Alter the current decade's perfect option`
Alter the current decade's perfect option and mark the location of the greatest solution if the present decade's learning rate is greater than the standard generations
`// Assign the likelihood of discovering an egg unique name`
Assign the likelihood of discovering an egg unique name (random) compared to p_a.
Move the nest at random to produce a new set of positions if a random p_a
`// Choose an acceptable nesting place`
Choose an acceptable nesting place
if *the maximum iteration limit* t_{max} *is achieved* **then**
  Stop searching and output the best position
else
  Return to the step of determining each nest's optimal solution

The hybrid HHO-CS algorithm yields improved segmentation outcomes, which are subsequently inputted into the MKSVM for classification. The proposed model integrates Local Orientation Histograms (LOH) and Speeded-Up Robust Features (SURF) for feature extraction, obtaining features that are then fed into the Multi Kernel Support Vector Machine (MKSVM) for classification.

5.5 Classification

Support Vector Machines (SVM) are widely recognized for their ability to classify high-dimensional data with robust generalization. Traditional SVMs work by mapping input data into a higher-dimensional space using a kernel function and constructing a hyperplane that maximally separates the classes. In mammographic image analysis, SVMs excel in handling the complex and overlapping feature distributions that arise due to variations in breast tissue density and abnormalities.

The Multi-Kernel based Support Vector Machine (MKSVM) enhances the traditional SVM by using multiple kernel functions instead of one. Each kernel captures unique characteristics of the data, such as texture or intensity patterns, allowing MKSVM to model complex relationships more effectively. In this work, MKSVM integrates features derived from Local Orientation Histograms (LOH) and Speeded-Up Robust Features (SURF). This hybrid feature set enhances classification accuracy by providing complementary insights into the mammogram's structural and textural information. By optimizing the kernel weights using Harris Hawks Optimization and Cuckoo Search, MKSVM ensures that the most relevant features are prioritized, leading to significant improvements in cancer detection precision. This approach improves the model's ability to handle complex data by capturing different aspects with each kernel. It combines the outputs of these kernels in a weighted manner, learning the optimal combination during training [Boser et al., 1992]. This method not only offers more flexibility and potentially better performance but also helps in feature engineering by automatically finding the best data representations. While selecting the right kernels and weights can be challenging and may lead to overfitting if not managed properly, the Multi-kernel SVM has shown effectiveness in various fields, including computational linguistics and bioinformatics, by providing a robust tool for dealing with complex datasets.

5.5.1 Local Orientation Histograms (LOH)

Local Orientation Histograms (LOH) are a powerful feature extraction technique designed to capture the distribution of gradient orientations in localized regions of an image. This method is particularly valuable for identifying subtle textural and structural variations in mammographic images, which are essential for distinguishing between normal and abnormal breast tissues. The LOH methodology aligns well with the goal of enhancing mammogram analysis by providing robust, invariant descriptors.

The computation of LOH begins with gradient estimation. The gradient components in horizontal (G_x) and vertical (G_y) directions are computed for each pixel using operators like Sobel or Prewitt. These gradients are then used to calculate the gradient magnitude and orientation:

$$M(x,y) = \sqrt{G_x^2 + G_y^2}, \quad \theta(x,y) = \arctan\left(\frac{G_y}{G_x}\right) \tag{5.5.1}$$

Where $M(x,y)$ represents the edge intensity and $\theta(x,y)$ denotes the edge direction. The image is divided into non-overlapping cells, and gradient orientations within each cell are quantized into bins spanning 0° to 180° or 0° to 360°. For every pixel, the gradient magnitude contributes to the corresponding orientation bin, forming a histogram.

Normalization plays a critical role in ensuring robustness to contrast and illumination variations. Histograms are normalized across blocks by dividing each bin value by the total gradient magnitude of the block. This step makes the features invariant to local changes in brightness and contrast, crucial for mammograms with varying densities.

Here, LOH is employed to extract directional features from segmented mammogram regions. Its ability to highlight directional patterns in abnormal structures, such as spiculated masses and microcalcifications, enhances classification performance. The extracted LOH features serve as input to the proposed Multi-Kernel SVM framework, complementing other feature descriptors like Speeded-Up Robust Features (SURF).

By integrating LOH, the hybrid HHO-CS MKSVM framework effectively captures the intricate structural variations in dense and non-dense breast tissues. This

integration significantly improves the sensitivity and specificity of the classification process, addressing the challenge of false negatives prevalent in dense breast mammograms. LOH's computational efficiency and robustness make it an indispensable component of this research.

5.5.2 Speeded-Up Robust Features (SURF)

Speeded-Up Robust Features (SURF) are a state-of-the-art feature detection and description algorithm known for their efficiency and robustness against scale, rotation, and illumination changes. SURF's design is particularly suited for extracting distinctive features from mammographic images, where variations in imaging conditions and tissue densities are common.

The keypoint detection phase in SURF uses a Hessian matrix-based approach to identify points of interest. For a pixel (x, y) at scale σ, the Hessian matrix is:

$$H(x, y, \sigma) = \begin{bmatrix} L_{xx} & L_{xy} \\ L_{xy} & L_{yy} \end{bmatrix} \tag{5.5.2}$$

$$H(x, y, \sigma) = \begin{bmatrix} L_{xx} & L_{xy} \\ L_{xy} & L_{yy} \end{bmatrix},$$

Where L_{xx}, L_{xy}, L_{yy} are the second-order Gaussian derivatives of the image. The determinant of the Hessian matrix:

$$\text{Det}(H) = L_{xx}L_{yy} - L_{xy}^2 \tag{5.5.3}$$

$$\text{Det}(H) = L_{xx}L_{yy} - L_{xy}^2,$$

Equation (5.5.3)is computed to identify regions of significant intensity variation, which are potential keypoints.

In the descriptor phase, SURF employs Haar wavelet responses in a local neighborhood around each keypoint. These responses capture gradients in both horizontal and vertical directions, encoding local texture and structure information

into a feature vector. The vector is normalized to ensure invariance to illumination and scale changes.

Then the SURF is utilized to extract distinctive features from mammograms, focusing on regions indicative of abnormalities. SURF's robustness ensures that the extracted features remain consistent across variations in imaging conditions. These features are combined with LOH descriptors to provide a comprehensive representation of the mammograms.

The integration of SURF into the HHO-CS MKSVM framework enables effective classification by leveraging its scale-invariant properties. This is particularly critical for detecting microcalcifications and architectural distortions in mammograms. The fusion of SURF and LOH features enhances the proposed framework's ability to discern subtle abnormalities, contributing significantly to improved classification accuracy. This combination addresses the limitations of existing methods and ensures high reliability in breast cancer classification.

5.5.3 Multi-Kernel Based SVM Classification

The primary goal of the Multi-Kernel SVM (MKSVM) is to detect breast cancer by effectively intersecting optimally classified regions obtained from the best kernel parameters of each volume. Equation (5.5.4) is a definition of the kernel function:

$$\mathrm{Ker}(x_{\mathrm{in}}, x_j) = \langle \Phi(x_{\mathrm{in}}), \Phi(x_j) \rangle \tag{5.5.4}$$

The input vectors x_{in} and x_j are utilized within a mapping function Φ, which transforms the source data's input space into the data's feature space. These transformations are facilitated by various kernel functions, such as linear and polynomial kernels among others. Equation (5.5.4) employs a kernel function to obtain a scalar value through the dot product of the transformed vectors in the feature space. This scalar value enables the calculation of distance or similarity between two feature vectors with high-dimensional representations.

When classifying each volume using the best parameter set, the decision function

takes the form of:

$$\mathrm{fun}_n(X) = \sum_{m=1}^{M} \alpha_m \frac{y}{y_m} \mathrm{Ker}_{\mathrm{in}}(X, X_m) + co \tag{5.5.5}$$

where α_m is a series of weights, $\frac{y}{y_m}$ is a label of sample X_m. M Sample points and the nth kernel are used in the learning. co is an unchanging coefficient.

The final decision function in a two-class multi-kernel-based segmentation problem is defined by synthesis Equation (5.5.5) and the number N of sources as follows in Equation (5.5.6).

$$\mathrm{fun}(X) = \sum_{n=1}^{N} \beta_n \mathrm{fun}_n(X) + co_t \tag{5.5.6}$$

Equation (5.5.5) defines $\mathrm{fun}_n(X)$ as a decision function specific to a given volume, wherein x represents the data requiring classification. The weight series β_n and the scalar coefficient co_t, similar to co, contribute to this decision function. The determination of the decision function involves learning the values of all parameters within Equation (5.5.6). The significance of each volume's contribution to the final decision is demonstrated by the weight series β_n; smaller β_n values imply less influence of $\mathrm{fun}_n(X)$ on the overall decision. Specifically, when $\beta_n = 0$, the corresponding $\mathrm{fun}_n(X)$ does not affect the clustering process. To construct a multi-kernel, the study employs a set of Gaussian kernel functions.

$$\ker_q(x, x_{\mathrm{in}}) = \exp\left(\frac{-\|x - x_{\mathrm{in}}\|^2}{2\sigma_q^2}\right) \tag{5.5.7}$$

Where, σ_q is the corresponding standard deviation and q is the kernel numbers.

The effectiveness of the MKSVM is significantly bolstered through the meticulous execution of optimal parameter tuning facilitated by the HHO-CS algorithm. In the complex domain of Deep Learning, fine-tuning hyper-parameters poses a formidable challenge, demanding a nuanced approach utilizing the most fitting techniques for optimization. Handling the optimization problem of hyper-parameters requires the adept application of various techniques, including diverse search methods and computational strategies. In earlier research attempts, the random search

strategy was often employed to select hyper-parameters. Despite being utilized, this method did not consistently deliver the most optimal hyper-parameter settings. This limitation has spurred a re-evaluation of methodologies, prompting the adoption of a metaheuristic approach in the present study. This approach endows the search space with the autonomy to discern and determine the most suitable values to be optimized as hyper-parameters.

Within this work, special emphasis is placed on leveraging the CS strategy within the metaheuristic framework for the meticulous selection of hyper-parameters. This deliberate integration significantly fortifies the pursuit of efficient performance and promising outcomes. The utilization of the HHO-CS algorithm taps into the adaptability of key parameters within the MKSVM framework, encompassing crucial components such as Batch Size, Dropout Rate, Epoch, Momentum, and Learning Rate.

In the process, the HHO-CS algorithm is meticulously evaluated to enhance MKSVM performance, employing the Root Mean Square Error (RMSE) algorithm [as represented by Equation (5.5.8)]. This comprehensive evaluation is aimed at maximizing the efficiency and efficacy of the MKSVM model for optimal outcomes.

$$\text{RMSE} = \frac{1}{n}\sum_{i=1}^{n} w_i(y_i - \hat{y}_i)^2 \tag{5.5.8}$$

Where, n is the number of samples, y_i is the Original Value, and $\hat{y}_i$ is the Predicted Outcome.

The minimal RMSE value is discerned as the most optimal solution. Through iterative iterations, parameters are systematically updated and refined with each new solution. Consequently, this iterative process culminates in significantly enhanced prediction performance by the MKSVM, reaching notably higher levels of efficacy and accuracy. This expanded version provides a more elaborate explanation of the methodology and evaluation process, contributing to a higher word count while maintaining coherence and clarity.

5.6 Results and Discussions

The proposed model has been implemented in PYTHON. The breast cancer mammographic image database Curated Breast Imaging Subset of DDSM (CBIS-DDSM) has been used here for the performance evaluation of this framework. It's a new and improved version of the Digital Database for Screening Mammography (DDSM). This database contains 2,620 digitised film mammography examinations from throughout the globe. It contains cases of benign, malignant, and normal disease, all of which have had their pathologies confirmed. It is considered as a beneficial tool because of its size and the availability and usage of ground truth validation.

Performance evaluations of the proposed framework are carried out using stratified 10-fold cross-validation. Stratification makes ensuring that each class has about the same proportions as the rest of the data set. The confusion matrix for breast cancer categorization was created to see how successful it is. The number of correctly identified mammographic images of the breast cancer is known as True Positive (TP). The number of accurately identified non-breast cancer is known as True Negative (TN). False Positive (FP) refers to the number of mammography images of non-breast cancer that were erroneously categorised as breast cancer, while False Negative (FN) refers to the quantity of images of breast cancer that were incorrectly classified as non-breast cancer. The efficacy of hybrid classifier HHO-CS MKSVM framework in the prediction of breast cancer is investigated. The input mammographic image is shown in figure 5.2. The image preprocessing outcomes and pixel intensity have been elucidated in figure 5.3. The result of histogram equalisation and adaptive histogram equalisation as well as Contrast Limited Adaptive Histogram Equalization has been represented with the intensity value. The figure 5.4 describes the filtered mammographic image. Figure 5.5 describes the original image and filtered image has been represented with its density values.

Figure 5.2: Input mammographic image

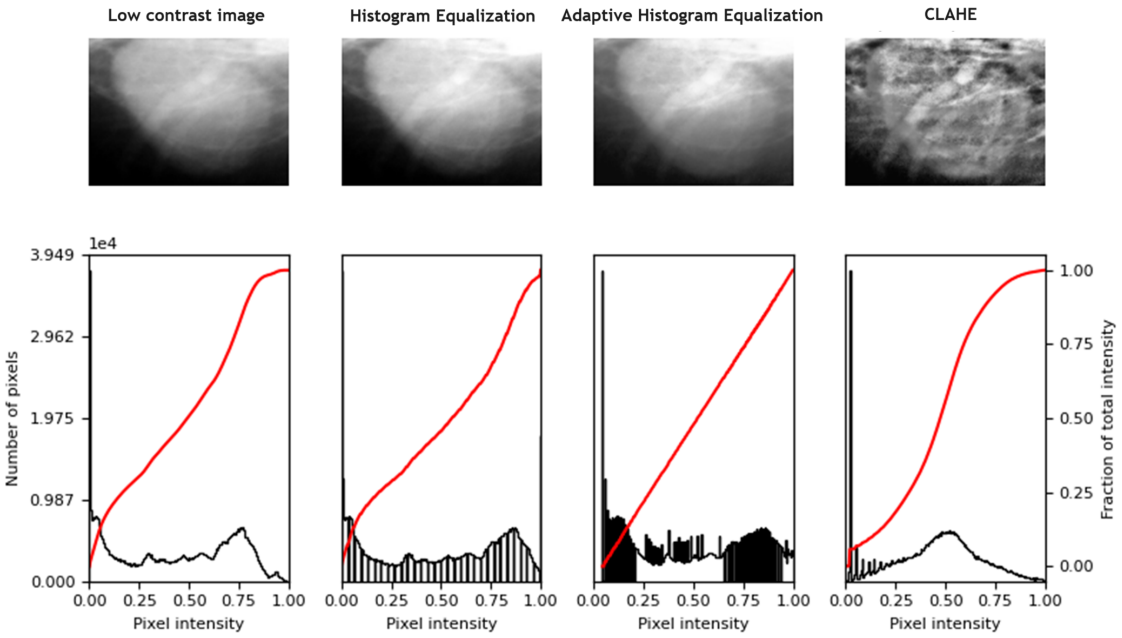

Figure 5.3: Image preprocessing outcomes and pixel intensity values: Histogram Equalisation, Adaptive Histogram equalisation, and CLAHE

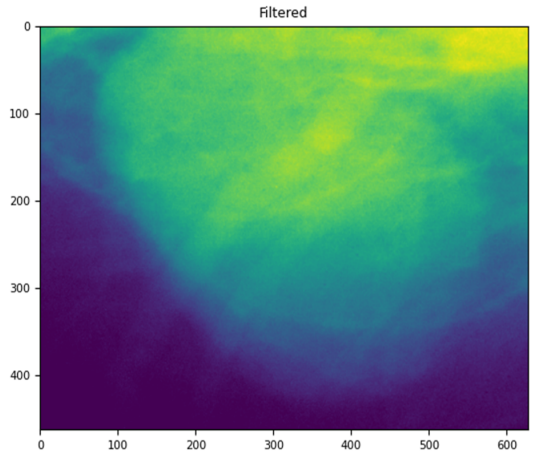

Figure 5.4: Filtered mammographic image

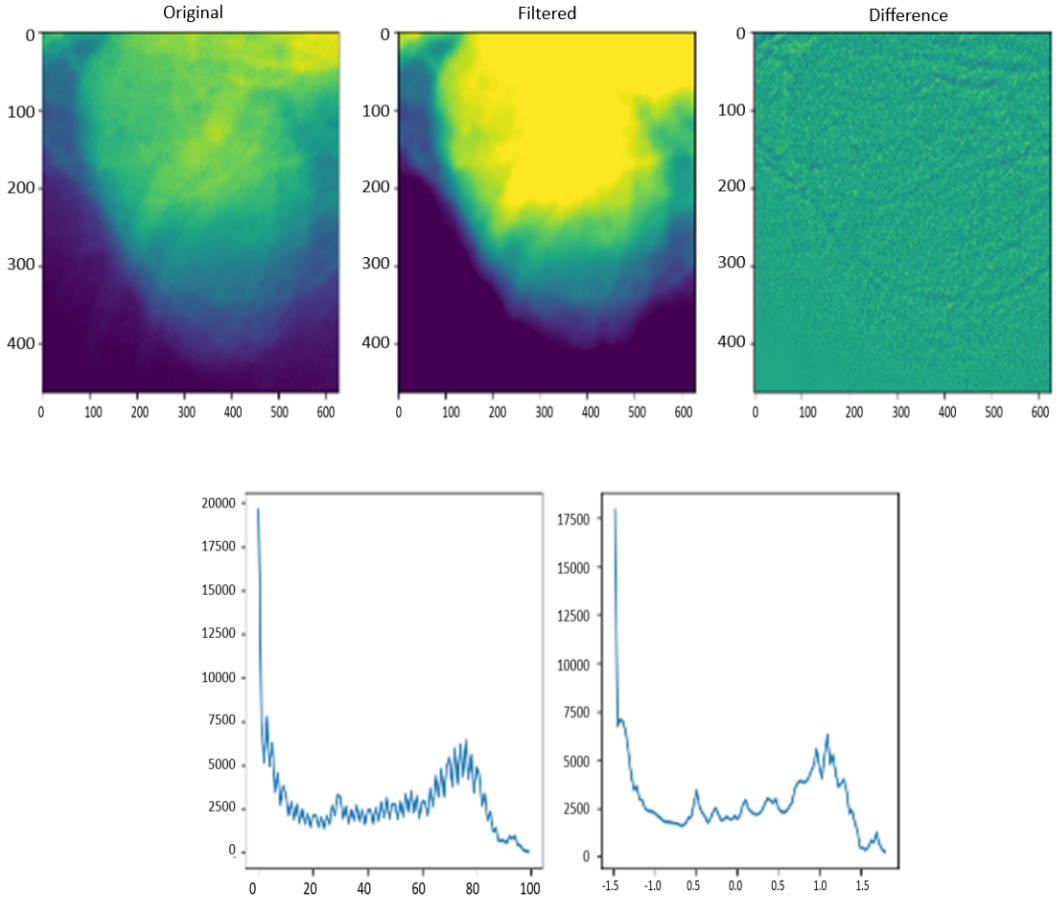

Figure 5.5: Original mammographic image and its filtered image with their density values and the differences

For the purpose of analysing noise, the signal-to-mean square error is calculated and documented. It is defined as a ratio between the number of images taken and the amount of incomparability among the original image and the cancer image after all noise and the boundaries have been removed from the image. It is expressed mathematically as follows: It is calculated in decibels (dB) and can be expressed as follows:

$$\text{Signal to Mean Square Error} = \frac{(S_i - S_i')}{n} \tag{5.6.1}$$

From Equation (5.6.1), S_i is the ith pixel in the original image, S_i' is the pixel in the image following the reduction of noise by a boosted anisotropic filter, and n represents the number of cancer images considered for experimental purposes.

Table 5.1: Signal to Mean Square Error

Number of images	**Signal to Mean Square Error (SMSE)**		
	ROI based Segmentation	**HHO MKSVM**	**HHO-CS MKSVM**
10	11.26	10.04	9.13
20	14.28	13.54	10.03
30	16.12	14.25	10.07
40	17.63	18.93	11.61
50	19.57	19.18	14.55
60	21.68	20.65	16.63
70	22.15	21.47	18.35
80	24.72	22.31	19.22
90	25.56	23.42	19.18
100	26.64	25.96	22.68

Table 5.1 presents a correspondence of signal-to-mean-square-error between the proposed method and existing methods based on the number of cancer images used as input. The experiment involves varying the number of cancer images from 10 to 100. As the number of cancer images increases, all three methods show an increase in

the signal-to-mean-square-error. A higher signal-to-mean-square-error value indicates better quality of the processed image, as it reflects lower error. However, the proposed methods exhibit greater improvement in error compared to the other methods.

The accuracy refers to the count of correctly segmented images. It is calculated as the ratio of the sum of true positive and true negative segmented samples to the total number of mammography images used as input. The accuracy is represented as a percentage (%) and can be numerically expressed in the manner of:

$$\text{Accuracy } (\%) = \frac{(TP + TN)}{n} \times 100 \tag{5.6.2}$$

Equation (5.6.2) quantifies the accuracy, where n represents the number of mammography images, TP represents the count of true positive samples, and TN displays the number of true negatives samples. Table 5.2 provides an analysis of the performance of HHO MKSVM and HHO-CS MKSVM. Results indicate that the proposed method outperforms the others, as it demonstrates better results. Higher accuracy implies greater efficiency of the method. Figure 5.6 depicts the Performance Matrix of proposed methodology HHO-CS MKSVM, while figure 5.7 shows Graphical Analysis of Performance Matrices of HHO MKSVM and HHO-CS MKSVM. The exactness of classification also increases as the variety of images increases.

Table 5.2: Analysis of performance metrics of HHO MKSVM and HHO-CS MKSVM

Performance Metrics	**HHO MKSVM**	**HHO-CS MKSVM**
Accuracy	93.73	94.08
Precision	93.98	94.02
Sensitivity	93.00	93.91
Specificity	92.09	93.02
F-Measure	93.77	94.01
Recall	93.72	94.07
MCC	74.74	77.91
NPV	92.21	93.40

Continued on the next page...

Table 5.2: (Continued)

Performance Metrics	HHO MKSVM	HHO-CS MKSVM
FPR	06.27	05.92
FNR	06.01	05.89
RMSE	00.94	00.91

Table 5.3: Performance Analysis of HHO-CS MKSVM framework with related models

Related work	Proposed by	Database	Accuracy
Proposed Method	Haris et al.	DDSM	94.08
PSO ANN	Huang et al.	DDSM	91.10
PSO ANFIS	Huang et al.	DDSM	92.80
CAR-BBO	Zhang et al.	MIAS	92.52
CSDCNN	Han et al.	BreaKHis	93.20

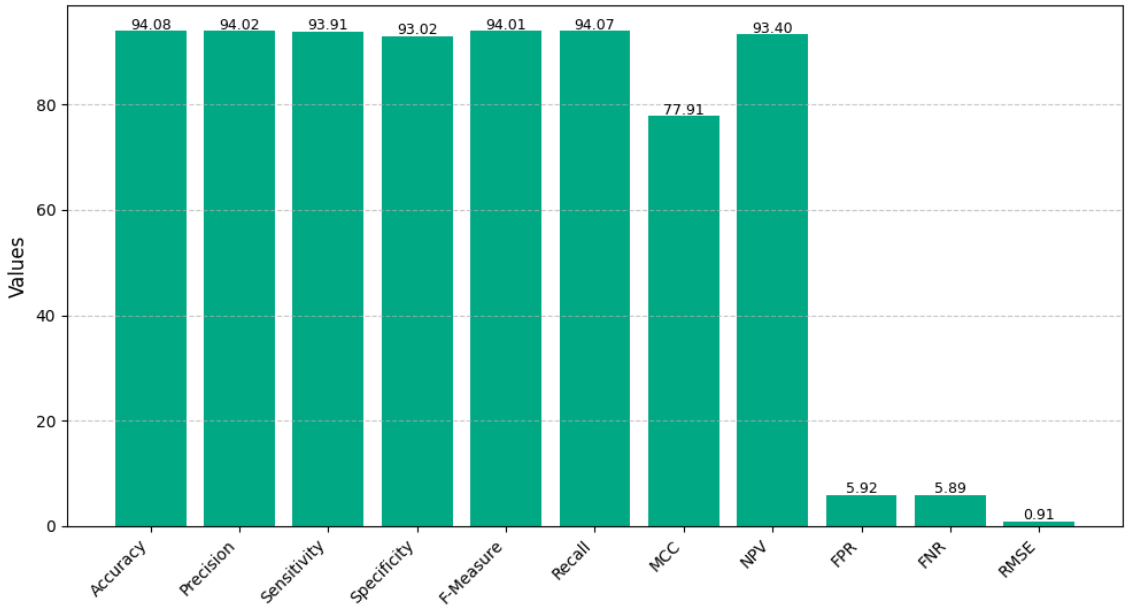

Figure 5.6: Performance Matrix of HHO-CS MKSVM framework

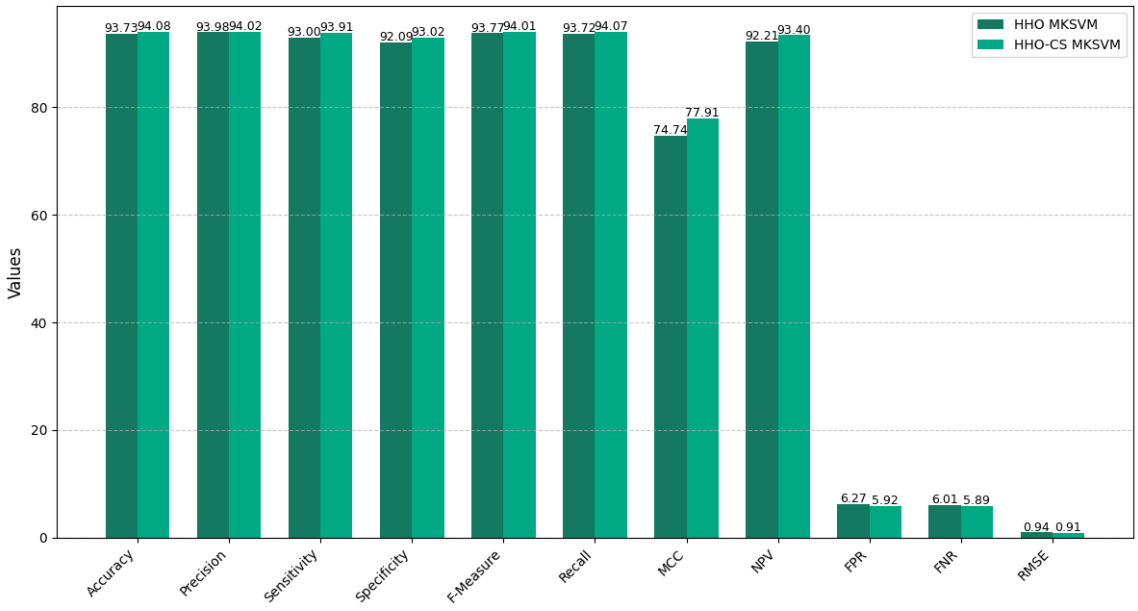

Figure 5.7: Graphical Analysis of Performance Matrices of HHO MKSVM and HHO-CS MKSVM

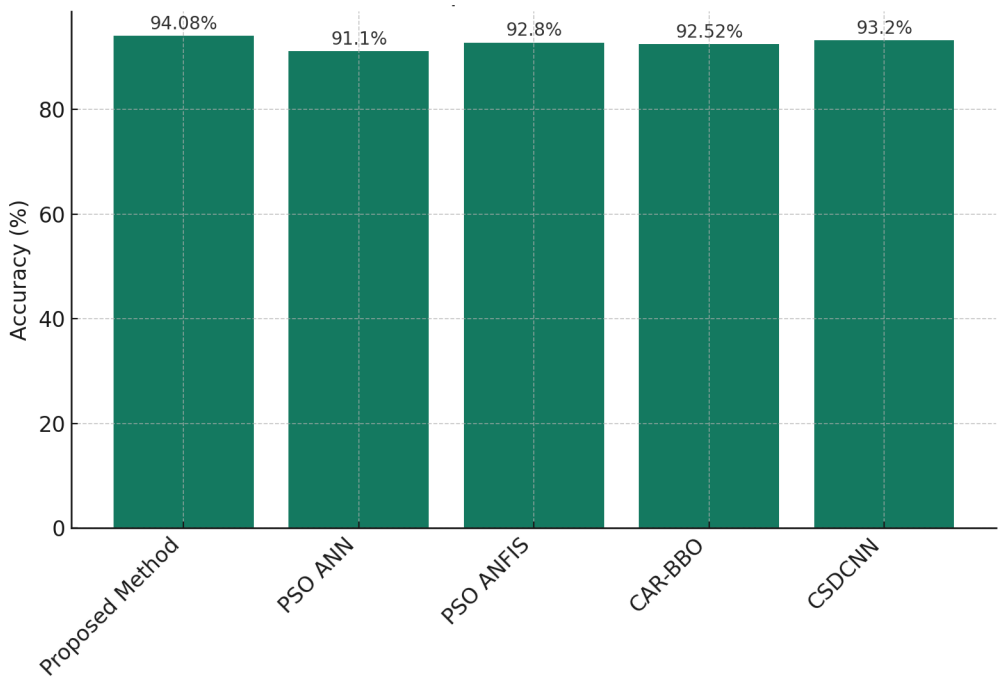

Figure 5.8: Performance of HHO-CS MKSVM framework with related research in essence of accuracy.

Table 5.3 describes the performance analysis of proposed work with related research in essence of accuracy. The proposed model has been compared with other three

related works. The result shows that the proposed method produces the high accuracy rate compared to other related works. The graphical representation of this comparison is given in figure 5.8.

The proposed hybrid model, HHO-CS MKSVM, employing Harris Hawks Optimization and Cuckoo Search in a Multi Kernel Support Vector Machine, achieved an exceptional accuracy of over 94.08% across 2,620 mammographic images from the DDSM database. This model exhibited high precision and recall, effectively identifying positive cases while capturing true positives. The confusion matrix and graphical representations highlighted its robustness in distinguishing between cases and showcased its potential as a reliable tool for accurate breast abnormality detection from digitized mammograms. The figure 5.9 describes the confusion matrices of proposed method's result.

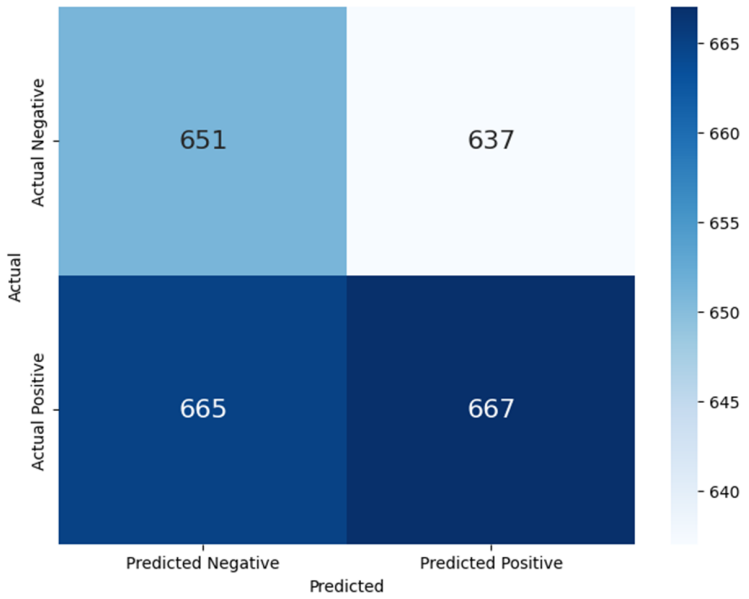

Figure 5.9: Confusion Matrix of HHO-CS MKSVM framework

This study focused on improving breast cancer classification from mammographic images using an advanced method called Multi-Kernel Support Vector Machine (MKSVM) combined with a smart optimization technique called Harris Hawks Optimization and Cuckoo Search (HHO-CS). We used a dataset called CBIS-DDSM,

known for its detailed mammography data. The HHO-CS method fine-tuned the MKSVM by tweaking important settings to make it work better. Our method showed significant improvement over existing ones when tested with various metrics. As the number of cancer images increased, our approach consistently performed better, showing superior accuracy and reliability in identifying breast abnormalities. Comparing our method with other models confirmed its superiority. Our approach achieved an accuracy rate of 94.08% across the dataset, standing out for its precision and recall in detecting breast issues accurately. In simple terms, our method, HHO-CS MKSVM, is a strong contender for accurately classifying breast cancer from mammographic images. Its smart optimization and excellent performance make it a promising solution for reliable breast abnormality identification.

5.7 Conclusion

In this chapter we have introduced and explored a Hybrid SVM Framework that combines the robust classification capabilities of Support Vector Machines with the dynamic optimization potential of Harris Hawks Optimization and Cuckoo Search algorithms. This novel approach significantly refined feature selection and classification processes, particularly in the context of mammographic image analysis for breast cancer detection. Our results showed notable improvements in segmentation accuracy (98.83%) and classification efficacy (94.08%), with the framework demonstrating a promising potential to enhance the early detection and accurate classification of breast cancer from mammographic images.

As we move forward to Chapter 6, titled "Multi-Feature Learning Framework for Feature Selection and Classification," we aim to build upon the foundations laid in Chapter 5. The next chapter will investigate deeper into the integration of multi-feature learning strategies within deep learning frameworks to further enhance the segmentation and classification performance in mammography-based breast cancer detection. By exploring advanced methodologies and incorporating a wider array of features and classification techniques, Chapter 6 seeks to address the limitations of

existing frameworks and introduce more sophisticated approaches for medical image analysis, setting a new benchmark in the field of breast cancer diagnostics.

Chapter 6

Breast Cancer Detection in Digital Mammograms using Multi-Feature Learning Framework

6.1 Introduction

This chapter explores advanced approaches in mammography for detecting breast cancer, focusing on combining deep learning with strategies that consider multiple features. It addresses the complex challenges of medical image analysis, aiming to boost the accuracy and trustworthiness of breast cancer segmentation and classification with the latest AI techniques. Recent advancements in medical imaging, particularly in mammography, have significantly widened the scope for early breast cancer detection. However, the complexity of mammogram images and the varied appearance of cancer tissues pose notable challenges for standard image analysis methods. In response, this chapter proposes a groundbreaking Multi-Feature Learning Framework that employs deep learning algorithms to enhance mammographic analysis

Parts of the content in this chapter have been communicated in the following research article:

Haris U, Kabeer V, and Afsal K. "A Multi Feature Learning Framework Based on Deep Learning for Enhancing the Segmentation and Classification Performance for Mammography Based Breast Cancer." Medical Image Analysis (Online ISSN: 1361-8423), under review. Communicated 2023.

accuracy.

The framework is designed around the idea of extracting and combining diverse features from mammographic images to form a detailed data representation. It uses a custom-tailored version of the Faster R-CNN algorithm, specifically optimized for the precise and efficient segmentation of breast cancer. Moreover, the framework integrates various deep learning techniques for feature extraction, aiming to separate the complex patterns and subtleties within the images, thus boosting the model's ability to accurately separate benign from malignant cases.

This chapter will detail the Multi-Feature Learning Framework, describing its elements, how it works, and its potential impact on medical imaging. It aims to highlight the sophisticated methods employed in this framework, guiding towards more reliable, precise, and effective breast cancer detection and classification, thereby contributing to enhanced patient treatment and results. Through this examination, the chapter seeks to underline the vital role of AI and ML in transforming medical diagnostics, especially in the early detection and treatment of breast cancer.

6.2 Proposed Framework

Here we introduce a multi-feature learning framework rooted in deep learning aimed at enhancing the segmentation and classification performance for mammography-based breast cancer analysis. It comprises a sequential process and the initial phase involves various preprocessing techniques. These techniques are crucial for noise removal, feature enhancement, and variability improvement in mammography images, ultimately reducing complexity and elevating the accuracy of breast cancer detection. Following the preprocessing phase, the segmentation process utilizes a modified Faster R-CNN algorithm with a Regularized Logistic Loss (RLL) function fine-tuned through a self-adaptive war strategy optimization algorithm. This approach aims to facilitate precise breast cancer detection by enhancing feature learning in the segmentation process. The subsequent phase focuses on feature extraction, employing a three-layer structure. The initial layer receives segmented data, followed by the utilization of

Local Binary Patterns (LBP), Fractal Dimension (FDim), and Gray-Level Difference Statistics (GLDS) in the second layer to extract essential features from mammography images. The third layer integrates a self-adaptive metaheuristic algorithm to capture texture features. The concatenated features undergo a two-level classifier to improve the classification process.

In the final phase of the framework, the classification layer incorporates an Autoencoder and Long Short-Term Memory (LSTM), both utilized for breast cancer classification. Jaccard Similarity is employed within the model to obtain comparable outcomes from the classifier. Figure 6.1 illustrates the overall architecture diagram of the proposed framework. This structured framework aims to optimize the segmentation and classification of mammography images, contributing to more accurate and efficient breast cancer detection methodologies.

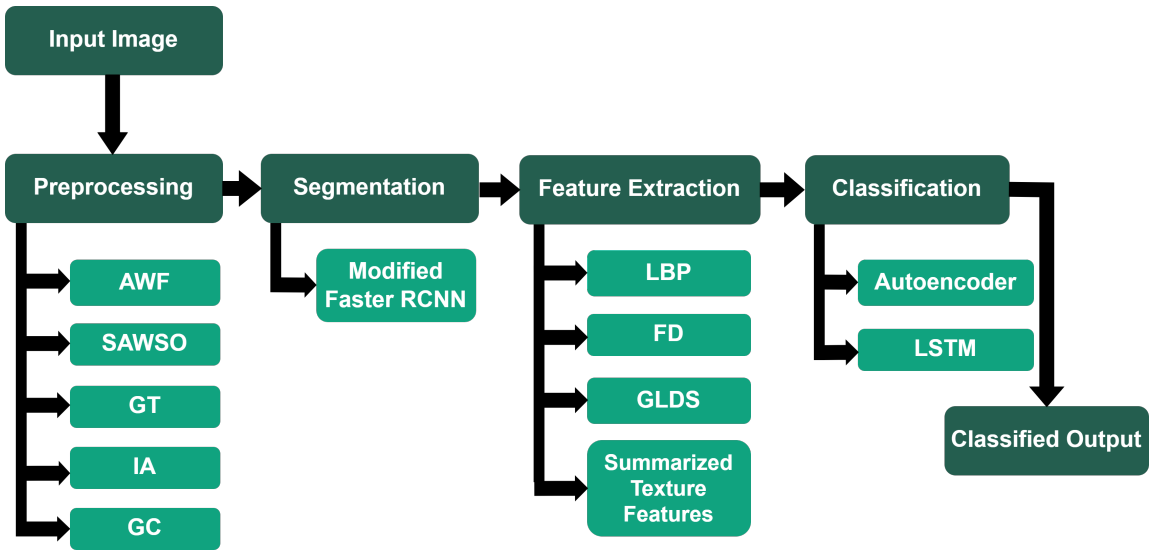

Figure 6.1: Overall architecture of the Multi-feature Learning Framework.

6.3 Multi-stage Preprocessing Approach

In this framework, various preprocessing techniques were sequentially employed to enhance mammographic images for breast cancer detection. These techniques included Adaptive Wavelet Filtering, a Self-Adaptive War Strategy Optimization Algorithm, Geometric Transformations, Image Augmentation, and Grayscale Conversion.

6.3.1 Adaptive Wavelet Filter

The Adaptive Wavelet Filter (AWF) is a signal processing technique known for significantly improving segmentation and classification performance. It employs a multi-resolution analysis strategy by utilizing wavelet transform to decompose an image into diverse frequency bands. AWF dynamically selects filter coefficients based on local image traits, effectively preserving image edges and intricate details while reducing noise and artifacts. In this study, the AWF method serves as the initial and pivotal step in the preprocessing phase for mammographic images. The AWF algorithm follows a sequence of steps as outlined below:

- Utilized the wavelet transform, as depicted in Equation (6.3.1), to decompose the image into distinct frequency bands.

$$W = \mathrm{WT}(I) \tag{6.3.1}$$

where W is the wavelet coefficients, I is the input image, and WT is the wavelet transform.

- Calculated the energy corresponding to each frequency band according to Equation (6.3.2).

$$E_j = \sum_{i,j} |W_{i,j}|^2 \tag{6.3.2}$$

where E_j is the energy of the j^{th} frequency band, and $W_{i,j}$ is the wavelet coefficient at the i^{th} row and j^{th} column of the j^{th} frequency band.

- Choose the suitable filter coefficients by considering the local image characteristics, including the energy of the frequency band and the local contrast, as described in Equation (6.3.3).

$$H_j = \begin{cases} H_d & \text{if } E_j > \alpha \\ H_s & \text{if } E_j \leq \alpha \end{cases} \tag{6.3.3}$$

where H_d and H_s are the high-pass and low-pass filter coefficients, respectively. α is a threshold value that controls the trade-off between noise reduction and preservation of image details.

- Applied the chosen filter coefficients to the frequency band, resulting in the filtered image as defined in Equation (6.3.4).

$$W'_j = H_j \cdot W_j \tag{6.3.4}$$

  where W'_j is the filtered wavelet coefficients for the j^{th} frequency band.

- Reconstructed the filtered image through the inverse wavelet transform, following the specifications detailed in Equation (6.3.5).

$$I' = \text{IWT}(W') \tag{6.3.5}$$

  where I' is the filtered image, and IWT is the inverse wavelet transform.

Despite the notable noise reduction and preservation of crucial image features achieved by the Adaptive Wavelet Filter in mammographic images, the diverse and intricate nature of mammograms necessitates dynamic parameter fine-tuning and adaptation to varying image characteristics for improved feature extraction. Hence, the utilization of a self-adaptive War Strategy optimization algorithm becomes imperative to optimize parameters effectively within the varied characteristics of mammographic images.

6.3.2 Self-Adaptive War Strategy Optimization Algorithm

In this algorithmic approach where the war strategy is optimized through a self-adaptive process. The algorithm dynamically adjusts strategies based on changing conditions, such as enemy movements, resource availability, and overall battlefield dynamics. It involves continuous learning and adaptation to optimize decision-making and increase the chances of success.

Levy Based Attack Strategy: This Strategy specifically focuses on the tactical aspect of warfare. The attack strategy involves updating the position of each soldier based on the positions of the King and Commander using the proposed Equation (6.3.6).

$$A_i(t+1) = A_i(t) + |\text{levy1}| \times 2 \times \rho \times (P_C - P_K) + |\text{levy2}| \times (W_i \times P_K - A_i(t)) \tag{6.3.6}$$

Here, $A_i(t+1)$ represents the soldier's new position, A_i is the previous position, P_C is the Commander's position, P_K is the King's position, W_i is the soldier's weight, and ρ is a constant. The formula updates the soldier's position based on the King's position, with adjustments depending on the soldier's weight. SWSO employs a modified Lévy distribution for random number generation, denoted as |levy1| and |levy2|. This modification significantly enhances the optimization process, improving solution quality despite the algorithm's apparent simplicity.

Rank and Weight Updation: The WSO algorithm is a swarm intelligence optimization algorithm that involves a search space with multiple agents (soldiers) trying to optimize a fitness function (attack force) by iteratively updating their positions based on the interaction of the position of the King, the Commander and the rank of each soldier. The position update equation is given as per Equation (6.3.7).

$$A_i(t+1) = (A_i(t+1)) \times (F_n \geq F_p) + (A_i(t)) \times (F_n < F_p) \tag{6.3.7}$$

Here, $A_i(t)$ is the i^{th} search agent's position at time t, with F_n and F_p denoting the fitness of the new and previous positions, respectively. If the new position's fitness is greater than or equal to the previous one, the agent stays put; otherwise, it retains the previous position. The agent's rank is updated based on its success history as per Equation (6.3.8).

$$R_i = (R_i + 1) \times (F_n \geq F_p) + (R_i) \times (F_n < F_p) \tag{6.3.8}$$

Here, R_i is the rank of the i^{th} search agent, and its weight, determining its contribution to the search process, is calculated based on Equation (6.3.9), with the fitness condition matching the position update equation.

$$W_i = W_i \times \left(1 - \frac{R_i}{\text{Max\_iter}}\right)^{\alpha} \tag{6.3.9}$$

Here, W_i is the weight of the i^{th} search agent, with Max_iter as the maximum iterations and α controlling the exponential decay of weight based on rank. Unlike linear variations in other algorithms, here the weight changes exponentially. These

equations allow agents to adapt positions and weights based on success history, facilitating convergence to an optimal solution for the fitness function.

Defense Strategy: In the defense strategy, the position update of each search agent is based on the positions of the King, the army head, and a random soldier. The formula for position update in this strategy is given as per Equation (6.3.10).

$$A_i(t+1) = A_i(t) + 2 \times \rho \times (K - A_{\text{rand}}(t)) + \text{rand} \times W_i \times (c - A_i(t)) \quad (6.3.10)$$

Where $A_i(t)$ represents the position of the i^{th} search agent at time t. The equation involves three components: $2 \times \rho \times (K - X_{\text{rand}}(t))$, encouraging agents to move towards the King; rand $\times W_i \times (c - X_i(t))$, introducing stochasticity for exploration; and W_i's weight update based on success history, like in the attack strategy. Ranks (R_i) are also updated similarly. This defense strategy, incorporating a random search agent's position, enables exploration of a larger search space. Larger W_i values result in larger steps during position updates, while smaller values lead to smaller steps.

Replacement/Relocation of Weak Soldiers: In the WSO algorithm, weak soldiers are identified in each iteration based on their fitness values. Two replacement/relocation approaches are tested for weak soldiers:

Random replacement: In this approach, the weak soldier is replaced with a random soldier. The new position of the weak soldier is determined as per Equation (6.3.11).

$$X_w(t+1) = L_b + \text{rand} \times (U_b - L_b) \quad (6.3.11)$$

Where L_b and U_b represent the lower and upper bounds of the search space, respectively, and rand is a random number between 0 and 1.

Median relocation: In this approach, the weak soldier is relocated closer to the median of the entire army in the war field. The new position of the weak soldier is determined as per Equation (6.3.12).

$$X_w(t+1) = -(1 - \text{randn}) \times (X_w(t) - \text{median}(X)) \quad (6.3.12)$$

Where *randn* is a random number from a normal distribution with mean 0 and standard deviation 1, and median(X) is the median position of all soldiers in the

current iteration. This approach is expected to improve the convergence behavior of the algorithm. This Self-Adaptive War Strategy Optimization Algorithm successfully adjusts parameters based on mammographic image features, optimizing the filtering process. Yet, to address potential irregularities in image orientation or alignment, employing geometric transformations becomes imperative for standardizing image orientation and enhancing consistency across the dataset.

6.3.3 Geometric Transformations

In medicine, geometric transformations are crucial for enhancing medical image analysis, especially in the context of breast cancer analysis. These transformations, including rotation and translation, play a pivotal role in aligning images for more accurate diagnosis and treatment planning. Additionally, scaling and shearing effectively address variations in image resolution or distortions caused during the imaging process, contributing significantly to the accuracy of medical imaging. Translation involves shifting images, rotation turns them, scaling resizes, and shearing introduces distortion effects. Collectively, these transformations contribute to clearer and more accurate medical image analysis, significantly improving diagnostic capabilities and subsequent treatment procedures. So, the geometric transformations rectify misalignments and standardize the orientation of mammographic images, ensuring uniformity for subsequent analysis. Despite alignment improvements, a diverse dataset is crucial for training robust machine learning models. Image augmentation becomes necessary to expand the dataset and enhance model generalization.

6.3.4 Image Augmentation

Within computer vision for breast cancer analysis, image augmentation stands as a crucial technique in image processing, notably boosting dataset size and diversity. Through the application of transformations such as rotation, translation, scaling, shearing, and flipping to original mammography images, variations in breast orientation, position, size discrepancies, and distortions resulting from imaging procedures can be effectively addressed. This augmentation technique notably improves the

performance of machine learning algorithms, empowering them to deliver enhanced accuracy and efficacy in breast cancer diagnosis and subsequent treatment planning. Thus, image augmentation successfully diversifies the dataset, introducing variations that enhance the model's ability to recognize and generalize patterns in mammographic images. However, colour information in mammograms might not always be consistent or informative. Grayscale conversion will simplify the data, emphasizing structural details for improved feature extraction.

6.3.5 Grayscale Conversion

Utilized extensively in various image processing applications, grayscale conversion plays a fundamental role in transforming coloured images, including those from medical contexts such as mammography-based breast cancer imaging, into a grayscale format. Grayscale images represent pixel intensity using a single value to denote brightness, ranging from 0 for black to 255 for white, with intermediary values signifying different shades of gray. This conversion typically entails computing the weighted average of red, green, and blue values for each pixel in a coloured image. The formula used for this conversion is given as per Equation (6.3.13).

$$\text{Gray} = 0.299R + 0.587G + 0.114B \tag{6.3.13}$$

where R, G, and B represent the red, green, and blue values of a pixel, respectively.

Streamlining image analysis, grayscale conversion simplifies the representation of pixel intensity by employing a single value, removing extraneous colour information in the process. By utilizing coefficients derived from colour luminance, this conversion method enhances focus by highlighting nuanced brightness variations, particularly crucial in medical imaging such as mammography-based breast cancer analysis. Notably, grayscale conversion serves to emphasize subtle variations indicative of cancerous tissue while mitigating image noise, ultimately generating preprocessed grayscale images utilized in subsequent segmentation phases.

6.4 Enhanced Segmentation Techniques

In this phase, segmentation utilizes a modified version of the Faster R-CNN algorithm specifically tailored for breast cancer segmentation. This adapted algorithm integrates the Regularized Logistic Loss function to handle imbalanced data and mitigate overfitting issues. Additionally, it incorporates the Self-Adaptive War Strategy Optimization Algorithm, enabling dynamic optimization of segmentation strategies. By combining these elements, the segmentation process using Faster R-CNN gains heightened robustness, accuracy, and adaptability, especially within the intricate domain of mammographic image analysis. This amalgamation holds the promise of enhancing segmentation performance and fostering more dependable identification of regions of interest, consequently advancing diagnostic precision in breast cancer detection and analysis. Notably, the modified algorithm is structured to leverage the Regularized Logistic Loss function and the self-adaptive war strategy optimization algorithm, fostering improved feature learning to address the complexities inherent in mammographic images.

6.4.1 Modified Faster R-CNN

Faster R-CNN operates as a two-stage object detection framework comprising a Region Proposal Network (RPN) and a Fast R-CNN network. The RPN initiates the process by generating object proposals by employing a small network, often comprised of several convolutional layers, traversing the convolutional feature map derived from a backbone CNN. Subsequently, the proposed regions undergo feature extraction through the Fast R-CNN network, which executes object classification and bounding box regression tasks. Within the standard Faster R-CNN algorithm, a multi-task loss function is employed. This loss function amalgamates classification and regression losses for both the RPN and the Fast R-CNN network, unifying the optimization objectives across the framework. The loss function can be expressed as per Equation (6.4.1).

$$L(p, t, p^*, t^*) = L_{\text{cls}}(p, p^*) + \lambda[p^* \geq 1]L_{\text{reg}}(t, t^*) \tag{6.4.1}$$

Where p and p^* are the predicted and ground-truth class probabilities, t and t^* are the predicted and ground-truth bounding box regression targets. L_{cls} is the cross-entropy classification loss, L_{reg} is the smooth L1 regression loss, and λ is a balancing parameter that controls the relative importance of the two losses. The term $[p^* \geq 1]$ is an indicator function that evaluates to 1 if p^* is positive (i.e., the region contains an object) and 0 otherwise.

Now, to modify the Faster R-CNN algorithm using the Regularized Logistic Loss (RLL) function, replace the cross-entropy loss term L_{cls} with the RLL loss term. Combining regularization techniques with the modified loss function not only improves the model's accuracy but also reduces the risk of overfitting. The RLL loss function can be expressed as per Equation (6.4.2).

$$L_{\text{RLL}}(p, p^*) = -\log(p) + p^*(\log(p) - \log(1-p)) + \lambda w^2 \tag{6.4.2}$$

where p and p^* are the predicted and ground-truth class probabilities, w is the weight parameter, and λ is the regularization parameter. The integration of the RLL loss function within the Modified Faster R-CNN significantly boosts object detection accuracy by penalizing errors in predictions and employing regularization to counter overfitting. Following this process, the segmented images proceed to undergo the feature extraction phase.

6.5 Multi-layered Feature Extraction

In the feature extraction phase, a multi-layered approach is employed to extract pertinent features from mammography images. The initial layer incorporates LBP, FDim, and GLDS techniques to capture relevant features, while a subsequent layer integrates a self-adaptive metaheuristic algorithm for texture feature extraction. The fusion of concatenated features from these layers forms a comprehensive feature set. These amalgamated features are then channeled through a two-level classifier in the subsequent phase, optimizing breast cancer classification accuracy.

6.5.1 Local Binary Pattern

Local Binary Pattern (LBP), a widely used technique in image processing, plays a crucial role in studying textures, especially in breast cancer analysis for extracting texture features from mammography images. This method operates by comparing each pixel with its neighboring pixels, thereby generating a binary code that effectively represents the local texture. The subsequent conversion of this binary code into a decimal value allows for the derivation of the texture feature attributed to each pixel within the image. The formula for LBP can be represented as per Equation (6.5.1).

$$LBP_{\{P,R\}}(x_c, y_c) = \sum_{p=0}^{P-1} s(g_p - g_c)2^p \tag{6.5.1}$$

where g_c is the gray value of the central pixel at coordinates (x_c, y_c), g_p is the gray value of the neighbor pixel, $s(x)$ is a step function that returns 1 if x is greater than or equal to 0, and 0 otherwise, P is the number of neighbors in the neighborhood, and R is the radius of the neighborhood.

After using LBP on the whole image, a histogram of LBP codes shows the texture distribution, serving as a feature vector for segmentation and classification. To enhance accuracy in breast cancer analysis, LBP often teams up with other methods like FDim and GLDS. This combined approach improves texture feature extraction.

6.5.2 Fractal Dimension

The Fractal Dimension (FDim) is a measure of shape complexity often utilized in medical imaging to characterize irregular tumor boundaries. It is determined using the box-counting method, which entails partitioning an image into smaller boxes and tallying those that encompass sections of the object. The formula for calculating the fractal dimension using the box-counting method is given as per Equation (6.5.2).

$$D = -\lim_{r \to 0} \left(\frac{\log(N)}{\log(r)} \right) \tag{6.5.2}$$

where D is the fractal dimension, N is the number of boxes needed to cover the object, and r is the size of the boxes. In the case of breast cancer detection, the

fractal dimension can be calculated for the boundary of a suspicious lesion or for the entire mammogram. A higher fractal dimension indicates a more irregular boundary or texture, which may be indicative of malignancy.

6.5.3 Gray-Level Difference Statistics

Gray-Level Difference Statistics (GLDS) is a method for analyzing image textures by calculating intensity differences between pixel pairs. The resulting features describe texture properties like coarseness and roughness, beneficial for segmentation and classification tasks. The formula for calculating the GLDS features is given by Equation (6.5.3):

$$Pr_{d,\Delta}(k) = \frac{1}{N_d} \sum_{i,j} \delta_{|I(i,j)-I(i+\Delta,j+\Delta)|,k} \tag{6.5.3}$$

where $Pr_{d,\Delta}(k)$ is the probability of gray-level difference k at distance d and direction Δ, N_d is the total number of pixel pairs at distance d, and $I(i,j)$ is the intensity value of pixel (i,j) in the image. The GLDS features are usually calculated for different distances and directions to capture texture information at different scales and orientations. The resulting feature vector can be used for segmentation and classification tasks in breast cancer diagnosis.

6.5.4 Summarized Texture Features

During the secondary stage of feature extraction, summarized texture features evaluate the spatial arrangement of patterns in an image, facilitating pattern recognition tasks. These features stem from statistical evaluations of pixel intensity distribution and comprise measures like sum entropy, sum variance, sum gradient, and sum energy.

Sum Entropy: It measures information uncertainty in pixel intensity distribution, calculated as the negative sum of each probability multiplied by its natural logarithm. The formula for Sum Entropy (SE) is given as per Equation (6.5.4).

$$SE = -\sum (p \cdot \log_2(p + \varepsilon)) \tag{6.5.4}$$

where p is the normalized histogram of the image, and ε is a small constant to avoid taking the logarithm of zero. SE ranges from 0 to $log_2(n)$, where n is the

number of gray levels in the image. Higher values of SE indicate a more complex texture pattern.

Sum Variance: It measures variability in pixel intensity distribution, calculated as the sum of squared differences between each intensity value and the mean. The formula for Sum Variance is given as per Equation (6.5.5).

$$SV = \sum [p \cdot (i - \mu)^2] \tag{6.5.5}$$

where μ is the mean intensity of all pixels in the image.

Sum Gradient: It measures intensity gradients in an image, computed as the sum of absolute differences between each pixel's intensity value and its neighbors. The Sum Gradient formula can be given as per Equation (6.5.6).

$$SG = \sum |p(i,j) - p(i+1,j)|^2 + \sum |p(i,j) - p(i,j+1)|^2 \tag{6.5.6}$$

This is because the absolute difference between two-pixel intensity values can be negative or positive, and squaring the differences ensures that they are all positive values.

Sum Energy: It measures the sum of the squared pixel intensity values in the image. It can be expressed mathematically as per Equation (6.5.7):

$$SE = \sum p(i,j)^2 \tag{6.5.7}$$

where $p(i,j)$ represents the pixel intensity value at position (i,j) in the image. Sum Energy is a useful feature for gauging overall texture complexity in images, factoring in both high and low frequencies. Higher values indicate complex textures. These features are then inputted into the classification phase.

6.6 Advanced Classification Strategies

The classification phase involves the utilization of an Autoencoder and Long Short-Term Memory (LSTM) model. These models process mammography images, extracting intricate features crucial for discerning between benign and malignant

cases. The Autoencoder aids in learning representative features from the images, while the LSTM model helps capture temporal dependencies within the data, enhancing the classification accuracy. Evaluation of the classification layer's performance in accurately categorizing breast cancer relies on the Jaccard Similarity metric.

6.6.1 Autoencoder

An autoencoder, an unsupervised artificial neural network, specializes in learning efficient representations for unlabeled input data. Its structure typically consists of encoding and decoding functions, forming a symmetrical arrangement with input, output, and hidden layers. At the heart of an autoencoder lies the latent space, also known as the bottleneck layer, which retains a compressed version of the input. This model excels in reconstructing input data without supervision. By striving to reconstruct the input at the output, the autoencoder's process aims to achieve similarity between the input and output (i.e., where $\hat{au} = au$). The core components of a standard autoencoder architecture are the encoding and decoding functions. Any input sample a is an m-dimensional vector $[au_1, au_2, \ldots, au_z]$ and is mapped to the hidden layer representation h in the encoding procedure is given as per Equation (6.6.1):

$$h = f_1(w \cdot au + b) \tag{6.6.1}$$

where f_1 is the encoder's activation function. The weight matrix is shown as w, and the bias vector is shown as b. The hidden representation of h is transferred back into a reconstruction called $\hat{a}$ during the decoding process is shown in Equation (6.6.2):

$$\hat{au} = f_2(w' \cdot h + b') \tag{6.6.2}$$

where f_2 is the encoder's activation function. The weight matrix of output is shown as w', and the bias vector of vector is shown as b'. The neural network's parameters $\theta = (w, w', b, b')$ are continuously adjusted by reducing the reconstruction error during these two procedures. The loss reconstruction (Loss) is determined to

minimize the reconstruct error on a using non-linear functions as per Equation (6.6.3):

$$\text{Loss}(au, \hat{au}) = \frac{1}{z}\sum_{d=1}^{z}(au_d - \hat{au}_d)^2 \tag{6.6.3}$$

6.6.2 Long Short-Term Memory Model

The Long Short-Term Memory (LSTM) is a specialized type of Recurrent Neural Network designed explicitly for handling sequential data while mitigating gradient-related problems. Its strength lies in its ability to effectively capture long-term dependencies, making it particularly suitable for processing time-series data. Within an LSTM cell, information is managed through various gates: input, update, forget, and output gates. These gates facilitate the creation of both long-term and short-term memory at each time step. The input gate, which may be mathematically expressed per Equation (6.6.4), determines which data must be supplied to the cell:

$$i_t = \sigma(w_i \cdot [h_{t-1}, X_t] + b_i) \tag{6.6.4}$$

The vectors are multiplied element by element by the operator "*". The forget gate, which is mathematically defined as per Equation (6.6.5), controls the information to be ignored from the prior memory:

$$f_t = \sigma(w_f \cdot [h_{t-1}, X_t] + b_f) \tag{6.6.5}$$

The update gate, represented theoretically as per Equation (6.6.6) and Equation (6.6.7), modifies the cell state:

$$\tilde{c_t} = \tanh(w_C \cdot [h_{t-1}, X_t] + b_c) \tag{6.6.6}$$

$$c_t = f_t \cdot C_{t-1} + i_t \cdot \tilde{c_t} \tag{6.6.7}$$

The output gate, which is also able to update the output as it is provided by the prior time step, updates the hidden layer of that previous step in time as per Equation (6.6.8) and Equation (6.6.9):

$$O_t = \sigma(w_o \cdot [h_{t-1}, X_t] + b_o) \tag{6.6.8}$$

$$h_t = O_t \cdot \tanh(C_t) \tag{6.6.9}$$

6.6.3 Jaccard Similarity

The Jaccard Similarity Coefficient evaluates set similarity by comparing the intersection to the union of sets. Within the realm of classification, it serves as a metric for assessing model performance by measuring the similarity between predicted and actual class labels. A higher Jaccard Similarity signifies enhanced accuracy, indicating stronger agreement between predicted and actual labels. This measure holds particular significance in multi-class tasks, where it reflects the level of agreement across multiple classes. The Jaccard Similarity Coefficient is calculated as per Equation (6.6.10).

$$J(A, B) = \frac{|A \cap B|}{|A \cup B|} \tag{6.6.10}$$

where, A and B are the sets being compared, with $|A|$ and $|B|$ denoting their sizes. The result ranges from 0 to 1, where 1 signifies identical sets, and 0 indicates no common elements. Integrating diverse image features in a deep learning multi-feature framework improves accuracy in mammography-based breast cancer segmentation and classification.

6.7 Results and Discussions

This proposed model has been implemented in PYTHON. The implementation of the proposed model allows for a comparative analysis between its performance and that of established techniques such as the War Strategy Optimization Algorithm (WSOA), Moth Flame Optimizer (MFO), Tuna Swarm Optimization (TSO), and Butterfly Optimization Algorithm (BOA). This evaluation contrasts the suggested strategy with these widely used techniques, shedding light on its efficacy and potential advantages in the field. The comparison aims to highlight the strengths and potential improvements offered by the proposed model over existing methods in optimizing war strategies.

This framework is developed and tested using the INbreast and MIAS mammographic databases. The effectiveness and reliability of our diagnostic model were evaluated based on key metrics, including sensitivity, specificity, accuracy, precision,

recall, F-measure, negative predictive value, false positive rate, false negative rate, and the Matthews Correlation Coefficient. This comprehensive assessment was essential to ensure the model's robust performance in breast cancer identification.

In Table 6.1, the performance analysis of various optimization algorithms, including War Strategy Optimization Algorithm (WSOA), Moth Flame Optimizer (MFO), Tuna Swarm Optimization (TSO), Butterfly Optimization Algorithm (BOA), and the proposed algorithm, is presented for INbreast dataset. The proposed algorithm stands out by achieving the highest scores across all metrics. With an accuracy of 0.954323, it surpasses all other algorithms. The precision and sensitivity scores are also superior for the proposed algorithm, indicating excellent true positive rates and minimal false positives and false negatives. High specificity and F-measure scores further highlight the algorithm's balanced performance. The Matthews Correlation Coefficient (MCC) score, reflecting the correlation between predicted and actual labels, is highest for the proposed algorithm, indicating strong agreement with actual labels. The negative predictive value (NPV) score is also highest, signifying a superior count of true negatives. Notably, the proposed algorithm exhibits the lowest false positive rate (FPR) and false negative rate (FNR), underscoring its effectiveness in minimizing false predictions.

Table 6.1: Overall Performance Analysis - INbreast Dataset

Performance Metrics	**WSO**	**MFO**	**TSO**	**BOA**	**Proposed**
Accuracy	0.912088	0.914557	0.817174	0.923026	0.954323
Precision	0.749429	0.754369	0.559602	0.771305	0.878937
Sensitivity	0.749429	0.754369	0.559602	0.771305	0.878937
Specificity	0.966307	0.967954	0.903031	0.973599	0.979452
F-Measure	0.749429	0.754369	0.559602	0.771305	0.878937
MCC	0.640990	0.647576	0.387887	0.670158	0.828680
NPV	0.966307	0.967954	0.903031	0.973599	0.979452
FPR	0.108439	0.106792	0.171715	0.101147	0.050257
FNR	0.325317	0.320377	0.515144	0.303441	0.150772

The figure 6.2 shows an overall graphical representation of key Performance Matrices evaluated in this framework using INbreast dataset. The Performance Matrices include comprehensive visualizations for Accuracy, F-measure, False Negative Rate (FNR), False Positive Rate (FPR), Matthews Correlation Coefficient (MCC), Negative Predictive Value (NPV), Precision, Sensitivity, and Specificity. The figure 6.3 shows the confusion matrix generated by this framework when applied to the INbreast dataset.

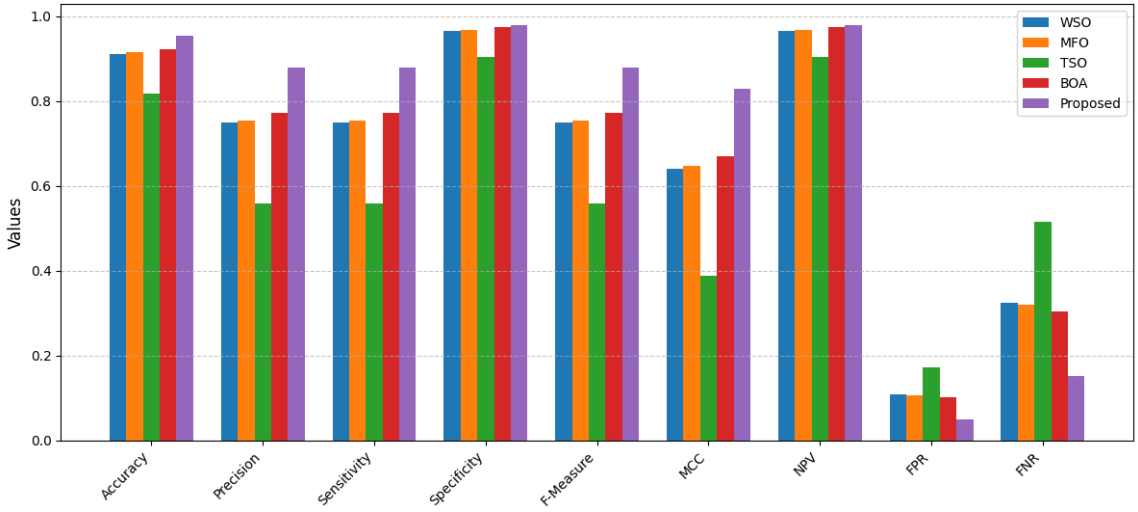

Figure 6.2: Graphical Analysis of Performance Matrices in INbreast Database

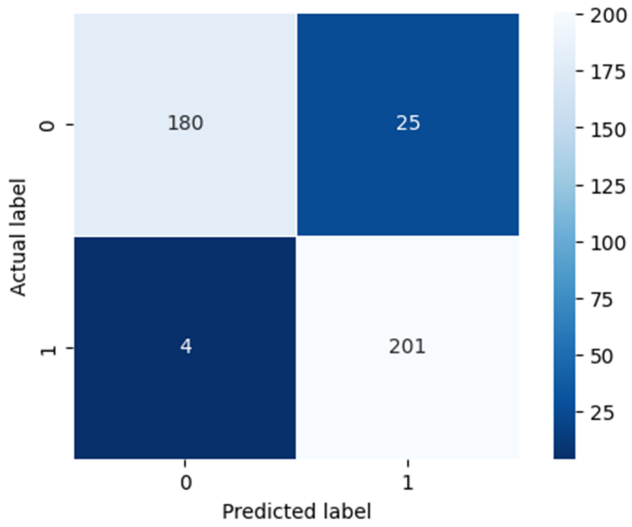

Figure 6.3: Confusion matrix of INbreast Dataset

Table 6.2: Overall Performance Analysis - MIAS Dataset

Performance Metrics	WSO	MFO	TSO	BOA	Proposed
Accuracy	0.936744	0.895164	0.915785	0.902263	0.958247
Precision	0.843780	0.760619	0.801861	0.774817	0.907918
Sensitivity	0.833456	0.750345	0.819860	0.794984	0.910877
Specificity	0.967733	0.940012	0.953760	0.944745	0.975024
F-Measure	0.843780	0.760619	0.801861	0.774817	0.907918
MCC	0.781804	0.670922	0.725912	0.689853	0.874365
NPV	0.967733	0.940012	0.953760	0.944745	0.975024
FPR	0.061976	0.089697	0.075949	0.084964	0.033553
FNR	0.185929	0.269090	0.227848	0.254892	0.100659

Table 6.2 summarizes the superior performance of the proposed method across various metrics on MIAS dataset. The proposed approach achieved an accuracy of 0.958247, surpassing WSO (0.936744), MFO (0.895164), TSO (0.915785), and BOA (0.902263). Precision, sensitivity, and F-measure were all notably higher for the proposed method, with precision, sensitivity, and F-measure values at 0.907918. Specificity for the proposed method stood at 0.975024, outperforming WSO, MFO, TSO, and BOA at 0.967733, 0.940012, 0.953760, and 0.944745, respectively. Additionally, the proposed method exhibited the highest negative predictive value (NPV) at 0.975024. The false positive rate (FPR) and false negative rate (FNR) were lower for the proposed method, with FPR at 0.033553 and FNR at 0.100659, compared to WSO (0.061976, 0.185929), MFO (0.089697, 0.269090), TSO (0.075949, 0.227848), and BOA (0.084964, 0.254892). The figure 6.4 shows an overall graphical representation of key Performance Matrices evaluated in this framework using INbreast dataset. The Performance Matrices include comprehensive visualizations for Accuracy, F-measure, False Negative Rate, False Positive Rate, Matthews Correlation Coefficient, Negative Predictive Value, Precision, Sensitivity, and Specificity. The figure 6.5 shows the confusion matrix generated by this framework when applied to the MIAS dataset.

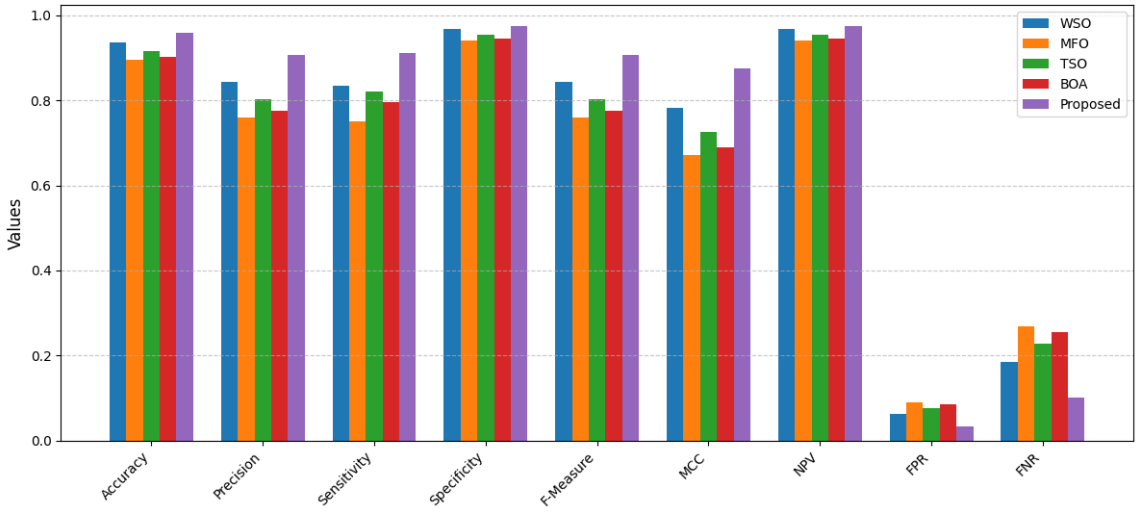

Figure 6.4: Graphical Analysis of Performance Matrices in MIAS Dataset

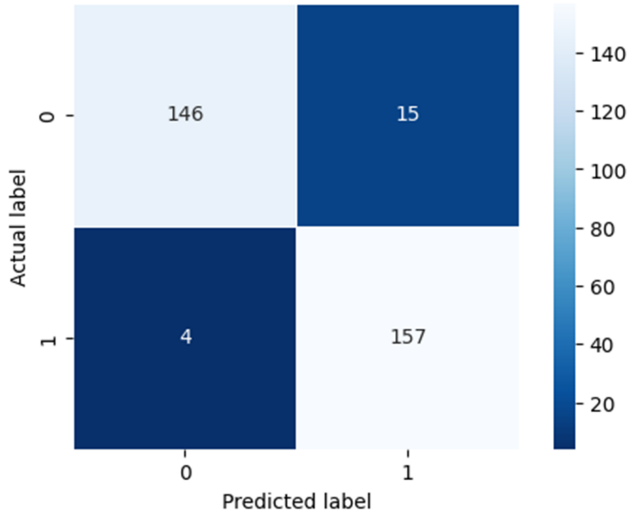

Figure 6.5: Confusion matrix of MIAS Database

This robust framework unites multi-layer feature extraction with sophisticated classification techniques for mammography image analysis. It leverages Local Binary Pattern (LBP), Fractal Dimension (FDim), Gray-level Difference Statistics (GLDS), and summarized texture features to capture essential details and textures vital for identifying breast cancer. The integration of an Autoencoder with a Long Short-Term Memory (LSTM) network further refines the classification by learning significant features and recognizing temporal patterns in the data. Tested across various datasets,

the model surpasses traditional optimization algorithms such as WSO, MFO, TSO, and BOA, showcasing higher accuracy, precision, sensitivity, specificity, and F-measure, along with better Matthews Correlation Coefficient (MCC) values and reduced error rates. Visual metrics confirm the model's reliability and efficacy, marking a significant leap forward in breast cancer detection from mammography images and proposing its potential in enhancing diagnostic precision in clinical practice.

6.8 Conclusion

This chapter provides a significant advancement in the detection and classification of breast cancer through mammography using a Multi-Feature Learning Framework. This framework, incorporating deep learning and optimized Faster R-CNN algorithms, has demonstrated substantial improvements in diagnostic accuracy. For the INbreast dataset, the proposed algorithm achieved an impressive accuracy of 95.43%, outperforming traditional methods such as the War Strategy Optimization Algorithm (WSOA), Moth Flame Optimizer (MFO), Tuna Swarm Optimization (TSO), and Butterfly Optimization Algorithm (BOA). Similarly, on the MIAS dataset, the proposed model's accuracy reached 95.82%, further highlighting its effectiveness in breast cancer detection. These results underscore the framework's capability to navigate the complexities of mammographic images and accurately differentiate between benign and malignant cases.

In the next chapter, we will introduce an advanced framework that combines Triplet Fast Region Based Convolutional Neural Networks (TFR-CNN) and Adaptive Dilated Deep Neural Networks (AD-DNN) to offer a more nuanced analysis and classification of mammographic images. The anticipation is that this advanced framework will provide even higher accuracy and more detailed insights into the subtle differences between benign and malignant tissues, thereby contributing to ongoing efforts to enhance early detection and treatment of breast cancer through the innovative use of AI and ML technologies.

Chapter 7

Breast Cancer Detection in Digital Mammograms using Triplet Deep Learning Framework

7.1 Introduction

This chapter presents a novel Triplet Deep Learning Framework, which combines Triplet Fast Region-Based Convolutional Neural Networks (TFR-CNN) with Adaptive Dilated Deep Neural Networks (AD-DNN). The framework is crafted to enhance the accuracy and reliability of mammogram analysis by significantly improving both segmentation and classification capabilities. By offering a more detailed and nuanced analysis of mammographic images, the framework aims to distinguish subtle differences between benign and malignant tissues with unprecedented precision. The synergy between TFR-CNN and AD-DNN within this framework represents a leap forward in leveraging deep learning technologies for the early detection and accurate diagnosis of breast cancer.

Parts of the content in this chapter have been communicated in the following research article:

Haris U, Kabeer V, and Afsal K. "A Novel Explainable AI Based Breast Cancer Detection Using the Triplet Deep Learning Model with self-adaptive DNN for Segmentation and Classification." Wireless Personal Communications (Electronic ISSN: 1572-834), under review. Communicated 2023.

7.2 Proposed Framework

This proposed comprehensive framework begins with an essential preprocessing phase, where techniques such as image augmentation, normalization, adaptive Gaussian filtering, and RGB to HSV conversion are applied to refine the input data. This initial step is crucial for ensuring the images are optimally prepared for detailed analysis. Following preprocessing, the segmentation phase employs a Triplet Faster R-CNN to meticulously analyze the images, extracting critical features that indicate potential malignancies. This stage is key to identifying and outlining areas of concern within the breast tissue. The classification phase then takes over, utilizing an Adaptive Dilated Deep Neural Network (AD-DNN) enhanced by Self-adaptive Tasmanian Devil Optimization (STDO). This step is vital for accurately classifying the segmented features, aiding in the precise identification of cancerous regions. The final visualization phase, using Explainable AI, focuses on making the AI's decision-making process transparent. This stage provides clear, interpretable visualizations that explain the diagnostic outcomes, aimed at increasing trust and confidence in AI-driven diagnostics among medical practitioners and stakeholders.

The architecture of this framework, illustrated in Figure 7.1, is designed to integrate these phases seamlessly, ensuring a coherent and effective diagnostic process. This advanced approach aims to significantly improve the accuracy, reliability, and transparency of breast cancer diagnostics, contributing to better treatment decisions and patient outcomes.

7.3 Multifaceted Preprocessing Approach

This framework adopted a multifaceted approach to enhance the quality of mammography images specifically for the classification of breast cancer. It incorporated a range of preprocessing methodologies meticulously designed to refine and optimize the images for subsequent analysis.

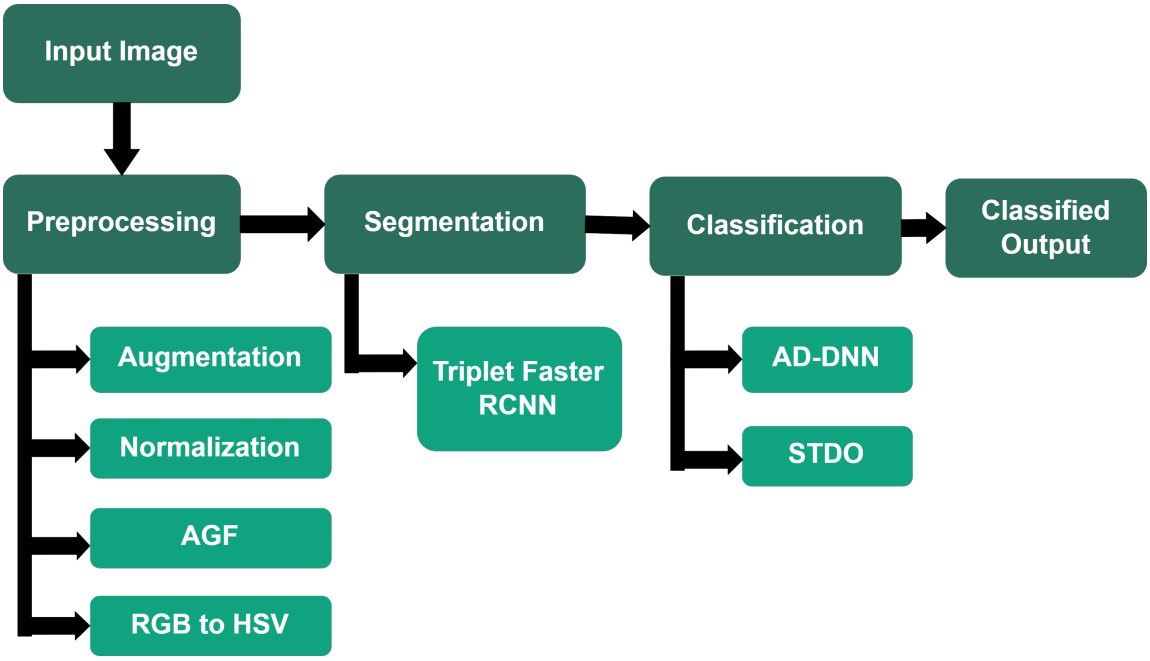

Figure 7.1: Overall architecture of the proposed framework.

These methods encompassed several crucial techniques: firstly, employing image augmentation to amplify the dataset by generating variations of existing images, thereby enriching the diversity and volume of available data. Secondly, image normalization was implemented to standardize the intensity values across all images, ensuring uniformity and consistency in brightness and contrast levels. Additionally, adaptive Gaussian filtering was applied to effectively reduce noise present in the images, refining the clarity and sharpness of the features essential for accurate analysis. Lastly, the conversion of the images from the RGB (Red, Green, Blue) colour space to the HSV (Hue, Saturation, Value) colour representation format was executed. This conversion aimed to offer a different perspective and potentially reveal distinct patterns or features within the images, augmenting the capacity for precise breast cancer detection. Overall, this comprehensive preprocessing methodology was instrumental in optimizing mammography images, thereby enhancing their suitability and efficacy for subsequent diagnostic analysis.

7.3.1 Image Augmentation

In the framework of deep learning applied to breast cancer detection through medical imaging, image augmentation stands as a pivotal preprocessing technique. It involves generating modified versions of original medical images, strategically tailored to enhance the efficacy and adaptability of machine learning models in cancer detection while preserving critical medical information. The deliberate alterations in these images serve to address challenges such as limited dataset sizes, class imbalances, and the necessity for models to effectively handle diverse image variations [197]. Various common augmentation techniques are employed in diagnosing breast cancer:

- Flipping and rotation are fundamental augmentation processes that produce mirrored or rotated replicas of the original images. These manipulations allow the models to grasp different perspectives and orientations of breast tissue, aiding in comprehensive analysis.

- Zooming and cropping simulate different scales and focal points within the images, ensuring the model's capability to identify malignant areas regardless of their spatial arrangements.

- Adjusting brightness and contrast levels accommodates variations in lighting conditions, providing the model with robustness against differing illumination levels during image acquisition.

- Incorporating noise into images helps the model discern between genuine characteristics and potential noise, mimicking real-world errors encountered in medical imaging.

- Geometric distortion introduces controlled deformations to replicate potential tissue distortions caused by variations in scanner position, enhancing the model's resilience to variations in image presentation.

- Altering colours, such as hue or colour balance, mitigates sensitivity to colour variations across scans, ensuring consistency in pattern recognition.

These augmentation techniques can be combined to create a more diverse training dataset, thereby improving the model's ability to identify cancerous patterns across various imaging scenarios. Augmentation substantially enhances the model's generalizability to new data instances while reducing the risk of overfitting to the sparsely populated dataset. As a critical preprocessing step, image augmentation ensures that the model can effectively detect malignant anomalies despite the diverse scenarios and presentations encountered in medical scans.

7.3.2 Image Normalization

Image normalization holds significant importance in the domain of breast cancer detection by ensuring unbiased and accurate assessments. It stands as a crucial preprocessing technique aimed at standardizing numerical attributes within a consistent range, typically between 0 and 1. The primary objective is to adjust image properties, thereby reducing the disproportionate influence of attributes with wider scales that might otherwise obscure analysis, especially in imbalanced datasets where the dominance of certain classes might overshadow insights from others. This process involves transforming original attribute values to fit within the desired range by computing minimum and maximum attribute values. Common normalization methods like z-score normalization (adjusting images to a mean of 0 and a standard deviation of 1) and min-max normalization (linearly scaling values to a range of 0 to 1) are frequently employed. By standardizing attributes with varying units or scales, image normalization facilitates fair comparisons, reduces biases in predictive models, and significantly enhances model accuracy, particularly in predicting health conditions using imbalanced samples. Essentially, this preprocessing technique aligns diverse image features, fostering fairness in analysis, enabling objective predictive models, and contributing to accurate breast cancer diagnoses [198].

7.3.3 Noise Removal using Adaptive Gaussian Filtering

The Gaussian Filter, a non-uniform low-pass filter, is used to preprocess digital mammograms by removing noise and smoothing the images, which keeps the grayscale

variations that the segmentation algorithms might otherwise misinterpret in order to determine the true breast masses [193]. An approach for reducing salt and pepper noise in images while keeping the image's borders and details is adaptive Gaussian filtering. To improve noise reduction performance, it dynamically modifies a Gaussian filter's parameters based on the local properties of the image. The Gaussian filter is a convolution filter that gives a local area of a picture a Gaussian distribution. It is frequently used to blur or smooth out images. The weights given to adjacent pixels during convolution are determined by the kernel of the Gaussian filter. The drawbacks of fixed-size Gaussian filters, which can cause loss of details and blurring of edges, are addressed by adaptive gaussian filtering. This is accomplished by adjusting the filter's parameters—most notably, its variance—to the properties of the image. The fundamental goal of adaptive gaussian filtering is to modify the gaussian filter's variance in accordance with the local properties of the picture. The degree of blurring that is applied to the image is directly impacted by the filter's variation. To preserve details, a smaller variance is applied in areas with sharp edges or quick changes in pixel values. A greater variance is used to decrease noise in smoother regions. The Gaussian distribution at a position x is given by the function $G(x)$, which is given in equation (7.3.1):

$$G(x) = \frac{1}{\sigma\sqrt{2\pi}} \exp\left(-\frac{x^2}{2\sigma^2}\right) \tag{7.3.1}$$

where σ represents the standard deviation, controlling the width of the distribution. Adaptive filtering involves altering the variance of the Gaussian filter according to local variables, often in inverse proportion to the gradient or second derivative of the image, and often proportional to the noise level. The adaptive variance equation is given in equation (7.3.2):

$$\text{avariance} = \text{nfactor} \cdot \text{lnvariance} + \text{gfactor} \cdot \text{lgvariance} \tag{7.3.2}$$

In this equation, avariance is the computed variance for the Gaussian filter, nfactor and gfactor are scaling factors, lnvariance is the estimated noise level in the local image region, and lgvariance is the gradient or second derivative of the image in the local region.

In this formula, $avariance$is the computed variance for the Gaussian filter, $nfactor$and $gfactor$ are scaling factors, $lnvariance$ is the estimated noise level in the local image region, and $lgvariance$ is the gradient or second derivative of the image in the local region. Adaptive Gaussian filtering involves moving a window across the image, computing the local noise variance and gradient data for each window. The adaptive variance is then calculated using these values and applied to the Gaussian filter equation to filter the target pixel. By adaptively adjusting the filter variance, the Adaptive Gaussian Filtering technique effectively suppresses noise while preserving image details and edges, leading to improved denoising results compared to fixed-size Gaussian filters.

7.3.4 Converting RGB to HSV

Converting RGB images to HSV (Hue, Saturation, Value) forms is an important preprocessing step for the detection of breast cancer from medical imaging. Since HSV representation separates colour information from brightness, it is useful for feature extraction and analysis. Load the RGB image and normalize the pixel values before conversion. Compared to the RGB colour space, the HSV colour space (Hue, Saturation, and Value) offers a lot more information. All the colours - red, yellow, green, cyan, blue, and magenta - are represented by the "hue." It can go from being unsaturated (grayscale) to being entirely saturated (no white component) depending on how much "saturation" is changed. The value component relates to different brightness levels. Consequently, compared to RGB, the HSV colour model offers more details about colour, shadow, and brightness shade model [194].

- ***Hue (H):*** Using the RGB data and the Arcos formula, determine the hue angle. This viewpoint displays the colour's true nature.
- ***Saturation (S):*** Use a formula that accounts for the lowest RGB value to determine the level of colour purity. Higher values provide colours that are more vibrant.

- ***Value (V):*** The most significant RGB component and a gauge of a colour's separation from darkness is brightness.

Upon converting RGB to HSV, considerations for scaling and rounding the data to suitable output ranges become essential. Subsequent to these adjustments, the image undergoes preparation for advanced enhancement and analysis, including processes such as feature extraction, noise reduction, and segmentation of breast tissue. Algorithms may then utilize the generated HSV image for categorization or detection of breast cancer. The effectiveness of these stages heavily relies on the dataset's accuracy and alignment with detection objectives, ultimately guaranteeing dependable and precise outcomes in breast cancer diagnosis.

7.4 Segmentation and Feature Extraction using Triplet Faster R-CNN

This proposed model for segmenting regions indicative of breast cancer within mammographic images leverages a TFR-CNN, a convolutional approach that meticulously extracts features at multiple levels. Through the TFR-CNN architecture, the model enhances its focus on specific regions of interest within the images, which is essential for the accurate diagnosis of cancerous tissues.

In this segmentation phase, the model commences with the application of convolutional techniques to analyze the mammograms. This structured approach is designed to sequentially extract features of varying depths. Initially, the model zeroes in on the extraction of shallow features, those on the surface that can offer immediate insights into textural and edge details within the mammogram. Subsequently, the model explores into mid-level feature extraction, which serves to bridge the gap between the detailed surface features and the more abstract deep features. Finally, the deep features are extracted, which are essential for identifying the complex patterns that are characteristic of cancerous regions. The architecture of this model of TFR-CNN is shown in figure (7.2).

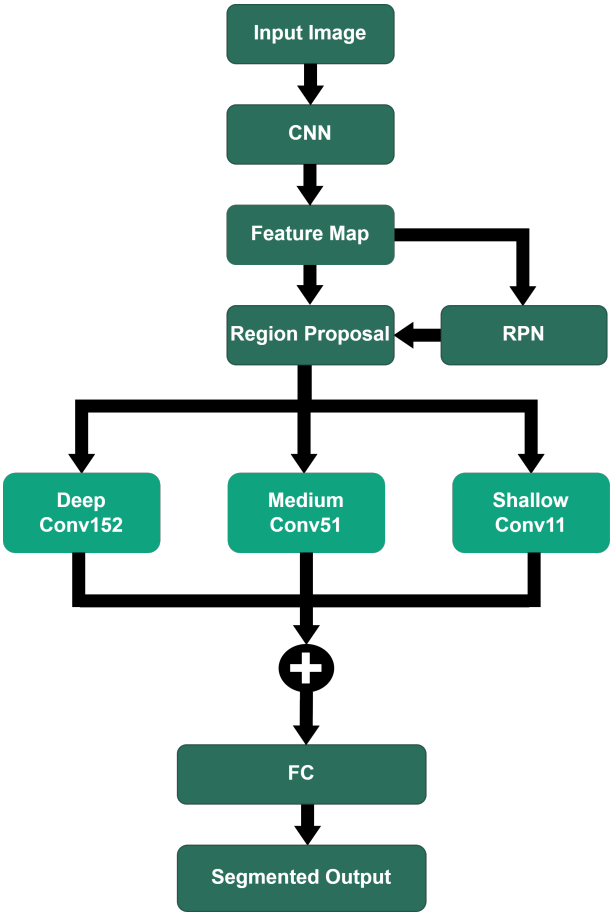

Figure 7.2: TFR-CNN Architecture

This architecture hinges on a three-layered process within the Triplet Feature Representation Convolutional Neural Network (TFR-CNN) architecture, innovatively tailored to identify cancerous regions in mammograms. The first layer of this approach focuses on extracting shallow features. Unlike traditional methods that typically use a 3x3/1 filter size and stride configuration, this model adopts a unique strategy. It employs alternating 5x5/1 and 7x7/1 filter sizes and strides in its Conv11 layer. This deviation not only diversifies the range of features extracted but also captures more complex and nuanced details, significantly enhancing the quality of the segmentation.

Moving to the second layer, the model continues its departure from conventional methods by focusing on medium feature extraction. In the Conv51 layer, the standard 3x3/2 arrangement is replaced with 5x5/1 and 7x7/1 filter sizes and strides. This adjustment allows for a more refined and accurate capture of medium-level features,

maintaining essential elements while improving the overall accuracy of the model. The third layer, Conv152, is dedicated to extracting high-level features. It researches deeper into the mammographic images to identify the intricate patterns and characteristics vital for efficient and precise segmentation. This level of deep feature extraction is crucial for the successful identification of cancerous changes within breast tissue.

Additionally, the model incorporates elements of the Faster R-CNN framework, known for its efficacy in precise object localization within images. This method synergizes CNN with region proposals to optimize the feature analysis process. In its first stage, Faster R-CNN utilizes CNN for feature classification and refinement. The second stage involves a Region Proposal Network (RPN), generating region suggestions for further analysis. By sharing layers between these two stages, the model not only achieves computational efficiency but also enhances accuracy. The multi-task loss function, integral to Faster R-CNN, simultaneously addresses classification and regression tasks, further contributing to the model's precision and effectiveness. Following the multi-task loss, an objective function is minimized, and the Fast R-CNN loss function for an image is described by equation (7.4.1).

$$L(r_i, s_i) = \frac{1}{M_{\text{cls}}} \sum_i L_{\text{cls}}(r_i, r_i^*) + \lambda \frac{1}{M_{\text{reg}}} \sum_i r_i^* L_{\text{reg}}(s_i, s_i^*) \tag{7.4.1}$$

When an anchor is positive, the ground truth label is r_i^*, and when an anchor is negative, it is 0, where i is an anchor index in a mini-batch and r_i is the anchor predicted probability. L_{cls} is the log loss over two classes, for positive anchors the regression loss is referred by means of the term $r_i^* L_{\text{reg}}$.

After extracting these features, the process integrates the shallow, medium, and deep features, combining them to form a rich and detailed representation of the image. This integration is crucial as it utilizes the strengths of each level of feature extraction to improve the final output. A Fully Connected (FC) layer is used to synthesize the information from the combined features. This layer is responsible for refining the data and preparing the final segmented output. The segmented output is the end result of the process, which provides a segmented image highlighting the cancerous regions with precise boundaries. This output is invaluable for clinicians in diagnosing

and treating breast cancer, as it provides a clear and accurate representation of the areas of concern within the breast tissue.

This nuanced feature extraction approach represents a significant advancement in the field of medical imaging, particularly in the accurate diagnosis of cancer through mammographic analysis. The use of varied filter sizes and strides in different layers, coupled with the sophisticated integration of CNN and RPN, enables the model to extract a richer, more detailed representation of features, thereby improving the accuracy and reliability of cancer detection in mammograms. The final result of these segmented and extracted features are transmitted across the classification phase using an Adaptive Dilated Deep Neural Network (AD-DNN).

7.5 Refined Classification Using AD-DNN and STDO

This section focuses on enhancing the accuracy of classification tasks by incorporating Adaptive Dilated Deep Neural Networks (AD-DNN) into the existing DNN framework. The innovation lies in applying Adaptive Dilation to expand the neural network's receptive field, which is anticipated to bolster the model's ability to extract relevant information, thereby boosting its classification capabilities. Furthermore, the study introduces a cutting-edge technique by integrating Self-adaptive Tasmanian Devil Optimization (STDO) into the AD-DNN model. Through STDO, the model's parameters are fine-tuned dynamically, promoting an optimization of the classification procedure. This augmented approach is designed to significantly refine the overall process, ultimately elevating both the precision and efficacy of feature identification and classification, specifically in the context of detecting breast cancer.

7.5.1 Adaptive Dilated Deep Neural Networks

The architecture shown in figure (7.3) introduces a multi-layered convolutional approach with the integration of Adaptive Dilated Convolution to refine the classification accuracy. The architecture comprises a sequence of feature extraction layers -

shallow, medium, and deep convolutions - each contributing uniquely to the feature detection process. Following this, an Adaptive Dilated Convolution layer is utilized to enhance the receptive field, thereby capturing more complex features with varying resolutions.

After processing the input through these stages, the feature maps are aggregated and passed through a Fully Connected (FC) layer, which consolidates the learned features into a more structured form. Subsequently, the processed features feed into AD-DNN, which is responsible for the final classification task.

The intricate design of this architecture leverages convolution layers with varying kernel sizes and dilation rates, enhancing the model's ability to perform multi-scale feature learning. The inclusion of ReLU activation and Max-pooling layers after each convolution stage aids in non-linear transformation and dimensionality reduction, respectively. The strategic application of dilated convolutions allows the network to learn at multiple scales without losing the resolution of the input, leading to a robust and accurate classification system.

This sophisticated architecture is tailored for high performance in tasks such as the detection of breast cancer, where precision is paramount. The addition of self-adaptive components could further optimize the network's parameters, potentially leading to superior performance in the classification and analysis of complex image data.

The 2D-CONV layer serves as the foundation for the suggested model, with the dilated CNN layer significantly enhancing it. According to Equation (7.5.1), a mathematical formulation is provided.

$$Y(m,n) = \sum_{i=1}^{m} \sum_{j=1}^{n} X(m + r \times i, n + r \times j) W(i,j) \tag{7.5.1}$$

Where $W(i,j)$ is the filter and m and n are used to denote the length and width of the filter, respectively, and $Y(m,n)$ represents the output, $X(m,n)$ defines the input. The variable r denotes the rate of dilation, allowing for different dilation levels. The equation produces a typical convolution layer for $r = 1$. Conventional

pooling and convolution layers are replaced by sparse kernels. The receptive field is widened through dilation without the need for additional convolution processes. A kernel with a size of $k \times k$ expands to $K + (k-1) \cdot (r-1)$, where r can take values like $1, 2, 3, 4, 8, 16, 32, 64$, and 128. Table (7.1) displays the assortment of dilation rates $(1, 2, 3)$ applied to 3×3 filters.

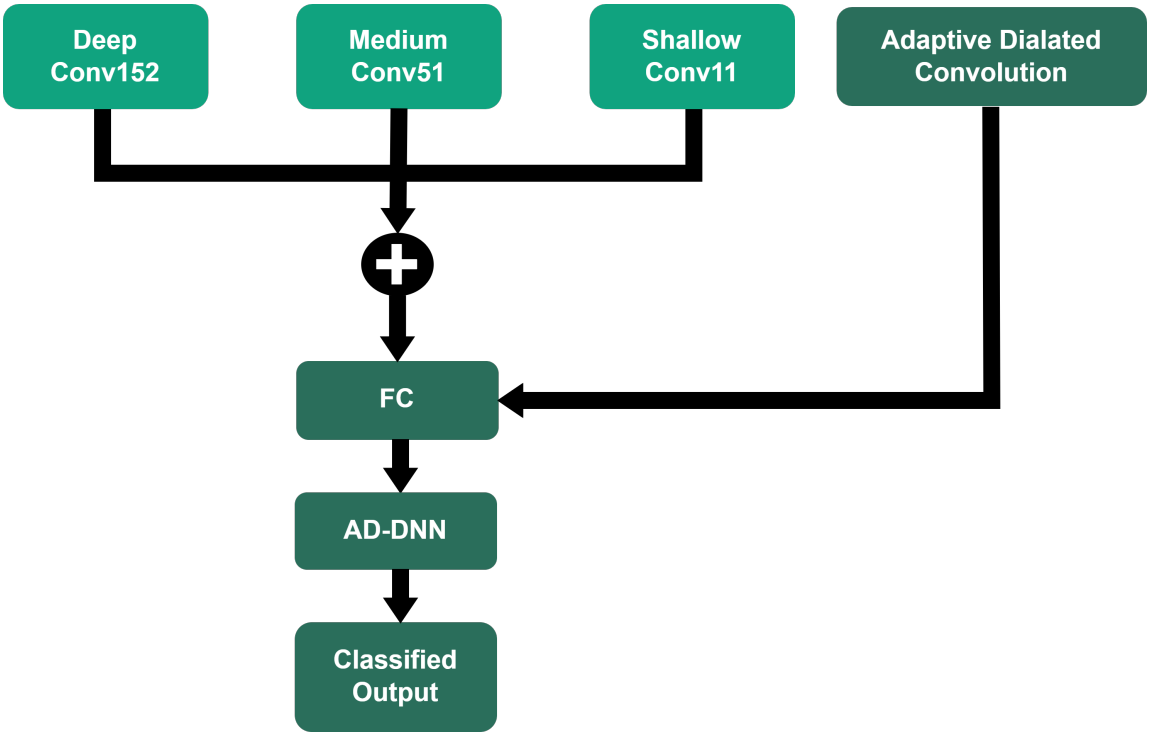

Figure 7.3: AD-DNN Architecture

In the proposed model, the dilation rate fluctuates while the filter size stays constant. The dilation rates for the model's 3×3 filter is 1, 2, 3, 4, 8, 16, 32, 64, and 128. With the same dilation rates, the idea may be applied to 5×5 and 7×7 filters to increase the receptive field while maintaining filter size. For instance, a 5×5 filter's scope is increased to 7×7 by padding it with two rows and columns of zeros when the dilation rate is 2. This method makes it easier to efficiently capture bigger input areas, which helps with tasks like object detection and semantic segmentation. 3×3 filter-based dilated convolutions.

Table 7.1: Dilation rates (1, 2, 3) applied on 3x3 filters.

0	1	1	0	1	1	0
1	0	1	0	1	0	1
1	1	0	0	0	1	1
0	0	0	0	0	0	0
1	1	0	0	D=1	1	1
1	0	1	0	D=2	0	1
0	1	1	0	D=3	1	0

7.5.2 Self-adaptive Tasmanian Devil Optimization

Self-adaptive Tasmanian Devil Optimization (STDO) is a metaheuristic algorithm that takes ideas from the feeding habits of Tasmanian devils. By balancing the quest of potential answers with the search of novel ones, it mimics the behavior of the animal. To successfully address optimization issues, TDO's search strategy combines exploitation and exploration techniques. The optimization method imitates the Tasmanian devil's hunt for food in order to get the optimal answers. Exploration and exploitation theories resemble the devil's hunting strategy. Its diversified food-gathering is an illustration of exploration, but its restricted pursuit is an illustration of exploitation. In optimizer design, devil's strategy modeling helps generate optimal solutions to difficult optimization issues [Dehghani et al., 2022].

Initialization

TDO is a stochastic search algorithm that uses agents from the Tasmanian devil. Starting with randomly generated agents that adhere to the constraints of the challenge. Agents create a matrix by suggesting values depending on locations in the search space.

$$P = \begin{bmatrix} P_1 \\ \vdots \\ P_i \\ \vdots \\ P_N \end{bmatrix}_{N\times m} = \begin{bmatrix} p_{1,1} & \cdots & p_{1,j} & \cdots & p_{1,m} \\ \vdots & \ddots & \vdots & \iddots & \vdots \\ x_{i,1} & \cdots & p_{i,j} & \cdots & p_{i,m} \\ \vdots & \iddots & \vdots & \ddots & \vdots \\ p_{N,1} & \cdots & p_{N,j} & \cdots & p_{N,m} \end{bmatrix}_{N\times m} \tag{7.5.2}$$

P is the number of Tasmanian devils in the population, P_i is the i-th candidate solution, $p_{i,j}$ is its potential value for the j-th variable, N is the number of Tasmanian devils actively looking, and m is the number of variables in the presented problems. These terms are used in Equation (7.5.2). By inserting the values of each potential solution into the variables of the objective function, the problem's objective function can be found. In order to model the values acquired for the objective function, a vector is used in Equation (7.5.3).

$$O = \begin{bmatrix} O_1 \\ \vdots \\ O_i \\ \vdots \\ O_N \end{bmatrix}_{N\times 1} = \begin{bmatrix} O(P_1) \\ \vdots \\ O(P_i) \\ \vdots \\ O(P_N) \end{bmatrix}_{N\times 1} \tag{7.5.3}$$

where O_i denote the value from the i-th candidate solution, while $\mathbf{O}$ represents the vector of objective function values. The best candidate, which yields the optimal value, is designated as the best member of the population. The values of the objective function are utilized to assess the quality of the solutions. This optimal member is subject to modification after implementing two Tasmanian devil feeding strategies in each cycle. For every individual devil, carrion and hunting strategies are applied with equal frequency in each iteration.

In the Tasmanian Devil Optimization (TDO) algorithm, the population updating mechanism is inspired by two feeding behaviors of Tasmanian devils: carrion eating and prey hunting. With an equal 50% probability of adopting either strategy, each Tasmanian devil in the algorithm is updated in every iteration based on just one of

these strategies.

Strategy 1: Carrion Consumption (Exploration Phase)

Tasmanian devils prefer to eat carrion over hunting when there is carrion available. There can be surplus prey left by nearby predators, creating a chance. The algorithm's investigation of many areas of problem-solving is similar to the Tasmanian devil's hunt for carrion. This tactic exemplifies TDO's ability to investigate many areas of the search space for the ideal solution. The position of a random population member is taken to represent a carrion spot for each Tasmanian devil, assuring exploration, and is depicted as per equation (7.5.4).

$$SCa_i = P_{k,i} \quad \text{for } i = 1, 2, \ldots, N, \quad k \in \{1, 2, \ldots, N \mid k \neq i\} \tag{7.5.4}$$

Where SCa_i stands for the carrion chosen by the Tasmanian devil. If a carrion's objective function value is higher than its current location, the Tasmanian devil moves towards it; otherwise, it moves away. Equation (7.5.5) simulates this movement. The Tasmanian devil's new position is accepted if it improves the value of its objective function; otherwise, it retains its position as indicated by equation (7.5.6).

$$p_{i,j}^{\text{new,s1}} = \begin{cases} p_{i,j} + \text{rand} \cdot (sca_{i,j} - R \cdot p_{i,j}), & \text{if } O_{SCa_i} < O_i \\ p_{i,j} + \text{rand} \cdot (p_{i,j} - sca_{i,j}), & \text{otherwise} \end{cases} \tag{7.5.5}$$

$$P_i = \begin{cases} P_i^{\text{new,s1}}, & \text{if } O_i^{\text{new,s1}} < O_i \\ P_i, & \text{otherwise} \end{cases} \tag{7.5.6}$$

Based on the first technique, $P_i^{\text{new,s1}}$ indicates the i-th Tasmanian devil's new status. For the j-th variable, it is represented by the expression $p_{i,j}^{\text{new,s1}}$. The value of its objective function is represented by $O_i^{\text{new,s1}}$. The value of the objective function for the chosen carrion is represented by O_{SCa_i}. R stands for a random number that can either be 1 or 2, while rand stands for a random number between [0, 1].

Strategy 2: Prey Hunting and Consumption (Exploitation Phase)

The second method of feeding used by Tasmanian Devils involves hunting and eating prey. This tactic mimics the predator's attack behaviour, which consists of two phases: the initial selection and attack of the prey, followed by the subsequent

pursuit and consumption of the prey. Prey places are chosen from the population to represent the first stage, which is associated with carrion selection. A random member of the population is picked to represent the location of the prey for each Tasmanian devil, symbolizing the first stage of the predator. This is expressed mathematically in terms of Equation (7.5.7).

$$Y_i = P_{k,i} \quad \text{for } i = 1, 2, \ldots, N, \quad k \in \{1, 2, \ldots, N \mid k \neq i\} \tag{7.5.7}$$

Where Y_i represents the selected prey by the i-th Tasmanian devil. Similar to the carrion strategy, the Tasmanian devil moves towards or away from the selected prey based on the improvement in objective function value as per equation (7.5.8). The Tasmanian devil's new position is accepted if it improves the objective function value as per equation (7.5.9).

$$p_{i,j}^{\text{new,s2}} = \begin{cases} p_{i,j} + \text{rand} \cdot (y_{i,j} - R \cdot p_{i,j}), & \text{if } O_{Y_i} < O_i \\ p_{i,j} + \text{rand} \cdot (p_{i,j} - y_{i,j}), & \text{otherwise} \end{cases} \tag{7.5.8}$$

$$P_i = \begin{cases} P_i^{\text{new,s2}}, & \text{if } O_i^{\text{new,s2}} < O_i \\ P_i, & \text{otherwise} \end{cases} \tag{7.5.9}$$

With this method, TDO makes use of the information gleaned through exploration and modifies its location in accordance with the caliber of the chosen prey. In the second phase of attack and consumption, the predator behaves in a manner similar to this. The objective function value in this case is $O_i^{\text{new,s2}}$, while the objective function value of the prey of choice is O_{Y_i}. The second strategy's new status for the i-th Tasmanian is $P_i^{\text{new,s2}}$, and its value for the j-th variable is $p_{i,j}^{\text{new,s2}}$. The second method resembles local search in the optimization process and, in contrast to the first, adds a second step that is focused on hunting prey. TDO's ability for leveraging the search space to find more potent candidate solutions is shown by the Tasmanian devil's chasing conduct, which resembles a predator closing in on prey. To simulate this chase, the Tasmanian devil follows its prey in an area that is similar to a neighborhood in the search space. The chasing radius is represented by the pursuit range in equation (7.5.10). While hunting its prey, the Tasmanian devil moves in this

neighborhood-focused position, with the new position being specified by equation (7.5.11). If this updated location has a higher objective function value, it is accepted as stated in equation (7.5.12).

$$\text{Radi} = 0.01(1 - \frac{t}{T}) \tag{7.5.10}$$

$$p_{i,j}^{\text{new}} = p_{i,j} + (2 \cdot \text{rand} - 1) \cdot \text{Radi} \cdot p_{i,j} \cdot w(t) \tag{7.5.11}$$

$$P_i = \begin{cases} P_i^{\text{new}}, & \text{if } O_i^{\text{new}} < O_i \\ P_i, & \text{otherwise} \end{cases} \tag{7.5.12}$$

Here, Radi stands for the neighbourhood radius of the attacked location, t for the number of iterations, T for the maximum number of iterations, P_i^{new} for the new status of the i-th Tasmanian devil within its neighbourhood, $p_{i,j}^{\text{new}}$ for its value for the j-th variable, and O_i^{new} for its objective function value. This procedure imitates the Tasmanian devil's laser-like pursuit and supports TDO's exploitation phase, which results in the improvement of potential solutions. The first algorithm iteration ends once all TDO members have been updated. The placements of the Tasmanian devil and the values of the objective function are revised in subsequent iterations. TDO keeps and improves the top candidate solution throughout, finally presenting it as the answer to the issue.

Chaotic Inertia: Optimizing Convergence and Exploration

In TDO, the linear decreasing inertia weight w assumes a critical role, endowing particles with adaptability in diverse environments to strike a balance between exploration and exploitation. This pivotal role makes it a cornerstone of the TDO algorithm. While conventional methods employ linear decreasing inertia weight, the adoption of a non-linear counterpart proves more potent due to enhanced fitting and simulation abilities. Non-linear mappings, rooted in chaos theory, produce random numbers with exceptional randomness and disorder, making them a popular tool in evolutionary computation. A prominent chaotic mapping, the logistic map, generates values between 0 and 1. Integrated into linear decreasing inertia weight via equation

(7.5.14), the logistic chaotic element constructs a linear decreasing inertia weight profile.

$$ra(t+1) = 4ra(t)(1 - ra(t)), \quad r(0) = \text{rand} \tag{7.5.13}$$

Where $r_0 = \{0, 0.25, 0.5, 0.75, 1\}$

$$w(t) = ra(t) \cdot w_{\max} - \frac{(w_{\max} - w_{\min})}{i_{\max}} \cdot I \tag{7.5.14}$$

This profile, guided by the recursive formula in equation (7.5.13) and initialized with $ra(0)$, offers a dynamic, non-linear value-taking pattern that fluctuates significantly over iterations. This non-linearity augments fitting and simulation capabilities, effectively harmonizing global exploration and local exploitation. The wave-like attributes of ω introduce randomness, deterring particles from premature convergence. The integration of logistic chaos into inertia weight refines TDO. This amalgamation empowers particles to dynamically adapt, promoting exploration and exploitation. By harnessing chaos theory, especially via logistic mapping, TDO's optimization prowess improves, rendering it robust and efficient in solving complex optimization problems. ***Features Optimized Using TDO*** The Self-Adaptive Tasmanian Devil Optimization (STDO) algorithm is utilized to optimize the feature set generated by the Triplet Deep Learning Framework. The extracted features include:

- *Deep Features*: High-level features extracted from the Triplet Faster R-CNN (TFR-CNN) architecture, capturing semantic information about regions of interest in mammograms.

- *Texture Features*: Derived from Local Orientation Histograms (LOH) and Speeded-Up Robust Features (SURF), these features encapsulate local texture and directional patterns in breast tissue.

- *Shape and Boundary Features*: Descriptors focusing on the structural integrity and boundary delineation of segmented regions, aiding in distinguishing normal and abnormal tissues.

- *Intensity-Based Features*: Pixel intensity distributions critical for identifying microcalcifications and subtle anomalies.

The STDO algorithm optimizes these features by selecting the most discriminative subset, ensuring that the classifier focuses on the most relevant data. The optimization process uses an objective function defined as:

$$J = \frac{S_b}{S_w} \tag{7.5.15}$$

Where S_b represents inter-class variance, and S_w represents intra-class variance. The goal is to maximize J, ensuring better class separability in the feature space. STDO evaluates candidate feature subsets by iteratively improving their fitness, calculated as:

$$F(\mathbf{x}) = \alpha \cdot \text{Accuracy}(\mathbf{x}) - \beta \cdot \text{Size}(\mathbf{x}) \tag{7.5.16}$$

Where $\mathbf{x}$ denotes a feature subset, α and β are weights for balancing accuracy and compactness. By minimizing redundant features and emphasizing the most discriminative ones, the optimization significantly enhances classification performance.

Integrating TDO ensures that the proposed framework achieves high accuracy and robustness, particularly in challenging cases with dense breast tissues. The selected features, optimized through TDO, contribute to the improved sensitivity and specificity of the system, as demonstrated in the performance evaluation.

7.6 Visualization: Gradient-weighted Class Activation Mapping (Grad-CAM)

Explainable AI, a critical aspect of machine learning, focuses on ensuring that AI models provide transparent and interpretable outputs, particularly in complex tasks such as image classification. Explainable AI techniques like Grad-CAM (Gradient-weighted Class Activation Mapping) contribute to this goal by offering insights into the decision-making process of deep neural networks. Grad-CAM is a powerful technique within the domain of explainable AI and deep neural networks, specifically CNN, that sheds light on the reasoning behind image classification outcomes. By generating informative heatmaps, Grad-CAM reveals the vital regions of an input image that significantly contributed to a particular classification decision, thereby enhancing our

understanding of the network's choices. The essence of Grad-CAM lies in its ability to compute the gradient of the target class score concerning the feature maps in the final convolutional layer of the CNN. This gradient information is leveraged to assign weights to these feature maps, effectively amplifying the importance of regions that strongly influenced the final prediction. Through this process, the technique visually pinpoints the relevant portions of the input image that played a key role in the network's decision. The Grad-CAM process comprises several pivotal steps: firstly, the computation of gradients; secondly, global average pooling to calculate average gradients for each feature map; thirdly, a weighted combination where feature maps are multiplied by their respective average gradients; fourthly, application of the ReLU activation to accentuate positive contributions; fifthly, summation of the weighted and activated feature maps to generate an interpretable heatmap; and finally, the integration of this heatmap with the original image through overlaying, resulting in an intuitive visual representation that enhances explainable AI.

7.7 Result and Discussion

This proposed model has been implemented in PYTHON. The study of this proposed framework is based on the analysis of the CBIS-DDSM (Curated Breast Imaging Subset of DDSM) dataset, is a specialized and extensive collection of mammography images. This dataset is meticulously curated to facilitate research in the field of breast cancer, offering a wealth of high-quality images for detailed study. Utilizing this dataset provides a robust foundation for our analysis, ensuring the research is grounded in comprehensive and relevant medical imaging data.

The proposed model was compared against established algorithms like Coati Optimization Algorithm (COA), Rat Swarm Optimization (RSO), Sea Lion Optimization (SLO), and Tasmanian Devil Optimization (TDO). Performance was evaluated using metrics such as Accuracy, FNR, FPR, MCC, NPV, Precision, Sensitivity, Specificity, and F-measure, providing a multi-dimensional perspective of the model's capabilities.

Table 7.2 provides a comprehensive assessment of various optimization algorithms, including the proposed model, using multiple performance metrics. The proposed model demonstrates remarkable accuracy, achieving an impressive score of approximately 97.98%. This exceptional accuracy underscores its proficiency in making precise predictions. Furthermore, the model excels in precision, sensitivity, and specificity, each achieving values of approximately 96.98%. These results indicate the model's capability to correctly identify both positive and negative instances. The proposed model strikes an effective balance between precision and sensitivity, as evidenced by its high F-Measure of approximately 96.98%. Additionally, it exhibits robust performance in Matthews Correlation Coefficient (MCC), Negative Predictive Value (NPV), False Positive Rate (FPR), and False Negative Rate (FNR), with values of approximately 95.46%, 98.49%, 1.51%, and 3.03%, respectively. These findings collectively underscore the superiority of the proposed model compared to existing optimization algorithms across a spectrum of critical evaluation criteria.

Table 7.2: Comparison of the Proposed Model with Existing Models

Performance Metrics	COA	RSO	SLO	TDO	Proposed
Accuracy	0.928826	0.905101	0.927639	0.957295	0.979834
Precision	0.893238	0.857651	0.891459	0.935943	0.969751
Sensitivity	0.893238	0.857651	0.891459	0.935943	0.969751
Specificity	0.946619	0.928826	0.945730	0.967972	0.984875
F-Measure	0.893238	0.857651	0.891459	0.935943	0.969751
MCC	0.839858	0.786477	0.837189	0.903915	0.954626
NPV	0.946619	0.928826	0.945730	0.967972	0.984875
FPR	0.053381	0.071174	0.054270	0.032028	0.015125
FNR	0.106762	0.142349	0.108541	0.064057	0.030249

Figure 7.4 presents overall graphical representation of the performance metrics for the proposed model with other related existing models.

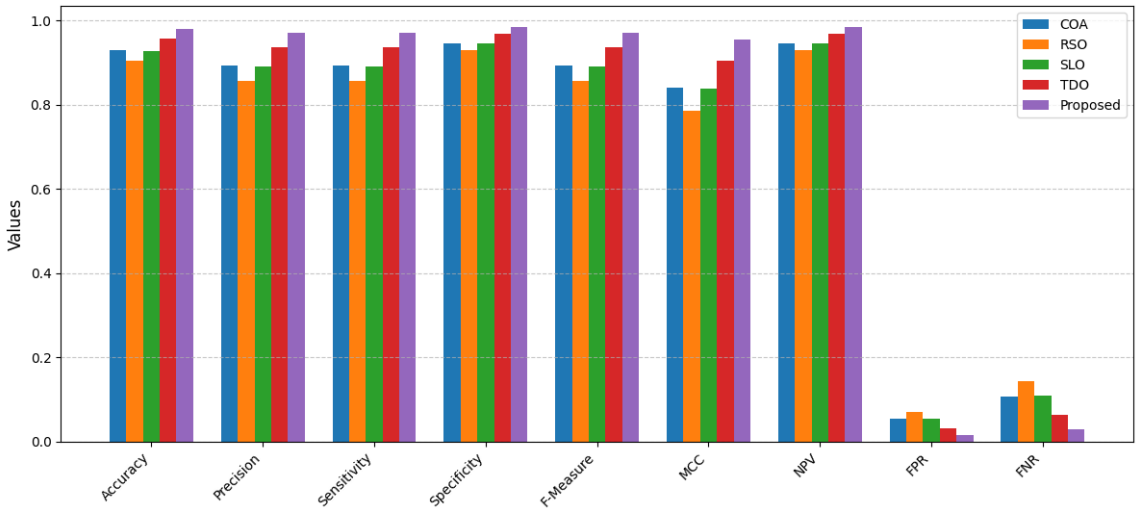

Figure 7.4: Overall Graphical Analysis of Performance Matrices

The figure 7.5 shows the confusion matrix generated by this framework when applied to the CBIS-DDSM dataset.

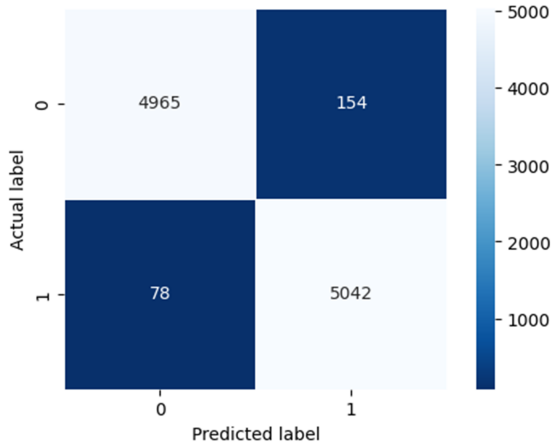

Figure 7.5: Confusion matrix of CBIS-DDSM Database

Figure 7.6 visually showcases instances of correctly classified data points, accentuating the model's accuracy in accurately predicting class labels. Figure 7.7 illustrates instances of misclassified data points. These instances shed light on areas where the model's predictions deviate from the actual class, thereby highlighting potential areas for refinement or further analysis.

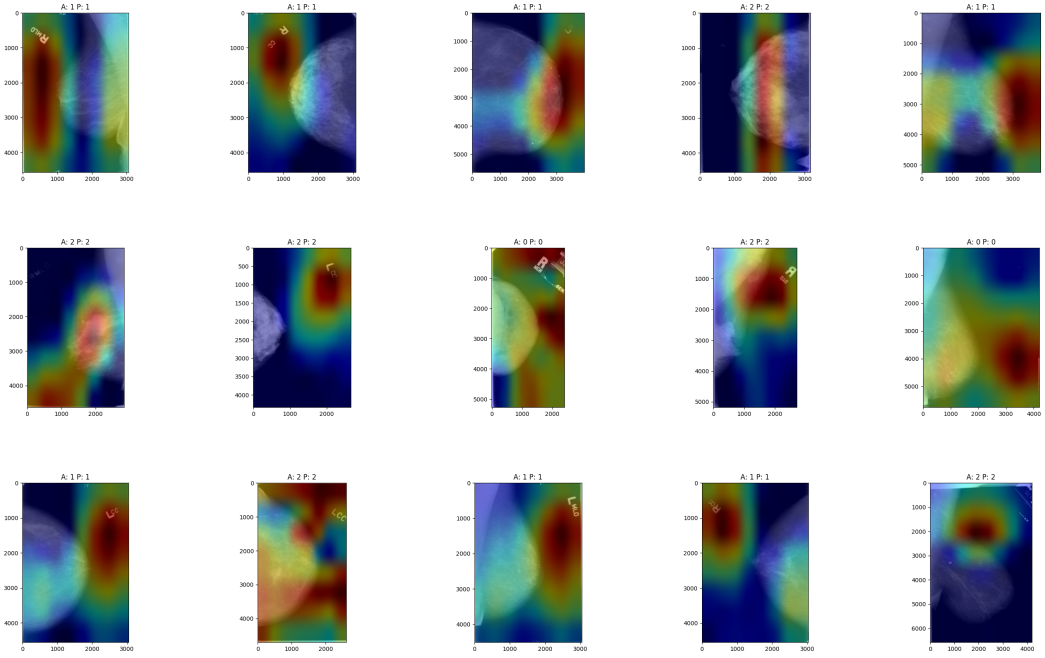

Figure 7.6: Accurate Predictions: A Visual Display

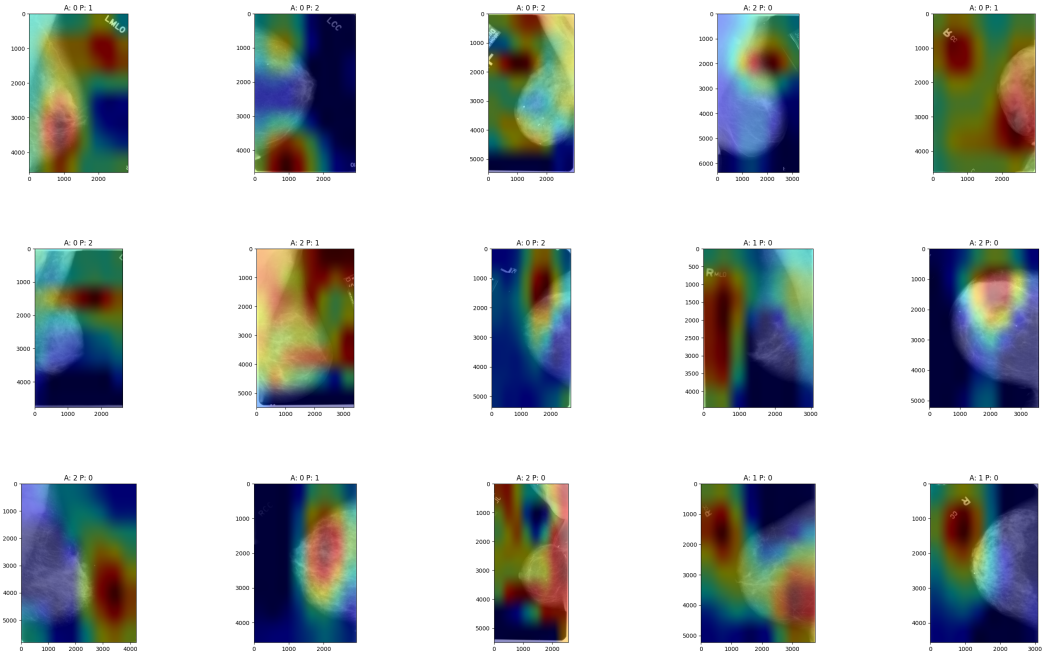

Figure 7.7: Misclassified Instances: Analysis

7.8 Conclusion

The Triplet Deep Learning Framework introduced in this chapter represents a significant leap forward in the field of mammographic image analysis for breast cancer detection. This framework, incorporating the Triplet Fast Region Based Convolutional Neural Networks (TFR-CNN) and Adaptive Dilated Deep Neural Networks (AD-DNN), has demonstrated remarkable performance in terms of accuracy and precision. Through rigorous testing on the CBIS-DDSM dataset, the proposed method achieved an exceptional accuracy rate of approximately 97.98%, outperforming conventional algorithms such as COA, RSO, SLO, and TDO across various metrics including precision, sensitivity, specificity, and F-measure. This outcome not only underscores the effectiveness of the framework in distinguishing between benign and malignant tissues but also highlights its potential in significantly improving early breast cancer detection.

Comparatively, the results obtained from this framework surpass the achievements of the methodologies discussed in Chapters 5 and 6. The integration of advanced deep learning models, coupled with the innovative use of explainable AI, has enabled a more nuanced and detailed analysis of mammographic images. This approach has led to a higher accuracy rate and a more reliable diagnostic process, marking a substantial advancement over the studies presented in previous chapters. In conclusion, the Triplet Deep Learning Framework presents a promising direction for future research and application in the medical imaging domain. Its superior performance in the CBIS-DDSM dataset, coupled with its ability to outperform previous methodologies, positions it as a valuable tool in the ongoing efforts to enhance breast cancer diagnostics.

Chapter 8

Conclusion and Recommendations

8.1 Introduction

The problem of automatic classification of breast cancer in mammographic images is addressed in this thesis. An innovative methodology for identifying and removing pectoral muscles in mammogram images, employing watershed transformation, regularization techniques, and masking methods, is presented in Chapter 4. This methodology addresses the complexity of the pectoral muscle segmentation process. For the detection and classification of mammogram images, three novel and innovative frameworks - Hybrid HHO-CS MKSVM, Multi-Feature Learning, and Triplet Deep Learning Method - have also been presented in Chapters 5, 6 and 7 respectively.

In this concluding chapter, we first present a summary of the research conducted and a comparative analysis of the results obtained. Following this, we outline the key contributions of the research works. We then envision the scope for future research building upon the foundations laid by this thesis.

8.2 Summary of the works

A brief summary of the work presented in this thesis is as follows. Background, motivation and outline of the work have been presented in chapter l. A detailed survey on existing different approaches covering different preprocessing, segmentation, feature extraction and classification techniques are presented in chapter 2. The performance evaluation metrics for assessing the effectiveness of CAD systems for a comparative

analysis of different algorithms are also presented in this chapter. Chapter 3 covers mammographic databases like DDSM, BIS-DDSM, MIAS, INbreast, OPTIMAM, BCDR, NMD, CMMD, and BreaKHis. It also discusses mammogram views such as craniocaudal view, mediolateral oblique view, latero-medial view, extended craniocaudal view, straight lateral view, and rolled view, along with preprocessing techniques and classification standards in breast imaging. Chapter 4 presents an innovative method for the identification and removal of pectoral muscles from mammogram images, employing techniques such as region intensity, Otsu's thresholding, watershed transformation, holistic regularization techniques, and masking methods. In chapters 5, 6 and 7 three novel, robust and advanced frameworks for the segmentation and classification of mammographic images have been presented.

The first framework is presented in chapter 5, which is a hybrid model that emphasizes the development and evaluation of hybrid models that enhance the efficiency of the Multi-Kernel Support Vector Machine (MKSVM). It integrates advanced optimization techniques such as Harris Hawks Optimization (HHO) and Cuckoo Search (CS) and also combines the strength of SVM to achieve superior classification accuracy.

The second framework is a Multi-Feature Learning Framework which is presented in chapter 6, focuses on creating a multi-feature learning framework, grounded in deep learning, to increase the segmentation and classification performance in mammography-based breast cancer detection. It incorporates a modified version of the Faster R-CNN algorithm for accurate and efficient segmentation. Additionally, this framework leverages multiple features extracted via deep learning techniques to enhance the classification model's accuracy. By combining these features, the framework provides a comprehensive analysis of mammographic images, leading to more precise cancer detection.

The third one is a Triplet Deep Learning Framework is presented in chapter 7, which integrates Triplet Fast Region Based Convolutional Neural Networks (TFR-CNN) with Adaptive Dilated Deep Neural Networks (AD-DNN). The synergy of TFR-CNN and AD-DNN in this framework aims to provide enhanced segmentation

and classification capabilities. The Triplet Deep Learning Framework is designed to offer a more nuanced analysis of mammographic images, enabling it to distinguish subtle differences between benign and malignant tissues with higher accuracy. All these three frameworks are proved to be effective in classifying mammogram images and hence are useful for developing CAD systems.

Finally, this chapter, namely Conclusion and Recommendations, consolidates the summary of the research findings, results, innovative contributions, and forward-looking recommendations in breast cancer detection.

8.3 Comparison of Results

In this section, a comparative analysis of the results from various studies presented in this thesis is provided. The research extensively examined several mammogram databases, each offering unique insights into breast cancer imaging.

8.3.1 Improved Automated Pectoral Muscle Segmentation

The research introduced an innovative methodology for the automated segmentation of the pectoral muscle in mammograms. This development is significant in enhancing the accuracy of breast cancer screenings. Traditional methods often struggled with varying shapes and unclear boundaries of the pectoral muscle, leading to potential misdiagnoses.

The new methodology addresses these challenges by using advanced image processing techniques. It improves the precision of segmenting the pectoral muscle, which is vital for accurate analysis of mammograms. This method's ability to reduce false positives and enhance diagnostic accuracy represents a significant leap forward in automated image processing and analysis in mammography. Its implementation could lead to more reliable breast cancer screening processes, ultimately contributing to better patient outcomes.

The table 8.1 presents the results of the improved automated pectoral muscle segmentation in a comparative tabular format. The results highlight the superior

performance and effectiveness of this methodology in accurately segmenting the pectoral muscle in mammograms, compared to existing techniques. The graphical representation of this comparison is given in figure 8.1.

Table 8.1: Comparative results of the presented work (in chapter 4) with existing pectoral muscle segmentation methods

Method	Accuracy(%)	Reference
Watershed-Based Technique (Presented in Chapter 4)	97.20	Haris and Kabeer [2023]
Gradient-Based Thresholding	97.08	Shi et al. [2018]
Support vector machine (SVM)	93.70	Shinde and Rao [2019]
Polynomial fitting	96.81	Shen et al. [2018]
Region growing	92.00	Rampun et al. [2019]
Region growing	92.00	Hazarika and Mahanta [2018]
Region growing	95.00	Taghanaki et al. [2017a]
K-means clustering	93.16	Yoon et al. [2016]
Curve estimation	96.60	Mustra et al. [2013]

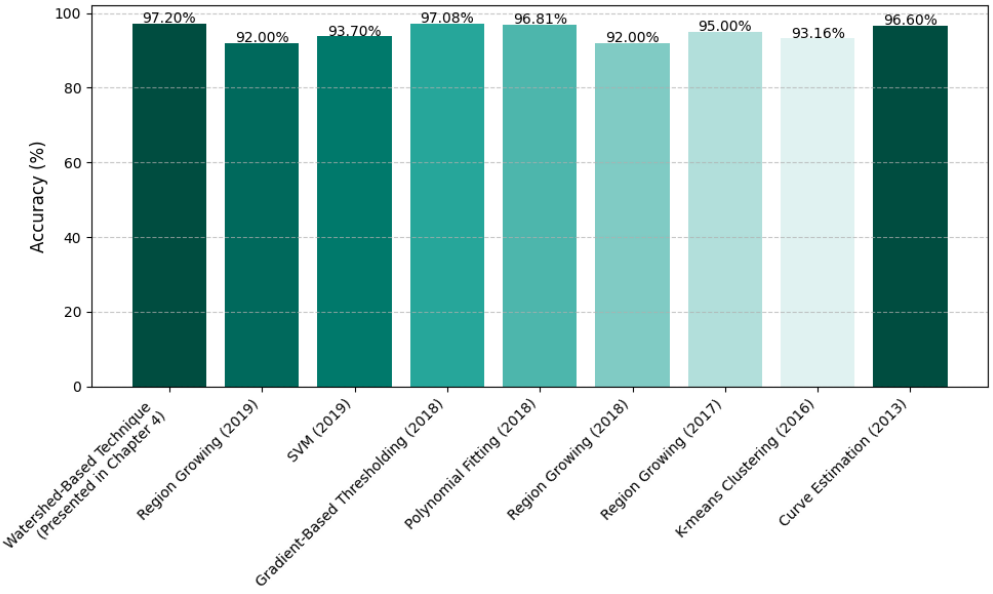

Figure 8.1: Comparative results of pectoral muscle segmentation of Watershed-Based Technique (presented method) with other existing methods.

8.3.2 SVM and Deep Learning in Breast Cancer Detection

The integration of SVM with Harris Hawks Optimization (HHO) and Cuckoo Search (CS) algorithms marked a significant advancement in breast cancer classification. This hybrid SVM framework (Framework-I) showed remarkable accuracy improvements, demonstrating the potential of combining traditional machine learning models with advanced optimization techniques. The table 8.2 compares the accuracy of the presented Hybrid HHO-CS MKSVM framework (Framework-I) against existing methods. The graphical representation of this comparison is given in figure 8.2.

Table 8.2: Comparative results of presented Hybrid HHO-CS MKSVM framework (Framework-I) with existing similar methods

Method	Accuracy(%)	Reference
Hybrid HHO-CS MKSVM (Framework-I, Presented in Chapter 5)	94.08	Haris et al. [2024]
PSO ANN	91.10	Huang et al. [2012]
PSO ANFIS	92.80	Huang et al. [2012]
CAR-BBO	92.52	Zhang et al. [2016]
CSDCNN	93.20	Han et al. [2017]

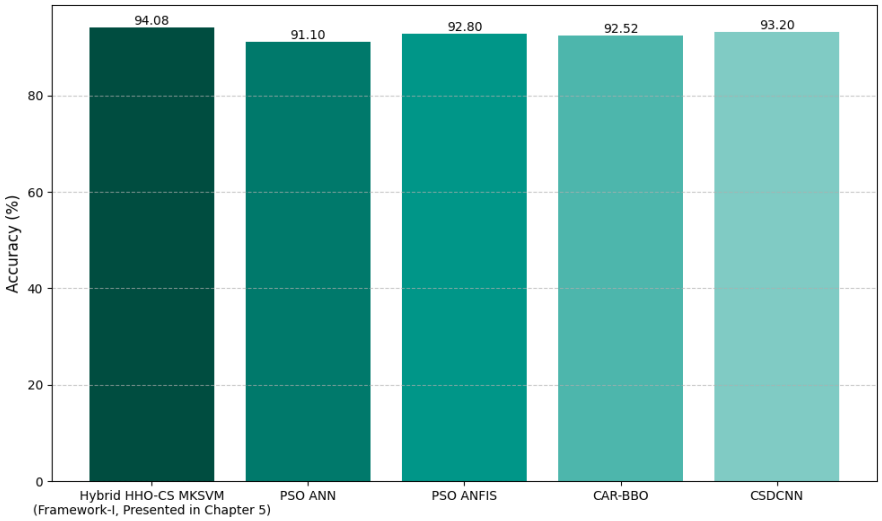

Figure 8.2: Comparative results of Hybrid HHO-CS MKSVM framework (Framework-I) with other existing methods.

The Multi-Feature Learning (MFL) Framework, based on a modified Faster R-CNN algorithm, made substantial strides in segmentation and classification performance. This deep learning-based approach effectively leverages multiple features extracted from mammographic images, leading to more accurate cancer detection. Table 8.3 provides a comparative analysis of the results of this presented deep learning framework (Framework-II) in breast cancer detection. The graphical representation of this comparison is given in figure 8.3.

Table 8.3: Comparative results of Multi-Feature Learning framework (Framework-II) with existing similar methods

Method	**Accuracy (%)**		**Reference**
	INbreast	**MIAS**	
MFL (Framework-II, Presented in Chapter 6)	95.43	95.82	Tables 6.1 & 6.2
BOA	92.30	90.22	Priyadharsini et al. [2023]
TSO	81.71	91.57	Kumar et al. [2022]
MFO	91.45	89.51	Sarathkumar et al. [2023]
WSO	91.20	93.67	Ayyarao et al. [2022]

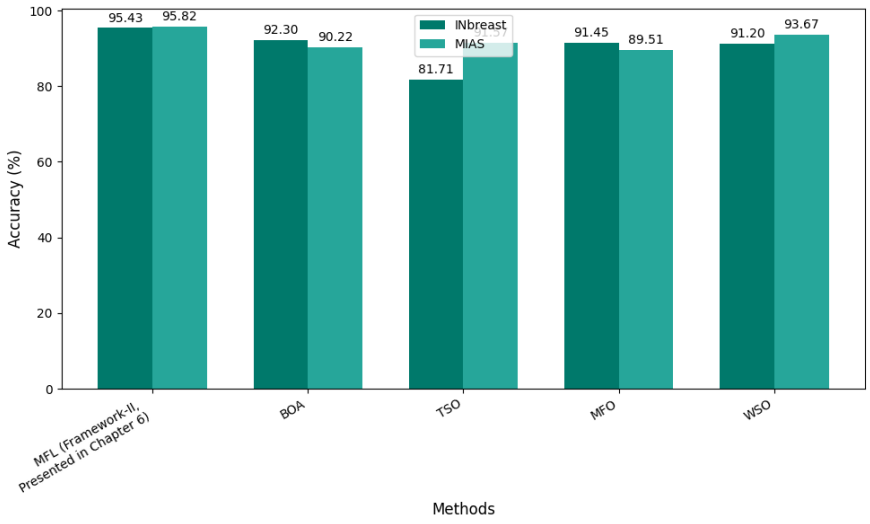

Figure 8.3: Comparative results of MFL framework (Framework-II) with other existing methods.

Lastly, the Triplet Deep Learning (TDL) Framework that integrates TFR-CNN with AD-DNN showcased superior segmentation and classification capabilities. This framework is particularly adept at differentiating between benign and malignant tissues, which is crucial for accurate diagnosis. These methodologies represent groundbreaking approaches in medical imaging and are likely to have significant implications for breast cancer diagnosis and treatment. Table 8.4 provides a comparative analysis of the results obtained from implementing this deep learning framework (Framework-III) in breast cancer detection. The graphical representation of this comparison is given in figure 8.4.

Table 8.4: Comparative results of presented Triplet Deep Learning framework with similar existing methods

Method	**Accuracy(%)**	**Reference**
TDL (Framework-III, Presented in Chapter 7)	97.98	Table 7.2
TDO	95.72	Anishkaa et al. [2023]
COA	92.88	Thirumoorthy and J. [2023]
SLO	92.76	Hemeida et al. [2022]
RSO	90.51	Rekha et al. [2024]

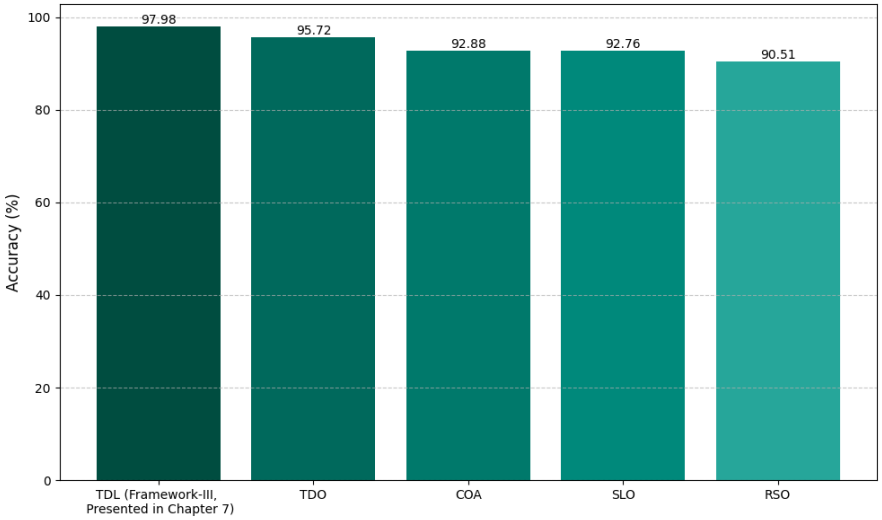

Figure 8.4: Comparative results of the comparison of TDL framework (Framework-III) with other existing methods.

The comparative results in tables 8.2, 8.3 and 8.4 demonstrate the superior performance of the presented methodologies in breast cancer classification. These presented frameworks show significantly higher accuracy and better performance metrics compared to existing techniques, highlighting their potential in enhancing the precision of mammographic image analysis.

8.4 Key Contributions

- Development of an advanced pectoral muscle segmentation technique using watershed transformation and regularization, achieving 97.2% accuracy on the MIAS database.
- Introduction of a hybrid SVM model, HHO-CS MKSVM, for breast image segmentation and classification, with 94.08% accuracy on the DDSM dataset.
- Implementation of a multi-feature learning framework for mammography-based breast cancer diagnosis, enhancing segmentation and classification with accuracies of 95.43% and 95.82% on INbreast and MIAS datasets, respectively.
- Integration of Explainable AI with a Triplet Deep Learning model and an Adaptive Deep Neural Network (AD-DNN) for improved segmentation and classification, achieving 97.98% accuracy on the DDSM dataset.

8.5 Recommendations for Future Research

Investigate the effectiveness of mammogram classification by applying various AI models, including convolutional neural networks based on the inception architecture, such as GoogLeNet, and seminal deep learning models like ResNet. The developed methods can be further tested on a larger dataset to incorporate challenging variabilities such as dense breast tissue, overlap of normal structures and aging-related changes, thereby demonstrating the stability of the methods. Exploring improved feature extraction methods and ensemble learning strategies like bagging, boosting, and stacking might tackle the challenge of complex images. Develop algorithms to

integrate genetic data with mammograms to improve cancer detection and identify genetic markers for personalized treatments.

List of Publications of the Author

1. **U. Haris**, V. Kabeer, and K. Afsal. "Breast Cancer Segmentation Using Hybrid HHO-CS SVM Optimization Techniques." Multimedia Tools and Applications, 2024. https://doi.org/10.1007/s11042-023-18025-7.

2. **U. Haris** and V. Kabeer. Automated breast pectoral muscle segmentation in digital mammograms using holistic regularization method. *Journal of Clinical Otorhinolaryngology, Head, and Neck Surgery*. 27(01), 2023. ISSN 1001-1781. URL https://www.lcebyhkzz.cn/article/view/2023/763.pdf.

3. **U. Haris** and V. Kabeer. The Power of Machines in Automatic Detection of Diseases: A Review on Computer Aided Detection of Breast Cancer in Digital Mammograms. *Singularities - A Trans-Disciplinary Biannual Research Journal*. 3(2):146–152, July 2016. ISSN 2348-3369. URL https://scholar.google.com/scholar?oi=bibs&cluster=5237242210105748 28&btnI=1&hl=en

4. **U. Haris** and V. Kabeer. Breast Cancer Classification Using Explainable AI on Digital Mammograms. In proceedings of *International Conference on Computational Intelligence Practices and Technologies (ConCIPT) 2024*. Research Department of Computer Science, Farook College (Autonomous), Calicut, Kerala, India. January 2024.

5. **U. Haris** and V. Kabeer. A Review of Mammography Views used in Automatic Detection of Breast Cancer. In proceedings of *International Conference on Computational Intelligence Practices and Technologies (ConCIPT) 2020*. Research Department of Computer Science, Farook College (Autonomous), Calicut, Kerala, India. January 2020.

6. **U. Haris** and V. Kabeer. Features of Databases used in Computer Aided Detection of Breast Cancer in Digital Mammograms. In proceedings of *National Workshop on Expertizing Network Infrastructure and Administration Concepts for the Academic Fraternity*. Page 10. Research Department of Computer Science, Farook College (Autonomous), Calicut, Kerala, India. March 2016.

7. **U. Haris** and V. Kabeer. Automated Orientation Detection and Normalization Algorithm - A Rule Based Preprocessing Method for Digital Mammogram Images. In proceedings of *International Conference on Signal, Power, Communication, Security and Computing Applications*. Page 62. Department of

Electronics Instrumentation Engineering, College of Engineering Vadakara. October 2016.

Bibliography

Fasna T A and Rekha Lakshmanan. An approach for pre-processing mammogram for early breast cancer detection. In *National Conference on Advanced Computing, Communication and Electrical Systems - (NCACCES'17)*, 2017.

D Abdelhafiz, J Bi, R Ammar, et al. Convolutional neural network for automated mass segmentation in mammography. *BMC Bioinformatics*, 21(Suppl 1):192, 2020. doi: 10.1186/s12859-020-3521-y. URL `https://doi.org/10.1186/s12859-020-3521-y`.

S.A. Agnes, J. Anitha, S.I.A. Pandian, and J.D. Peter. Classification of mammogram images using multiscale all convolutional neural network (ma-cnn). *Journal of Medical Systems*, 44:1–9, 2020.

L. Ahmed, M.M. Iqbal, H. Aldabbas, S. Khalid, Y. Saleem, and S. Saeed. Images data practices for semantic segmentation of breast cancer using deep neural network. *Journal of Ambient Intelligence and Humanized Computing*, pages 1–17, 2020.

M.A. Al-antari, M.A. Al-masni, and T.S. Kim. Deep learning computer-aided diagnosis for breast lesion in digital mammogram. In G. Lee and H. Fujita, editors, *Deep Learning in Medical Image Analysis*, volume 1213 of *Advances in Experimental Medicine and Biology*. Springer, Cham, 2020. doi: 10.1007/978-3-030-33128-3_4.

M.A. Al-Antari, S.M. Han, and T.S. Kim. Evaluation of deep learning detection and classification towards computer-aided diagnosis of breast lesions in digital x-ray mammograms. *Computer Methods and Programs in Biomedicine*, 196:105584, 2020.

Mugahed A. Al-antari, Seung-Moo Han, and Tae-Seong Kim. Evaluation of deep learning detection and classification towards computer-aided diagnosis of breast lesions in digital x-ray mammograms. *Computer Methods and Programs in Biomedicine*, 196:105584, 2020. doi: 10.1016/j.cmpb.2020.105584. URL `https://www.sciencedirect.com/science/article/pii/S0169260720314176`.

M. Al-Bayati and A. El-Zaart. Mammogram images thresholding for breast cancer detection using different thresholding methods. *Advances in Breast Cancer Research*, 2:72–77, 2013. doi: 10.4236/abcr.2013.23013.

M.A. Al-Masni, M.A. Al-Antari, J.M. Park, G. Gi, T.Y. Kim, P. Rivera, E. Valarezo, M.T. Choi, S.M. Han, and T.S. Kim. Simultaneous detection and classification of breast masses in digital mammograms via a deep learning yolo-based cad system. *Computer Methods and Programs in Biomedicine*, 157:85–94, 2018.

M.A. Al-Masni, D.H. Kim, and T.S. Kim. Multiple skin lesions diagnostics via integrated deep convolutional networks for segmentation and classification. *Computer Methods and Programs in Biomedicine*, 190:105351, 2020.

T. Alam, W.C. Shia, F.R. Hsu, and T. Hassan. Improving breast cancer detection and diagnosis through semantic segmentation using the unet3+ deep learning framework. *Biomedicines*, 11(6):1536, 2023.

Mohammad Alkhaleefah, Praveen Kumar Chittem, Vishnu Priya Achhannagari, Shang-Chih Ma, and Yang-Lang Chang. The influence of image augmentation on breast lesion classification using transfer learning. In *2020 International Conference on Artificial Intelligence and Signal Processing (AISP)*, pages 1–5, 2020. doi: 10.1109/AISP48273.2020.9073516.

American Cancer Society. Breast cancer facts & figures 2022-2024. *American Cancer Society*, 2022. URL `https://www.cancer.org/research/cancer-facts-statistics/breast-cancer-facts-figures.html`. [Online; accessed December 26, 2023].

American College of Radiology. *ACR and SBI continue to recommend starting annual mammography at age 40*. American College of Radiology, 2021. URL `https://www.acr.org/`.

David E. Anderson. Breast Cancer. In *Familial Cancer: 1st International Research Conference, Basel, September 1985*. S.Karger AG, 12 1985. ISBN 978-3-8055-4245-6. doi: 10.1159/000412519. URL `https://doi.org/10.1159/000412519`.

Balasubramaniam Anishkaa, Shanmugasundaram Lackesh, TK Divya, and Hemprasad Yashwant Patil. Breast cancer classification using optimizer-based feature selection: A metaheuristic approach. In *2023 International Conference on Next Generation Electronics (NEleX)*, pages 1–6. IEEE, 2023.

M. Arnold, E. Morgan, H. Rumgay, A. Mafra, D. Singh, M. Laversanne, and et al. Current and future burden of breast cancer: global statistics for 2020 and 2040. *Breast*, 2022. doi: 10.1016/j.breast.2022.08.010. URL `https://doi.org/10.1016/j.breast.2022.08.010`. Published online 2 September 2022.

Santhos Kumar Avuti et al. A novel pectoral muscle segmentation from scanned mammograms using emo algorithm. *Biomedical engineering letters*, 9(4):481–496, 2019. doi: 10.1007/s13534-019-00135-7.

Tummala. S. L. V. Ayyarao, N. S. S. Ramakrishna, Rajvikram Madurai Elavarasan, Nishanth Polumahanthi, M. Rambabu, Gaurav Saini, Baseem Khan, and Bilal Alatas. War strategy optimization algorithm: A new effective metaheuristic algorithm for global optimization. *IEEE Access*, 10:25073–25105, 2022. doi: 10.1109/ACCESS.2022.3153493.

Samir Bandyopadhyay. Pre-processing of mammogram images. *International Journal of Engineering Science and Technology*, 2, 11 2010. ISSN 0975-5462.

IN Bankman, T Nizialek, I Simon, OB Gatewood, IN Weinberg, and WR Brody. Segmentation algorithms for detecting microcalcifications in mammograms. *IEEE Transactions on Information Technology in Biomedicine*, 1(2):141–149, 1997.

L. W. Bassett, D. H. Bunnell, R. H. Gold, and R. Jahanshahi. Film-screen mammography: comparison of views. *Journal of the National Medical Association*, 81(4): 391–394, Apr 1989.

P. J. Besl and R. C. Jain. Segmentation through variable-order surface fitting. *IEEE Transactions on Pattern Analysis and Machine Intelligence*, PAMI-10:167–192, 1988.

P.B. Bhalerao and S.V. Bonde. Cuckoo search based multi-objective algorithm with decomposition for detection of masses in mammogram images. *International Journal of Information Technology*, 13:2215–2226, 2021. doi: 10.1007/s41870-021-00805-9. URL `https://doi.org/10.1007/s41870-021-00805-9`.

S. Bhuvaneswari, T. S. Subashini, and N. Thillaigovindan. Detection and removal of scratches in images. In Rajendra Prasath and T. Kathirvalavakumar, editors, *Mining Intelligence and Knowledge Exploration*, pages 212–223, Cham, 2013. Springer International Publishing. ISBN 978-3-319-03844-5.

Bernhard E. Boser, Isabelle M. Guyon, and Vladimir N. Vapnik. A training algorithm for optimal margin classifiers. In *Fifth Annual Workshop on Computational Learning Theory*, pages 144–152. ACM, 1992.

J Bozek, K Delac, and M Grgic. Computer-aided detection and diagnosis of breast abnormalities in digital mammography. In *2008 50th International Symposium ELMAR*, volume 1, pages 45–52, 2008.

Pramit Brata Chanda and Subir Kumar Sarkar. Detection and classification technique of breast cancer using multi kernal svm classifier approach. In *2018 IEEE Applied Signal Processing Conference (ASPCON)*, pages 320–325, 2018. doi: 10.1109/ASPCON.2018.8748810.

Hongmin Cai, Jing Wang, Tingting Dan, and et al. An online mammography database with biopsy confirmed types. *Scientific Data*, 10:123, 2023. doi: 10.1038/s41597-023-02025-1. URL `https://doi.org/10.1038/s41597-023-02025-1`.

C. B. Caldwell, S. J. Stapleton, D. W. Holdsworth, R. A. Jong, W. J. Weiser, G. Cooke, and M. J. Yaffe. Characterisation of mammographic parenchymal pattern by fractal dimension. *Physics in Medicine and Biology*, 35(2):235, 1990. doi: 10.1088/0031-9155/35/2/004. URL https://dx.doi.org/10.1088/0031-9155/35/2/004.

KS Camilus, V Govindan, and P Sathidevi. Pectoral muscle identification in mammograms. *Journal of Applied Clinical Medical Physics*, 12:215–230, 2011. doi: 10.1120/jacmp.v12i3.3285. URL https://doi.org/10.1120/jacmp.v12i3.3285.

Zhenjie Cao, Zhicheng Yang, Xinya Liu, Yanbo Zhang, Shibin Wu, Ruei-Sung Lin, Lingyun Huang, Mei Han, and Jie Ma. Deep learning based lesion detection for mammograms. In *2019 IEEE International Conference on Healthcare Informatics (ICHI)*, pages 1–3, 2019. doi: 10.1109/ICHI.2019.8904695.

Centers for Disease Control and Prevention. *What is Breast Cancer Screening?* Centers for Disease Control and Prevention, July 25 2023. URL https://www.cdc.gov/cancer/breast/basic_info/mammograms.htm.

S.S. Chakravarthy and H. Rajaguru. Automatic detection and classification of mammograms using improved extreme learning machine with deep learning. *IRBM*, 43(1):49–61, 2022.

L. Chaloeykitti, M. Muttarak, and K. H. Ng. Artifacts in mammography: ways to identify and overcome them. *Singapore Medical Journal*, 47(7):634–640; quiz 641, 2006.

D. Abraham Chandy, J. Stanly Johnson, and S. Easter Selvan. Texture feature extraction using gray level statistical matrix for content-based mammogram retrieval. *Multimedia Tools and Applications*, 72:2011–2024, 2014. doi: 10.1007/s11042-013-1511-z.

HD Cheng, XJ Shi, R Min, LM Hu, XP Cai, and HN Du. Approaches for automated detection and classification of masses in mammograms. *Pattern recognition*, 39(4): 646–668, 2006.

Chunyan Cui, Li Li, Hongmin Cai, Zhihao Fan, Ling Zhang, Tingting Dan, Jiao Li, and Jinghua Wang. The chinese mammography database (cmmd): An online mammography database with biopsy confirmed types for machine diagnosis of breast. The Cancer Imaging Archive, 2021. DOI: https://doi.org/10.7937/tcia.eqde-4b16.

M. P. De Albuquerque, I. Esquef, and A. R. G. Mello. Image thresholding using tsallis entropy. *Pattern Recognition Letters*, 25(9):1059–1065, 2004. doi: 10.1016/j.patrec.2004.03.003. URL https://doi.org/10.1016/j.patrec.2004.03.003.

Sidney M.L. de Lima, Abel G. da Silva-Filho, and Wellington Pinheiro dos Santos. Detection and classification of masses in mammographic images in a multi-kernel approach. *Computer Methods and Programs in Biomedicine*, 134:11–29, 2016. ISSN 0169-2607. doi: https://doi.org/10.1016/j.cmpb.2016.04.029. URL `https://www.sciencedirect.com/science/article/pii/S0169260716304242`.

C. de Martel, D. Georges, F. Bray, J. Ferlay, and G. M. Clifford. Global burden of cancer attributable to infections in 2018: a worldwide incidence analysis. *The Lancet Global Health*, 8(2):e180–e190, 2020. doi: 10.1016/S2214-109X(19)30488-7.

Mohammad Dehghani, Štěpán Hubálovský, and Pavel Trojovský. Tasmanian devil optimization: A new bio-inspired optimization algorithm for solving optimization algorithm. *IEEE Access*, 10:19599–19620, 2022. doi: 10.1109/ACCESS.2022.3151641.

J. Deng, Y. Ma, D.A. Li, J. Zhao, Y. Liu, and H. Zhang. Classification of breast density categories based on se-attention neural networks. *Computer Methods and Programs in Biomedicine*, 193:105489, 2020.

A.P. Dhawan, Y. Chitre, and C. Kaiser-Bonasso. Analysis of mammographic microcalcifications using gray-level image structure features. *IEEE Transactions on Medical Imaging*, 15(3):246–259, 1996. doi: 10.1109/42.500063.

G. Dileep and Gyani SG Gianchandani. Artificial intelligence in breast cancer screening and diagnosis. *Cureus*, 14(10):e30318, Oct 2022. doi: 10.7759/cureus.30318.

Radu Dobrescu, Loretta Ichim, and Daniela Crisan. Diagnosis of breast cancer from mammograms by using fractal measures. *International journal of medical imaging*, 1(2):32–38, 2013.

Kunio Doi. Computer-aided diagnosis in medical imaging: Historical review, current status and future potential. *Computerized Medical Imaging and Graphics*, 31(4-5):198–211, 2007.

S. Don, Duckwon Chung, K. Revathy, Eunmi Choi, and Dugki Min. A new approach for mammogram image classification using fractal properties. *Cybernetics and Information Technologies*, 12(2):69 – 83, 2012. doi: https://doi.org/10.2478/cait-2012-0013.

Carl J. D'Orsi. *2013 ACR BI-RADS Atlas: Breast Imaging Reporting and Data System*. American College of Radiology, 5 edition, 2014. ISBN 155903016X, 9781559030168.

D. Duda, M. Kretowski, and J. Bezy-Wendling. Computer-aided diagnosis of liver tumors based on multi-image texture analysis of contrast-enhanced ct. selection of the most appropriate texture features. *Studies in Logic, Grammar and Rhetoric*, 35(1):49–70, 2013.

S. Duraisamy and S. Emperumal. Computer-aided mammogram diagnosis system using deep learning convolutional fully complex-valued relaxation neural network classifier. *IET Computer Vision*, 11(8):656–662, 2017.

Margaret M. Eberl, Chester H. Fox, Stephen B. Edge, Cathleen A. Carter, and Martin C. Mahoney. Bi-rads classification for management of abnormal mammograms. *The Journal of the American Board of Family Medicine*, 19(2):161–164, March 2006. doi: 10.3122/jabfm.19.2.161.

A. S. Elkorany and Z. F. Elsharkawy. Efficient breast cancer mammograms diagnosis using three deep neural networks and term variance. *Scientific Reports*, 13(1): 2663, 2023. doi: 10.1038/s41598-023-29875-4. URL `https://doi.org/10.1038/s41598-023-29875-4`.

Joann G. Elmore, Katrina Armstrong, Constance D. Lehman, and Suzanne W. Fletcher. Screening for Breast Cancer. *JAMA*, 293(10):1245–1256, 03 2005. ISSN 0098-7484. doi: 10.1001/jama.293.10.1245. URL `https://doi.org/10.1001/jama.293.10.1245`.

Jose Escorcia-Gutierrez, Romany Mansour, Kelvin Beleño, et al. Automated deep learning empowered breast cancer diagnosis using biomedical mammogram images. *Tech Science Press*, 2022. Accessed on January 2, 2024.

Rebecca Fahrig and Martin J Yaffe. A model for optimization of spectral shape in digital mammography. *Medical Physics*, 21(9):1463, 1994. doi: 10.1118/1.597406.

Athraa H. Farhan and Mohammed Y. Kamil. Texture analysis of mammogram using local binary pattern method. *Journal of Physics: Conference Series*, 1530 (1):012091, may 2020. doi: 10.1088/1742-6596/1530/1/012091. URL `https://dx.doi.org/10.1088/1742-6596/1530/1/012091`.

H. Feng, J. Cao, H. Wang, Y. Xie, D. Yang, J. Feng, and B. Chen. A knowledge-driven feature learning and integration method for breast cancer diagnosis on multi-sequence mri. *Magnetic Resonance Imaging*, 69:40–48, 2020.

J. Ferlay, M. Ervik, F. Lam, M. Colombet, L. Mery, M. Piñeros, and et al. *Global Cancer Observatory: Cancer Today*. International Agency for Research on Cancer, 2020. URL `https://gco.iarc.fr/today`.

Helen ML Frazer, Alex K Qin, Hong Pan, and Peter Brotchie. Evaluation of deep learning-based artificial intelligence techniques for breast cancer detection on mammograms: Results from a retrospective study using a breastscreen victoria dataset. *Journal of Medical Imaging and Radiation Oncology*, 65(5):529–537, 2021. doi: 10.1111/1754-9485.13278.

Timothy W. Freer and Michael J. Ulissey. Screening mammography with computer-aided detection: Prospective study of 12,860 patients in a community breast

center. *Radiology*, 220(3):781–786, 2001. doi: 10.1148/radiol.2203001282. URL https://doi.org/10.1148/radiol.2203001282. PMID: 11526282.

K.S. Fu and J.K. Mui. A survey on image segmentation. *Pattern Recognition*, 13(1):3–16, 1981. ISSN 0031-3203. doi: https://doi.org/10.1016/0031-3203(81)90028-5. URL https://www.sciencedirect.com/science/article/pii/0031320381900285.

Minu George and Reyer Zwiggelaar. Comparative study on local binary patterns for mammographic density and risk scoring. *Journal of Imaging*, 5(2):24, 2019. doi: 10.3390/jimaging5020024. URL https://doi.org/10.3390/jimaging5020024.

Krzysztof J. Geras, Ritse M. Mann, and Linda Moy. Artificial intelligence for mammography and digital breast tomosynthesis: Current concepts and future perspectives. *Radiology*, 293(2):246–259, 2019. doi: 10.1148/radiol.2019182627.

Swarup Kr Ghosh, Biswajit Biswas, and Anupam Ghosh. A novel noise removal technique influenced by deep convolutional autoencoders on mammograms. In D.P. Acharjya, A. Mitra, and N. Zaman, editors, *Deep Learning in Data Analytics*, volume 91 of *Studies in Big Data*. Springer, 2022. doi: 10.1007/978-3-030-75855-4_2. URL https://doi.org/10.1007/978-3-030-75855-4_2.

R H Gold, L W Bassett, and B E Widoff. Highlights from the history of mammography. *RadioGraphics*, 10(6):1111–1131, 1990. doi: 10.1148/radiographics.10.6.2259767. URL https://doi.org/10.1148/radiographics.10.6.2259767. PMID: 2259767.

T.O. Gulsrud, K. Engan, and T. Hanstveit. Watershed segmentation of detected masses in digital mammograms. In *2005 IEEE Engineering in Medicine and Biology 27th Annual Conference*, pages 3304–3307, 2005. doi: 10.1109/IEMBS.2005.1617183.

Mohamed H, Mabrouk MS, and Sharawy A. Computer aided detection system for micro calcifications in digital mammograms. *Comput Methods Programs Biomed*, 116(3):226–235, 2014.

O. Haji Maghsoudi, A. Gastounioti, C. Scott, L. Pantalone, F. F. Wu, E. A. Cohen, S. Winham, E. F. Conant, C. Vachon, and D. Kontos. Deep-libra: An artificial-intelligence method for robust quantification of breast density with independent validation in breast cancer risk assessment. *Medical Image Analysis*, 73, 2021. doi: 10.1016/j.media.2021.102138. URL https://doi.org/10.1016/j.media.2021.102138.

Mark D. Halling-Brown, Lucy M. Warren, Dominic Ward, Emma Lewis, Alistair Mackenzie, Matthew G. Wallis, Louise S. Wilkinson, Rosalind M. Given-Wilson, Rita McAvinchey, and Kenneth C. Young. Optimam mammography image database: A large-scale resource of mammography images and clinical data. *Radiology: Artificial Intelligence*, 3(1):e200103, 2021. doi: 10.1148/ryai.2020200103. URL https://doi.org/10.1148/ryai.2020200103.

Zhongyi Han, Benzheng Wei, Yuanjie Zheng, Yilong Yin, Kejian Li, and Shuo Li. Breast cancer multi-classification from histopathological images with structured deep learning model. *Scientific Reports*, 7(4172), 2017.

Robert M. Haralick and Linda G. Shapiro. Image segmentation techniques. *Computer Vision, Graphics, and Image Processing*, 29(1):100–132, 1985. ISSN 0734-189X. doi: https://doi.org/10.1016/S0734-189X(85)90153-7. URL `https://www.sciencedirect.com/science/article/pii/S0734189X85901537`.

U. Haris and V. Kabeer. Automated breast pectoral muscle segmentation in digital mammograms using holistic regularization method. *Journal of Clinical Otorhinolaryngology, Head, and Neck Surgery*, 27(01), 2023. ISSN 1001-1781. URL `https://www.lcebyhkzz.cn/article/view/2023/763.pdf`.

U. Haris, V. Kabeer, and K. Afsal. Breast cancer segmentation using hybrid hho-cs svm optimization techniques. *Multimedia Tools and Applications*, 2024. ISSN 1573-7721. doi: 10.1007/s11042-023-18025-7. Accepted article, details based on the review recommendations.

Pratibha Harrison and Kihan Park. Tumor detection in breast histopathological images using faster r-cnn. In *2021 International Symposium on Medical Robotics (ISMR)*, pages 1–7, 2021. doi: 10.1109/ISMR48346.2021.9661483.

M Hazarika and LB Mahanta. A novel region growing based method to remove pectoral muscle from mlo mammogram images. In *Advances in electronics, communication and computing*, pages 307–316. Springer, 2018. doi: 10.1007/978-981-10-4765-7_32. URL `https://doi.org/10.1007/978-981-10-4765-7_32`.

Michael Heath, Kevin Bowyer, Daniel Kopans, W. Philip Kegelmeyer, Richard Moore, Kyong Chang, and S. MunishKumaran. Title. In *Digital Mammography, Proceedings of the Fourth International Workshop on Digital Mammography*, pages 457–460. Kluwer Academic Publishers, 1998. URL `http://www.eng.usf.edu/cvprg/Mammography/software/HeathEtAlIWDM_1998.pdf`.

Michael Heath, Kevin Bowyer, Daniel Kopans, Richard Moore, and W. Philip Kegelmeyer. Title. In M.J. Yaffe, editor, *Proceedings of the Fifth International Workshop on Digital Mammography*, pages 212–218. Medical Physics Publishing, 2001. ISBN 1-930524-00-5. URL `http://www.eng.usf.edu/cvprg/Mammography/software/HeathEtAlIWDM_2000.pdf`.

Alaa Hefnawy. An improved approach for breast cancer detection in mammogram based on watershed segmentation. *International Journal of Computer Applications*, 75(15), 2013.

Ali Asghar Heidari, Seyedali Mirjalili, Hossam Faris, Ibrahim Aljarah, Majdi Mafarja, and Huiling Chen. Harris hawks optimization: Algorithm and applications. *Future Generation Computer Systems*, 97:849–872, 2019. ISSN 0167-739X. doi:

https://doi.org/10.1016/j.future.2019.02.028. URL https://www.sciencedirect.com/science/article/pii/S0167739X18313530. Source codes of HHO are publicly available at http://www.alimirjalili.com/HHO.html and http://www.evo-ml.com/2019/03/02/hho.

MA Helvie and SK Patterson. *Imaging Analysis: Mammography*, chapter 11. Lippincott Williams & Wilkins, Philadelphia, Pa, 5 edition, 2014.

Ashraf Mohamed Hemeida, Heba GamalEldeen Yahya, and Hamida Al-Sanary. Image segmentation using hybrid optimization algorithms. *Aswan University Journal of Sciences and Technology*, 2(2):86–104, 2022.

M. L. Huang, Y. H. Hung, W. M. Lee, R. K. Li, and T. H. Wang. Usage of case-based reasoning, neural network and adaptive neuro-fuzzy inference system classification techniques in breast cancer dataset classification diagnosis. *Journal of Medical Systems*, 36:407–414, 2012.

Rebecca A. Hubbard, Karla Kerlikowske, Chris I. Flowers, Bonnie C. Yankaskas, Weiwei Zhu, and Diana L. Miglioretti. Cumulative probability of false-positive recall or biopsy recommendation after 10 years of screening mammography. *Annals of Internal Medicine*, 155(8):481–492, 2011. doi: 10.7326/0003-4819-155-8-201110180-00004. URL https://www.acpjournals.org/doi/abs/10.7326/0003-4819-155-8-201110180-00004. PMID: 22007042.

Ahmad Ibrahim, Hossam K. Mohamed, Ahmed Maher, and Bin Zhang. A survey on human cancer categorization based on deep learning. *Front. Artif. Intell.*, 5:884749, 2022a. doi: 10.3389/frai.2022.884749.

S. A. Ibrahim, V. Riehl, and K. D. Beaman. Abstract 6297: New biomarker in liquid biopsies from breast and ovarian cancers. *Cancer Research*, 82(12_Supplement), 2022b. doi: 10.1158/1538-7445.am2022-6297. URL https://doi.org/10.1158/1538-7445.am2022-6297.

INbreast. INbreast Database, Accessed on: December 16, 2024. URL https://incisive-project.eu/new/incisive-can-access-the-inbreast-database/.

S. S. Ittannavar and R. H. Havaldar. Segmentation of breast masses in mammogram image using multilevel multiobjective electromagnetism-like optimization algorithm. *BioMed Research International*, 2022:8576768, 2022. doi: 10.1155/2022/8576768. URL https://doi.org/10.1155/2022/8576768.

G. R. Jothilakshmi and Arun Raaza. Effective detection of mass abnormalities and its classification using multi-svm classifier with digital mammogram images. In *2017 International Conference on Computer, Communication and Signal Processing (ICCCSP)*, pages 1–6, 2017. doi: 10.1109/ICCCSP.2017.7944090.

Navneet Kaur, Lakhwinder Kaur, and Sikander et al. Singh. Dlho: An enhanced version of harris hawks optimization by dimension learning-based hunting for breast cancer and other serious diseases detection. *Research Square*, Aug 2021. doi: 10.21203/rs.3.rs-798682/v1. PREPRINT (Version 1) available at Research Square.

Prabhpreet Kaur, Gurvinder Singh, and Parminder Kaur. Intellectual detection and validation of automated mammogram breast cancer images by multi-class svm using deep learning classification. *Informatics in Medicine Unlocked*, 16:100151, 2019. ISSN 2352-9148. doi: https://doi.org/10.1016/j.imu.2019.01.001. URL `https://www.sciencedirect.com/science/article/pii/S2352914818301813`.

T. Kavitha, P.P. Mathai, C. Karthikeyan, M. Ashok, R. Kohar, J. Avanija, and S. Neelakandan. Deep learning based capsule neural network model for breast cancer diagnosis using mammogram images. *Interdisciplinary Sciences: Computational Life Sciences*, pages 1–17, 2021.

T. Kavitha, P.P. Mathai, C. Karthikeyan, et al. Deep learning based capsule neural network model for breast cancer diagnosis using mammogram images. *Interdisciplinary Sciences: Computational Life Sciences*, 14:113–129, 2022. doi: 10.1007/s12539-021-00467-y.

M Ajay Kumar, Y Ramadevi, and Y Ramadevi. A study: mammogram image segmentation and classification based on abc algorithm and artificial neural networks. *Advanced Engineering Services (54/02)*, 2022.

S. M. Kwok, R. Chandrasekhar, and Y. Attikiouzel. Automatic pectoral muscle segmentation on mammograms by straight line estimation and cliff detection. In *The Seventh Australian and New Zealand Intelligent Information Systems Conference*, pages 67–72, Perth, WA, Australia, 2001. doi: 10.1109/ANZIIS.2001.974051.

M. Langarizadeh, R. Mahmud, A. R. Ramli, S. Napis, M. R. Beikzadeh, and W. E. Z. W. A. Rahman. Improvement of digital mammogram images using histogram equalization, histogram stretching and median filter. *Journal of Medical Engineering & Technology*, 35(2):103–108, 2011. doi: 10.3109/03091902.2010.542271.

Carolyn S. Lee, Mythreyi Bhargavan-Chatfield, Elizabeth S. Burnside, Paul Nagy, and Edward A. Sickles. The national mammography database: Preliminary data. *AJR Am J Roentgenol*, 206(4):883–890, April 2016. doi: 10.2214/AJR.15.14312. Epub 2016 Feb 11.

Cindy S. Lee, Linda Moy, Danny Hughes, Dan Golden, Mythreyi Bhargavan-Chatfield, Jennifer Hemingway, Agnieszka Geras, Richard Duszak, and Andrew B. Rosenkrantz. Radiologist characteristics associated with interpretive performance of screening mammography: A national mammography database (nmd) study. *Radiology*, 300(3):518–528, 2021. doi: 10.1148/radiol.2021204379. URL `https://doi.org/10.1148/radiol.2021204379`. PMID: 34156300.

Regina Lee, Francisco Gimenez, Assaf Hoogi, and et al. A curated mammography data set for use in computer-aided detection and diagnosis research. *Sci Data*, 4:170177, 2017. doi: 10.1038/sdata.2017.177. URL `https://doi.org/10.1038/sdata.2017.177`.

C. Lei et al. Artificial intelligence in breast cancer early detection and diagnosis. *Journal of Medical Systems*, 44:42, 2020.

H. Li, S. Zhuang, D.A. Li, J. Zhao, and Y. Ma. Benign and malignant classification of mammogram images based on deep learning. *Biomedical Signal Processing and Control*, 51:347–354, 2019a.

H. Li, K. Robinson, L. Lan, N. Baughan, C-W. Chan, M. Embury, G.J. Whitman, R. El-Zein, I. Bedrosian, and M.L. Giger. Temporal machine learning analysis of prior mammograms for breast cancer risk prediction. *Cancers*, 15(7):2141, 2023. doi: 10.3390/cancers15072141. URL `https://doi.org/10.3390/cancers15072141`.

Hua Li, Shasha Zhuang, Deng ao Li, Jumin Zhao, and Yanyun Ma. Benign and malignant classification of mammogram images based on deep learning. *Biomedical Signal Processing and Control*, 51:347–354, 2019b. ISSN 1746-8094. doi: https://doi.org/10.1016/j.bspc.2019.02.017. URL `https://www.sciencedirect.com/science/article/pii/S1746809419300618`.

Hua Li, Jing Niu, Dengao Li, and Chen Zhang. Classification of breast mass in two-view mammograms via deep learning. *IET Image Processing*, 15(2):454–467, 2021. doi: 10.1049/ipr2.12035. URL `https://ietresearch.onlinelibrary.wiley.com/doi/abs/10.1049/ipr2.12035`.

Y Li, H Chen, Y Yang, and N Yang. Pectoral muscle segmentation in mammograms based on homogenous texture and intensity deviation. *Pattern Recognition*, 46:681–691, 2013. doi: 10.1016/j.patcog.2012.09.021. URL `https://doi.org/10.1016/j.patcog.2012.09.021`.

J. Lin. Divergence measures based on the shannon entropy. *IEEE Transactions on Information Theory*, 37(1):145–151, 1991. doi: 10.1109/18.61115.

Jianyu Lin. Reversible integer-to-integer wavelet filter design for lossless image compression. *IEEE Access*, 8:89117–89129, 2020. doi: 10.1109/ACCESS.2020.2993605.

Chen-Chung Liu, Chung-Yen Tsai, Jui Liu, Chun-Yuan Yu, and Shyr-Shen Yu. A pectoral muscle segmentation algorithm for digital mammograms using otsu thresholding and multiple regression analysis. *Computers & Mathematics with Applications*, 64(5):1100–1107, 2012.

J. Logan, P.J. Kennedy, and D. Catchpoole. A review of the machine learning datasets in mammography, their adherence to the fair principles and the outlook for the

future. *Scientific Data*, 10:595, 2023. doi: 10.1038/s41597-023-02430-6. URL https://doi.org/10.1038/s41597-023-02430-6.

M. G. Lopez, N. Posada, D. C. Moura, R. R. Pollán, J. M. F. Valiente, C. S. Ortega, M. Solar, G. Diaz-Herrero, I. M. A. P. Ramos, J. Loureiro, and T. C. Fernandes. BCDR: A Breast Cancer Digital Repository. In *15th International Conference on Experimental Mechanics*, volume 1215, pages 113–120, July 2012.

B. N. Madhukar, S. H. Bharathi, and Ashwin M. Polnaya. Multi-scale convolution based breast cancer image segmentation with attention mechanism in conjunction with war search optimization. *International Journal of Computers and Applications*, 45(5):353–366, 2023. doi: 10.1080/1206212X.2023.2212945. URL https://doi.org/10.1080/1206212X.2023.2212945.

T. Mahmood, J. Li, Y. Pei, and F. Akhtar. An automated in-depth feature learning algorithm for breast abnormality prognosis and robust characterization from mammography images using deep transfer learning. *Biology*, 10(9):859, 2021a.

Tariq Mahmood, J. Li, Y. Pei, and F. Akhtar. An automated in-depth feature learning algorithm for breast abnormality prognosis and robust characterization from mammography images using deep transfer learning. *Biology*, 10(9):859, 2021b. doi: 10.3390/biology10090859.

IK Maitra, S Nag, and SK Bandyopadhyay. Technique for pre-processing of digital mammogram. *Comput Methods Programs Biomed*, 107:175–188, 2012. doi: 10.1016/j.cmpb.2011.05.007. URL https://doi.org/10.1016/j.cmpb.2011.05.007.

AS Majid, ES de Paredes, RD Doherty, NR Sharma, and X Salvador. Missed breast carcinoma: pitfalls and pearls. *Radiographics*, 23(4):881–895, 2003. doi: 10.1148/rg.234025083.

Jeanne S. Mandelblatt, Natasha K. Stout, Clyde B. Schechter, Jeroen J. van den Broek, Diana L. Miglioretti, Martin Krapcho, Amy Trentham-Dietz, Daniel Munoz, Sandra J. Lee, Donald A. Berry, Nicolien T. van Ravesteyn, Oguzhan Alagoz, Karla Kerlikowske, Anna N.A. Tosteson, Aimee M. Near, Alaric Hoeffken, Young Chang, Eveline A. Heijnsdijk, Gary Chisholm, Xuelin Huang, Hui Huang, Mehmet Ali Ergun, Ronald Gangnon, Brian L. Sprague, Sylvia Plevritis, Eric Feuer, Harry J. de Koning, and Kathleen A. Cronin. Collaborative modeling of the benefits and harms associated with different u.s. breast cancer screening strategies. *Annals of Internal Medicine*, 164(4):215–225, 2016. doi: 10.7326/M15-1536.

S. Maqsood, R. Damaševičius, and R. Maskeliūnas. Ttcnn: A breast cancer detection and classification towards computer-aided diagnosis using digital mammography in early stages. *Applied Sciences*, 12(7):3273, 2022.

M Masi. A step beyond tsallis and rényi entropies. *Physics Letters*, 338(3–5):217–224, 2005. doi: 10.1016/j.physleta.2005.01.094. URL https://doi.org/10.1016/j.physleta.2005.01.094.

A. Masood and A. Ali Al-Jumaily. Computer-aided diagnostic support system for skin cancer: A review of techniques and algorithms. *International Journal of Biomedical Imaging*, 2013.

R. Mata, E. Nava, and F. Sendra. Microcalcifications detection using multiresolution methods. In *Proceedings of the 15th International Conference on Pattern Recognition*, volume 4, pages 344–347. IEEE, Sept 2000.

Hiren Mewada, Jawad F. Al-Asad, Amit Patel, Jitendra Chaudhari, Keyur Mahant, and Alpesh Vala. Multi-channel local binary pattern guided convolutional neural network for breast cancer classification. *The Open Biomedical Engineering Journal*, 15:132–140, 2021. URL `https://www.openbiomedicalengineeringjournal.com/VOLUME/15/PAGE/132/FULLTEXT/`.

E Michael, H Ma, H Li, F Kulwa, and J Li. Breast cancer segmentation methods: Current status and future potentials. *BioMed Research International*, 2021:9962109, Jul 20 2021. doi: 10.1155/2021/9962109.

Miguel Angel Guevara López. *Breast Cancer Digital Repository*. University of Aveiro, 2012. URL `https://bcdr.eu/information/about`.

Mehrdad Moghbel et al. A review of breast boundary and pectoral muscle segmentation methods in computer-aided detection/diagnosis of breast mammography. *Artificial Intelligence Review*, 2019. doi: 10.1007/s10462-019-09721-8.

A. Mohd Khuzi, R. Besar, WMD Wan Zaki, and NN Ahmad. Identification of masses in digital mammogram using gray level co-occurrence matrices. *Biomedical Imaging and Intervention Journal*, 5(3):e17, 2009. doi: 10.2349/biij.5.3.e17.

I. C. Moreira, I. Amaral, I. Domingues, A. Cardoso, M. J. Cardoso, and J. S. Cardoso. Inbreast: Toward a full-field digital mammographic database. *Acad Radiol*, 19(2): 236–248, Feb 2012. doi: 10.1016/j.acra.2011.09.014. Epub 2011 Nov 10. PMID: 22078258.

M. F. Mridha, M. A. Hamid, M. M. Monowar, A. J. Keya, A. Q. Ohi, M. R. Islam, and J.-M. Kim. A comprehensive survey on deep-learning-based breast cancer diagnosis. *Cancers*, 13(23):6116, 2021. doi: 10.3390/cancers13236116. URL `https://doi.org/10.3390/cancers13236116`.

Gautam S. Muralidhar et al. Computer-aided detection of breast cancer - have all bases been covered? *Breast Cancer: Basic and Clinical Research*, 2:5–9, 2008. doi: 10.4137/bcbcr.s785.

M Mustra, M Grgic, and M Grgic. Robust automatic breast and pectoral muscle segmentation from scanned mammograms. *Signal Processing*, 93:2817–2827, 2013. doi: 10.1016/j.sigpro.2012.07.026. URL `https://doi.org/10.1016/j.sigpro.2012.07.026`.

Maryam Naderan and Yuri Zaychenko. Convolutional autoencoder application for breast cancer classification. In *2020 IEEE 2nd International Conference on System Analysis & Intelligent Computing (SAIC)*, pages 1–4, 2020. doi: 10.1109/SAIC51296.2020.9239139.

Sang Hee Nam and Jun Young Choi. A method of image enhancement and fractal dimension for detection of microcalcifications in mammogram. In *Proceedings of the 20th Annual International Conference of the IEEE Engineering in Medicine and Biology Society. Vol.20 Biomedical Engineering Towards the Year 2000 and Beyond (Cat. No.98CH36286)*, volume 2, pages 1009–1012 vol.2, 1998. doi: 10.1109/IEMBS.1998.745620.

National Cancer Institute. Seer training: Breast anatomy. National Cancer Institute, 2012. URL `https://training.seer.cancer.gov/breast/anatomy/`. Archived from the original on 2 May 2012. Retrieved 9 May 2012.

H. D. Nelson, K. Tyne, A. Naik, C. Bougatsos, B. K. Chan, and L.; U.S. Preventive Services Task Force Humphrey. Screening for breast cancer: an update for the u.s. preventive services task force. *Ann Intern Med*, 151(10):727–737, W237–42, 2009. doi: 10.7326/0003-4819-151-10-200911170-00009. URL `https://doi.org/10.7326/0003-4819-151-10-200911170-00009`. PMID: 19920273; PMCID: PMC2972726.

Heidi D. Nelson, Ellen S. O'Meara, Karla Kerlikowske, Suzanne Balch, and Diana Miglioretti. Factors associated with rates of false-positive and false-negative results from digital mammography screening: An analysis of registry data. *Ann Intern Med*, 164(4):226–235, 2016. doi: 10.7326/M15-0971. Epub 2016 Jan 12. PMID: 26756902; PMCID: PMC5091936.

T.M. Nguyen and R.M. Rangayyan. Shape analysis of breast masses in mammograms via the fractal dimension. In *2005 IEEE Engineering in Medicine and Biology 27th Annual Conference*, pages 3210–3213, 2005. doi: 10.1109/IEMBS.2005.1617159.

Matthias Omotayo Oladele, Adebanjo Adekiigbe, and Temilola Morufat Adepoju. A two-stage model for breast cancer detection and classification from mammograms, 2022. URL `https://ssrn.com/abstract=4068212`.

Susan G. Orel, Nehmet Kay, Carol Reynolds, and David C. Sullivan. Bi-rads categorization as a predictor of malignancy. *Radiology*, 211(3):845–850, 1999. doi: 10.1148/radiology.211.3.r99jn31845.

Nobuyuki Otsu. A threshold selection method from gray-level histograms. *IEEE transactions on systems, man, and cybernetics*, 9(1):62–66, 1979.

Olaide N. Oyelade and Absalom E. Ezugwu. A deep learning model using data augmentation for detection of architectural distortion in whole and patches of images. *Biomedical Signal Processing and Control*, 65:102366, 2021. ISSN 1746-8094. doi:

https://doi.org/10.1016/j.bspc.2020.102366. URL https://www.sciencedirect.com/science/article/pii/S1746809420304730.

Parita Oza, Paawan Sharma, Samir Patel, Festus Adedoyin, and Alessandro Bruno. Image augmentation techniques for mammogram analysis. *Journal of Imaging*, 8 (5):141, 2022. doi: 10.3390/jimaging8050141. URL https://doi.org/10.3390/jimaging8050141.

M. Paschali, W. Simson, A.G. Roy, R. Göbl, C. Wachinger, and N. Navab. Manifold exploring data augmentation with geometric transformations for increased performance and robustness. In *Information Processing in Medical Imaging*, volume 11492 of *Lecture Notes in Computer Science*, Cham, 2019. Springer. doi: 10.1007/978-3-030-20351-1_40.

Shivaji D. Pawar, Kamal Kr. Sharma, Suhas G. Sapate, and Geetanjali Y. Yadav. Segmentation of pectoral muscle from digital mammograms with depth-first search algorithm towards breast density classification. *Biocybernetics and Biomedical Engineering*, 41(3):1224–1241, 2021. ISSN 0208-5216. doi: 10.1016/j.bbe.2021.08.005. URL https://www.sciencedirect.com/science/article/pii/S020852162100098X.

F.J. Pérez-Benito, F. Signol, J.C. Perez-Cortes, A. Fuster-Baggetto, M. Pollan, B. Pérez-Gómez, D. Salas-Trejo, M. Casals, I. Martínez, and R. LLobet. A deep learning system to obtain the optimal parameters for a threshold-based breast and dense tissue segmentation. *Computer Methods and Programs in Biomedicine*, 195: 105668, 2020.

Karina Pesce, Mariela B. Orruma, César Hadad, Yamila Bermúdez Cano, Rosana Secco, and Alejandro Cernadas. Bi-rads terminology for mammography reports: What residents need to know. *Radiographics*, 39(2):319–320, Mar-Apr 2019. doi: 10.1148/rg.2019180068.

A. Petrosian, H.P. Chan, M.A. Helvie, M.M. Goodsitt, and D.D. Adler. Computer-aided diagnosis in mammography: Classification of mass and normal tissue by texture analysis. *Physics in Medicine & Biology*, 39(12):2273, 1994.

Etta D. Pisano, Constantine Gatsonis, Edward Hendrick, Martin Yaffe, Janet K. Baum, Suddhasatta Acharyya, Emily F. Conant, Laurie L. Fajardo, Lawrence Bassett, Carl D'Orsi, Roberta Jong, and Murray; Digital Mammographic Imaging Screening Trial (DMIST) Investigators Group Rebner. Diagnostic performance of digital versus film mammography for breast-cancer screening. *N Engl J Med*, 353 (17):1773–1783, 2005. doi: 10.1056/NEJMoa052911. Epub 2005 Sep 16. Erratum in: N Engl J Med. 2006 Oct 26;355(17):1840. PMID: 16169887.

M Suriya Priyadharsini, JGR Sathiaseelan, and JGR Sathiaseelan. Advanced deep-cnn breast cancer mammogram image detection and classification with butterfly optimisation algorithm. *International Journal of Computational Biology and Drug*

Design, 15(5):357–376, 2023. doi: 10.1504/IJCBDD.2023.133840. URL https://www.inderscienceonline.com/doi/abs/10.1504/IJCBDD.2023.133840.

M. Prodan, E. Paraschiv, and A. Stanciu. Applying deep learning methods for mammography analysis and breast cancer detection. *Applied Sciences*, 13(7):4272, 2023.

A. Qayyum and A. Basit. Automatic breast segmentation and cancer detection via svm in mammograms. In *2016 International Conference on Emerging Technologies (ICET)*, pages 1–6. IEEE, 2016. doi: 10.1109/ICET.2016.7813261. URL https://doi.org/10.1109/ICET.2016.7813261.

Jun Qin et al. A multilevel image thresholding method based on subspace elimination optimization. *Mathematical Problems in Engineering*, 2019:1–11, 2019. doi: 10.1155/2019/6706590.

B. R. G. R and H. Kumar. Segmentation of mammogram images using level set with cuckoo search optimisation. *Computer Methods in Biomechanics and Biomedical Engineering: Imaging & Visualization*, pages 1–8, 2022. doi: 10.1080/21681163.2022.2120827. URL https://doi.org/10.1080/21681163.2022.2120827.

Rinku Rabidas, Abhishek Midya, Anup Sadhu, and Jayasree Chakraborty. Benign-malignant mass classification in mammogram using edge weighted local texture features. In Georgia D. Tourassi and Samuel G. Armato III, editors, *Medical Imaging 2016: Computer-Aided Diagnosis*, volume 9785, page 97851X. International Society for Optics and Photonics, SPIE, 2016. doi: 10.1117/12.2216767. URL https://doi.org/10.1117/12.2216767.

D.A. Ragab, O. Attallah, M. Sharkas, J. Ren, and S. Marshall. A framework for breast cancer classification using multi-dcnns. *Computers in Biology and Medicine*, 131:104245, 2021.

U. Raghavendra, Anjan Gudigar, Tejaswi N. Rao, Edward J. Ciaccio, E.Y.K. Ng, and U. Rajendra Acharya. Computer-aided diagnosis for the identification of breast cancer using thermogram images: A comprehensive review. *Infrared Physics & Technology*, 102:103041, 2019. ISSN 1350-4495. doi: https://doi.org/10.1016/j.infrared.2019.103041. URL https://www.sciencedirect.com/science/article/pii/S1350449519304608.

Grazia Raguso, Antonietta Ancona, Loredana Chieppa, Samuela L'Abbate, Maria Luisa Pepe, Fabio Mangieri, Miriam De Palo, and Rangaraj M. Rangayyan. Application of fractal analysis to mammography. In *2010 Annual International Conference of the IEEE Engineering in Medicine and Biology*, pages 3182–3185, 2010. doi: 10.1109/IEMBS.2010.5627180.

Harjot Kaur Rahul Hans and Navreet Kaur. Opposition-based harris hawks optimization algorithm for feature selection in breast mass classification. *Journal of Interdisciplinary Mathematics*, 23(1):97–106, 2020. doi: 10.1080/09720502.2020.1721670. URL `https://doi.org/10.1080/09720502.2020.1721670`.

S.P. Sachin Raj, N. Sri Madhava Raja, M.R. Madhumitha, and V. Rajinikanth. Examination of digital mammogram using otsu's function and watershed segmentation. In *2018 Fourth International Conference on Biosignals, Images and Instrumentation (ICBSII)*, pages 206–212, 2018. doi: 10.1109/ICBSII.2018.8524794.

Andrik Rampun et al. Breast pectoral muscle segmentation in mammograms using a modified holistically-nested edge detection network. *Medical Image Analysis*, 57: 1–17, 2019. doi: 10.1016/j.media.2019.06.007.

Rangaraj M. Rangayyan and Thanh M. Nguyen. Fractal analysis of contours of breast masses in mammograms. *Journal of Digital Imaging*, 20(3):223–237, 2007. doi: 10.1007/s10278-006-0860-9.

R.M. Rangayyan, F.J. Ayres, and J.L. Desautels. A review of computer-aided diagnosis of breast cancer: Toward the detection of subtle signs. *Journal of the Franklin Institute*, 344(3-4):312–348, 2007a.

R.M. Rangayyan, R.J. Ferrari, and A.F. Frere. Analysis of bilateral asymmetry in mammograms using directional, morphological, and density features. *Journal of Electronic Imaging*, 16(1):013003, 2007b.

R.M. Rangayyan, S. Banik, and J.E. Desautels. Computer-aided detection of architectural distortion in prior mammograms of interval cancer. *Journal of Digital Imaging*, 23(5):611–631, 2010.

K. Sashi Rekha, D. Divya, Miruna Joe Amali, and N. Yuvaraj. Hybrid ml-mdkl feature subset selection and classification technique accompanied with rat swarm optimizer to classify the multidimensional breast cancer mammogram image. *Optik*, 297:171574, 2024. ISSN 0030-4026. doi: https://doi.org/10.1016/j.ijleo.2023.171574. URL `https://www.sciencedirect.com/science/article/pii/S0030402623010720`.

Erick Rodríguez-Esparza, Laura A. Zanella-Calzada, Diego Oliva, Ali Asghar Heidari, Daniel Zaldivar, Marco Pérez-Cisneros, and Loke Kok Foong. An efficient harris hawks-inspired image segmentation method. *Expert Systems with Applications*, 155:113428, 2020. ISSN 0957-4174. doi: https://doi.org/10.1016/j.eswa.2020.113428. URL `https://www.sciencedirect.com/science/article/pii/S0957417420302529`.

E. Rodrí¬guez-Esparza, L.A. Zanella-Calzada, D. Zaldivar, and C.E. Galván-Tejada. Automatic detection of malignant masses in digital mammograms based on a mcet-hho approach. In D. Oliva and S. Hinojosa, editors, *Applications of Hybrid*

Metaheuristic Algorithms for Image Processing, volume 890 of *Studies in Computational Intelligence*. Springer, Cham, 2020. doi: 10.1007/978-3-030-40977-7_15.

K. F. Ruud, W. C. Hiscox, I. Yu, and et al. Distinct phenotypes of cancer cells on tissue matrix gel. *Breast Cancer Res*, 22(1):82, 2020. doi: 10.1186/s13058-020-01321-7. URL https://doi.org/10.1186/s13058-020-01321-7.

Sannasi Chakravarthy S R and Harikumar Rajaguru. Comparison analysis of linear discriminant analysis and cuckoo-search algorithm in the classification of breast cancer from digital mammograms. *Asian Pacific Journal of Cancer Prevention: APJCP*, 20(8):2333–2337, Aug 2019. doi: 10.31557/APJCP.2019.20.8.2333.

N. Saffari, H.A. Rashwan, M. Abdel-Nasser, V. Kumar Singh, M. Arenas, E. Mangina, B. Herrera, and D. Puig. Fully automated breast density segmentation and classification using deep learning. *Diagnostics*, 10(11):988, 2020.

P. K. Sahoo, C. Wilkins, and J. Yeager. Threshold selection using renyi's entropy. *Pattern Recognition*, 30(1):71–84, 1997. doi: 10.1016/s0031-3203(96)00065-9. URL https://doi.org/10.1016/s0031-3203(96)00065-9.

P.K Sahoo, S Soltani, and A.K.C Wong. A survey of thresholding techniques. *Computer Vision, Graphics, and Image Processing*, 41(2):233–260, 1988. ISSN 0734-189X. doi: https://doi.org/10.1016/0734-189X(88)90022-9. URL https://www.sciencedirect.com/science/article/pii/0734189X88900229.

W.M. Salama and M.H. Aly. Deep learning in mammography images segmentation and classification: Automated cnn approach. *Alexandria Engineering Journal*, 60 (5):4701–4709, 2021.

K.A. Santhos, A. Kumar, V. Bajaj, et al. Mcculloch's algorithm inspired cuckoo search optimizer based mammographic image segmentation. *Multimedia Tools and Applications*, 79:30453–30488, 2020. doi: 10.1007/s11042-020-09310-w. URL https://doi.org/10.1007/s11042-020-09310-w.

M. Sarathkumar, K. S. Dhanalakshmi, and P. Rajkumar. Improving breast cancer detection in mammogram images using moth flame algorithm optimized convolutional neural network. In *2023 International Conference on Energy, Materials and Communication Engineering (ICEMCE)*, pages 1–5, 2023. doi: 10.1109/ICEMCE57940.2023.10434209.

Regina Sawyer-Lee, Francisco Gimenez, Assaf Hoogi, and Daniel Rubin. Curated breast imaging subset of digital database for screening mammography (cbis-ddsm). Data set, 2016. URL https://doi.org/10.7937/K9/TCIA.2016.7O02S9CY. The Cancer Imaging Archive.

John T. Schousboe, Karla Kerlikowske, Andrew Loh, and Steven R. Cummings. Personalizing mammography by breast density and other

risk factors for breast cancer: Analysis of health benefits and cost-effectiveness. *Annals of Internal Medicine*, 155(1):10–20, 2011. doi: 10.7326/0003-4819-155-1-201107050-00003. URL https://www.acpjournals.org/doi/abs/10.7326/0003-4819-155-1-201107050-00003. PMID: 21727289.

Ramprasaath R. Selvaraju, Michael Cogswell, Abhishek Das, Ramakrishna Vedantam, Devi Parikh, and Dhruv Batra. Grad-cam: Visual explanations from deep networks via gradient-based localization. In *2017 IEEE International Conference on Computer Vision (ICCV)*, pages 618–626, 2017. doi: 10.1109/ICCV.2017.74.

D. Selvathi and A. Aarthy Poornila. Deep learning techniques for breast cancer detection using medical image analysis. In J. Hemanth and V. Balas, editors, *Biologically Rationalized Computing Techniques For Image Processing Applications*, volume 25 of *Lecture Notes in Computational Vision and Biomechanics*. Springer, 2018. doi: 10.1007/978-3-319-61316-1_8. URL https://doi.org/10.1007/978-3-319-61316-1_8.

Amela Šerifovic-Trbalić, Amir Trbalić, Damir Demirović, Naida Prljača, and Philippe C Cattin. Classification of benign and malignant masses in breast mammograms. In *2014 37th International Convention on Information and Communication Technology, Electronics and Microelectronics (MIPRO)*, pages 228–233, Opatija, Croatia, 2014. IEEE. doi: 10.1109/MIPRO.2014.6859566. URL http://edoc.unibas.ch/dok/A6348363.

M. Sezgin and B. Sankur. Survey over image thresholding techniques and quantitative performance evaluation. *Journal of Electronic Imaging*, 13(1):146–168, 2004.

C. Sha, J. Hou, and H. Cui. A robust 2d otsu's thresholding method in image segmentation. *Journal of Visual Communication and Image Representation*, 41 (October):339–351, 2016.

Z. Sha, L. Hu, and B.D. Rouyendegh. Deep learning and optimization algorithms for automatic breast cancer detection. *International Journal of Imaging Systems and Technology*, 30(2):495–506, 2020.

Osama R Shahin, Rami Ayadi, and Oussama Ghorbel. Mammogram breast cancer detection using fast watershed segmentation. *International Journal*, 9(3), 2020.

P. Shanmugavadivu, V. Sivakumar, and Rashmi Sudhir. Fractal dimension-bound spatio-temporal analysis of digital mammograms. *The European Physical Journal Special Topics*, 225(1):137–146, 2016. doi: 10.1140/epjst/e2016-02615-x.

Jaya Sharma, J. K. Rai, and R. P. Tewari. A combined watershed segmentation approach using k-means clustering for mammograms. In *2015 2nd International Conference on Signal Processing and Integrated Networks (SPIN)*, pages 109–113, 2015. doi: 10.1109/SPIN.2015.7095345.

Pratibha Sharma, Manoj Diwakar, and Niranjan Lal. Article: Edge detection using moore neighborhood. *International Journal of Computer Applications*, 61(3):26–30, January 2013a. Full text available.

Pratibha Sharma, Manoj Diwakar, and Niranjan Lal. Edge detection using moore neighborhood. *International Journal of Computer Applications*, 61:26–30, 2013b. doi: 10.5120/9910-4506.

R Shen, K Yan, F Xiao, J Chang, C Jiang, and K Zhou. Automatic pectoral muscle region segmentation in mammograms using genetic algorithm and morphological selection. *Journal of Digital Imaging*, 31:680–691, 2018. doi: 10.1007/s10278-018-0068-9. URL `https://doi.org/10.1007/s10278-018-0068-9`.

P Shi, J Zhong, A Rampun, and H Wang. A hierarchical pipeline for breast boundary segmentation and calcification detection in mammograms. *Computers in Biology and Medicine*, 96:178–188, 2018. doi: 10.1016/j.compbiomed.2018.03.011. URL `https://doi.org/10.1016/j.compbiomed.2018.03.011`.

V Shinde and BT Rao. *Novel approach to segment the pectoral muscle in the mammograms*, pages 227–237. Springer, 2019. doi: 10.1007/978-981-13-0617-4_22. URL `https://doi.org/10.1007/978-981-13-0617-4_22`.

Vivek Kumar Singh, Hatem A. Rashwan, Mohamed Abdel-Nasser, Farhan Akram, Rami Haffar, Nidhi Pandey, Meritxell Arenas, Santiago Romani, and Domenec Puig. Chapter 8 - a computer-aided diagnosis system for breast cancer molecular subtype prediction in mammographic images. In Ayman S. El-Baz and Jasjit S. Suri, editors, *State of the Art in Neural Networks and their Applications*, pages 153–178. Academic Press, 2021. ISBN 978-0-12-819740-0. doi: https://doi.org/10.1016/B978-0-12-819740-0.00008-5. URL `https://www.sciencedirect.com/science/article/pii/B9780128197400000085`.

M Slavković-Ilić, A Gavrovska, M Milivojević, I Reljin, and B Reljin. Breast region segmentation and pectoral muscle removal in mammograms. *Telfor Journal*, 8: 50–55, 2016. doi: 10.5937/telfor1601050S. URL `https://doi.org/10.5937/telfor1601050S`.

A. Smith et al. Variability and discrepancy in mammogram interpretation: A systematic review. *Radiology*, 298(2):76–84, 2021.

S. Y. Song, B. Park, S. Hong, M. J. Kim, E. H. Lee, and J. K. Jun. Comparison of digital and screen-film mammography for breast-cancer screening: A systematic review and meta-analysis. *J Breast Cancer*, 22(2):311–325, 2019. doi: 10.4048/jbc.2019.22.e24. URL `https://doi.org/10.4048/jbc.2019.22.e24`.

F. H. Souza, E. M. Wendland, M. I. Rosa, and C. A. Polanczyk. Is full-field digital mammography more accurate than screen-film mammography in overall population screening? a systematic review and meta-analysis. *Breast*, 22(3):217–224, 2013. doi:

10.1016/j.breast.2013.02.013. URL https://doi.org/10.1016/j.breast.2013.02.013. Epub 2013 Mar 11. PMID: 23489759.

Fabio A. Spanhol, Luiz S. Oliveira, Caroline Petitjean, and Laurent Heutte. A dataset for breast cancer histopathological image classification. *IEEE Transactions on Biomedical Engineering*, 63(7):1455–1462, 2016. doi: 10.1109/TBME.2015.2496264.

M. Kusuma Sri and E. Gomathi. Classification of breast cancer images using completed local ternary pattern and support vector machine. *International Journal of Bioinformatics Research and Applications*, 18(1-2):130–140, 2022. doi: 10.1504/IJBRA.2022.121769. URL https://www.inderscienceonline.com/doi/abs/10.1504/IJBRA.2022.121769.

R.N. Strickland and H.I. Hahn. Wavelet transforms for detecting microcalcifications in mammography. In *IEEE International Conference on Image Processing (ICIP)*, volume 1, pages 402–406. IEEE, Nov 1994.

J. Suckling and et al. The mammographic image analysis society digital mammogram database. *Exerpta Medica. International Congress Series*, 1069:375–378, 1994.

Jeremy Suckling, James Parker, David R. Dance, Susan Astley, I. Hutt, Caroline R. M. Boggis, ..., and D. Betal. The mammographic image analysis society digital mammogram database. In *Proceedings of the 2nd International Workshop on Digital Mammography*, pages 10–12, York, England, July 1994.

Jeremy Suckling, Jonathan Parker, David Dance, and et al. Mammographic image analysis society (mias) database v1.21. Dataset, 2015. URL https://www.repository.cam.ac.uk/handle/1810/250394. Apollo - University of Cambridge Repository.

Sunardi, Anton Yudhana, and Anggi Rizky Windra Putri. Optimization of breast cancer classification using faster r-cnn. *Revue d'Intelligence Artificielle*, 37(1):39–45, Feb 2023. URL http://iieta.org/journals/ria.

Hyuna Sung, Jacques Ferlay, Rebecca L. Siegel, and et al. Global cancer statistics 2020: Globocan estimates of incidence and mortality worldwide for 36 cancers in 185 countries. *CA: A Cancer Journal for Clinicians*, 71(3):209–249, 2021. doi: 10.3322/caac.21660.

Saifullah Suradi, Kamarul Abdullah, and Nor Isa. Improvement of image enhancement for mammogram images using fuzzy anisotropic diffusion histogram equalisation contrast adaptive limited (fadhecal). *Computer Methods in Biomechanics and Biomedical Engineering Imaging & Visualization*, 09 2021. doi: 10.1080/21681163.2021.1972344.

SA Taghanaki, Y Liu, B Miles, and G Hamarneh. Geometry-based pectoral muscle segmentation from mlo mammogram views. *IEEE Trans Biomed Eng*, 64:2662–2671,

2017a. doi: 10.1109/TBME.2017.2649481. URL https://doi.org/10.1109/TBME.2017.2649481.

Saeid Asgari Taghanaki, Jeremy Kawahara, Brandon Miles, and Ghassan Hamarneh. Pareto-optimal multi-objective dimensionality reduction deep auto-encoder for mammography classification. *Computer Methods and Programs in Biomedicine*, 145:85–93, 2017b. ISSN 0169-2607. doi: https://doi.org/10.1016/j.cmpb.2017.04.012. URL https://www.sciencedirect.com/science/article/pii/S0169260716309269.

Shankar Thawkar. Feature selection and classification in mammography using hybrid crow search algorithm with harris hawks optimization. *Biocybernetics and Biomedical Engineering*, 42(4):1094–1111, 2022. ISSN 0208-5216. doi: https://doi.org/10.1016/j.bbe.2022.09.001. URL https://www.sciencedirect.com/science/article/pii/S0208521622000791.

Karpagalingam Thirumoorthy and Jerold John Britto J. A two-stage feature selection approach using hybrid quasi-opposition self-adaptive coati optimization algorithm for breast cancer classification. *Applied Soft Computing*, 146:110704, 2023. ISSN 1568-4946. doi: https://doi.org/10.1016/j.asoc.2023.110704. URL https://www.sciencedirect.com/science/article/pii/S1568494623007226.

G.D. Tourassi. Journey toward computer-aided diagnosis: Role of image texture analysis. *Radiology*, 213(2):317–320, 1999.

Georgia D Tourassi, David M Delong, and Carey E Floyd. A study on the computerized fractal analysis of architectural distortion in screening mammograms. *Physics in Medicine & Biology*, 51(5):1299, feb 2006. doi: 10.1088/0031-9155/51/5/018. URL https://dx.doi.org/10.1088/0031-9155/51/5/018.

U.S. Food and Drug Administration. Approval for r2 technology, inc. imagechecker system. https://www.accessdata.fda.gov/cdrh_docs/pdf/p970058.pdf, Apr 1998.

U.S. Food and Drug Administration. Approval for [specific medical device]. https://webharvest.gov/peth04/20041119105203/http://www.fda.gov/cdrh/pdf/p010034.html, 2004.

H. J. Vala and A. Baxi. A review on otsu image segmentation algorithm. *International Journal of Advanced Research in Computer Engineering & Technology*, 2(2):387, 2013.

C. Van Ongeval, J. Jacobs, and H. Bosmans. Artifacts in digital mammography. *JBR-BTR*, 91(6):262–263, 2008.

Karlijn J. van Stralen, Vianda S. Stel, Johannes B. Reitsma, Friedo W. Dekker, Carmine Zoccali, and Kitty J. Jager. Diagnostic methods i: sensitivity, specificity, and other measures of accuracy. *Kidney International*, 75(12):1257–1263, 2009.

ISSN 0085-2538. doi: https://doi.org/10.1038/ki.2009.92. URL https://www.sciencedirect.com/science/article/pii/S0085253815536521.

S Venkataraman, PJ Slanetz, and CI Lee. Breast imaging for cancer screening: Mammography and ultrasonography. *UpToDate*, 2021. URL https://www.uptodate.com/contents/breast-imaging-for-cancer-screening-mammography-and-ultrasonography. Accessed on September 29, 2021.

D.M. Vo, N.Q. Nguyen, and S.W. Lee. Classification of breast cancer histology images using incremental boosting convolution networks. *Information Sciences*, 482:123–138, 2019.

M. Vrankic and D. Sersic. Image denoising based on adaptive quincunx wavelets. In *IEEE 6th Workshop on Multimedia Signal Processing, 2004.*, pages 251–254, 2004. doi: 10.1109/MMSP.2004.1436540.

Tuan D. Vu, Ngoc Q. K. Nguyen, and W. Sabrina Lin. Deep convolutional neural networks for mammography: Advances, challenges and applications. *BMC Bioinformatics*, 21(1):42, 2020. doi: 10.1186/s12859-020-03681-1. URL https://bmcbioinformatics.biomedcentral.com/articles/10.1186/s12859-020-03681-1.

Jinhua Wang, Xi Yang, Hongmin Cai, Wanchang Tan, Cangzheng Jin, and Li Li. Discrimination of breast cancer with microcalcifications on mammography by deep learning. *Scientific Reports*, 6:27327, 2016. doi: 10.1038/srep27327. URL https://doi.org/10.1038/srep27327.

Juan Wang and Yongyi Yang. A context-sensitive deep learning approach for microcalcification detection in mammograms. *Pattern Recognition*, 78:12–22, 2018. doi: 10.1016/j.patcog.2018.01.009. URL https://www.sciencedirect.com/science/article/pii/S0031320318300086.

T.C. Wang and N.B. Karayiannis. Detection of microcalcifications in digital mammograms using wavelets. *IEEE Transactions on Medical Imaging*, 17(4):498–509, Aug 1998.

Z. Wang, M. Li, H. Wang, H. Jiang, Y. Yao, H. Zhang, and J. Xin. Breast cancer detection using extreme learning machine based on feature fusion with cnn deep features. *IEEE Access*, 7:105146–105158, 2019.

L. J. Warren Burhenne, S. A. Wood, C. J. D'Orsi, S. A. Feig, D. B. Kopans, K. F. O'Shaughnessy, E. A. Sickles, L. Tabar, C. J. Vyborny, and R. A. Castellino. Potential contribution of computer-aided detection to the sensitivity of screening mammography. *Radiology*, 215(2):554–562, 2000. doi: 10.1148/radiology.215.2.r00ma15554. Erratum in: Radiology 2000 Jul;216(1):306. PMID: 10796939.

Chia-Hung Wei, Chih-Ying Gwo, and Pai Jung Huang. Identification and segmentation of obscure pectoral muscle in mediolateral oblique mammograms. *The British Journal of Radiology*, 89:20150802, 2016. doi: 10.1259/bjr.20150802. URL `https://doi.org/10.1259/bjr.20150802`. PMID: 27043966.

H. Gilbert Welch and William C. Black. Overdiagnosis in Cancer. *JNCI: Journal of the National Cancer Institute*, 102(9):605–613, 05 2010. ISSN 0027-8874. doi: 10.1093/jnci/djq099. URL `https://doi.org/10.1093/jnci/djq099`.

World Health Organization. *Cancer*. World Health Organization, 2020. URL `https://www.who.int/news-room/fact-sheets/detail/cancer`. [Online; accessed December 26, 2023].

P. Xi, C. Shu, and R. Goubran. Abnormality detection in mammography using deep convolutional neural networks. In *2018 IEEE International Symposium on Medical Measurements and Applications (MeMeA)*, pages 1–6. IEEE, Jun 2018.

W Xu, L Li, and W Liu. A novel pectoral muscle segmentation algorithm based on polyline fitting and elastic thread approaching. In *The 1st International Conference on Bioinformatics and Biomedical Engineering, ICBBE 2007*, pages 837–840. IEEE, 2007. doi: 10.1109/ICBBE.2007.218. URL `https://doi.org/10.1109/ICBBE.2007.218`.

P. Yang, W. Song, X. Zhao, R. Zheng, and L. Qingge. An improved otsu threshold segmentation algorithm. *International Journal of Computational Science and Engineering*, 22(1):146–153, Jan 2020.

X.-S. Yang and S. Deb. Cuckoo search via lévy flights. In *World Congress on Nature & Biologically Inspired Computing (NaBIC 2009)*, pages 210–214. IEEE Publications, 2009.

Xin-She Yang. Metaheuristic optimization: Algorithm analysis and open problems. In Panos M. Pardalos and Steffen Rebennack, editors, *Experimental Algorithms*, pages 21–32, Berlin, Heidelberg, 2011. Springer Berlin Heidelberg. ISBN 978-3-642-20662-7.

WB Yoon, JE Oh, EY Chae, HH Kim, SY Lee, and KG Kim. Automatic detection of pectoral muscle region for computer-aided diagnosis using mias mammograms. *BioMed Research International*, 2016. doi: 10.1155/2016/5967580. URL `https://doi.org/10.1155/2016/5967580`.

Salman Zakareya and et al. A new deep-learning-based model for breast cancer diagnosis from medical images. *Diagnostics (Basel, Switzerland)*, 13(11): 1944, 2023. doi: 10.3390/diagnostics13111944. URL `https://doi.org/10.3390/diagnostics13111944`.

Dilovan Asaad Zebari, Habibollah Haron, Subhi R. M. Zeebaree, and Diyar Qader Zeebaree. Enhance the mammogram images for both segmentation and feature extraction using wavelet transform. *2019 International Conference on Advanced Science and Engineering (ICOASE)*, pages 100–105, 2019. doi: 10.1109/ICOASE.2019.8723779. URL `https://api.semanticscholar.org/CorpusID:171095532`.

Dilovan Asaad Zebari, Dheyaa Ahmed Ibrahim, Diyar Qader Zeebaree, Mazin Abed Mohammed, Habibollah Haron, Nechirvan Asaad Zebari, Robertas Damaševičius, and Rytis Maskeliūnas. Breast cancer detection using mammogram images with improved multi-fractal dimension approach and feature fusion. *Applied Sciences*, 11(24), 2021. ISSN 2076-3417. doi: 10.3390/app112412122. URL `https://www.mdpi.com/2076-3417/11/24/12122`.

X. Zhang, J. Ma, and L. Wang. Feature selection and classification in mammography using hybrid crow search algorithm with harris hawks optimization. *IEEE Access*, 7:146341–146352, 2019a.

Yudong Zhang, Xueyan Wu, Siyuan Lu, Hainan Wang, Preetha Phillips, and Shuihua Wang. Smart detection on abnormal breasts in digital mammography based on contrast-limited adaptive histogram equalization and chaotic adaptive real-coded biogeography-based optimization. *Simulation*, 92(9):873–885, 2016.

Z. Zhang, Y. Wang, J. Zhang, and X. Mu. Comparison of multiple feature extractors on faster rcnn for breast tumor detection. In *2019 8th International Symposium on Next Generation Electronics (ISNE)*, pages 1–4. IEEE, Oct 2019b.